Purification and Characterisation of the Ectodomain of the Scavenger Receptor CD36

David John Sanders

A thesis submitted for the degree of
Doctor of Philosophy

2014

Centre for Cutaneous Research

The Blizard Institute

Barts and The London School of Medicine and Dentistry

Queen Mary, University of London

Acknowledgements

First and foremost I would like to thank my supervisor Kenny Linton who throughout my doctoral studies provided me with impeccable support and advice; he truly has the patience of a saint.

I would also like to thank all past and present members of the Membrane Transport Biology Group who have provided me with inspiration, support and at times a much needed laugh!

Finally I would like to thank all my family and friends for their unconditional support over the last four years.

Statement of Originality

I, David J. Sanders, confirm that the research included within this thesis is my own work or that where it has been carried out in collaboration with, or supported by others, that this is duly acknowledged below and my contribution indicated.

I attest that I have exercised reasonable care to ensure that the work is original, and does not to the best of my knowledge break any UK law, infringe any third party's copyright or other Intellectual Property Right, or contain any confidential material. I accept that the College has the right to use plagiarism detection software to check the electronic version of the thesis. I confirm that this thesis has not been previously submitted for the award of a degree by this or any other university.

David J. Sanders

24/09/2014

Abstract

Introduction

Human CD36 is a class B scavenger receptor expressed in a variety of cell types including macrophages and endothelial cells. This heavily glycosylated membrane protein has a large ectodomain (ED) responsible for binding a variety of ligands. These include oxidised LDL and long chain fatty acids, which link CD36 to the development of atherosclerosis and insulin resistance, respectively. CD36 has also been implicated in the phagocyte-uptake of apoptotic cells, anti-angiogenic effects in endothelial cells and development of a variety of fibrotic diseases, through interaction with thrombospondin-1. The main objective of this study was to express, purify and characterise the ligand binding ectodomain of CD36 with a view to better understanding how CD36 binds multiple ligands.

Methods

A baculovirus expression system was used to express and secrete CD36 ED with a 12-His tag from insect cells using an N-terminal secretion sequence. Subsequent purification was performed using nickel affinity chromatography with functionality of the ED assessed through the ability to bind modified LDL in a solid phase binding assay. The N-glycosylation status of the purified ED was explored through use of the N-glycosidase PNGase F and mass spectrometric analysis. Initial studies to measure binding kinetics involved use of surface plasmon resonance (SPR) and binding of

commercially available antibodies, mAb1955, mAb1258 and mAbFA6-152, to purified CD36 ED immobilised on an NTA SPR sensor chip.

Results

The N-glycosylation status of CD36 ED produced in Sf21 and Hi5 insect cells was different with heterogeneous N-glycosylation being identified at individual glycosylation sites. Solid-phase ligand binding revealed that both glycosylated and deglycosylated ED retain affinity for modified LDL. The purified CD36 ED was found to homo-oligomerise particularly at higher concentrations. MAb1955 and mAb1258 were found to bind to the nickel on the sensor chip precluding microkinetic analysis of binding to CD36. However, mAbFA6-152 was found to bind to the immobilised CD36 ED with high avidity and two-step binding kinetics.

Conclusions and future direction

This study shows for the first time that N-glycosylation is not important for the binding of modified LDL to CD36. Furthermore it was demonstrated that native CD36 ED produced in Sf21 insect cells can be deglycosylated without denaturation, which may be critical for the success of future crystallisation trials. The characterisation of mAbFA6-152 binding by SPR is proof-of-principle that CD36 ED can be studied using this technique paving the way for future biophysical analysis of ligand binding.

Contents

List of Figures

List of Tables

List of Equations

Abbreviations

12His	12xHistidine
Å	Angstrom
AcLDL	Acetylated LDL
AcMNPV	*Autographa californica* multiple nuclear polyhedrosis virus
AGE	Advanced glycation end products
AIM	Apoptosis inhibitor of macrophages
AMPK	AMP-activated protein kinase
AP	Alkaline phosphatase
ApoE	Apolipoprotein E
Asn	Asparagine
Asp	Aspartic acid
bFGF	basic fibroblast growth factor
BSA	Bovine serum albumin
BV	Budded virus
C/EBP	CCAAT/enhancer-binding protein
CD5L	CD5 antigen-like
CD36	Cluster of differentiation 36
CD36	Human protein
CD36	Human gene
Cd36	Rodent protein

Cd36		Rodent gene
	hCD36	Human protein
	mCd36	Mouse protein
cDNA		Complementary deoxyribonucleic acid
CHO		Chinese hamster ovary
CID		Collision-induced dissociation
CLA		CD36 and LIMP-2 analogous
CLESH		CD36 LIMP-2 emp SR-BI homology
Da		Daltons
dH_2O		Distilled water
DiI		(2Z)-2-[(E)-3-(3,3-dimethyl-1-octadecylindol-1-ium-2-yl)prop-2-enylidene]-3,3-dimethyl-1-octadecylindole; perchlorate
DMEM		Dulbecco's Modified Eagle Medium
DNA		Deoxyribonucleic acid
DPP		Dolichol pyrophosphate
DTT		Dithiothreitol
ECL		Enhanced chemiluminescence
ED		Ectodomain
EDTA		Ethylenediaminetetraacetic acid
Emp		Epithelial membrane protein
ER		Endoplasmic reticulum
ESI		Electrospray ionisation

ETD	Electron-transfer dissociation
Fab	fragment antigen-binding
FABP$_{pm}$	Plasma membrane fatty acid binding protein
FAF	Fatty acid free
FAT	Fatty acid translocase
FB	*flashBAC*
FBG	*flashBAC Gold*
FBS	Foetal bovine serum
EGFP	Enhanced green fluorescent protein
GLUT	Glucose transporter
GST	Glutathione-S-transferase
HCD	Higher energy collision-induced dissociation
HDL	High-density lipoprotein
HDMEC	Human dermal microvascular endothelial cells
HEK	Human embryonic kidney
HEL	Human erythroleukemia
Hi5	High-Five insect cells
His	Histidine
HMSS	Honey bee melittin secretion signal
HRP	Horseradish peroxidase
IMAC	Immobilised metal ion affinity chromatography
JNK	c-jun N-terminal kinase
Kb	kilobases

kDa	Kilodaltons
LB	Lysogeny broth
LC	Liquid chromatography
LCFA	Long chain fatty acids
LDL	Low-density lipoprotein
LIMP-2	Lysosomal integral membrane protein 2
hLIMP-2	Human protein
LMP-Ag	Low-melting point agarose
LOX-1	Lectin-like oxidised low-density lipoprotein receptor-1
LSB	Laemmli sample buffer
LTA	Lipotechoic acid
m/z	Mass/ charge ratio
mAb	Monoclonal antibody
MAPK	mitogen-activated protein kinase
MFGM	Milk fat globule membranes
Min	Minute
mLDL	Modified LDL
MOI	Multiplicity of infection
mRNA	messenger ribonucleic acid
MS/MS	Tandem mass spectrometry
Ni	Nickel
NHS	sulfo-N-hydroxy-succinimidyl
NMWCO	Nominal molecular weight cut off

NTA	Nitrilotriacetic acid
ODV	Occlusion-derived virus
OET	Oxford Expression Technologies
OPPF	Oxford Protein Production Facility
OST	oligosaccharyltransferase
oxLDL	Oxidised LDL
PAGE	Polyacrylamide gel electrophoresis
PBS	Phosphate-buffered saline
PEI	Polyethylenimine
PES	Polyethersulfone
PDI	Protein disulphide isomerase
Pfemp	*P. falciparum* erythrocyte membrane protein
Pfu	Plaque forming units
PKC	Protein kinase C
PMA	phorbol 12-myristate 13-acetate
PNGase F	Peptide N-glycosidase F
PPARγ	Peroxisome proliferator activated receptor gamma
PRO	*Profold ER-1*
PROS	photo-receptor outer segments
PTM	Post-translational modification
PVDF	Polyvinylidene fluoride
ROS	Reactive oxygen species
RPEs	Retinal pigment epithelial cells

Rpm	Revolutions per minute
RU	Response units
SAB	Salvianolic acid B
SD	Standard deviation
SEC	Size-exclusion chromatography
Selk	Selenoprotein K
Ser	Serine
SDS	Sodium dodecyl sulphate
SE	Standard error
SFM	Serum-free media
SHR	Spontaneously hypertensive rat
SNMP	Sensory neuron membrane protein
SNP	Single nucleotide polymorphism
SPR	Surface plasmon resonance
SR-BI	Scavenger receptor class B member 1
hSR-BI	Human protein
SSO	sulfo-N-hydroxy-succinimidyl oleate
TBS	Tris-buffered saline
TEMED	N, N, N', N'-tetramethylethane-1,2-diamine
TGF-β	Transforming growth factor-beta
Thr	Threonine
TLR	Toll-like receptor
TNF-α	Tumour necrosis factor-alpha

TSP	Thrombospondin
U	Units
UGT	UDP-Glc: glycoprotein glucosyltransferase
UTR	Untranslated region
VEGF	Vascular endothelial growth factor
VLDL	Very low-density lipoprotein
X-gal	5-bromo-4-chloro-3-indolyl-β-D-galactopyranoside

1. Introduction

1.1. Scavenger Receptors

Scavenger receptors, first identified by Brown and Goldstein in 1979, are membrane proteins originally recognised by their ability to bind and to mediate the endocytosis of chemically modified low density lipoproteins (LDL), such as the natural and clinically important oxidised LDL (oxLDL) and the synthetic acetylated LDL (acLDL) (Brown and Goldstein, 1979, Brown et al., 1979, Itabe et al., 2011). The ability to scavenge was attributed to particular membrane receptors being able to differentiate between normal self-molecules and altered self-molecules, with preferential binding of oxidised LDL over native LDL (Greaves and Gordon, 2009, Henriksen *et al*., 1981). With the discovery of many more scavenger receptors in recent years it has become apparent that the range of ligands recognised by individual members of this family are diverse including unmodified endogenous proteins, and a number of exogenous microbial structures (Areschoug and Gordon, 2009, Pluddemann *et al*., 2006). To account for this ligand polyspecificity it was proposed by Hartvigsen *et al.*, that epitopes generated by oxidation of endogenous proteins are similar to those found on exogenous microbial structures (Hartvigsen *et al*., 2009).

Scavenger receptors are a family of structurally heterogeneous membrane proteins that are subdivided into classes (A-H) depending on common structural features. Despite having the same general function, there is very little similarity between

classes (Canton *et al*., 2013). The first scavenger receptors to be isolated and cloned were designated type I and type II scavenger receptors (Kodama et al., 1990, Rohrer et al., 1990). These two proteins generated by alternative splicing of the same gene were later designated as class A scavenger receptors (Emi *et al*., 1993, Freeman *et al*., 1990). Composed of 6 domains, 5 of which are identical (the C-terminal being different), these receptors bind poly-anionic ligands through a collagenous extracellular domain (Acton *et al*., 1993, Doi *et al*., 1993).

1.2.   Class B Scavenger Receptors

The class B scavenger receptor CD36 was originally identified in 1983 on the surface of monocytes using the monoclonal antibody (mAb) OKM5 (Talle *et al*., 1983). However, it was not recognised as a scavenger receptor until 1991 when it was shown that CD36 expressed on the surface of macrophages could recognise and facilitate the uptake of apoptotic cells (Savill et al., 1991). CD36 was further demonstrated as a scavenger receptor by binding oxLDL when expressed on the surface of transiently transfected human embryonic kidney (HEK) 293 cells (Endemann *et al*., 1993). Initially known as glycoprotein IV, CD36 was also shown at the time to be expressed on the surface of platelets (Asch *et al*., 1987) and endothelial cells (Swerlick *et al*., 1992). CD36 was also able to bind thrombospondin-1 (TSP-1) (Asch *et al*., 1987), collagen (Tandon et al., 1989a) and to be responsible for the cytoadherance of erythrocytes infected with *Plasmodium falciparum* (Oquendo *et al.*, 1989). Despite this, CD36 was not classified as a class B scavenger receptor until hamster SR-BI was cloned and identified as a new member

of the CD36 family (Acton *et al*., 1994). Through use of direct binding and competition assays it was found that CD36 and SR-BI bound modified LDL with a similar high affinity but lacked the ability to bind the same range of poly-anionic ligands that class A scavenger receptors could bind. Following this observation, CD36 and SR-BI were designated as the new class B scavenger receptors (Acton *et al*., 1994).

Since the inception of the new term, other class B scavenger receptors have been identified including the human membrane glycoproteins, lysosomal integral membrane protein II (LIMP-2) (Vega *et al*., 1991) and the CD36 and LIMP-2 Analogous-1 (CLA-1). Other additions include the *Drosophila* proteins epithelial membrane protein (emp) (Hart and Wilcox, 1993), *Croquemort* (Franc *et al*., 1996*)* and sensory neuron membrane protein (SNMP) which was originally identified in *Lepidoptera* (Nichols and Vogt, 2008*)*.

LIMP-2 is a lysosomal protein that is important for activity and correct localisation of the enzyme β-glucocerebrosidase. LIMP-2 shares 34% primary amino acid identity with human CD36 (Reczek *et al*., 2007). CLA-1 shares 32% primary amino acid identity with human CD36. CLA-1 is mainly located at the plasma membrane, acting as a high affinity receptor for HDL, VLDL and LDL as well as modified LDL (Calvo *et al*., 1997). CLA-1 is the human homologue of SR-BI, the main difference being that SR-BI is not expressed in the hamster placenta (Acton *et al*., 1994, Cao *et al*., 1997). Hamster SR-BI and CLA-1 (hSR-BI) share 85% primary amino acid sequence identity (Murao et al., 1997).

In insects, *croquemort* is expressed on the surface of macrophages and haemocytes and is required for phagocytosis of apoptotic corpses. It has a 23% amino acid

identity to CD36 (Franc *et al*., 1996). Emp is expressed in precursor cells and is thought to be required for proper development and function of epithelial cells. It has 32% amino acid identity to CD36 (Hart and Wilcox, 1993). SNMPs are membrane bound proteins involved in odour detection, for example pheromones (Benton *et al*., 2007). Numerous homologues have been identified across many insect orders (Nichols and Vogt, 2008). A CD36 ortholog in *C. elegans,* C03F11.3, has been shown to mediate binding and engulfment of fungal pathogens (Means, 2010).

1.3.   The Scavenger Receptor CD36

1.3.1.   Structure of CD36

A defining feature that is thought to distinguish class B scavenger receptors from other scavenger receptors is the presence of two hydrophobic transmembrane domains and a large hydrophilic ectodomain (ED). This was first demonstrated in the study of LIMP-2 where it was found that both hydrophobic domains serve to anchor LIMP-2 within the lysosomal membrane with the 'ED' in the lumen (Vega *et al*., 1991). Since the primary amino acid sequence of CD36 (472 amino acids) contains two hydrophobic regions next to amino- and carboxy-termini, a ditopic topology model was proposed with short cytoplasmic tails at the amino-terminus (GCDRNC-) and carboxy-terminus (-CACRSKTIK). This model was further supported by Tao *et al*., who showed that cysteines on both of the short amino-terminal and carboxy-terminal tails were palmitoylated (Tao et al., 1996). Despite this ditopic model now being generally agreed upon, other models have been proposed in the past including

one with a single transmembrane domain. Pearce *et al.,* reported that deletion of the carboxy-terminal putative transmembrane domain resulted in secretion of CD36 as opposed to membrane anchorage. This led to the hypothesis that only the carboxy-terminus spans the membrane and the amino-terminus was suggested to be an uncleaved signal peptide that translocates to the extracellular space (Pearce *et al*., 1994). A later study by Gruarin *et al*., disproved this theory. It was shown that truncation of the carboxy-terminal domain was not sufficient to result in CD36 secretion. Only when both amino-terminal and carboxy-terminal domains were deleted was CD36 secretion observed. Additionally, a FLAG epitope attached to the amino-terminal domain of wild type CD36 expressed in transiently transfected COS-7 cells, could only be detected when the cells were first permeabilised (Gruarin *et al*., 1997). This further reinforced the idea of two transmembrane domains with two short cytoplasmic tails.

The majority of CD36 can be found in the large ED, predicted to have a molecular weight of 46kDa (the full-length protein is predicted to have a molecular weight of 53kDa) (Figure 1.1). The transmembrane domains and cytoplasmic tails therefore make up only a small portion of the total protein. The extracellular domain is heavily modified post-translationally by glycosylation, phosphorylation and disulphide bridging. It is this ED that is also responsible for the binding a wide range of ligands.

In 2013, Neculai *et al*., crystallised the ectodomain of human LIMP-2 and solved the structure to a medium resolution of 3Å (Figure 1.2). The structure includes a previously unidentified fold with an anti-parallel β-barrel core with many short α-helical segments (Neculai *et al*., 2013). The β-barrel is imperfect, with one of the 13 slats being replaced with a short loop that partly occupies the centre of the barrel. It was reported by Neculai *et al*., that the β-barrel is also asymmetric with four β-

strands extending the full length of the LIMP-2 ectodomain structure, creating a prolate spheroid (Neculai *et al*., 2013). Furthest from the membrane at the end of the β-barrel is a three α-helix bundle that was proposed to be a binding site for β-glucocerebrosidase and also thought to be responsible for the observed homo-oligomerisation of the purified protein (Neculai *et al*., 2013).

Due to the primary amino acid similarity shared by the ectodomains of all class B scavenger receptors, the crystal structure of LIMP-2 has been used as a template to homology model both CD36 and SR-BI. Electrostatic mapping of both of the homology models suggested the accumulation of cationic residues at the apex distal from the membrane (Neculai *et al*., 2013), which fits well with the theory that this helical bundle is also responsible for ligand binding in CD36 and SR-BI which are known to bind anionic ligands.
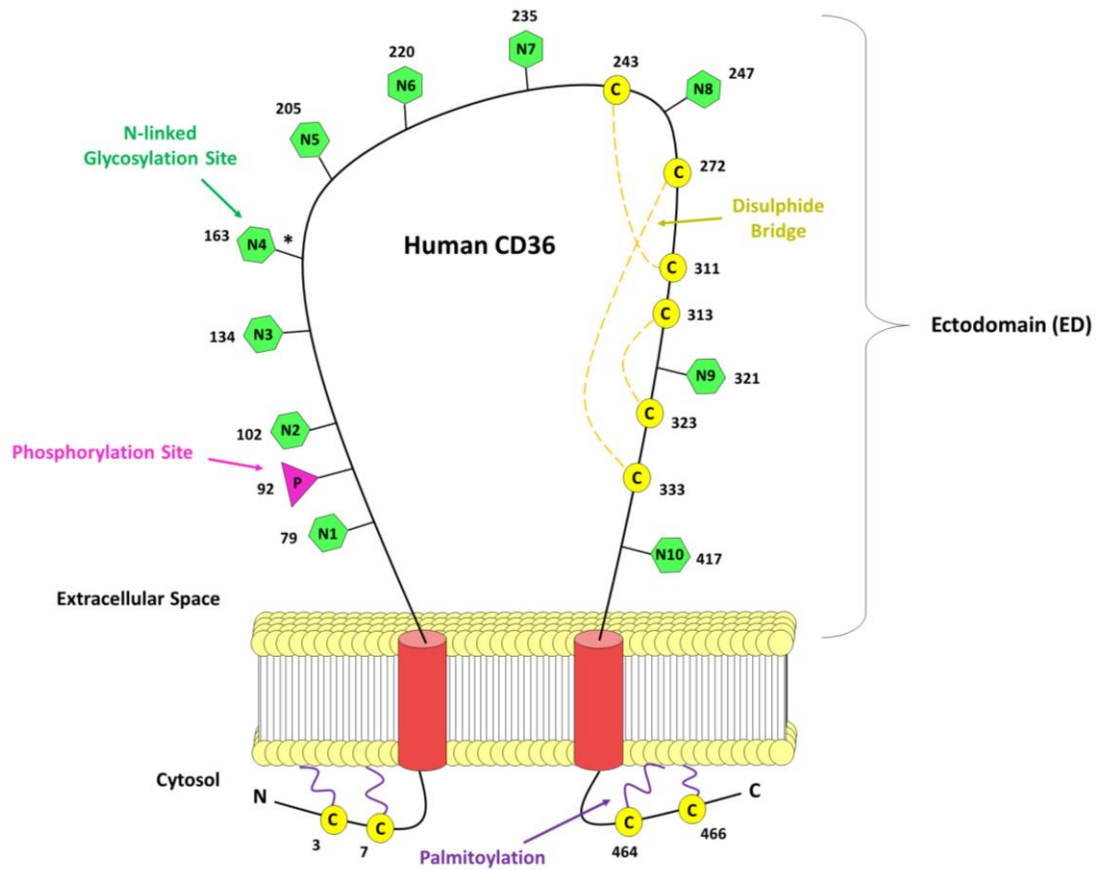
Figure 1.1. Cartoon representation of the predicted topology of human CD36.
CD36 is a ditopic protein with short cytoplasmic amino-terminal and carboxy-terminal tails. Two cysteines on each tail are palmitoylated. The majority of the protein can be found in a large ectodomain that is heavily modified post-translationally, and which is known to be responsible for ligand binding. The ectodomain is N-linked glycosylated at nine out of ten putative sites. The site shown to lack a glycan is highlighted by '*'. Three pairs of cysteines in the ectodomain form disulphide bridges, drawn based on pattern observed in bovine CD36. Two cysteines located within both the amino-terminal and carboxy-terminal tails are palmitoylated. A phosphorylation site at Thr92 is known to regulate TSP-1 binding. The numbers shown indicate which amino acid residues within human CD36 are modified.
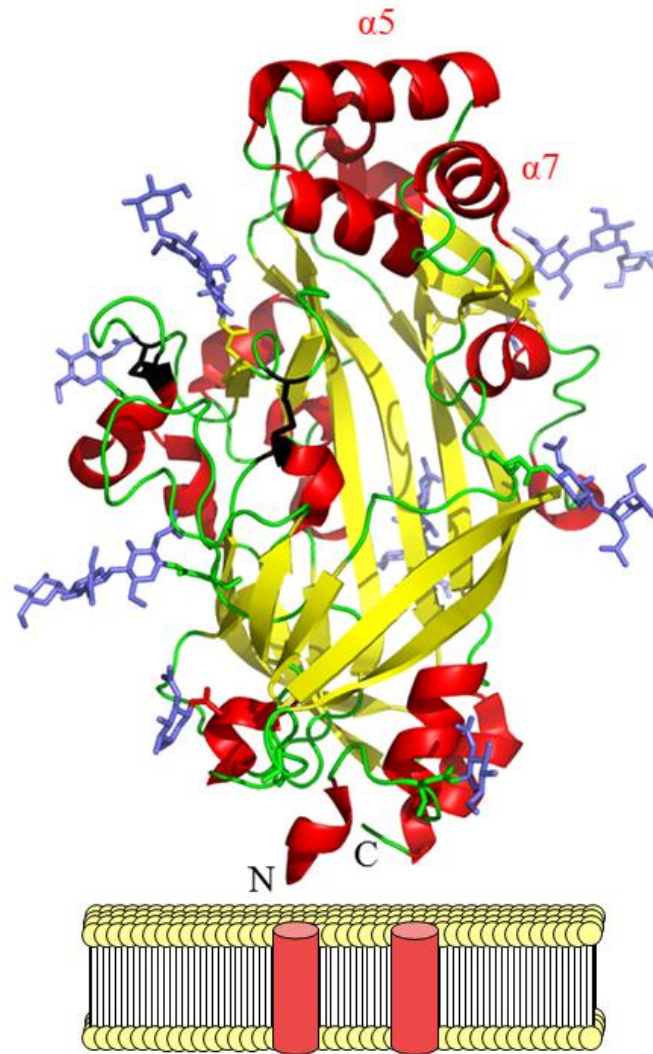
Figure 1.2. Structure of the human LIMP-2 ectodomain.
The α-helices and β-strands are shown in ribbon format coloured red and yellow, respectively. The asparagines of N-linked glycosylation sites are shown in stick format coloured slate blue. The two disulphide bridges are coloured black. The apex of the protein is made up of an α-helix bundle, devoid of glycosylation sites, thought to be a primary ligand binding site and additionally through interactions between α5 and α7 helices of different LIMP-2 molecules, a site for homo-oligomerisation (Neculai *et al.*, 2013).

1.3.2. Ligands of CD36 and localisation of binding sites

CD36 is capable of binding a diverse group of ligands. Through the use of glutathione S-transferase (GST)/CD36 fusion proteins, the binding domain for TSP-1 was investigated (Frieda *et al*., 1995). It had previously been proposed, using small synthetic peptides to represent putative CD36 domains, that TSP-1 bound to CD36 via a complex two-step process requiring low affinity binding to one region (amino acids from 139-155) which then allowed high affinity binding to a second region (amino acids 93-110) (Leung *et al*., 1992). Through use of a battery of GST/CD36 fusion proteins which covered CD36 entirely, and radiolabelled TSP-1, it was shown by Freida *et al.,* that amino-acid residues 93-120 was likely to be the main CD36 binding site for TSP-1. It may be that binding to amino acid residues 93-120 can be modulated by the downstream amino acid sequence 139-155 (Frieda *et al*., 1995). By mapping the regions of CD36 implicated in ligand binding onto the LIMP-2 structure (Figure 1.3 (a)), assuming CD36 has a similar fold, the TSP-1 binding site (amino acids 93-120) can be found along one of the β-strands which makes up part of the anti-parallel β-barrel core. The downstream sequence containing amino acid residues 139-155 is located within the α-helix bundle at the apex of the protein. Interestingly, antibodies that bind the sequence containing amino acid residues 155-183 can block TSP-1 binding (Dawson *et al*., 1997), further highlighting the possibility of modulating TSP-1 binding to CD36 either through steric hindrance or an allosteric effect.

 The further revelation that LIMP-2 also bound TSP-1 led to the identification of a conserved TSP-1 binding sequence found in the CD36 family which was called

<u>C</u>D36 <u>L</u>IMP-2 <u>e</u>mp <u>S</u>R-BI <u>h</u>omology or CLESH. It is composed of three conserved motifs, a protein kinase C (PKC) phosphorylation recognition site and two TSP-1 motif binding blocks (Crombie and Silverstein, 1998). Following on from this many other non-CD36 related proteins have been discovered with CLESH domains and subsequently shown to bind TSP-1 (Crombie *et al*., 1998, Simantov *et al*., 2001).

The identification of the oxLDL binding domain was achieved by Puente Navazo *et al*., who showed how monoclonal antibodies against the CD36 region containing amino acids 155-183 could inhibit oxLDL binding to human CD36 on the surface of transiently transfected COS cells, whereas an antibody against the CD36 region containing amino acids 30-76 could not (Puente Navazo *et al*., 1996). In contrast, Pearce *et al*., reported a different oxLDL binding region, mapped to amino acids 120-155, with a second lower affinity region around amino acids 28-93 (Pearce *et al*., 1998). This study was performed using a similar method to Frieda *et al*., except in this study radiolabelled oxLDL was used (Frieda *et al*., 1995, Pearce *et al*., 1998). Later studies, by Kar *et al*., using GST/CD36 fusion proteins and site-directed mutagenesis, proposed that amino acids 160-168 contained the binding site of oxLDL and that Lys164 and Lys166 were crucial for the interaction (Kar *et al*., 2008). By mapping the regions of CD36 implicated in modified LDL binding onto the LIMP-2 structure (Figure 1.3 (b)), these proposed binding sites fit from the α-helical bundle at the apex of the protein down through the β-barrel to the N-terminus of the ectodomain which would be attached to a transmembrane region. Neculai *et al*., reported that the centre of the LIMP-2 ectodomain consists of a large cavity that transverses the entire length of the protein. It was proposed, having used mutagenesis and an inhibitor of SR-BI-dependent lipid transport from HDL, that a similar cavity within SR-BI is responsible for delivering cholesterol(esters) from lipoproteins to the

outer leaflet of the plasma membrane (Neculai *et al*., 2013). A similar process may exist for lipophilic ligands of CD36, however, without a true structure for CD36, the presence of a cavity in CD36 cannot be confirmed. Interestingly, a similar structure has been reported for fatty acid binding proteins (FABPs). These small highly conserved proteins are responsible for binding hydrophobic ligands and trafficking them around cellular compartments. They consist of a water-filled, binding pocket surrounded by ten anti-parallel beta sheets, forming a beta barrel, capped by two alpha helices which are thought to regulate ligand binding (Smathers and Petersen, 2011). CD36 has also been reported to be capable of binding native lipoproteins HDL, VLDL and LDL (Calvo *et al*., 1998).

Plasmodium falciparum is one of four species of *Plasmodium* that naturally infects humans, being responsible for most malarial disease and resultant mortality (Gardner *et al*., 2002). *P. falciparum* is thought to have a survival mechanism which involves the adherence of infected erythrocytes to the microvasculature of vital organs, limiting exposure to the immune system (Baruch *et al*., 1999). A number of receptors have been implicated in the cytoadherence of *P. falciparum*-infected erythrocytes to endothelial cells including CD36. The binding of these erythrocytes to CD36 can be inhibited by CD36 antibodies that recognise amino acids 155-183, the same antibodies that can block TSP-1 binding (Daviet *et al*., 1995, Daviet *et al*., 1997). Using CD36 peptides to block the binding of infected erythrocytes, Baruch *et al*., identified amino acids 139-184 as the likely binding site (Baruch *et al*., 1999). *P. falciparum* erythrocyte membrane protein 1 (Pfemp1) has since been identified on the surface of the infected erythrocytes as a ligand for CD36 (Yipp *et al*., 2003). This binding region when mapped on to the LIMP-2 structure overlaps the modified LDL binding site as well as the region thought to possibly modulate TSP-1 binding

(Figure 1.3 (c)). This overlap would suggest the possibility of one ligand being able to modulate or prevent the binding of another ligand to CD36.

Other ligands that bind CD36 include anionic phospholipids and long chain fatty acids (LCFA). The binding of anionic phospholipids (which also bind to SR-BI) was determined by incubating radiolabelled liposomes containing different phospholipids with COS cells transiently expressing CD36 or SR-BI. Both phosphatidylserine and phosphatidylinositol, phospholipids normally restricted to the inner leaflet of the plasma membrane, were identified as ligands of CD36 (Rigotti *et al*., 1995). It was proposed by Greenberg *et al*., that when cell membranes undergo lipid peroxidation, during senescence or apoptosis, the hydrophobic component of fatty acids from within the lipid bilayer move to the aqueous exterior, becoming available for recognition by pattern recognition receptors, such as CD36 (Greenberg et al., 2008). In 1993, Harmon and Abumrad, identified an 88kDa membrane protein on the surface of rat adipocytes that when labelled with a derivative of LCFA led to inhibition of LCFA transport . This protein was designated as a fatty acid translocase (FAT), however it was later discovered to be the rat CD36 (Abumrad et al., 1993, Harmon and Abumrad, 1993). Further studies showed that the membrane impermeable sulfo-N-hydroxy-succinimidyl (NHS) ester of oleate (SSO), which binds to CD36 irreversibly, was able to prevent binding of not just LCFA but also oxLDL to the surface of macrophages. It was proposed that oxLDL and LCFA share the same binding site on CD36. Subsequently it was demonstrated that mutation K164A on CD36 resulted in poor LCFA uptake (Kuda et al., 2013a). This is agreement with Kar *et al*., who suggested that Lys164 was critical for oxLDL binding (Kar *et al*., 2008). Neculai *et al*., showed using Chinese hamster ovary (CHO) cells transiently transfected with CD36 with particular point mutations, that

L158, L161, K164 and K166 were required for binding DiI-labelled oxLDL (Neculai *et al*., 2013).

CD36 has been shown to bind to microbial cell wall constituents, such as lipotechoic acid (LTA). This forms part of an innate immune response involving the association of CD36 with toll like receptors (TLR) 2 and 6 (Hoebe *et al*., 2005, Jimenez-Dalmaroni *et al*., 2009). Fibrillar β-amyloid, which is a marker of Alzheimer's disease, has also been shown to bind CD36, also with a possible association with toll like receptors, in this case, TLR4 and TLR6 (Bamberger *et al*., 2003, Stewart *et al*., 2010).

The interaction between advanced glycation end products (AGE) and CD36 has been linked to the progression of chronic inflammation and diabetes (Ohgami *et al*., 2002, Basta *et al*., 2004, Zhu *et al*., 2012). AGEs which form in hyperglycemic environments are lipids or proteins that have been excessively non-enzymatically glycated or oxidised after contact with aldose sugars (Schmidt *et al*., 1994). The accumulation of AGE in many different cell types can affect the structure and function of both the extracellular and intracellular environments by binding cell surface receptors, producing reactive oxygen species (ROS) and cross-linking proteins (Schmidt *et al*., 1994, Brownlee *et al*., 1985). It was shown that CHO cells overexpressing CD36 could recognise radiolabelled AGE which was then taken up by endocytosis (Ohgami *et al*., 2002). However, later studies showed that uptake of AGE by liver endothelial cells was not via CD36 and furthermore that CD36 was not involved with clearance of AGE from the circulation (Nakajou *et al*., 2005). Instead, AGE binding to mouse adipocytes via Cd36 was shown to induce oxidative stress and inhibition of leptin expression (Horiuchi *et al*., 2005). The hyper-reactivity of platelets from patients suffering from type 2 diabetes has been linked to the

accumulation of AGE (Hasegawa *et al*., 2002). In 2012, Zhu *et al*., showed that platelets from *Cd36*-null mice under hyperglycemic conditions did not form blood clots as readily as wild-type mice under the same conditions, leading to the conclusion that vascular dysfunction in type 2 diabetes is linked to AGE-CD36-mediated platelet signalling pathways and subsequent platelet hyper-reactivity (Zhu *et al*., 2012).

CD36 is also a receptor for growth hormone protein hexarelin and its derivative EP 80317 (Bodart *et al*., 2002). EP 80317, which has no growth hormone properties, has been shown to interfere with the binding of oxLDL to CD36 (Marleau *et al*., 2005). Another ligand capable of blocking oxLDL binding to CD36 is salvianolic acid B (SAB), which is an abundant water-soluble compound extracted from the Danshen plant. SAB was shown to bind CD36 and furthermore inhibit uptake of modified LDL into macrophages in a CD36-dependent manner (Bao *et al*., 2012). Ursolic acid, a pentacyclic triterpenoid, has been shown to inhibit binding of β-amyloid protein to the surface of CD36-transfected CHO cells (Wilkinson *et al*., 2011). Together these ligands show promise as pharmaceutical agents for the treatment of a number of CD36-dependent disease states such as atherosclerosis, type 2 diabetes and Alzheimer's disease.
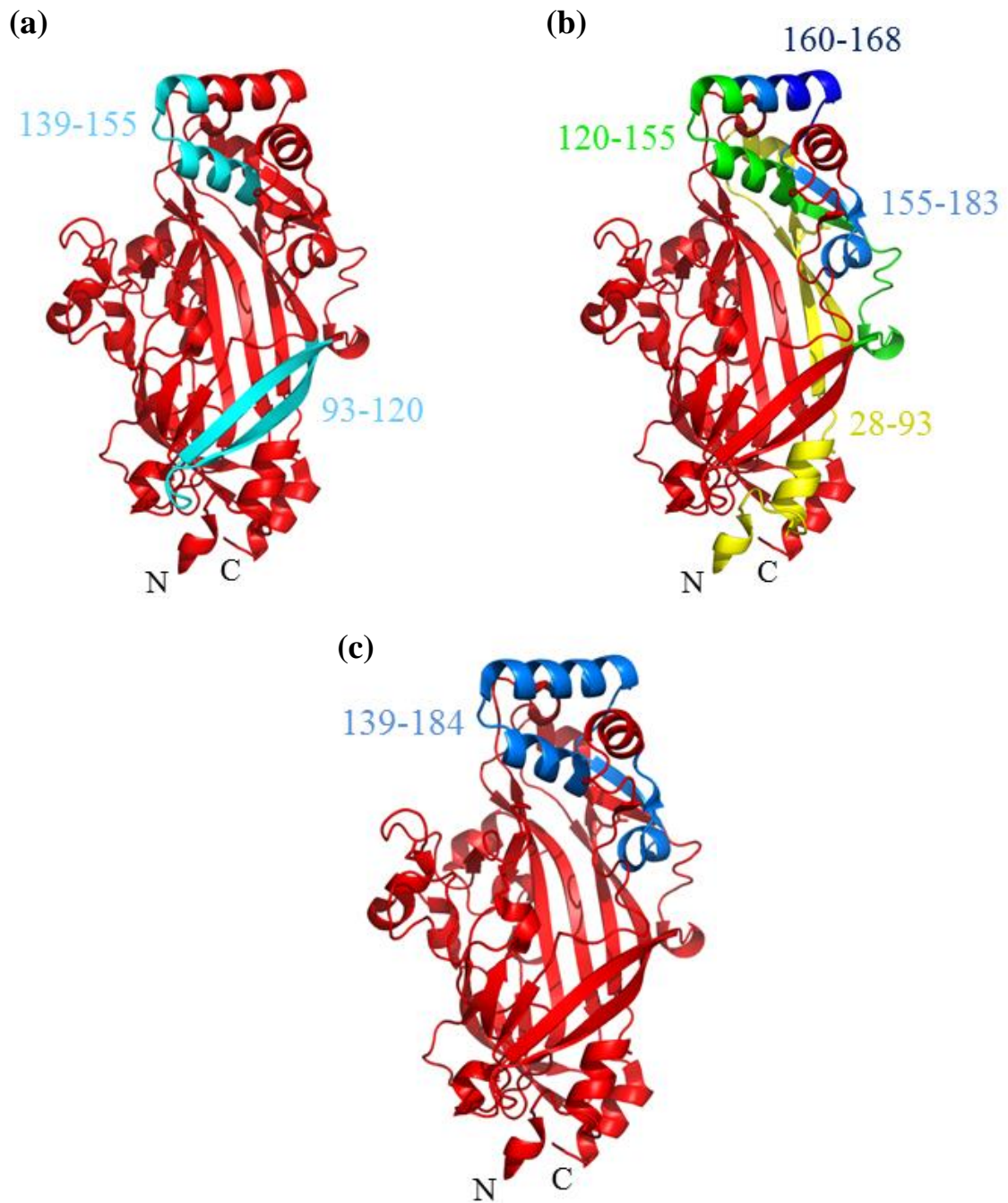
Figure 1.3. Mapping regions of CD36 implicated in ligand binding onto the LIMP-2 crystal structure.

Regions highlighted have been implicated in CD36 binding to **(a)** TSP-1, **(b)** modified LDL and **(c)** *P. falciparum* infected erythrocytes. Equivalent regions on LIMP-2 are highlighted based on a CD36/LIMP-2 primary sequence alignment. Coloured segments indicate possible ligand binding sites that have been identified based on different studies (see 1.3.2).

1.4.   Expression and Regulation of *CD36*

1.4.1.   Regulation of *CD36*

The human *CD36* gene is more than 35kb long and is located on chromosome *7, band q11.2* (Fernandez-Ruiz *et al*., 1993, Armesilla and Vega, 1994). The gene has 15 exons, and the coding sequence begins in exon 3 and finishes in exon 14 (Figure 1.4) (Armesilla and Vega, 1994). Alternative splicing of the mRNA transcript, however, is known to occur, and exons 4 and 5 can be skipped resulting in a protein lacking amino acids 43-143 which includes the TSP-1 binding domain and three putative N-linked glycosylation sites in the ectodomain. Transient expression of this variant in COS-1 and HEL cells was found to reach the cell surface, however it is unknown whether it adopts the wild-type fold. A similar exon skipping event can be seen with CLA-1 (Tang *et al*., 1994). Alternative splicing in exon 1 that lacks TATA boxes and CpG islands leads to the generation of different transcripts, regulated specifically by the tissue (Andersen *et al*., 2006, Sato *et al*., 2002, Zingg *et al*., 2002). CD36 gene regulation is therefore complex, reflecting the broad expression pattern of the protein in many different cells types. This is in addition to multiple forms of post-translational modification which are likely to also be tissue specific and affect ligand interaction. It has been documented that CD36 is upregulated in response to different CD36 ligands. For example, CD36 is upregulated by oxLDL via a signalling pathway involving PKC and peroxisome proliferator-activated receptor gamma (PPAR-γ) (Feng *et al*., 2000) with the *CD36* gene containing a PPAR-γ responsive element (Nagy *et al*., 1998). CCAAT/enhancer-binding proteins (C/EBP) α and β, whose transcriptional activity is upregulated in type 2 diabetes by

p38-mediated serine phosphorylation has been shown to increase *CD36* expression in different cells types. A C/EBP-responsive element has been identified within the *CD36* promoter, suggesting another mechanism for regulating expression (Qiao *et al.*, 2008, Qiao *et al.*, 2006).

Figure 1.4. Schematic representation of the human *CD36* gene.
The human *CD36* gene consists of 15 exons. The 5'-untranslated region (5'-UTR) consists of exons 1, 2 and part of 3. The remainder of exon 3, 4-13 and part of 14 encode human CD36. The 3'-UTR consists of part of exon 14 and exon 15. Alternative splicing of exon 1 allows tissue specific regulation. Modified from Collot-Teixeira, S., Martin, J., McDermontt-Roe, C., Poston, R. & McGregor, J. L. 2007. CD36 and macrophages in atherosclerosis. *Cardiovasc Res,* 75**,** 468-77 by permission of Oxford University Press.

1.4.2.   *CD36* mutants and variants

Many mutations have been identified within the coding sequence of the human *CD36* gene including small and gross deletions, insertions, rearrangements, variant repeats and duplications (Rac *et al.*, 2007). Two types of *CD36* deficiency have been

identified from mutations, designated type I and type II. Type I is characterised by absence of *CD36* expression in both monocytes and platelets, whereas type II is characterised by the absence of *CD36* expression only in platelets. There are over twenty types of mutation which, as homozygous or compound heterozygous mutations, lead to type I *CD36* deficiency (Rac *et al*., 2007). One of the most common of these mutations is *C478T* which results in an 81kDa protein (as opposed to the wild-type 88kDa protein), possibly with glycosylation defects, which leads to protein degradation (Kashiwagi *et al*., 1993, Kashiwagi *et al*., 1995, Kashiwagi *et al*., 2001). Related observable phenotypes of type I *CD36* deficiency include abnormal glucose and lipid metabolism.

The mechanism behind type II *CD36* deficiency is unclear, however, it has been observed in individuals who have a heterozygous mutation in the *CD36* gene, in particular *C478T*. Studies performed by Kashiwagi *et al*., found that both *C478* and *T478* forms of CD36 were present in monocytes from two patients with type II deficiency, but only *T478* was present in the platelets of the same individuals, suggesting a platelet-specific regulation contributing to the phenotype (Kashiwagi *et al*., 1995).

Considerable variability has been observed in *CD36*, especially in individuals of African and Asian descent, with naturally occurring polymorphisms being linked to a variety of diseases. Five intronic SNPs present within the African-American population were shown to be linked to a significant increase in risk of metabolic syndrome (Love-Gregory *et al*., 2008). Five SNPs in the Caucasian population have been linked to an increased incidence of cardiovascular disease (Ma *et al*., 2004). Three polymorphisms in Thai patients infected with *P. falciparum*, *T14C*, *G53T* and

a TG_{12} repeat within intron 3, were associated with protection against severe malaria (Omi et al., 2003).

1.5. Post-translational modification of CD36

1.5.1. Phosphorylation

Protein phosphorylation is the most commonly observed post-translational modifications (Khoury et al., 2011). Through recognition of kinase consensus sequences, present on many proteins, phosphorylation and dephosphorylation is known to regulate a number of physiological processes (Ubersax and Ferrell, 2007, Hunter, 1995, Ehrlich et al., 1990).

In work carried out by Asch et al., a single phosphorylation site was identified on human CD36. CD36 domains were randomly expressed in a recombinant expression system and subsequently screened using a peptide (amino acids 504-509, CSVTCG) which corresponds to the TSP-1 sequence that is known to bind CD36. The binding site on CD36 (amino acids 88-99, RGPYTYRVRFLA) that recognises this TSP-1 peptide was identified as a PKC consensus target sequence. When CD36 was incubated with PKC and phosphorylated, TSP-1 peptide binding was reduced by 60%, suggesting that binding of TSP-1 to CD36 may be regulated by phosphorylation. Site-directed mutagenesis and repeat binding experiments identified Thr92 as the site of phosphorylation. It was proposed based on these findings that CD36 is constitutively phosphorylated but can be dephosphorylated extracellularly leading to increased TSP-1 binding. This could then be reversed by

phosphorylation by PKC (Asch *et al*., 1993). However, PKC is an intracellular kinase and so is unlikely to be able to phosphorylate the site which is extracellular. In 2012, Chu and Silverstein showed that phorbol 12-myristate 13-acetate (PMA), an activator of PKC, substantially increased the phosphorylation of CD36 intracellularly, and proposed that regulation of the amount of phosphorylated CD36 on the cell surface involved synthesis of new protein rather than an external unknown kinase (Chu and Silverstein, 2012).

The same phosphorylation site (Thr92) has also been shown to be important for the cytoadherence of *P. falciparum*-infected erythrocytes to microvascular endothelium. Studies have shown endogenously expressed CD36 on the surface of human dermal microvascular endothelial cells (HDMECs) allows the adhesion of infected erythrocytes, regulated by the Src family of kinases and alkaline phosphatase (AP). With the ectodomain of CD36 constitutively phosphorylated (recognised by a phospho-specific antibody), infected erythrocytes can bind CD36, however, maximal binding was achieved when the ectodomain is dephosphorylated by AP (Ho *et al*., 2005).

1.5.2. Glycosylation

The theoretical molecular mass of CD36, based on the primary sequence, is 53kDa, yet it has been reported that depending on the cell type in which it is expressed, the molecular weight of CD36 will vary, for example, in human platelets (88kDa), mammary epithelial (85kDa) and erythroblasts (78kDa) (Greenwalt et al., 1990, Kieffer et al., 1989, Tandon et al., 1989a). As the primary amino acid sequences for

CD36 are identical in all these cell types, the differences have been attributed to cell-specific post-translational modifications, in particular N-linked glycosylation (Nakata *et al*., 1993).

There are ten putative N-linked glycosylation sites within human CD36 (recognised by the consensus sequence Asn-X-Ser/Thr, also referred to as a sequon, where X is any amino acid except proline). By using mass spectrometry on purified CD36 that had been deglycosylated by peptide N-glycosidase F, and by measuring the electrophoretic mobility of different N-linked glycosylation site mutants, 9 of the 10 putative sites were identified as occupied by a glycan (Hoosdally *et al*., 2009). In the same study it was shown by flow cytometry that mammalian cells, transiently-transfected with these glycosylation site mutants that glycosylation was important for CD36 trafficking to the plasma membrane, but no individual site was essential for this process (Hoosdally *et al*., 2009). The nature and the pattern of N-linked glycosylation was also not important for binding of modified LDL (Hoosdally *et al*., 2009), however it has been suggested by Lauzier *et al*., that the glycosylation status of Cd36 in the Spontaneously Hypertensive Rat (SHR), which is altered (along with the primary amino acid sequence and abundance in cardiac membranes) affects the ability of Cd36 to utilise LCFA in cardiac tissues (Lauzier *et al*., 2011).

In CD36 purified from platelets, alkali-labile O-linked glycosylation has also been identified (Tandon et al., 1989b), with some groups suggesting that O-linked glycosylation has a role in Cd36 membrane recruitment in the cardiac tissue of both normal and SHR rats (Lauzier *et al*., 2011, Laczy *et al*., 2011). Polysialylated O-linked glycans, absent on CD36 in platelets, have been found on CD36 secreted in human milk and are thought to be important for protection and nutrition for neonates (Yabe *et al*., 2003). Sialic acid is known to be a binding target for many viral and

bacterial pathogens and so it is thought that the presence of polysialylated structures on Cd36 could bind and prevent invasion into neonates (Karlsson, 1998, Yabe *et al*., 2003). Several studies have shown the exogenous administration of sialic acids orally or by intraperitoneal injection increased production of gangliosides and improved the development of the neural system in the brains of nourished and malnourished young rats (Carlson and House, 1986, Morgan and Winick, 1980). Human milk is rich in sialic acid (Carlson, 1985). The level of CD36 polysialation varies during lactation with the highest levels occurring 1 month after parturition (Yabe *et al*., 2003). Polysialic acid on CD36 may therefore provide an extra source of sialic acid in early human development.

1.5.3.   Disulphide Bonds

Disulphide bonds (or bridges) are covalent bonds between the two thiol groups of separate cysteine residue side-chains (to form covalently linked cystine residues). These bonds that are formed in the endoplasmic reticulum (ER) of eukaryotic cells are highly conserved features that are important for protein folding, stabilisation and overall protein structure (Sevier and Kaiser, 2002, Thornton, 1981, Creighton, 1988).

Human CD36 has ten cysteines in total, however, four of these (C3, C7, C463 and C466) are intracellular and are palmitoylated (Tao et al., 1996). The remaining six cysteines (C243, C272, C311, C313, C323, C333) can all be found within the carboxy-terminal half of the ectodomain of CD36. These cysteines are highly conserved within the CD36 family with only C311 not being conserved between SR-BI, CLA-1, LIMP-2 and emp. C313 is also not conserved in emp.

It was originally reported that the electrophoretic mobility of native CD36 under reducing and non-reducing conditions was the same leading to the assumption that Cd36 does not contain either intrachain or interchain disulphide bridges (Oquendo *et al*., 1989). This was later disproved by Gruarin *et al*., who showed that disulphide bridges do form in human CD36 and the reason for not being able to visualise a change in electrophoretic mobility is due to the extensive glycosylation. Prior deglycosylation of CD36 using PNGase F allowed the change in electrophoretic mobility to be observed under reducing conditions. It was further shown that in the presence of the reducing agent DTT, newly formed CD36 is retained within the ER, providing evidence that disulphide bridge formation is required for CD36 to traffic through the secretory pathway to the membrane (Gruarin *et al*., 1997).

In 1998, the pattern of disulphide bridge formation was elucidated for bovine Cd36 purified from milk fat globule membranes (MFGMs). From the lack of incorporation of ^{14}C labelled iodoacetic acid, no free cysteines were identified. Fragments of Cd36 generated from CnBr degradation were separated and analysed by amino acid sequencing and mass spectrometry, with the assumption that any disulphide bridges present had remained intact. The subsequent bonding pattern was identified: C243-C311, C272-C333 and C313-C323 (Rasmussen *et al*., 1998). As all these cysteines are conserved between bovine and human CD36, it is highly likely that the bonding pattern is also conserved.

1.5.4. Palmitoylation

Palmitoylation, or protein S-acylation, is a common post-translation modification involving the covalent attachment of the sixteen carbon, saturated fatty acid palmitate through a thioester linkage to a cysteine residue (Smotrys and Linder, 2004, Khoury *et al*., 2011). The main role of palmitoylation is thought to be to facilitate the reversible tethering of proteins to the cytosolic face of the cell membrane (Conibear and Davis, 2010, Rocks *et al*., 2005). Palmitoylation has also been shown to be involved with protein trafficking, membrane localisation, signalling and protein-protein interactions (Aicart-Ramos *et al*., 2011, Linder and Deschenes, 2007).

Using site directed mutagenesis and radiolabelled palmitate, it was shown that the two most amino-terminal and carboxy-terminal cysteines of CD36 (C3, C7, C463 and C466) were palmitoylated (Tao et al., 1996). Despite palmitoylation being thought to be important for membrane localisation, site directed mutagenesis of the carboxy-terminal cysteines of CD36 indicated that modification of these residues was unnecessary for plasma membrane localisation (Malaud *et al*., 2002). Palmitoylation of CD36 has been shown to be inhibited by the antifungal antibiotic cerulenin (Jochen *et al*., 1995). Studies involving either the inhibition of palmitoylation with cerulenin or site directed mutagenesis of cysteines resulted in delayed processing of CD36 in the endoplasmic reticulum (ER) and passage through the secretory pathway (Thorne *et al*., 2010). Additionally, it was shown that the lack of palmitoylation reduced the half-life of CD36 and that palmitoylation deficient CD36 mutants failed to localise efficiently within lipid rafts (Thorne *et al*., 2010).

Localisation within lipid rafts is thought to be a prerequisite for efficient uptake of modified LDL by CD36 (Rios *et al*., 2013, Zeng *et al*., 2003). It has been suggested that selenoprotein K (Selk), a selenium incorporated ER-resident protein (Lu *et al*., 2006) may play a role in the palmitoylation of CD36. Selk$^{-/-}$ macrophages showed decreased CD36 palmitoylation, lower CD36 stability and poor lipid raft localisation (Meiler *et al*., 2013).

1.5.5. Ubiquitination

Ubiquitination is a post-translational modification that involves the addition of one or more ubiquitin proteins to a target protein (Komander, 2009). The addition of ubiquitin can have a number of effects on the target protein including tagging it for degradation via the proteasome, altering cellular localisation, modifying activity or regulating protein-protein interactions (Herrmann *et al*., 2007). These different effects are mediated by different types of ubiquitination. Mono-ubiquitination which is the addition of one ubiquitin protein to one target protein residue is thought to be involved with membrane trafficking and endocytosis. Polyubiquitination involves the extension of monoubiquitinated residues. The ubiquitin molecules bind to one another via lysine rich regions. Depending on which of these residues are used to form the polyubiquitin chain affects the ultimate fate of the target protein. Lysine 48-linked polyubiquitin chains target proteins for degradation by the proteasome whereas lysine 63-linked polyubiquitin chains, are associated with changes to protein cellular localisation and function (Komander, 2009).

CD36 was shown to be polyubiquitinated, with both lysine 48 and lysine 63 linkages when expressed in CHO and HEK 293 cells (Smith *et al*., 2008). It was further shown using CHO cells expressing both the insulin receptor and CD36, that addition of insulin resulted in a reduction of CD36 ubiquitination whereas addition of fatty acids resulted in increased ubiquitination, suggesting a mechanism for regulating the level of CD36 at the plasma membrane (Smith *et al*., 2008). Mutation of the lysine residues in the intracellular C-terminal tail of CD36 resulted in reduced ubiquitination, increased CD36 levels and enhanced fatty acid uptake, which could be blocked with the CD36 inhibitor SSO (Smith *et al*., 2008).

In 2011, Kim *et al*., demonstrated that the ubiquitin ligase Parkin was capable of ubiquitinating CD36. When mice are fed a high fat diet, the levels of Parkin in hepatocytes rose in parallel to increased expression of lipid binding proteins such as Cd36. It was also reported that knockout mice deficient in Parkin resisted weight gain and did not acquire insulin resistance when fed a high fat diet. It was subsequently shown that addition of fatty acids to HeLa cells engineered to constitutively express CD36 resulted in the reduction of CD36 expression whereas in the presence of Parkin, there was an increase in CD36 expression levels, suggesting a ubiquitination-dependent mechanism to stabilise CD36 levels and in turn modulate fatty acid uptake (Kim *et al*., 2011). These two studies present contradictory roles for ubiquitination in the regulation of CD36. Nevertheless these two studies would suggest that ubiquitination of CD36 can have multiple effects depending on the cell type and possibly the ubiquitin ligase involved.

1.6. CD36 in normal and disease pathology

1.6.1. Innate Immunity

In 1991, CD36 was first recognised as a scavenger receptor by *Savill et al.,* during an investigation of the uptake of apoptotic cells by mononuclear phagocytes (Savill et al., 1991). BLAST searches have shown that CD36 homologues are found in primitive to immunologically advanced organisms. By comparing the functions of these proteins it was suggested that uptake of apoptotic cells during normal homeostasis is one of the most ancient roles of CD36 (Febbraio and Silverstein, 2007). The membrane of an apoptotic cell is different from that of other cells in that the outer leaflet becomes enriched in anionic phospholipids, such as phosphatidylserine (Pittoni and Valesini, 2002). Oxidation of phosphatidylserine, and to a lesser extent phosphatidylcholine, on the surface of apoptotic cells is recognised by CD36. It is thought that this interaction is required for the clearance of apoptosing cells by macrophages (Greenberg *et al*., 2006). In the eye, the removal of shed photo-receptor rod outer segments (PROS) has been shown to be another example apoptotic cell clearance mediated by CD36. Expression of CD36 on the surface of retinal pigment epithelial cells (RPEs) mediates the uptake of PROS which are shed regularly and need to be cleared to maintain normal vision. Antibodies to CD36 can inhibit the uptake of PROS by RPEs by 20% leading to the suggestion that there may be a co-receptor, with inhibition of both CD36 and the integrin $\alpha_v\beta_5$ reducing uptake of PROS by 80% (Ryeom *et al*., 1996). Further studies, however, have suggested that these receptors likely work independently (Finnemann and Silverstein, 2001).

In addition to apoptotic cell recognition, CD36 has been shown to recognise bacterial and fungal pathogens (Means *et al*., 2009, Hawkes *et al*., 2010a, Hoebe *et al*., 2005). It was suggested by Hoebe *et al*., that CD36 functions as a non-redundant sensor for the constituents of the cell wall of gram-positive bacteria, such as LTA, signalling through a toll-like receptor complex (TLR2/TLR6), to initiate an immune response (Hoebe *et al*., 2005). It was further proposed by Jimenez-Dalmaroni *et al*., that CD36 together with CD14 bind pathogenic signals initially before presenting them to TLR complexes within the plasma membrane to initiate an immune response (Jimenez-Dalmaroni *et al*., 2009). The immune response is therefore instigated by TLRs, but the initial recognition of the pathological ligand by macrophages is proposed to be via CD36 and CD14, independent of TLRs (Shamsul *et al*., 2010).

1.6.2. CD36 and Atherosclerosis

Atherosclerosis is described as a progressive chronic inflammatory disease involving the eventual hardening and thickening of the arterial wall. This results in a reduction in the diameter of the arterial lumen eventually leading to ischemia with possible plaque rupture. One of the first stages of atherosclerotic plaque formation is in the dysfunction of the endothelium, which recruits, through release of cytokines, circulating monocytes into the arterial intima. It is thought that this endothelial dysfunction may be initially induced by the presence of oxLDL (Collot-Teixeira *et al*., 2007). Once within the arterial intima, CD36 on the surface of macrophages is able to bind and endocytose oxLDL, ultimately leading to the formation of lipid-laden macrophages, called foam-cells. It is the accumulation of these foam cells

within the arterial intima that is a major contributor to plaque formation (Singh et al., 2002).

Despite oxLDL being identified as a ligand of CD36 (Endemann et al., 1993), its function in atherogenesis was not known until the development of suitable mouse models. It is now widely accepted, based on both *in vitro* and *in vivo* evidence, that the binding and endocytosis of oxLDL plays a key role in the formation of atherosclerotic lesions. Perhaps most important was the generation of the *ApoE/Cd36* double knockout mouse. The *ApoE* single knockout results in high circulating cholesterol levels and the more rapid development of atherosclerotic lesions when compared to wild-type mice (van Ree *et al*., 1994). *ApoE/Cd36* double knockout mice, fed a high-fat western diet, showed a significant 76.5% reduction in the number aortic tree lesions detected at 12 weeks old when compared to *ApoE* single knockout mice of the same age. Additionally, macrophages isolated from *ApoE/Cd36* double knockout mice displayed a 60% reduction in the amount of internalised oxLDL (Febbraio *et al*., 2000). Reintroduction of *CD36* into *ApoE/Cd36* deficient mice, by stem cell transfusion resulted in an increase in the size of atherosclerotic lesions (Febbraio *et al*., 2004). A similar result was observed with older mice at the age of 35-weeks fed a high-fat western diet (Guy *et al*., 2007). In addition, it was shown that the CD36 ligand EP80317, a hexarelin derivative, reduced the lesion area (up to 51%) in *ApoE* single knockout mice, supposedly by competing for the oxLDL binding site on Cd36 (Marleau *et al*., 2005).

However, further studies carried out by Moore *et al*., appear to contradict the conclusions drawn by Febbraio *et al*., that loss of *Cd36* in an *ApoE* null background could reduce the size of atherosclerotic lesions. In the follow up studies *ApoE*/*Cd36* double knockout mice were fed a high-fat western diet for 8 weeks and the size of

atherosclerotic lesions formed over the aorta sinus and tree were measured. The results differed depending on the sex of the animal, with male mice having no significant reduction in aortic lesion size and female mice showing reduced lesion area through the aortic tree but increased lesion area in the aortic sinus. From these observations it was concluded that uptake and endocytosis of oxLDL was independent of scavenger receptors such as Cd36 (Moore *et al*., 2005). The apparent contradiction of these results have since been re-examined with questions raised in regards to the latter study; for example, the size of the lesions in the aortic sinus may have a non-linear relationship with the area of aortic tree lesions (Curtiss, 2006), and since the aortic sinus undergoes remodelling, only the lesion size in the constant aortic tree should be measured. The reappraisal of the two studies has found the results to be similar overall, consistent with CD36 having a role in atherogenesis. Slight variations in the congenic strains of mice used in the study could have also resulted in altered function of macrophages and endothelial cells, as well as exposure to pathogens such as *Chlamydia pneumonia* that may have increased the size of lesions in the absence of Cd36 (Witztum, 2005, Burnett *et al*., 2001).

CD36 deficiency in macrophages (type I deficiency) has been identified in around 3% of the Japanese population (Nozaki *et al*., 1995). Clinical observations in this population has identified a 40-50% reduction in the binding and uptake of oxLDL into macrophages, although no anti-atherosclerotic advantage is reported (Hirano *et al*., 2003). In contrast, several patients with type I *CD36* deficiency have been shown to suffer from hypertension, hyperlipidemia and elevated fasting glucose levels, and one study has shown type I *CD36* deficiency to be linked to a higher incidence of coronary heart disease (Yamashita *et al*., 2007).

It has recently been suggested that CD36-mediated uptake of oxLDL by macrophages to form foam cell is increased in the presence of AIM (Apoptosis inhibitor of macrophages) (Amezaga *et al*., 2014). AIM, also called CD5 antigen-like (CD5L), is a soluble scavenger receptor known to bind oxLDL and to inhibit apoptosis of macrophages and other cell types (Sarrias *et al*., 2004, Arai *et al*., 2005, Haruta *et al*., 2001).

1.6.3.   CD36 and Angiogenesis

The activity of both CD36 and TSP-1 as a receptor/ligand complex was first demonstrated as anti-angiogenic and pro-apoptotic in tumour cells, and was shown to be effective in countering most angiogenic inducers such as basic fibroblast growth factor (bFGF) and vascular endothelial growth factor (VEGF) (Good *et al*., 1990). CD36, with TSP-1, is now known to function as a negative regulator of angiogenesis in microvascular endothelial cells that is important in any roles that require neovascularisation, such as tumour growth, inflammation and wound healing (Kaur *et al*., 2009, Dawson *et al*., 1997). CD36 inhibits pro-angiogenic signals (such as bFGF and VEGF) which stimulate cell proliferation, migration and tube formation, while triggering pro-apoptotic signals. The proposed pathway for these effects requires the association of the nonreceptor protein kinase Fyn, to CD36. The kinase becomes activated and leads to the activation of the mitogen-activated protein kinase (MAPK) p38 and c-Jun N-terminal kinase (JNK), which ultimately leads to DNA cleavage by caspases and apoptosis of the cell (Jimenez *et al*., 2000). Additional

effectors of apoptosis, such as Fas ligand and tumour necrosis factor-α (TNF-α) are also upregulated as a result of this pathway (Volpert *et al*., 2002, Rege *et al*., 2009).

1.6.4. Role of CD36 in the pathogenesis of Malaria and Sickle Cell Anaemia

A key factor that influences the outcome of malarial infection is related to the ability of parasitized erythrocytes to adhere to the host microvasculature. Infection with *P. falciparum* can lead to erythrocytes adhering to the microvasculature of the brain, leading to cerebral malaria, causing encephalopathy (Miller *et al*., 2013). Ockenhouse *et al*, suggested that CD36 on the surface of vascular endothelium was involved in the sequestration and adherence of infected erythrocytes in the brain via the ligand Pfemp-1, or possible changes to the erythrocyte membrane as a result of infection (Ockenhouse *et al*., 1991). The CD36-mediated sequestration and adherence of infected erythrocytes was suggested to enable the parasite to propagate and avoid spleen-mediated immunity. A study by Aitman *et al*., tested this theory by looking at common CD36 frame shift and deletion mutations within the African population (nucleotides *T1264G*, *G1439C* and *1888delA*) which all result in the production of a truncated CD36 without the carboxy-terminal half. The frequency of these mutations was significantly higher in those patients with cerebral malaria compared to the control group, in disagreement with the hypothesis (Aitman *et al*., 2000). In contrast, another study found that the CD36 nonsense mutation *T188G* protected patients against severe malaria (Pain *et al*., 2001). Despite other studies reporting similar conflicting findings, these early population studies were generally

limited by small sample sizes and by the control groups used as comparators (Ayodo *et al*., 2007, Sinha *et al*., 2008, Omi *et al*., 2003). In 2009, a genetic analysis of 3420 individuals from 66 ethnic groups showed that the *T1264G* polymorphism was abundant in sub-Saharan Africa groups but absent from nearly all non-African groups. However, the study, with a greater sample size than all previous studies combined, showed that CD36 was not linked to severe malaria (Fry *et al*., 2009). The authors, and others, have speculated that the common CD36 mutations in African populations may have arisen in response to evolutionary pressure of other severe infections or conditions that overlap with the geographical areas in which malaria is endemic (Fry *et al*., 2009, Hawkes *et al*., 2010b).

Patients who suffer from sickle cell anaemia are, for example, more resistant to malaria. Sickle cell anaemia which is prevalent in sub-Saharan Africa (Grosse *et al*., 2011), is caused by a mutation in the haemoglobin gene (Serjeant, 2013). As a result, erythrocytes are 'sickle'-shaped, transiting more slowly through the vascular system, promoting ligand/receptor recognition and formation of complexes which contribute to a vascular pathology (Hebbel *et al*., 1980). CD36 on the surface of microvascular endothelial cells is considered a receptor for sickle cells although the identity of relevant ligand is less clear. Possible ligands include TSP-1 (Trinh-Trang-Tan *et al*., 2010, Sugihara *et al*., 1992) and anionic phospholipids made accessible on the surface of the distorted sickle cell membrane (Setty *et al*., 2002). There is a selective pressure, therefore, to develop and maintain CD36 deficiency to alleviate the pathology of sickle-cell anaemia. This would suggest that, in sub-Saharan Africa, malaria, sickle-cell anaemia and CD36 deficiency, may have co-evolved.

1.6.5. CD36 and Fatty Acid Transport

Cd36 was identified as a fatty-acid translocase by Abumrad and Harmon, through fatty acid uptake inhibition studies in rat adipocytes using sulfo-N-succinimidyl derivatives of LCFAs (Harmon and Abumrad, 1993). LCFA had previously been thought to simply diffuse across the plasma membrane down a concentration gradient. However, the distribution of Cd36 in highly metabolically active tissues such as adipose tissue (Abumrad *et al*., 1993), heart muscle (Luiken *et al*., 1999) and skeletal muscle (Bonen *et al*., 1999), suggested a possible transport function. In 2000, this hypothesis was reinforced when it was shown that in *Cd36* knock-out mice, LCFA transport is dramatically reduced in the heart, skeletal muscle and adipose tissue (Coburn *et al*., 2000). A perfused heart system from the same mouse strain was found to rely heavily on glucose as an energy source instead of fatty acids (Kuang *et al*., 2004). Transgenic mice which overexpressed Cd36 in skeletal muscle were shown to have enhanced fatty acid oxidation, with a decrease in circulating fatty acids and triglycerides, and decreased fat deposition, consistent with a role of Cd36 in catabolism of LCFA (Ibrahimi *et al*., 1999).

The precise mechanism for the uptake of LCFA by CD36 remains unknown, however, it is thought that CD36 does not act as a typical transporter. It has been proposed that CD36 (in conjunction with the plasma membrane fatty acid binding protein; $FABP_{pm}$) facilitates the disassociation of LCFA from albumin (Stremmel *et al*., 2001, Glatz *et al*., 2003) and promotes diffusion across the lipid bilayer by mediating the integration of protonated LCFA into the outer leaflet of the membrane. The LCFA may then flip spontaneously to the inner leaflet of the membrane, down

its concentration gradient where it can become activated by the addition of coenzyme A (Stremmel *et al*., 2001). Despite being shown to facilitate LCFA uptake with CD36, the precise role that FABP$_{pm}$ plays is unclear. It has been proposed that FABP$_{pm}$ may function to bind LCFA creating a local fatty acid concentration gradient at the plasma membrane and/or may help to localise CD36 to particular sites within the plasma membrane where the uptake of LCFA is most required (Glatz and Luiken, 2014).

The uptake of LCFA is likely to be a rate limiting step in energy generation from fatty acid oxidation, therefore the cell surface expression of CD36 is metabolically important. Regulation of CD36 can be affected by muscle contraction or insulin release (Glatz *et al*., 2010). Recent studies have also suggested that plasma membrane localisation of CD36 for LCFA uptake is regulated by post-translational modifications such as ubiquitination (Smith *et al*., 2008, Kim *et al*., 2011). Glycosylation has also been suggested to regulate plasma membrane localisation of CD36 for LCFA uptake (Lauzier *et al*., 2011), however these studies were based on the SHR Cd36 which has an altered primary amino acid sequence (Aitman et al., 1999).

1.6.6. CD36, Insulin Resistance and Metabolic Syndrome

Insulin resistance is a feature of a number of complex human disorders such as type 2 diabetes, obesity, combined hyperlipidaemia and primary hypertension (Aitman *et*

al., 1997a, Aitman *et al*., 1997b, Groop *et al*., 1989, Reaven, 1988, Reaven *et al*., 1996). The SHR is used as a model organism in the study of these disorders because it displays similar symptoms of insulin resistance, hypertriglyceridemia, abdominal obesity and hypertension (Iritani *et al*., 1977, Reaven *et al*., 1989). By using a combination of cDNA microarrays, quantitative trait loci mapping and radiation hybrid mapping, it was shown by Aitman *et al*, that some SHR strains have a defective Cd36 gene (Aitman *et al*., 1999). Replacement of the mutant allele with a wild-type copy allowed the reversal of glucose tolerance and increased insulin responsiveness, although hypertension remained unaffected. These observations led to the conclusion that Cd36 deficiency was the cause of the insulin resistance in SHR (Pravenec *et al*., 2001). This was not surprising considering at the time CD36 had just been identified as a possible transport protein for LCFA, with insulin resistance syndromes being attributed to defects in fatty acid metabolism (Aitman *et al*., 1997a). Further studies however, working with different SHR lines showed the Cd36 mutations were absent from these strains, suggesting that mutations in Cd36 did not necessarily contribute to the symptoms observed (Gotoda *et al*., 1999). Furthermore, in Cd36 knock-out mice insulin resistance is not observed (Febbraio *et al*., 1999). Cd36 knock-out mice were, however, shown to have higher whole body glucose uptake and lower glucose storage in basal conditions compared to wild type mice. Under hyperinsulinemic conditions the whole body glucose uptake was higher than observed in the wild type (Goudriaan *et al*., 2003). These data are consistent with studies performed by Kuang *et al*., showing that in the absence of efficient LCFA uptake and subsequent oxidation, glucose is used as the main source of energy, especially in the heart (Kuang *et al*., 2004). However, under these conditions it was also noted that hepatic glucose production was not inhibited suggesting some hepatic

insulin resistance (Goudriaan *et al*., 2003). The differences observed between the mouse and rat models could be attributed to differences in genetic background or nutritional intake. A simple relationship between Cd36 status and insulin resistance seems unlikely, and Kennedy *et al,* using Cd36 knock-out mice, have demonstrated the presence of an oxLDL-Cd36 dependent paracrine loop between macrophages and adipocytes that links inflammation, oxidative stress, hyperlipidaemia and insulin resistance (Kennedy *et al*., 2011).

Studies of the causes of insulin resistance in humans remain inconclusive. There have are conflicting reports of whether the type I CD36 deficiency in the Japanese population results in insulin resistance (Furuhashi *et al*., 2003, Furuhashi *et al*., 2004, Kajihara *et al*., 2001, Kuwasako *et al*., 2003, Miyaoka *et al*., 2001, Yanai *et al*., 2000). CD36 polymorphisms have also been reported to be associated with insulin resistance (Corpeleijn *et al*., 2006, Lepretre *et al*., 2004).

It is currently thought that insulin resistance and cardiac disease involves interplay between CD36 and the glucose transporter GLUT4. Cd36 facilitated LCFA uptake and GLUT4 mediated glucose uptake in the cardiac and skeletal muscle of rats showed that both are subject to short-term cellular redistribution on muscle contraction (Bonen *et al*., 2000, Steinbusch *et al*., 2011). Furthermore it has been shown that in rats with insulin resistance and type 2 diabetes that Cd36 becomes permanently localised to the sarcolemma in cardiomyocytes whereas GLUT4 is internalised (Ouwens *et al*., 2007, Steinbusch *et al*., 2011).

There is increasing evidence to suggest that the use of pharmacological agents to bind and inhibit the CD36-mediated uptake of LCFA could provide a means to restrict the progression of a number of conditions such as insulin resistance and

cardiac failure (and also atherosclerosis). As a result of myocardial infarction and ischaemia insult the heart shifts metabolic substrate preference from fatty acids to glucose, the substrate with highest oxygen efficiency (Glatz et al., 2006). Despite a lower contribution from fatty acids for energy production under acute hypoxic conditions, localisation of Cd36 at the sarcolemma has been shown not to be diminished. Studies working with rat myocytes and perfused hearts have shown that acute hypoxic conditions activates AMP-activated protein kinase (AMPK) actually induces translocation of Cd36 to the sarcolemma, increasing fatty acid uptake (Chabowski et al., 2006). Due to reduced beta-oxidation, incoming fatty acids are redirected into intracellular lipid droplets. The accumulation of these lipid droplets is associated with the development and progression of cardiac contractile dysfunction (Sharma et al., 2004, Glatz et al., 2010). This increase in fatty acid uptake despite a reduction of beta-oxidation has also been associated with insulin resistance of skeletal muscle and the heart in obesity and type 2 diabetes (Glatz et al., 2010).

Inhibition of Cd36-mediated uptake using the small molecules AP5055 and AP5258 have been shown in rodent models to alleviate atherosclerosis (46% reduction in plaque size) and diabetes (>50% reduction in plasma glucose levels) with a reduction of plasma triglyceride concentration (Geloen *et al*., 2012). Additionally, the Cd36 peptide EP 80317 has been shown to protect mice from post-ischemic myocardial damage (Bessi *et al*., 2012) and antibody inhibition of Cd36 in a cardiomyocyte cell model enhanced basal glucose uptake while reducing elevated palmitate uptake (Angin *et al*., 2012). These studies highlight the importance of CD36 as a therapeutic target and the requirement of a better understanding of ligand binding to help development pharmacologically effective agents.

1.6.7. CD36 and Fibrosis

Fibrosis is characterised by overgrowth, hardening and scaring of dysfunctional tissue with excess deposition of collagen as the end result of chronic inflammatory reactions (Wynn, 2008). This can be caused by a number of factors including a persistent infection, an autoimmune response, radiation, chemical insults and/or physical tissue damage (Wynn, 2008). CD36 has been implicated in a number of fibrotic states including pulmonary (Yehualaeshet *et al*., 1999) and renal fibrosis (Yang *et al*., 2007). Pulmonary fibrosis involving CD36 has been suggested to involve the interplay of CD36, TSP-1 and the transforming growth factor (TGF)-β1. Using a rat model of pulmonary fibrosis it has been shown that blocking the interaction of TSP-1 with macrophage Cd36 reduces the inflammation, most likely by preventing the activation of TGF-β1 (Yehualaeshet *et al*., 2000). Through the use of monoclonal antibodies against TSP-1 and Cd36 it was concluded that TSP-1 bound to inactive TGF-β1 which bound, as a complex, to Cd36 on the alveolar macrophage where the protease plasmin was recruited to cleave and activate TGF-β1 (Yehualaeshet *et al*., 1999). A role for Cd36 in pulmonary fibrosis was further supported by a study which used a lentiviral vector to silence expression of Cd36 in rat alveolar macrophages following silica-induced fibrosis. Silencing of Cd36 resulted in a decrease in the level of active TGF-β1 and subsequent fibrosis (Wang *et al*., 2009, Wang *et al*., 2013).

In renal fibrotic disease a similar process of TGF-β1 activation that induces an inflammation response is thought to be responsible, however it should be noted that in both organs TGF-β1 activation can occur via other membrane receptors such as

integrin αvβ6 (Munger *et al*., 1999, Nishimura, 2009, Sheppard, 2005). Yang *et al*., have also demonstrated that albumin-induced renal tubule fibrosis could be supressed using siRNA against Cd36, resulting in a decrease in active TGF-β1 and fibronectin, further supporting the potential of Cd36 as a target for anti-fibrotic therapies (Yang *et al*., 2007).

1.6.8.   CD36 and Alzheimer's Disease

Alzheimer's disease is the most common neurodegenerative disorder in adults and is characterised by the formation of senile plaques in the brain parenchyma, composed of insoluble fibrillar β-amyloid protein surrounded by activated microglia, astrocytes, and dystrotrophic neurites (Selkoe, 2000, Salawu *et al*., 2011). One school of thought believes the pathogenesis of Alzheimer's disease is caused by the inflammatory response triggered by the deposition of insoluble fibrillar β-amyloid (Akiyama, 1994). Microglia are thought to be the main cell type involved in mediating this inflammatory reaction (Pan *et al*., 2011, Krabbe *et al*., 2013). A potential role for CD36 was suggested by Coraci *et al*., who showed that transient expression of the scavenger receptor allowed cells to specifically bind to surfaces coated with fibrillar β-amyloid (Coraci *et al*., 2002). CD36 is upregulated in microglia and the vascular endothelial cells in patients with Alzheimer's disease. Futhermore, it has been shown that monoclonal antibodies against CD36 can inhibit the production of pro-inflammatory ROS from N9 microglia and human macrophages adhered to β-amyloid coated surfaces by around 50% (Coraci *et al*., 2002). This ROS production could be inhibited by anti-CD36 antibodies however it

did not affect adherence, leading to the suggestion that other receptors also play a role in adherence to fibrillar β-amyloid such as class A scavenger receptors and SR-BI (El Khoury *et al.*, 1996, Husemann *et al.*, 2001). In 2003 it was further reported that microglia and macrophages isolated from Cd36 knock-out mice showed a significant reduction in the response to fibrillar β-amyloid, with reduced release of pro-inflammatory cytokines, chemokines and ROS, highlighting the role of Cd36 in the initiation of the inflammatory response in Alzheimer's disease (El Khoury *et al.*, 2003). From a study of THP-1 macrophages and mouse microglia binding to immobilised fibrillar β-amyloid Bamberger *et al.*, propose that a cell surface receptor complex consisting of Cd36, Cd47 and integrin $\alpha_6\beta_1$ mediate microglial activation (Bamberger *et al.*, 2003). More recently it was demonstrated that the inflammatory pathways triggered by β-amyloid (or oxLDL) were initiated through formation of a complex including CD36, TLR4 and TLR6 (Stewart *et al.*, 2010).

1.7.   Objectives of the current study

How the relatively small ectodomain of CD36 can bind such a diverse range of ligands remains unexplained. We can speculate on the nature of the polyspecificity from homology models based upon the LIMP-2 structure, but the lack of resolution, and the evolutionary distance and separation of function of LIMP-2, will always limit the relevance of conclusions drawn. An actual CD36 structure derived from a crystal remains elusive. CD36 binds a wide range of ligands which links the receptor to an equally wide range of disease states, however, a detailed understanding of the binding kinetics, of ligands and also of inhibitors that are being identified, is lacking.

The main objectives of this doctoral study is to develop an expression and purification system to purify significant amounts (milligram quantities) of human CD36 suitable for crystallisation studies, and also ligand binding experiments in order to calculate the microkinetics of interaction.

In chapter 3, insect and mammalian cell systems are compared to drive the synthesis and secretion of the CD36 ED tagged with a polyhistidine tail. The ED is purified from insect cells using nickel affinity chromatography and the retention of the native protein fold demonstrated by binding of fluorescently-labelled acLDL. The process is then scaled up to offer the possibility of milligram quantities of highly enriched CD36 ED. In chapter 4, the glycosylation status of the purified protein is explored, and mass spectrometric analysis used to determine the diversity and complexity of the actual glycan structures present. Finally, in chapter 5, purified CD36 ED is immobilised on a sensor chip for surface plasmon resonance experiments and, as proof of principle, the microkinetics of monoclonal antibody binding to CD36 are determined.

2. Materials and Methods

2.1. Bacteria culture medium

Lysogeny Broth (LB):   1% tryptone, 0.5% yeast extract, 1% NaCl

LB Agar: 1% tryptone, 0.5% yeast extract, 1% NaCl

SOC Medium: 2% tryptone, 0.5% yeast extract, 0.05% NaCl, 0.02% KCl, 0.04% glucose, 0.01M $MgCl_2$, 0.01M $MgSO_4$

Solid or liquid growth media were supplemented with ampicillin to a final concentration of 100μg/ml, where appropriate.

2.2. Bacterial Culture and Storage

Bacteria were grown in liquid growth media with shaking (230rpm), or on plates in an incubator set to 37°C. Bacteria were frozen for long term storage at -80°C in a mixture of LB medium and 15% glycerol.

2.3. Molecular Biology

2.3.1. Plasmids

The baculovirus transfer vector, pBacPAK9-CD36 ED-12His, provided by Kenneth Linton, encodes human CD36 ED (amino acids 36-435) with a C-terminal 12 histidine tag and an N-terminal honeybee melittin secretory signal. The vector was constructed in three steps. First, the coding sequence for the ED was amplified by mutagenic primers: CD36-ED-*Sac*I 5'-TGGAGACCTGCT<u>GAGCTC</u>GAAGACAATTAAAAAGC-3' and CD36-ED-*Bst*EII 5'-GGCCAAGGAGGTTTA<u>GGTGACC</u>AGTTACTTGAC-3' which introduce sites for the restriction enzymes *Sac*I and *Bst*EII (underlined), respectively at the 5' and 3' end of the coding sequence for the ED. The PCR product was digested with *Sac*I and *Bst*EII and cloned into similarly digested BlueBac-CD36-12His, described previously (Hoosdally *et al*., 2009). Cloning into the *Bst*EII site fused the ED coding sequence in frame with the coding sequence for a 12 x histidine carboxy-terminal tag and a translation stop codon. Second, the coding sequence was excised from the BlueBac vector using SacI and *Sal*I (the latter being 3' to the stop codon) and cloned into similarly digested pMelBac B (Invitrogen). This fused the coding sequence for the honeybee melittin secretion signal (HMSS) in frame at the 5' end of the CD36-ED. Third, the entire coding sequence of the HMSS-CD36-ED-12His was excised from the MelBac vector using the *Eco*RV site in the polyhedrin promoter and the *Xba*I site (that is 3' to the translation stop codon but 5' to the *Sal*I site of BlueBac-CD36-12His) and subcloned into equivalent sites in pBacPAK9 to

generate pBacPAK9-CD36 ED-12His. The construct was sequenced to ensure veracity. The relevant sequence elements are shown in Appendix 1.

The mammalian expression plasmid pOPING-CD36ED-6His was generated by Dr Joanne Nettleship at the Oxford Protein Production Facility (OPPF). CD36 ED was subcloned from pBacPAK9-CD36ED-12His into the pOPING vector (Oxford Protein Production Facility, UK) resulting in a construct encoding CD36 ED with an N-terminal RPTPmu secretory signal and a C-terminal 6 histidine tag.

2.3.2. Preparation of plasmid DNA

Small-scale (µg-quantities) plasmid DNA preparations were generated using the GenElute HP Plasmid Miniprep Kit, following the manufacturer's protocol (Sigma-Aldrich). The protocol is based upon the rapid alkaline lysis procedure to isolate plasmid DNA, first described by Birnboim and Doby (Birnboim and Doly, 1979). Bacterial cells from a 3ml overnight culture were harvested by centrifugation for 10 minutes at 14,000rpm (EBA 12, Hettich, Germany). The cell pellet was resuspended in 200µl Resuspension solution (50mM Tris-HCl pH 8, 10mM EDTA, 100µg/ml RNase A). Once the cell pellet was completely resuspended, 200µl Lysis buffer (1% SDS, 0.2M NaOH) was added to the solution, mixed by inversion and incubated at room temperature for 5 minutes. Nucleic acids and proteins within the lysate were subsequently denatured due to the alkalinity of the Lysis buffer. Following incubation in Lysis Buffer, 350µl of Neutralisation Buffer (3M potassium acetate, pH 5.5) was added to the solution, causing the aggregation of insoluble genomic DNA and high molecular weight RNA as well as the precipitation of protein-SDS

complexes. To remove these aggregates, the lysate was centrifuged at 14,000rpm for 10 minutes. GenElute HP Miniprep Binding Columns were prepared by adding 800μl of Column Preparation Solution (50mM MOPS pH7.0, 0.75M NaCl, 15% ethanol, 0.15% Triton X-100) followed by centrifugation at 14,000rpm for 2 minutes. The supernatant from the cell lysate was then added to the prepared columns and incubated for 2 minutes at room temperature before centrifugation at 14,000rpm for 2 minutes. The columns were washed by adding 500μl of Wash Solution (50mM MOPS pH8.5, 1M NaCl, 15% ethanol) and centrifuging at 14,000rpm for 2 minutes. The flow through was discarded and the columns were centrifuged as before to remove traces of Wash Solution. Plasmid DNA was eluted by adding 50μl Tris-HCl (pH 8.5) to the columns and incubating at room temperature for 5 minutes followed by centrifugation for 2 minutes at 14,000rpm. Recovered plasmid DNA was quantified using a NanoDrop (ND-100, Thermo Scientific), measuring the optical density at a wavelength of 260nm. Estimation of purity of the plasmid DNA was achieved through measuring the A260:A280 ratio; a ratio of 1.8-2.0 was indicative of a pure sample.

Large-scale (mg-quantities) plasmid DNA preparations were generated using the Plasmid Mega Kit (Qiagen), following a similar protocol as before. Bacterial cells from a 500ml overnight culture were harvested by centrifugation for 20 minutes at 6,000xg, 4°C in a Sorvall RC-5C Plus centrifuge (Thermo Scientific). The resulting cell pellet was resuspended in 50ml Resuspension Buffer. Following complete resuspension, Lysis Buffer was added before mixing by inversion and incubation at room temperature for 5 minutes. Chilled Neutralisation Buffer (50ml) was added, and the solution was mixed by inversion and incubated at 4°C for 30 minutes. Centrifugation for 30 minutes at 20,000xg, 4°C in a Sorvall RC-5C Plus centrifuge

(Thermo Scientific) was then used to clear the lysate. The supernatant was decanted onto a Qiagen 2500 column, pre-equilibrated with 35ml Column Preparation Solution. The column was washed with 200ml of Wash Solution before elution of the DNA with 35ml of Buffer QF (50mM Tris-HCl pH 8.5, 1.25M NaCl, 15% ethanol). Eluted DNA was precipitated by adding 100% isopropanol (24.5ml), and pelleted by centrifugation for 30 minutes at 15,000xg, 4°C, in a Sorvall RC-5C Plus centrifuge (Thermo Scientific). The resulting pellet was carefully rinsed with 70% ethanol (7ml), centrifuged as before, air-dried and then resuspended in 200µl Tris-HCl (pH 8.5). Recovered plasmid DNA was quantified as before.

2.4.   Insect Cell Culture

2.4.1.   Insect Cell Culture Medium and Reagents

Sf900 II SFM and TC100 insect cell media was purchased from Life Technologies. Ex-cell 405 media insect cell media was purchased from Sigma-Aldrich. Antibiotic-antimycotic solution (GE Healthcare) was added to all insect cell culture media to a final concentration of 100units/ml penicillin G, 100µg/ml streptomycin sulphate, and 25µg/ml amphotericin B, unless otherwise stated. In addition, TC100 media was routinely supplemented with 10% foetal bovine serum (FBS; Sigma-Aldrich). All manipulations were performed in a sterile environment, with disposable plasticware and glassware reserved specifically for that purpose. All suspension cultures of insect cells were grown at 27°C with shaking at 110rpm or within a Wave Bioreactor

Cellbag with variable rocking per minute and rocking angle depending on culture size (see 2.4.6).

2.4.2. Insect Cell Co-transfection and Baculovirus Generation

Sf21 cells were co-transfected with transfer vector and *flashBAC* (Oxford Expression Technologies, OET), *flashBAC Gold* (OET) or *Profold-ER1* (AB Vector) genomic DNA as instructed by the manufacturer. 1.5×10^6 cells were seeded onto a 35mm tissue culture dish (BD Biosciences, San Jose, CA) in TC100 medium without FBS or antibiotics.

For each co-transfection, the following reagents were mixed:

100ng	Baculoviral genomic DNA
500ng	Transfer Plasmid – pBacPAK9-CD36 ED-12His)
5μl	Lipofectamine transfection reagent (Life Technologies)
1ml	TC100 media without FBS or antibiotics

The solution was gently mixed and incubated at room temperature for 15 minutes. Medium was then aspirated from the monolayer of insect cells and replaced quickly, but carefully, with the transfection mixture. Each dish was then incubated overnight at 27°C in a humidified sealed box containing (lined with paper soaked in 50mM

EDTA). After 24hrs, 1ml TC100 containing 10% FBS and antibiotics was added to each dish and incubated for a further 120 hours, as before. Following incubation, the medium was recovered as 'Co-T' baculovirus.

2.4.3.   Plaque assay to determine baculovirus titre

Plaque assays were used to assess the titre of recombinant baculoviruses. For each baculovirus, six 35mm tissue culture dishes (BD Biosciences) were seeded with 1.5×10^6 Sf21 insect cells in TC100 medium, and left to settle on a flat surface. A series of dilutions of the baculovirus stock were made (10^{-4}, 10^{-5}, 10^{-6}) in TC100 media. The culture medium was aspirated from the dishes, replaced by 200µl of each baculovirus dilution. Each infection was performed in duplicate. The cells were incubated at room temperature for 2 hours. The medium covering the insect cells was aspirated and replaced with a 1.5ml layer of 1% low melting point agarose (LMP-Ag; Sigma-Aldrich) prepared from a 4% stock in dH_2O diluted to 1% using prewarmed TC100 media plus FBS and antibiotic-antimycotic. The dishes were placed on a flat surface and incubated at room temperature to allow the agarose to solidify after which 1ml of TC100 media was added onto the agarose 'plug' and the dishes placed inside a humidified box and incubated at 27°C for 72 hours. To visualise plaques, 1ml solution of 0.03% neutral red (Sigma-Aldrich) in PBS was added to each dish and incubated for 3-4 hours. The liquid medium was then aspirated, the dishes inverted and left at room temperature, overnight in the dark. Neutral red stains live cells, allowing the visualisation of virus plaques of lysed or dying cells as clear regions within the red background monolayer.

The titre (in plaque forming units/ml; pfu/ml) was calculated as the number of plaques multiplied by the dilution factor.

2.4.4. Amplification of Baculovirus

To obtain working stocks, baculovirus was amplified over a number of stages. At each stage the premise remains the same; with a low ratio of virus particles to insect cells (multiplicity of infection; MOI) used to permit cell growth to continue whilst allowing multiple cycles of viral infection, replication and budding to occur.

Co-T-to-intermediate stock amplification

A suspension culture containing 25ml Sf21 insect cells at a density of $1x10^6$ cells/ml in Sf900 II SFM media was infected with 250µl Co-T baculovirus. The cells were incubated overnight, before being diluted with 25ml of fresh Sf900 II SFM media. After a total of 5 days, the cells were removed by centrifugation at 1000xg for 10 minutes (Hettich rotanta 46R). The supernatant was recovered, filtered through a 0.2µm syringe filter (Minisart, filters, Sartorius) and stored at 4°C as 'intermediate stock'. The baculovirus titre was calculated by plaque assay.

Intermediate stock-to-working stock amplification

A suspension culture containing 100ml Sf21 insect cells at a density of $2x10^6$ cells/ml ($2x10^8$ cells/ml in total) in Sf900 II SFM media was infected with $1x10^7$ pfu/ml intermediate stock baculovirus (MOI=0.05). The cells were incubated overnight, before being diluted with 100ml fresh SF900 II SFM media. After a total of 5 days, the cells were removed by centrifugation at 1000xg for 10 minutes

(Hettich rotanta 46R). The supernatant was recovered, filtered through a 0.2µm syringe filter (Sartorius) and stored at 4°C as 'working stock'. The baculovirus titre was calculated by plaque assay.

2.4.5. Small-scale infection for protein production

Small-scale infections were performed in either 35mm tissue culture dishes or in 100ml suspension cultures.

Small-scale infection in tissue culture dishes

Tissue culture dishes were seeded with either $1x10^6$ Hi5 insect cells (in Ex-cell 405 media) or Sf21 insect cells (in Sf900 II SFM media) which were left to settle on a flat surface. For synchronous infection, a high MOI of 3 (3 virus particles per insect cell) was used. The culture medium was aspirated from the dishes and replaced with 1ml of baculovirus dilution containing $3x10^6$ pfu. The cells were incubated for 3 hours at 27°C. Following this, medium containing the baculovirus was aspirated and replaced with 2ml of fresh media. Cells were incubated at 27°C for a total of 72 hours before harvesting spent media by centrifugation at 1000xg for 10 minutes to remove cells and cell debris. Spent media was filtered through a 0.2µm syringe filter (Sartorius) and stored at 4°C.

Small-scale infection of suspension cultures

A suspension culture containing 50ml of either Hi5 insect cells (in Ex-cell 405 media) or Sf21 insect cells (in Sf900 II SFM media) at a density of $2x10^6$cell/ml (totalling $1x10^8$ cells) was infected with $3x10^8$ pfu of working stock baculovirus for a

Hi5 insect cell culture (MOI=3) or with 5×10^6 pfu of working stock baculovirus for a Sf21 insect cell culture (MOI=0.05) (see 3.3.2). Cells were incubated at 27°C for a total of 72 hours before harvesting spent media by centrifugation at 1000xg for 10 minutes to remove cells and cell debris. Spent media was filtered through a 0.2µm syringe filter (Sartorius) and stored at 4°C.

2.4.6.   Large-scale infection for protein production

A 2.5 litre suspension culture containing Sf21 insect cells in Sf900 II SFM media at a density of 2×10^6 cells/ml (5×10^9 cells in total) was grown in a 10L Cellbag bioreactor chamber (GE Healthcare) on a Wave Bioreactor (20/50EHT, GE Healthcare), rocking at 15 rocks per minute with a rocking angle of 8°. The cells were infected with 2.5×10^8 pfu of working stock baculovirus (MOI=0.05) (see 3.3.2) and incubated overnight at 27°C, at 18 rocks per minute with rocking gradient of 8°, before being diluted to 5L with fresh Sf900 II SFM media. At 100% capacity (5L for a 10L Cellbag) the rocking was adjusted to 25 rocks per minute with a rocking angle of 10°. The culture was harvested 72 hours post-infection by centrifugation at 1500xg for 20 minutes to remove cells and cellular debris. Spent media was filtered through 0.2µm 500ml bottle top filter units (Corning) and stored at 4°C.

2.5. Mammalian Cell Culture

2.5.1. Mammalian Cell Culture Medium and Reagents

TrypLE Express and Dulbecco's Modified Eagle Medium (DMEM) plus glutamax, were purchased from Life Technologies. The cationic polymer polyethyleneimine (PEI), used as a transfection agent, and FBS were supplied by Sigma-Aldrich.

Human embryonic kidney cells (HEK293T) were grown as monolayers and maintained by regular passage in DMEM supplemented with 10% FBS under 5% CO_2 at 37°C within a water vapour-saturated atmosphere. All manipulations were performed in a sterile environment, with disposable plasticware and glassware reserved specifically for that purpose.

2.5.2. Transient transfection of HEK293T cells

For transfection in a 35mm tissue culture dish (BD Biosciences), HEK293T cells were grown to 80% confluency as a monolayer. A solution containing 5µg DNA (pOPING-CD36ED-6His) at a concentration of 0.5µg/µl in 5% glucose was mixed with 1.5µl PEI solution (prepared by addition of 45mg 25kDa PEI (Sigma-Aldrich) to 8ml dH2O, pH to 7.2 with dilute HCl) and incubated at room temperature for 5 minutes. DMEM (2ml) with 10% FBS was added to the transfection mixture before applying to the cells. After 48 hours, spent media was harvested and any cells or cell

debris removed by centrifugation at 1000xg for 10 minutes. Spent media was filtered through a 0.2um syringe filter (Sartorius) and stored at 4°C.

2.6. Protein Biochemistry

2.6.1. Materials used for protein biochemistry

General chemicals were purchased from Sigma-Aldrich. EDTA-free protease cocktail tablets (cOmplete) were purchased from Roche, and used at a final concentration of 1x, according to manufacturer's recommendations.

2.6.2. Buffer exchange with concentration of harvested media

2.6.2.1. Small-scale buffer exchange and sample concentration

Harvested media from small-scale suspension cultures (100ml) was buffered exchanged and concentrated using a 30kDa nominal molecular weight cut-off (NMWCO) polyethersulfone (PES) VivaFlow 200 cassette as part of a tangential cross-flow diafiltration system, following manufacturer's protocols (Sartorius). Harvested media was buffer exchanged against 1L of purification buffer (50mM

HEPES pH7.4, 300mM NaCl, 20mM Imidazole) before concentration of the sample to around 20-30ml.

2.6.2.2. Large-scale buffer exchange and sample concentration

Harvested media from large-scale suspension cultures (5L) was first concentrated and then buffer exchanged using 30kDa NMWCO Xampler Ultrafiltration Hollow Fiber Cartridge along with a QuixStand Benchtop System as part of a tangential cross-flow diafiltration system, following manufacturer's protocols (GE Healthcare). Harvested media was first concentrated to around 500ml and then buffer exchanged against 5L of purification buffer (50mM HEPES pH 7.4, 300mM NaCl, 20mM Imidazole). The sample was then further concentrated to around 300-400ml.

2.6.3. Purification of CD36 ED-12His using affinity chromatography

2.6.3.1. Batch affinity chromatography

CD36 ED-12His from small-scale suspension cultures was purified in batch using Ni-NTA agarose (Qiagen). Ni-NTA agarose was washed in dH$_2$O (1ml of 50% agarose slurry/10ml of sample) and pre-equilibrated with purification buffer (50mM HEPES, 300mM NaCl, 20mM Imidazole, pH7.4) at a volumetric ratio of 1:10 (packed resin to purification buffer). At each stage of the purification process, the

resin was packed by centrifugation at 300rpm for 1 minute, 4°C (Hettich rotanta 46R). A low concentration of imidazole (20mM) was present in the initial purification buffer to reduced non-specific binding between other proteins and the resin. Protein sample and resin were incubated with continuous gentle mixing for 2 hours at 4°C to ensure binding of the 12 histidine tag of CD36 ED. The non-bound proteins were decanted (flow-through), and the resin washed seven times with 20-bed volumes of ice-cold purification buffer containing increasing concentrations of imidazole (20-100mM). Bound CD36 ED-12His was then eluted using four 8-bed volumes of purification buffer containing 500mM imidazole.

2.6.3.2. Column affinity chromatography

CD36 ED-12His from large-scale suspension culture was purified using a 5ml HisTrap HP column (GE Healthcare) on an AKTA Prime Plus automated protein purification system (GE Healthcare), within a refrigerated room (4°C). The HisTrap HP column was first washed with 10 column volumes of dH_2O and then equilibrated with 10 column volumes of purification buffer (50mM HEPES, 300mM NaCl, 20mM Imidazole, pH7.4) at a flow rate of 1ml/min. The protein sample was loaded onto the column at a low flow rate (0.3ml/min) overnight to ensure efficient binding of the 12 histidine tag of CD36 ED. Protein flowing through the column was measured by absorbance at 280nm (A280). The column was then washed with purification buffer containing 100mM imidazole at 0.5ml/min, until the A280 dropped to around baseline levels. Purification buffer containing 500mM imidazole

was passed through the column to elute CD36 ED-12His with 2ml fractions collected using the automated fraction collector.

2.6.4. Concentration of purified protein samples

Proteins eluted from the chromatography procedures were concentrated using Amicon Ultra-4 and Amicon Ultra-15 centrifugal devices with a 30kDa NMWCO (EMD Millipore), spun at 4000xg, 8°C (Hettich rotanta 46R), for between 10 and 30 minutes until the sample volume had reduced to 20% of the starting volume.

2.6.5. Dialysis

Dialysis was performed using Slide-a-Lyzer G2 dialysis cassettes with a 20kDa NMWCO (Thermo Scientific), following the manufacturer's protocol. Briefly, protein samples were added to dialysis cassettes and dialysed against 300x the volume of sample with dialysis buffer (50mM HEPES, 300mM NaCl, pH 7.4), in a beaker at 4°C for 1 hour with gentle stirring. The process was repeated for another hour with fresh dialysis buffer and then allowed to dialyse overnight in a third batch of dialysis buffer.

2.6.6. Size-exclusion chromatography

Purified proteins from a large-scale suspension culture, dialysed into dialysis buffer were further separated using size-exclusion chromatography (SEC). SEC was performed using a Superdex 200 10/300 GL column (GE Healthcare) attached to an AKTA Explorer 100 automated protein purification system (GE Healthcare), operated at room temperature. The column has a globular protein separation range of 10-600kDa. A concentrated purified protein sample (500µl) was passed down the SEC column at a flow rate of 0.5ml/min, with 1ml fractions being collected by an automated fraction collector.

2.6.7. Trichloroacetic acid precipitation of protein samples

Dilute protein solutions were precipitated using tricholoroacetic acid. This was performed prior to separating dilute protein samples by SDS-PAGE. 0.1% (v/v) of 0.15% sodium deoxycholate was added to the protein sample and incubated at room temperature for 5 minutes. Following this, 0.1% 72% trichloroacetic acid was added, the sample mixed well and incubated at room temperature for 5 minutes. Protein was recovered by centrifugation at 20000xg for 15 minutes (Hettich EBA 12). The supernatant was carefully removed and discarded, and the pellet resuspended in 10µl resuspension buffer (4% SDS, 0.2M Tris pH 7.4, 0.15M NaOH).

2.6.8. Preparation of protein samples for SDS-polyacrylamide gel electrophoresis (SDS-PAGE)

Protein samples were prepared for SDS-PAGE as described by Laemmli (Laemmli, 1970). Laemmli sample buffer (LSB; 100mM Tris-HCl pH 6.8, 20% glycerol, 10% 2-mercaptoethanol, 4% SDS, 0.1% bromophenol blue) was added to the protein sample (2:1 v/v, sample to LSB) and incubated at 75°C for 10 minutes prior to loading the gel. LSB without 10% 2-mercaptoethanol was used when preparation samples under non-reducing conditions.

2.6.9. SDS-PAGE

Proteins were separated by electrophoresis through vertical 1mm thick polyacrylamide gels (0.1% SDS, 8% acrylamide), using the procedure described by Laemmli (Laemmli, 1970). The required reagents and volumes to make the separating and stacking gel, along with SDS-PAGE running buffer were as follows:

10X SDS-PAGE running buffer: 250mM Tris Base

1.92M glycine

1% SDS

Separating gel: 1.3ml 1.5M Tris-HCl (pH8.8)

2.3ml H_2O

1.3ml 30% Acrylamide/Bis-acrylamide mix (37:5:1 ratio)

50µl 10% SDS

50µl 10% ammonium persulphate

3µl TEMED

Stacking gel: 380µl 1.0M Tris-HCl (pH6.8)

2.1ml H_2O

500µl 30% Acrylamide/Bis-acrylamide mix (37:5:1 ratio)

30µl 10% SDS

30µl 10% ammonium persulphate

3µl TEMED

Polymerisation of the separating gel was initiated by the addition of N,N,N',N'-tetramethylethan-1,2-diamine (TEMED). The stacking gel was overlaid onto the polymerised separating gel after addition of TEMED to initiate polymerisation. Prior

to sample loading, the wells of the gel were rinsed with running buffer. Gels were run at 100V for 2 hours or until the dye front had reached the bottom of the gel.

2.6.10. Detection of protein by colloidal blue staining

Following separation by SDS-PAGE, proteins were visualised using the colloidal blue staining kit (Life Technologies), according to the manufacturer's protocol. Briefly, following electrophoresis, the SDS-PAGE gel was placed in freshly made colloidal blue solution (per gel: 20ml Stainer A solution, 5ml Stainer B solution, 20ml 100% methanol and 55ml dH_2O) and incubated for 3-12 hours at room temperature on an orbital shaker. Staining solution was then removed and the gel washed three times, for 5 minutes, 1 hour and then overnight in dH_2O at room temperature on an orbital shaker to de-stain.

2.6.11. Protein Quantification

The protein content of samples were calculated using a BSA standard curve. Serially diluted protein samples and BSA standards were separated by SDS-PAGE and stained with colloidal blue stain. The gel was scanned and the density of the BSA standards was measured using ImageJ software (NIH) and the standard curve plotted using GraphPad Prism software version 5 (CA, USA). Using the BSA standard curve, the linear equation (Equation 1) was used to measure the concentration of protein based on the density of protein bands.

$$y = mx + c$$

Equation 2.1. The Linear Equation

Where y and x are the co-ordinates that satisfy the equation, m is the gradient of the straight line and c is the intercept on the y-axis.

The percentage purity of a protein sample was also calculated using the ImageJ analysis of stained SDS-polyacrylamide gels by comparing the density of the protein of interest (as a percentage) against the summed densities of all proteins bands in the sample (representing 100%).

2.6.12. Detection of proteins by western blotting

For western blotting analysis, proteins were separated by SDS-PAGE and then electroblotted onto a polyvinylidene fluoride (PVDF) membrane (EMD Millipore, MA, USA). The method is based on the western blotting procedures first demonstrated in 1979 (Towbin *et al*., 1979). The PVDF membrane was prepared by soaking in 100% methanol for 5 minutes, followed by a 5 minute wash in dH$_2$O. Finally, both the PVDF membrane and 3MM filter paper (Whatman, Maidstone, UK) were soaked in transfer buffer (25mM Tris-HCl pH8.3, 192mM glycine, 20% methanol). Electroblotting was carried out at 400mA for 1 hour at room temperature using a Mini Trans-blot cell (Biorad, CA, USA), according to manufacturer's

instructions. Following electroblotting, the PVDF membrane was washed for 5 minutes with PBST (0.1% v/v Tween 20 in PBS) before being incubated in block buffer (5% w/v skimmed milk powder in PBST) for 1 hour at room temperature on an orbital shaker. The membrane was then incubated with 1ml primary antibody diluted in blocking buffer inside a heat-sealed pocket for 2 hours at room temperature, shaking on an orbital shaker. For detection of CD36, a rat monoclonal anti-CD36 antibody, clone 1955 (R&D systems) was used at a dilution of 1:1000. For detection of the C-terminal poly-histidine tag, a mouse monoclonal anti-His antibody, clone 3D5 (Life Technologies) was used at a dilution of 1:5000. Following incubation with primary antibody, the membrane was given three 15 minutes washes with PBST before incubation with 1ml of secondary antibody, conjugated with to horseradish peroxidase (HRP) diluted in blocking buffer inside a heat-sealed plastic pocket for 1 hour at room temperature, shaking on an orbital shaker. The secondary antibodies used (Dako) were either a rabbit-anti rat (for anti-CD36 blots) or a goat-anti mouse (for anti-His). The membrane was subsequently given four 15 minute washes with PBST before visualisation of protein-bound HRP using Immobilon Western Chemiluninescence HRP Substrate (EMD Millipore, MA, USA), together with ECL Hyperfilm (GE Healthcare).

2.6.13. Glycosidase digestion of glycoproteins

Proteins were deglycosylated using Peptide-N-glycosidase F (PNGase F) (New England Biolabs) according to the manufacturer's protocol. Briefly, 1-20µg of protein was incubated for 10 minutes at 100°C in the presence of denaturing buffer (0.5% SDS, 1% 2-mercaptoethanol) and incubated on ice for 2 minutes. 500U of PNGase F was added with G7 buffer (50mM Sodium phosphate) supplemented with 1% NP40 and incubated at 37°C for 2 hours.

For deglycosylation of native purified protein, 1µg of protein was incubated with 500U of PNGase F in the presence of G7 buffer and incubated at 37°C for up to 72 hours.

2.6.14. Solid-phase ligand binding assay

1µg of purified CD36 ED-12His in 100µl binding buffer (PBS, 1mM $MgCl_2$, 1mM $CaCl_2$) was added to each well of a Ni-NTA HisSorb white plate (Qiagen) and incubated at 4°C overnight with gentle agitation. After unbound purified CD36 ED-12His had been aspirated, the wells were rinsed with 200µl binding buffer before addition of diluted alexa fluor 488-acLDL (Life Technologies). Alexa fluor 488-acLDL was diluted in ice-cold ligand binding buffer (binding buffer plus 1% fatty-acid free (FAF) BSA) to the following concentrations: 0, 2.5, 5, 10, 20, 30, 40µg/ml each in a final volume of 100µl. The plate was incubated for 2 hours at room temperature with gentle agitation. After removal of unbound alexa fluor 488-acLDL

by aspiration, the wells of the plate were rinsed three times with 100µl wash buffer (binding buffer with 0.2% FAF BSA). The bound fluorescence was measured using a microplate reader with an absorption and excitation maxima of 495 and 519nm, respectively (Synergy HT, Bio-Tek).

2.7. Mass Spectrometry

Following separation of purified CD36 ED-12His by SDS-PAGE and staining with colloidal blue, the protein was excised and sent to the Advanced Mass Spectrometry Facility at Birmingham University. The protein was digested in-gel using either trypsin or chymotrypsin, with subsequent peptide fragments being dissolved in 0.1% formic acid prior to separation by liquid chromatography and analysis using tandem mass spectrometry (LC-MS/MS).

Protein samples were analysed using a Dionex 3000 Ultimate nano-LC instrument (Dionex, CA, USA) with a zwitterionic hydrophilic interaction liquid nano chromatography column, 150mm x 75µm, 5µm, 200Å (ZIC-HILIC, Sequant, UK) coupled with a Triversa Nanomate nanospray source (Advion Biosciences, NY, USA) which was further interfaced with an LTQ Orbitrap Velos ETD mass spectrometer (Singh *et al*., 2012).

The data from LC-MS/MS was analysed using the software Mascot (Matrix Services) and Byonics (Protein Metrics, CA, USA) to identify peptide sequences and glycan structures, respectively.

2.8. Biacore

All studies were performed at 25°C using a Biacore T200 (GE Healthcare) using NTA S series sensor chips, following manufacturer's protocols (GE Healthcare). Data was analysed using BIAevaluation software. A working temperature of 25°C was used as this was the temperature recommended for optimal surface activation and ligand immobilisation following manufacturer's instructions.

Prior to use, NTA sensor chips were removed from their sealed pouch and allowed to equilibrate at room temperature for 15 minutes. Following docking of the sensor chip into the Biacore T200, the instrument was equilibrated with filtered running buffer (10mM HEPES, 150mM NaCl, 0.05% v/v Surfactant P20, 50μM EDTA). Addition of 50μM EDTA to the running buffer counteracted the effect of metal ion contaminants present in the buffer, without stripping nickel from the activated sensor chip surface. The NTA sensor chip was activated by passing 0.5mM $NiCl_2$ in dH_2O over the surface of the chip. Purified CD36 ED-12His (ligand) and antibodies (analytes) were diluted into running buffer prior to use. Regeneration of the NTA sensor was achieved by passing 350mM EDTA in dH_2O over the sensor surface.

3. Expression and Purification of the Ectodomain of CD36

3.1. Introduction

Protein expression and purification of recombinant proteins has become fundamental in many areas of academia as well as the pharmaceutical industry. The first recombinant protein produced more than 30 years ago was human insulin (Johnson, 1983). Expressed in *E. coli,* this recombinant protein replaced animal sourced insulin (primarily porcine) providing a readily available supply with enhanced purity. Now the use of recombinant proteins has become widespread ranging from diagnostic tools and enzymes used within the laboratory to vaccines and therapeutic agents used within the clinic. Despite these advances, the ever increasing drive to learn more about protein structure and function through use of sophisticated biophysical techniques has driven the need to produce substantial quantities of high purity protein. Through exploitation of a number of expression systems it has become increasingly possible to express high yields of heterologous protein and in turn challenge these ever increasing demands.

Bacteria, yeast, insect cells and mammalian cells, are the four most commonly used hosts for expression of recombinant proteins, each with their own advantages and disadvantages. For expression of heterologous proteins, a bacterial host (in particular *E. coli*) is usually the first and most preferred choice, mainly because it is inexpensive, divides rapidly and has the ability to produce high protein yields.

However, for more complex recombinant proteins, particularly those from higher eukaryotes, difficulties in efficient expression can be encountered as bacteria lack the same biochemical pathways required for post-translational modifications, such as N-linked glycosylation. This can lead to misfolding and aggregation, ultimately resulting in the formation of insoluble inclusion bodies. Yeast, like bacteria are also inexpensive and capable of producing high protein yields but have the added advantage, as a simple eukaryote, to produce some of the modifications observed on native mammalian proteins. Nevertheless, these modifications are limited with many mammalian recombinant proteins still being expressed incorrectly and tending to also end up within inclusion bodies. With insect and mammalian cells, much longer incubation times (with an 18-24 hour doubling time) are necessary to achieve the biomass required. Mammalian and insect cells generally tend to be more expensive to culture and harder to maintain than both bacteria and yeast. Insect cells can be particularly difficult to manipulate, with expression of recombinant proteins primarily relying on the use of baculovirus expression vectors. Despite these inconveniences, both insect and mammalian cells can be used to generate recombinant proteins with more complex post-translational modifications and often produce recombinant proteins more closely resembling the native form. Although mammalian cells may well be the vehicle of choice to express recombinant mammalian proteins and are more likely to produce more native-like post-translational modifications, higher protein yields can usually be obtained using insect cells, with scale-up of insect cell cultures easily achievable. Perhaps counter-intuitively, the use of insect cells to produce proteins with simpler and more uniform glycans can be an advantage for downstream biophysical and structural studies.

The scavenger receptor CD36 was first described nearly 40 years ago and has since been implicated in a large variety of roles both in normal and patho-physiology. Despite the physiological importance there is still no crystal structure for CD36 and data characterising ligand binding remains poor. In 2013, the crystal structure of the soluble domain of a related scavenger receptor found in lysosomes (LIMP-2) was solved to a resolution of 3Å (Neculai *et al.*, 2013). Although molecular models of CD36 were generated based on the LIMP-2 crystal structure, more reliable structural information is needed to model interactions with the diverse ligands of CD36 and this will only be obtained through studying the ligand binding domain of CD36 directly.

Previous attempts to express CD36 in both bacteria and yeast have led to the formation of insoluble inclusion bodies (Linton, K; personal communication). On the other hand, insect cells have been shown to be a good host for expression of CD36 (Jimenez-Dalmaroni *et al.*, 2009, Martin *et al.*, 2007, Hoosdally *et al.*, 2009), and little data is available on the recombinant expression of CD36 in mammalian cells. This chapter describes the use of baculovirus/insect cell expression systems to express recombinant CD36 with a C-terminal 12xHistidine tag (-12His) for subsequent purification using nickel affinity chromatography. The general aim is to produce milligram quantities of soluble functional CD36 to allow biochemical, biophysical and structural studies.

3.1.1. Full-length CD36 vs. Ectodomain of CD36

Although membrane proteins make up around 30% of the proteome of most organisms (Krogh *et al*., 2001), they continue to be a challenging target for structural and biophysical studies. Many difficulties are encountered when working with membrane proteins, one of which being their typically low expression level in their native environment (Seddon *et al*., 2004). Even with the use of heterologous expression systems to produce higher levels of membrane-targeted recombinant protein, obstacles still remain. Membrane proteins with their amphiphilic nature must first be solubilised from the membrane, usually through the use of detergents. Much time has to be spent in selecting the right detergent as well as deducing the most suitable ratio of detergent to protein to ensure that the membrane is solubilised efficiently without protein denaturation in the process (Prive, 2007). Detergents may also have a detrimental impact on subsequent chromatography steps leading to reduced yield and negatively affect the activity of the purified recombinant protein (Hammond and Zarenda, 1996, Tan and Ting, 2000).

The most common way to improve the expression and subsequent handling of a membrane protein, particularly a receptor with a large ectodomain that is simply anchored in the membrane, is to remove the transmembrane portion of the protein and just express the ectodomain (ED) as a secreted protein (Hulst *et al*., 1993). This is of course dependent on the assumption that the secreted protein retains the fold and function to permit reliable biophysical studies. The majority of CD36 is extracellular in what is likely to be a single domain. It is this large, heavily glycosylated, ED that is responsible for ligand binding. In 2009, mCd36 ED was

expressed and secreted from insect cells and used to demonstrate the binding negatively-charged diacylglycerol ligands to the ED. This highlighted the ability of this domain to be expressed independently of the rest of the protein and still retain the ability to bind ligand (Jimenez-Dalmaroni *et al*., 2009). Through expression and subsequent secretion of soluble CD36 ED, the need for detergents is removed, making the subsequent purification more straightforward, negating a number of possible complications with downstream applications. The additional advantage of this method is that the recombinant protein can be secreted into the surrounding media, acting as a crude preliminary purification step and avoiding the need to lyse cells.

3.1.2. Baculovirus Expression Systems

Originally harnessed for use as biological pesticides to control insect populations (Cory and Bishop, 1997), baculovirus expression systems have since become powerful tools for the expression of genes in insect cells (Smith *et al*., 1983). The most commonly used baculovirus for infection of insect cells is the *Autographa californica* multiple nuclear polyhedrosis virus (AcMNPV), which primarily relies on members of the lepidopteran species such as *Spodoptera frugiperda* and *Trichoplusia ni* as host insects for viral replication. The life-cycle of wild-type AcMNPV is biphasic involving the formation of two forms of virus: budded virus (BV) and occlusion-derived virus (ODV). These two forms are functionally and morphologically distinct (Miller, 1989). *In vivo*, the baculoviral infection process begins with ingestion of foliage contaminated with baculovirus, leading to the uptake

of baculoviral capsids into the epithelia of the midgut by direct fusion with the microvillus membrane. Once inside the epithelium, baculoviral capsids translocate to the nucleus, aided by the actin-cytoskeleton (Ohkawa *et al*., 2010), where upon uncoating of the viral genome occurs in preparation for transcription and viral replication. Around 10-12 hours following initial infection, new baculoviral capsids translocate through the cytoplasm to the plasma membrane where they bud from the cell surface, enclosed in a membrane envelope modified with the viral fusion protein gp64 (Blissard and Wenz, 1992). These highly infectious BV particles are then free to diffuse throughout the surrounding extracellular matrix, infecting neighbouring cells through uptake by endocytosis, leading to a systemic infection. Approximately 20-24 hours post-infection, formation of BV greatly diminishes while ODV begins to be synthesised. During ODV synthesis baculoviral capsids become embedded within large proteinaceous occlusion bodies consisting of a matrix of polyhedrin protein (Summers and Smith, 1978, Rohrmann, 1986). ODV synthesis continues for another 50 hours (up until ~72 post-infection), driven by the strong transcriptional activity of the polyhedrin gene (*polh*) promoter. During this period the level of polyhedrin protein within each cell can represent up to 50% of the total protein content (Possee and Howard, 1987). When the insect host cuticle begins to break down following systemic cell lysis, ODV is released allowing infection of new hosts. The polyhedrin occlusion body protects the virus from environmental stresses, only to be degraded once inside the alkaline environment of the midgut in the next host.

Under cell culture conditions, baculoviruses no longer need to resist the environmental stresses encountered in the wild, making the expression of the polyhedrin protein and formation of ODV redundant. As a consequence by exchanging the polyhedrin gene with cDNA encoding a protein of interest, the strong

polh promoter can be exploited to drive the expression of recombinant protein in cultured insect cells. This results in the formation of large quantities of BV early in the infection process, capable of infecting other cells, followed by expression of large quantities of recombinant protein under the control of the *polh* promoter at the late stage of the infection.

Although infection of insect cells with baculoviruses exploiting the *polh* promoter (such as Bac-to-Bac from Life Technologies and BacPAK6 from Clontech) have been shown to be effective at producing high levels of recombinant proteins, the increasing demand to produce more complex mammalian-like proteins has driven the development of more advanced baculovirus expression systems. These advances go beyond the use of baculoviruses lacking only the *polh* gene. Systems have been engineered with other non-essential baculoviral genes removed, thus reducing the burden on the cell machinery during recombinant protein expression (e.g. *FlashBAC* expression systems), or with additional mammalian chaperone proteins included that when co-expressed, help to stabilise recombinant mammalian proteins which may be prone to misfold in the heterologous host (e.g. the *Profold ER1* expression system).

3.1.2.1.   The *FlashBAC* Expression System

Although the genome of the baculovirus AcMNPV has been sequenced (133804bp; NC_001623), most of the 156 predicted protein-coding genes remain uncharacterised (Ayres *et al*., 1994, Chen *et al*., 2013). Despite this, many genes have been shown to not be required for the efficient propagation of baculovirus in cell culture (Li *et al*.,

2008, Wang *et al*., 2007, Carpentier *et al*., 2008). In the *flashBAC* expression system (Oxford Expression Technologies, OET), in addition to the removal of the *polh* gene, the non-essential chitinase gene (*ChiA*) has been deleted from the baculovirus genome. The *ChiA* gene encodes an enzyme with both endo- and exo-chitinase activity (Hawtin *et al*., 1995) that, in partnership with the enzyme cathepsin, facilitates the breakdown and liquefaction of the chitin-rich cuticle of insect host during the very late stages of the infection process allowing release of ODV to infect more hosts (Hawtin *et al*., 1997). Observations using confocal and electron microscopy of AcMNPV-infected insect cells has shown chitinase to accumulate within the endoplasmic reticulum (ER) where it is packed into a para-crystalline array, reducing the function and efficiency of the secretory pathway (Thomas *et al*., 1998, Saville *et al*., 2004). The deletion of the *ChiA* gene therefore is designed to improve efficiency of the secretory pathway and in turn improve the yield of secreted and membrane-targeted recombinant proteins.

3.1.2.2.   The *FlashBAC Gold* Expression System

The *FlashBAC Gold* expression system (also from OET) is an improvement on the *FlashBAC* system with an additional non-essential gene deleted to further aid recombinant protein production. In the *FlashBAC Gold* system the *v-cath* gene is deleted in addition to the *ChiA* gene (Hitchman *et al*., 2010). The *v-cath* gene encodes V-cath endopeptidase which is a papain-like cysteine protease (Slack *et al*., 1995). V-cath accumulates in the ER as an inactive precursor form (Pro-v-cath). Upon cell death the proenzyme is processed by chitinase into its active form

whereupon it facilitates breakdown of the host cuticle (Hom *et al.*, 2002, Hom and Volkman, 2000). The deletion of both *ChiA* and *v-cath* from the *flashBAC Gold* baculovirus genome is therefore designed to free up more processing space within the ER, potentially enhancing the yield of secreted and membrane-targeted proteins.

3.1.2.3. The *Profold-ER1* Expression System

As nascent proteins traffic through the ER to the Golgi apparatus, a number of chaperones facilitate post-translational modification of the membrane or secreted proteins and drive correct folding into the appropriate three-dimensional conformation. Although much is now known about protein folding and quality control mechanisms in the ER of mammalian cells (Braakman and Bulleid, 2011, van Anken and Braakman, 2005), less is known about similar processes in insect cells. To improve the folding of complex mammalian-like recombinant proteins in insect cells, a number of baculoviral expression systems have been engineered to co-express mammalian chaperones (Hsu and Betenbaugh, 1997, Hsu *et al.*, 1996). In the *Profold-ER1* expression system (AB Vector) the baculovirus genome encodes the human molecular chaperones calreticulin and protein disulphide isomerase (PDI). Both calreticulin and PDI are known to aid protein folding in the ER (Williams, 2006, Appenzeller-Herzog and Ellgaard, 2008). Calreticulin is a lectin chaperone that aids the folding of nascent glycoproteins only allowing correctly folded and processed glycoproteins to traffic from the ER to the Golgi apparatus (Williams, 2006). PDI is chaperone that participates in the formation of disulphide bonds and also facilitates correct protein folding (Appenzeller-Herzog and Ellgaard, 2008).

Several studies have shown that co-expression of these chaperones in a baculovirus expression system enhances the production of biologically active secreted and membrane-targeted recombinant proteins (Zhang *et al*., 2003, Hsu *et al*., 1996).

3.1.2.4. Generation of recombinant baculoviruses by homologous recombination

Due to the large size of the AcMNPV baculovirus genome (Ayres *et al*., 1994), direct manipulation and insertion of cDNA to encode recombinant protein is difficult. Instead, production of recombinant baculoviruses usually takes place in two steps, the first involving the cloning of the target gene into a transfer vector with sequences that flank the *polh* gene in the baculovirus genome. The second step involves introducing both the baculoviral genome and the transfer vector together into host insect cells, allowing simultaneous homologous recombination between the common flanking sequences (Smith *et al*., 1983). This results in the insertion of the target gene of interest into the baculovirus genome in place of the *polh* gene, under the control of the strong *polh* promoter.

The use of homologous recombination within insect cells to produce recombinant baculoviruses has generally resulted in a mixture of wild-type parental baculovirus in addition to recombinant baculovirus (recombination frequency was low initially at less than 1%) (Fraser, 1989). The consequence of this was the need to use labour intensive, time-consuming plaque assay and plaque purification techniques to isolate the recombinant baculovirus. This was not usually a one-off process as recombinant

baculovirus was often enriched but not pure and, eventually, the parental baculovirus would out-compete the recombinant baculovirus and necessitate the re-isolation of the recombinant form.

Many improvements to the baculoviral system have since been made to allow the separation of recombinant and parental baculoviruses. Initial attempts to address this involved insertion of the *lacZ* gene from *E. coli* into the transfer vector along with the target gene of interest. The *lacZ* gene encodes β-galactosidase, an enzyme that breaks down lactose. Through use of the stain X-gal (5-bromo-4-chloro-3-indoyl β-D-galactopyaranoside), an analogue of lactose, insect cells containing recombinant baculovirus would stain blue compared to cells containing parental virus that remained colourless. Although this improved identification of recombinant baculovirus, it did not improve the frequency of recombinant baculovirus formation that still required plaque purification. There was also the added problem of β-galactosidase contamination in the subsequent recombinant protein sample.

The problem of identification and separation of recombinant and parental baculovirus was partially solved by the use of linearised baculovirus DNA which could not become infectious unless rescued by recombination with a transfer vector (Kitts *et al*., 1990). In this method a unique enzyme restriction site (*Bsu*36 I) was introduced into the polyhedrin gene of the baculovirus DNA. By linearising the baculovirus DNA prior to homologous recombination, parental baculovirus became up to 150 times less infectious than the circularised form (Kitts *et al*., 1990). Only after homologous recombination between transfer vector and linearised baculoviral DNA would re-circularisation take place, restoring infectivity and allowing baculovirus replication. Despite this improvement in the selectivity of recombinant

baculovirus over parental baculovirus, the frequency of successful homologous recombination events remained around 30% (Kitts *et al*., 1990).

Shortly thereafter a more efficient method was devised which resulted in ~100% frequency of recombination baculovirus generation (Kitts and Possee, 1993). In this system, the baculovirus genome was engineered with two *Bsu*36 I restriction sites flanking the *polh* gene locus. Restriction digestion of the baculoviral DNA using *Bsu*36 I resulted in the formation of two DNA fragments (Figure 3.1 (a)). The smaller of these fragments included part of a downstream gene (*ORF1629*), essential for replication of the baculovirus (Possee *et al*., 1991). If the larger fragment were to re-circularise in the absence of the smaller fragment, the lack of a complete *ORF1629* gene would prevent the resultant baculovirus from replicating. However, through a double homologous recombination event between the linearised baculovirus DNA and a transfer vector containing the complete sequence of the *ORF1629* gene, in addition to the recombinant gene of interest, the baculoviral DNA could re-circularise allowing a viable baculovirus to be rescued (Figure 3.1 (b)). Both the *Profold-ER1* and *flashBAC* expression systems work using this methodology.
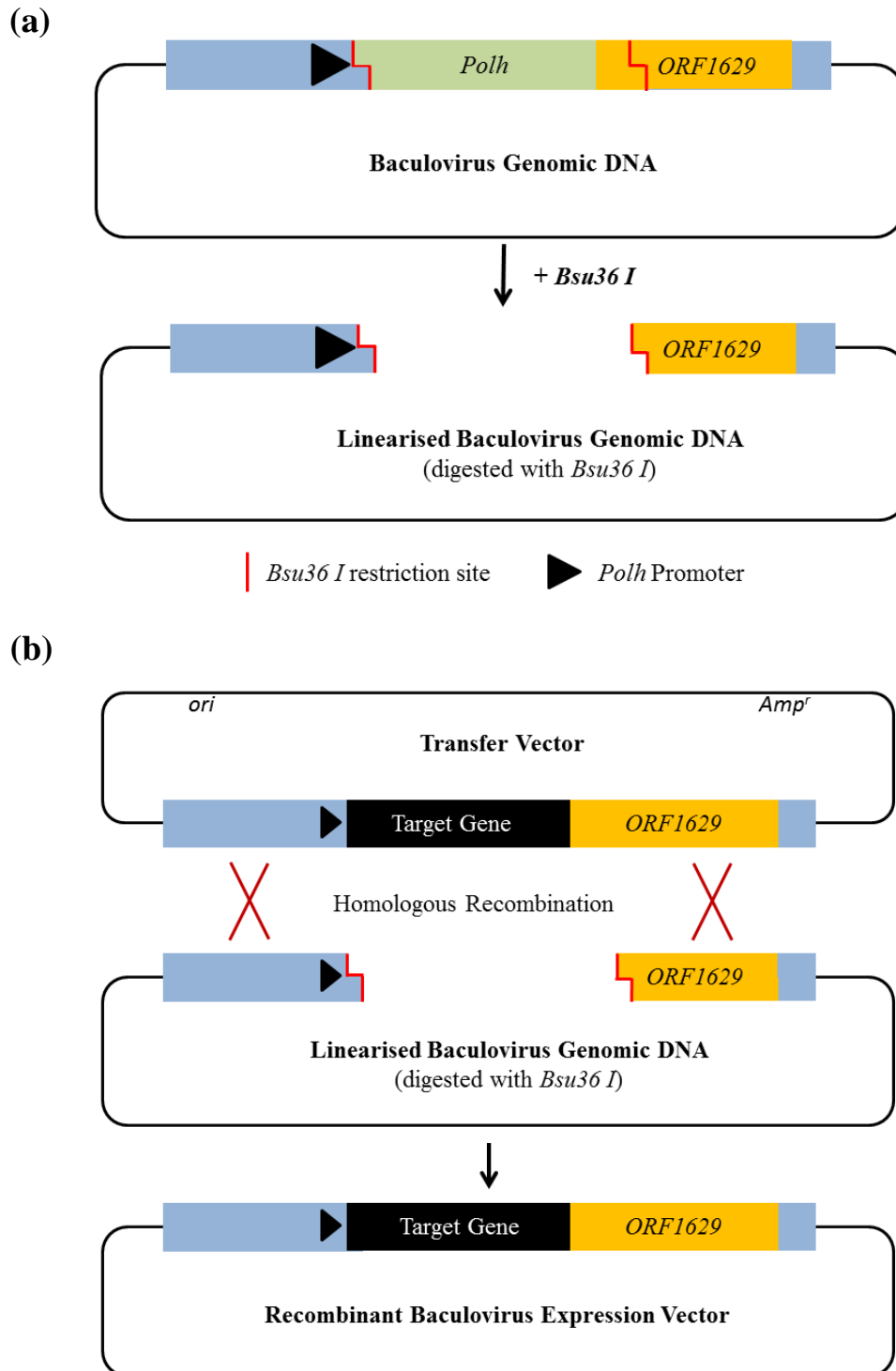
Figure 3.1 Schematic representation of recombinant baculovirus expression vector generation by double homologous recombination.
(a) Digestion of the baculovirus genomic DNA with *Bsu*36 I results in removal of the polyhedrin gene (*polh*) along with part of the essential *ORF1629* gene. Lack of a complete *ORF1629* gene prevents baculoviral synthesis if the baculoviral genomic DNA were to self-ligate. **(b)** Double homologous recombination between the linearised baculoviral genomic DNA and a transfer vector containing a complete copy of the *ORF1629* gene, along with target gene results in the restoration of the *ORF1629* gene and insertion of the target gene under the control of the strong polyhedrin promoter. With a complete *ORF1629* gene the resultant baculoviruses can replicate.

3.1.3. Insect Cells

Combined with the use of customised baculoviruses, insect cells have become a good option for the generation of large quantities of eukaryotic recombinant proteins. The main advantage of using insect cells is in their ability to incorporate post-translational modifications similar to those found in mammalian cells while still producing high yields of cytosolic, membrane and secreted proteins. Although N-linked glycosylation reliably occurs within the same sequon (Asn-X-Ser/Thr) in both insect and mammalian cells, glycosylation in insect cells has been shown to be less complex (Salmon *et al*., 1997, Jarvis, 2003). For some proteins, like full-length CD36, this simplicity in glycosylation is sufficient for the protein to be properly expressed, folded, trafficked to the plasma membrane and retain ligand binding activity (Hoosdally *et al*., 2009). Other proteins, like the influenza A virus hemagglutinin, show decreased function when expressed in insect cells due to the difference in glycosylation (de Vries *et al*., 2010). Glycosylation, in particular glycan heterogeneity, can lead to difficulties in producing good structural and biophysical data. For example, the ability the produce suitable crystals for use in X-ray crystallography can be hindered by large, complex and heterogeneous glycan structures. This therefore makes insect cells, which recognise mammalian glycosylation sites but modify with simpler glycan structures, a popular alternative host for production of mammalian recombinant proteins. Although many insect cell lines have been derived from over a 100 insect species (Lynn, 1996), three lepidopteran cell lines have become most frequently used for the baculovirus expression system: Sf21/Sf9 and Hi5 insect cells.

3.1.3.1.   Sf21 Insect Cells

Sf21 insect cells (officially called IPLB-Sf21AE) are derived from the pupal ovarian tissue of the fall army worm, *Spodoptera frugiperda* (Vaughn *et al*., 1977). Sf21 cells and Sf9 cells, a clonal isolate of the Sf21 cell line, grow well in both adherent monolayers and in suspension cultures. Both cell lines are suitable for baculovirus generation, amplification and plaque assay as well as for the expression of recombinant proteins. It has been suggested previously that Sf21 insect cells can express more recombinant protein that Sf9 insect cells with some baculoviruses (Hink *et al*., 1991).

3.1.3.2.   High-Five™ Insect Cells

High Five™ insect cells (Hi5, officially called BTI-TN-5BI-4), commercially sold by Life Technologies, are derived from the ovarian cells of the cabbage looper, *Trichoplusia ni* (Wickham *et al*., 1992). Hi5 insect cells have become one of the most commonly used insect cell lines for the expression of recombinant proteins using baculoviruses, having been shown in a number of cases to express more recombinant protein than other lepidopteran cell lines such as Sf9 and Sf21 cells (Davis *et al*., 1992, Wickham and Nemerow, 1993). Despite having a doubling time of around 24 hours and being able to grow well in serum-free media in suspension as well as in adherent cultures, Hi5 cells form irregular monolayers which makes

baculovirus generation and plaque assay difficult in this cell line. Virus amplification from Hi5 cells is also inefficient.

3.1.4. Aims of Chapter 3

- Test three different baculovirus expression systems to determine which produces the highest yield of secreted CD36 ED.

- Determine the amount of baculovirus required to infect insect cells for the generation of a high yield of secreted CD36 ED.

- Determine on a small scale the conditions required for efficient purification of CD36 ED using nickel affinity chromatography.

- Explore the ability to deglycosylate CD36 ED

- Test ligand binding to purified CD36 ED to ensure it is properly folded

- Scale up expression and purification of CD36 ED to generate milligram quantities of protein for biophysical analyses

3.2. Results

3.2.1. Comparison of expression systems

The pBacPAK9 transfer vector was engineered to express human CD36 ED (residues 36-435) with an N-terminal honeybee melittin secretory signal (HMSS) and a C-terminal 12 histidine tag (Figure 3.2; Linton, personal communication). Through homologous recombination in insect cells, three baculoviruses: *FlashBAC-CD36ED*, *FlashBAC Gold-CD36ED* and *Profold-ER1-CD36ED*, were generated as described in section 2.4.2. The recombinant baculoviruses were used in a series of Sf21 insect cell infections to amplify the baculovirus titre. Each infection was performed using a low multiplicity of infection (MOI; 0.05 = 5 viruses per 100 cells) to produce intermediate and then working stocks of baculovirus. Baculovirus titres were estimated by plaque assay.

HMSS	CD36 ED	12-His Tag

Figure 3.2. Schematic representation of recombinant CD36 ED expressed in insect cells.
The fusion protein has an N-terminal honeybee melittin secretory signal (HMSS; amino acids 1-25), the CD36 ED (amino acids 26-425) with a C-terminal 12 histidine tag (amino acids 426-440). HMSS is cleaved upon secretion. For full sequence see Appendix 1.

To identify the baculovirus that gave the highest protein yield, Sf21 and Hi5 insect cell monolayers (1×10^6 cells) adhered to 35mm tissue culture dishes were infected with each of the baculovirus at an MOI=3 in an equal volume of culture media (2ml). Expression and secretion of CD36 ED-12His was allowed to proceed for 72 hours, at which point spent culture media was harvested and analysed by western blot (Figure 3.3). Equal volumes of harvested media were loaded to allow direct comparison of secreted CD36 ED-12His protein levels. In parallel, a mammalian expression vector (pOPING; generated by Dr Joanne Nettleship, Oxford Protein Purification Facility) encoding CD36 ED-6His with a N-terminal secretory signal (RPTPmu) was used in the transient transfection of HEK293T mammalian cells (1×10^6) adhered to the surface of a 35mm tissue culture dish, again grown in 2ml media.
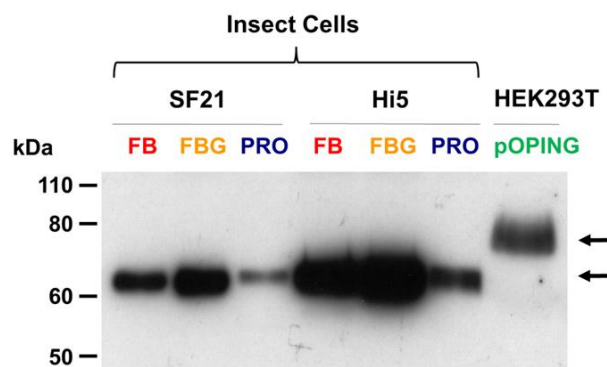
Figure 3.3. Western blot analysis showing CD36 ED-12His secretion from insect cells and HEK293T mammalian cells.
Adherent Sf21 and Hi5 cells (1×10^6) were infected in 35mm dishes with recombinant baculoviruses engineered to express human CD36 ED-12His. HEK293T cells (1×10^6) were transiently transfected with pOPING encoding human CD36 ED-6His. The culture media (2ml) was recovered 72 hours post-infection (insect cells) or 48 hours post-transfection (HEK293T cells). Samples (10μl) were loaded onto a SDS polyacrylamide gel and the proteins separated by electrophoresis. The blot was prepared on PVDF membrane and probed using anti-CD36 antibody clone 1955 (R&D systems). FB, *FlashBAC*; FBG, *FlashBAC Gold*; Pro, *Profold-ER1*. Arrows indicate two different glycosylation forms of CD36 ED-12His.

With both insect cells lines, the *flashBAC gold* baculovirus produced a higher yield of secreted CD36 ED-12His compared to the other baculoviruses. *Profold-ER1* baculoviruses produced the least amount of secreted CD36 ED-12His in both Sf21 and Hi5 insect cells. The levels of CD36 ED-12His secreted from Hi5 insect cells using the *flashBAC* and *flashBAC Gold* baculoviruses appeared to be higher than the level obtained from mammalian cells. The level of CD36 ED-12His secreted from Sf21 using the *flashBAC Gold* baculovirus appeared comparable to the level of CD36 ED-12His secreted from mammalian cells. The difference in electrophoretic mobility between CD36 ED-12His produced in insect cells and mammalian cells was expected due to the differences in glycosylation. Mammalian cells are known to add complex glycans to secreted and membrane proteins, but this has previously been shown not to be important for CD36 interaction with its ligand acetylated-LDL (Hoosdally *et al*., 2009). Based on these findings it was determined that insect cells would be suitable for the expression and secretion of CD36 ED-12His and that maximal expression is from the *flashBAC Gold* baculovirus.

3.2.2. Determining the multiplicity of infection required for maximum CD36 ED-12His expression.

When using baculoviruses to infect insect cells for the production of recombinant protein, determination of the optimal MOI is important. For maximum recombinant protein production, many studies have used a high MOI (at least 3) (Lazarte *et al.*, 1992, Yamaji *et al.*, 1999). Using a high MOI results in a synchronous infection with all insect cells expressing protein at the same time. This approach requires using large amounts of baculovirus, making the protein production process costly and time-consuming, requiring baculovirus stocks to be replenished more frequently. In contrast to using a high MOI, there is growing evidence that the use of very low MOI could be a good alternative for generating recombinant protein (Nguyen *et al.*, 1993, Licari and Bailey, 1992), especially for large-scale protein production which would otherwise require a significant volume of baculovirus stock. Using this method only a small percentage of cells are infected allowing the rest to grow and divide. The uninfected cells and their progeny only become infected later on by baculovirus budded from the originally infected cells. Compared to a high MOI infection where the kinetics of infection are simple (all cells becoming infected and expressing protein simultaneously), a low MOI infection produces more complicated kinetics arising from the serial infection of cells in the population and the ensuing protein synthesis (Wong *et al.*, 1996).

To explore the effect of low MOI on expression and secretion of CD36 ED-12His from Sf21 and Hi5 insect cells, adherent cells (1×10^6 cells) in 35mm tissue culture dishes were infected with *flashBAC Gold* baculovirus encoding CD36 ED-12His at

a range of MOIs (0.001-3) in equal volumes of culture media (2ml). Expression and

secretion of CD36 ED-12His was allowed to proceed for 72 hours, at which point

spent culture media was harvested and analysed by western blot (Figure 3.4). Equal

volumes of harvested media were loaded to allow direct comparison of secreted

CD36 ED-12His protein levels.

(a)

(b)
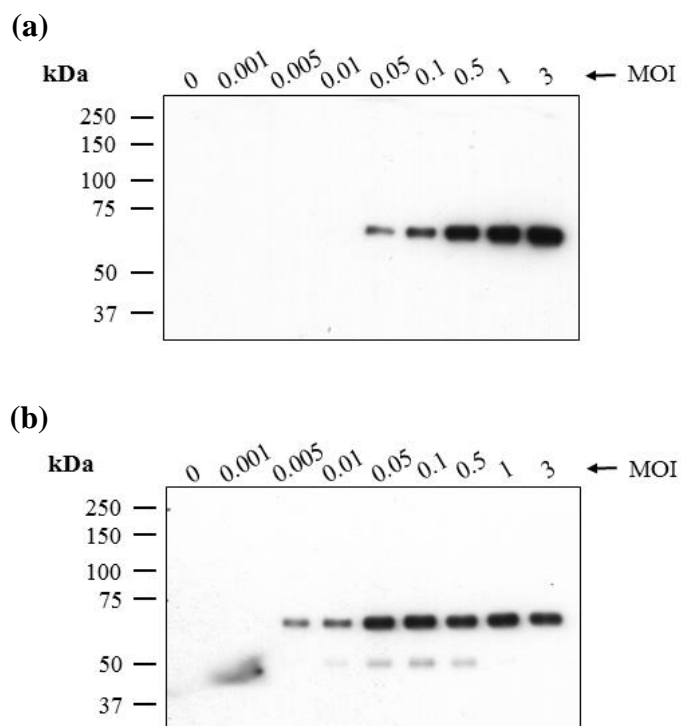
Figure 3.4. Effect of MOI on the expression and secretion of CD36 ED-12His from Sf21 and Hi5 insect cells.
Adherent (**a**) Hi5 and (**b**) Sf21 cells (1×10^6) were infected in 35mm dishes with *flashBAC Gold* baculovirus encoding CD36 ED-12His at a range of MOIs. The culture media (2ml) was recovered 72 hours post-infection. Samples (10µl) were loaded onto a SDS polyacrylamide gel and the proteins separated by electrophoresis. The blot was prepared on PVDF membrane and probed using anti-CD36 antibody clone 1955 (R&D systems). MOI, multiplicity of infection.

When Hi5 insect cells were infected with a range of MOIs (Figure 3.4 (a)), increasing levels of secreted CD36 ED-12His were detected from MOI=0.05 to MOI=3, suggesting that a higher MOI is favourable for maximum CD36 ED-12His yields in Hi5 insect cells. This is consistent with inefficient budding of recombinant virus from Hi5 cells and a requirement for high MOI to infect all cells in the population. However, when Sf21 insect cells were infected with the same range of MOI (Figure 3.4 (b)), CD36 ED-12His secretion was detected with an MOI as low as 0.005. Maximum CD36 ED-12His was observed with an MOI of 0.05. No further increase in CD36 ED-12His production was detected at higher MOI. This result showed that a low MOI could be used when infecting Sf21 insect cells, producing the same amount of CD36 ED-12His as that achieved when using a high MOI. Although Sf21 insect cells were shown to express and secrete less CD36 ED-12His than Hi5 insect cells overall, the ability to generate more CD36 ED-12His using a lower MOI, and therefore less demand for high viral titres, suggests that Sf21 may be a good compromise and a suitable host for large-scale cultures.

3.2.3. Buffer exchange is necessary prior to nickel affinity purification of CD36 ED-12His

Using the recombinant *flashBAC Gold*-CD36ED, small-scale insect cell infections were performed in suspension (100ml) to optimise purification by nickel affinity chromatography. Spent insect cell media containing secreted CD36 ED-12His was collected and centrifuged to pellet any cells or cell debris present. Before purification

could be performed the spent media was buffered exchanged into purification buffer (50mM HEPES, 300mM NaCl, 20mM imidazole, pH 7.4) using a tangential cross-flow diafiltration system (Vivaflow 200, Sartorius), increasing the low pH (to ~pH 7.4) and removing small contaminants (e.g. divalent cations, histidine, glycine) which would interfere with the purification process. The same system was also used to concentrate the sample to a final volume of 20ml. Samples were taken before and after diafiltration and analysed by western blot to measure any loss of CD36 ED-12His during the process (

Figure 3.5).
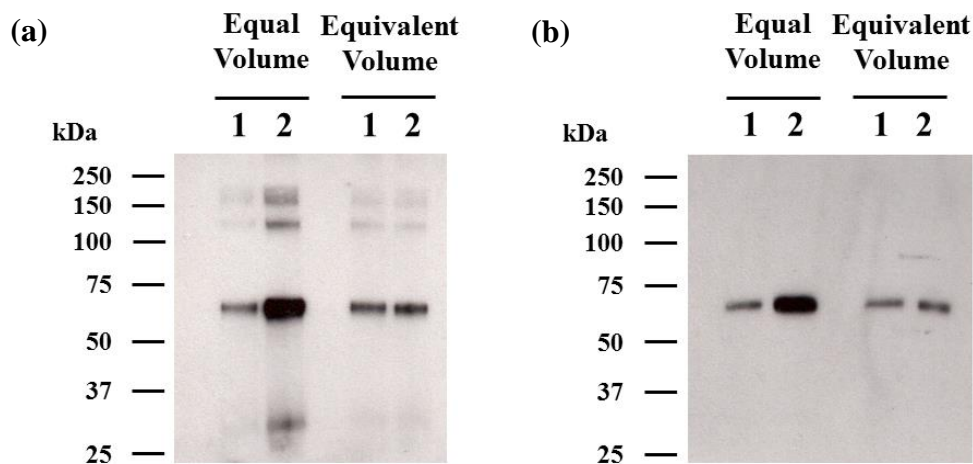
Figure 3.5. Western blot analysis of harvested CD36 ED-12His before and after diafiltration.
Spent Sf21 insect cell media (100ml) containing secreted CD36 ED-12His was buffer exchanged using a tangential flow diafiltration system (Vivaflow 200, Sartorius) into 50mM HEPES, 300mM NaCl, 20mM Imidazole, pH 7.4 and concentrated to a final volume of 20ml. Samples pre- (1) and post- (2) diafiltration were taken and loaded onto an SDS polyacrylamide gel and the proteins separated by electrophoresis. The blot was prepared on PVDF membrane and probed using either **(a)** anti-CD36 antibody clone 1955 (R&D systems) or **(b)** anti-His (C-term) antibody clone 3D5 (Life Technologies). For equal volume lanes, 5µl of either pre- and post-diafiltration samples were loaded. For equivalent volume lanes, 5µl of pre- and 1µl of post-diafiltration samples were loaded to account for differences in total sample volume. A similar result was obtained using CD36 ED-12His secreted from Hi5 insect cells in spent Hi5 insect cell media (not shown).

Following diafiltration of spent culture media into purification buffer, no loss of CD36 ED-12His was observed. Additionally, probing the western blot with an anti-His antibody (Figure 3.5 (b)) confirmed that the secreted CD36 ED retained the poly-histidine tag required for nickel affinity purification.

3.2.4. Batch purification of CD36 ED-12His by nickel affinity chromatography

Once the spent media had been buffer exchanged and concentrated, nickel affinity chromatography was performed to purify CD36 ED, utilizing the C-terminal 12x histidine tag. In nickel affinity chromatography, nickel ions are immobilised by the chelator nitrilotriacetic acid (NTA) (Hochuli *et al*., 1987), which for these batch purification processes, is bound to an agarose resin (Ni-NTA agarose Qiagen). The poly-histidine tag of CD36 ED has a high affinity for Ni-NTA allowing separation of CD36 ED from other proteins present. Any proteins which may bind to the resin non-specifically (or with low avidity) can be removed by washing the resin with low concentrations of imidazole which competes with the imidazole ring of histidine for binding sites on the Ni-NTA. CD36 ED-12His can then be eluted from the resin using a high concentration of imidazole.

CD36 ED-12His in purification buffer (50mM HEPES, 300mM NaCl, 20mM Imidazole, pH 7.4) was incubated with Ni-NTA agarose at a sample to resin volumetric ratio of 10:1. The resin was washed seven times with 20 bed volumes of purification buffer containing 20-100mM imidazole. Bound CD36 ED-12His was

eluted using purification buffer containing 500mM imidazole (4x4ml). Samples from each stage of the purification process were separated by SDS-PAGE and stained with colloidal blue to show total protein present (Figure 3.6 (a)). A corresponding western blot, probed with an anti-CD36 antibody confirmed purification of CD36 ED-12His (Figure 3.6 (b)). The major eluted protein was also confirmed as CD36 ED-12His using LC-MS/MS (see chapter 4).

Elution fractions were pooled and concentrated using an Amicon Ultra-15 centrifugation device (Millipore). The concentration of protein was estimated using densitometry in comparison with a BSA standard curve. Densitometric analysis was also used to measure the purity of sample. From a 100ml insect cell suspension culture infected with *flashBAC Gold* baculovirus encoding CD36 ED-12His, maximum yields of 115µg and 55µg were purified from Hi5 and Sf21 insect cells, respectively. Purity was estimated to be ~91% and ~82%, for purified CD36 ED-12His from Hi5 and Sf21 insect cells, respectively.

(a)

(b)
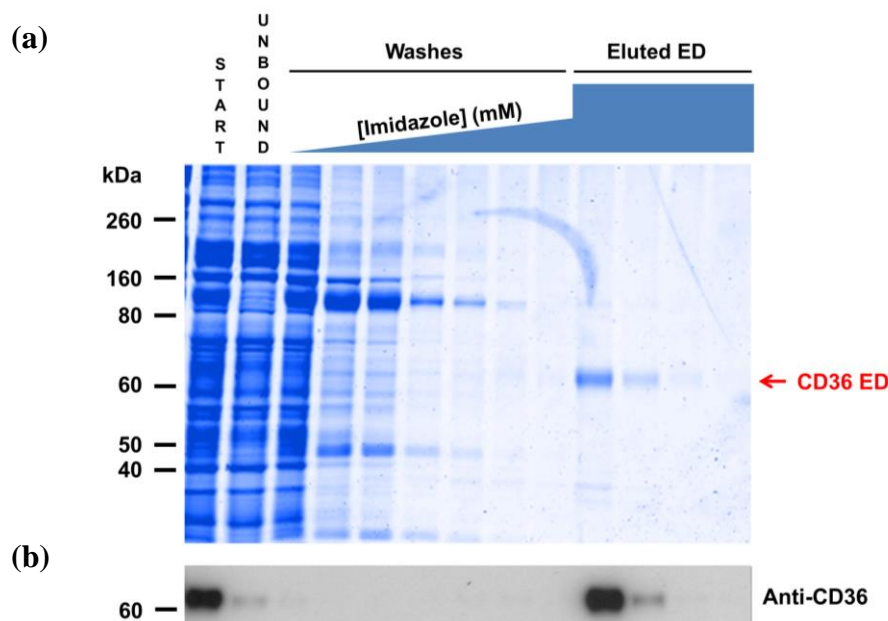
Figure 3.6. Small-scale nickel affinity purification of CD36 ED-12His secreted from Hi5 insect cells.
(a) Crude protein sample (start, 0.4% of total) was incubated with Ni-NTA agarose at a sample to resin volumetric ratio of 10:1. Unbound sample (0.4% of total) contains protein not bound to resin. Washes with increasing concentration of imidazole (20-100mM, 4% of total) were used to remove protein bound non-specifically. CD36 ED-12His was eluted with 4x4ml washes of 500mM imidazole (4% of total). Samples were loaded onto a SDS polyacrylamide gel and the proteins separated by electrophoresis and stained with colloidal blue stain. **(b)** Equivalent samples were diluted 1 in 1000 and loaded onto a SDS polyacrylamide gel and the proteins blotted onto PVDF membrane and probed using anti-CD36 antibody clone 1955 (R&D systems). A similar profile was obtained for purification from Sf21 insect cells (not shown).

3.2.5.   Deglycosylation of purified CD36 ED-12His

CD36 is heavily glycosylated at nine asparagines in the ED (Hoosdally *et al*., 2009). Although this post-translational modification could serve many roles including modulation of ligand binding, providing protease resistance or ensuring correct folding and trafficking to the membrane, the addition of large heterogeneous glycans can be detrimental to crystal formation. Despite insect cells not producing glycans with the same complexity as those seen in mammalian cells, these simple glycans may still present difficulties for later structural studies. To overcome this possible

114

difficulty, the enzyme PNGase F was used to try and remove N-linked glycans present on CD36 ED-12His secreted from both Hi5 and Sf21 insect cells. PNGase F is an endoglycosidase capable of cleaving nearly all forms of glycan from the asparagine residues of N-linked glycoproteins (Tretter et al., 1991).

Spent culture media from Hi5 and Sf21 insect cells infected with *flashBAC Gold* encoding CD36 ED-12His was denatured and treated with PNGase F before analysis by western blot (Figure 3.7).
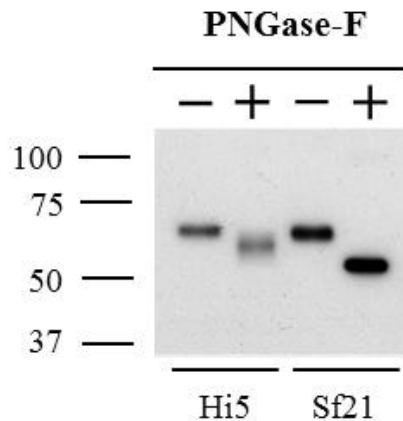
Figure 3.7. Deglycosylation of CD36 ED-12His secreted from Hi5 and Sf21 insect cells using PNGase-F.
Spent media containing, 3μl and 9μl, CD36 ED-12His from Hi5 and Sf21 insect cells, respectively, was treated with 500U of PNGase-F for 2 hours at 37°C. Samples were loaded onto a SDS polyacrylamide gel and the proteins separated by electrophoresis. The blot was prepared on PVDF membrane and probed using anti-CD36 antibody clone 1955 (R&D systems).

Digestion of CD36 ED-12His secreted from Sf21 insect cells with PNGase F resulted in an increase in electrophoretic mobility and formation of a sharp band migrating with an electrophoretic mobility corresponding to a molecular weight just above 50kDa. The predicted molecular weight of the mature CD36 ED-12His (in the absence of the cleaved signal sequence) without post-translational modifications is

48kDa. Digestion of CD36 ED-12His secreted from Hi5 insect cells also resulted in an increase in electrophoretic mobility but the effect was not as pronounced with the treated protein migrating as a diffuse band around 60kDa suggesting failure to remove all glycan groups. These data suggest that the glycans introduced by Hi5 cells are distinct from those introduced by Sf21 cells.

Having found that the maximum yield of recombinant protein from Sf21 insect cells could be achieved by using a low MOI and that the glycans introduced by Sf21 cells could be removed from CD36 ED-12His using PNGase F, it was decided that further experiments to optimise expression and purification of CD36 ED-12His should be performed using the Sf21 insect cell line.

3.2.6.   Native CD36 ED-12His produced from Sf21 cells can be deglycosylated by PNGase F

The standard protocol for using PNGase F to deglycosylate proteins requires the sample to first be heated to 95°C in the presence of detergent and reducing agent. This causes the protein to unravel allowing PNGase F to gain access to all glycans that may have otherwise been buried within the tertiary structure. Although the resulting protein lacks heterogeneous glycan groups, it has also lost its three-dimensional structure making subsequent structural studies pointless. Having deglycosylated the CD36 ED-12His under denaturing conditions, experiments were undertaken to determine whether deglycosylation could be achieved under native conditions, thus preserving protein structure important for future biochemical and

biophysical studies. Purified protein was therefore treated with PNGase F without detergent or reducing agents, for a period of up to 3 days (Figure 3.8). The results suggest that it is possible to deglycosylate native CD36 ED-12His secreted from Sf21 insect cells within 2hrs and that the molecular weight of the deglycosylated protein is stable for several days thereafter.
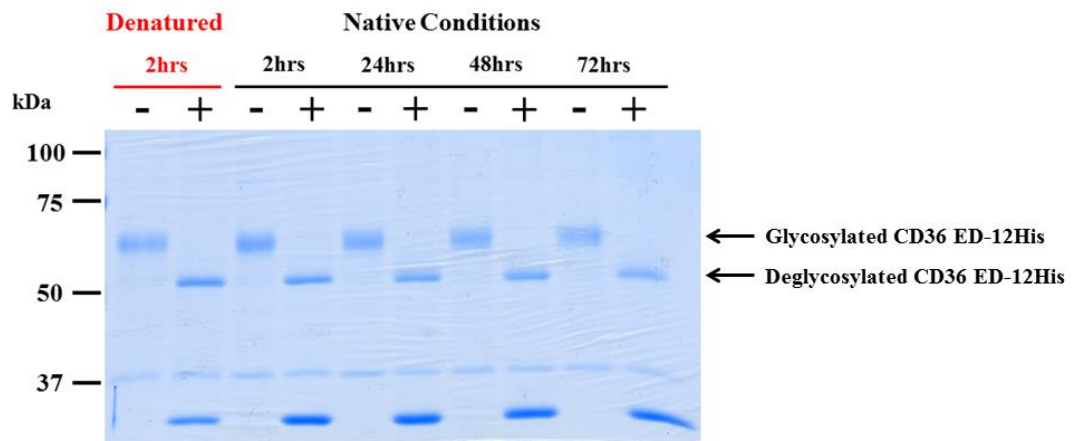
Figure 3.8. Deglycosylation of purified CD36 ED-12His secreted from Sf21 insect cells under native conditions.
Purified ED produced in Sf21 cells was treated with PNGase F (500U) under denaturing conditions for 2 hours at 37°C or for 2, 24, 48 or 72 hours at 37°C, without detergent or reducing agents. Samples were loaded onto a SDS polyacrylamide gel and the proteins separated by electrophoresis. The gel was stained with colloidal blue. − CD36 ED-12His not treated with PNGase F. + treated with PNGase F.

3.2.7. Affinity of purified CD36 ED for modified LDL

Although it was shown that CD36 ED-12His can be expressed and secreted from insect cells and purified, there was no evidence as yet to show that the protein was folded correctly and able to bind ligand. A ligand binding assay was therefore performed using fluorescently-labelled acetylated low-density lipoprotein (alexa fluor 488-acLDL, Life Technologies) to mimic the modified lipoprotein ligand, oxidised low-density lipoprotein (oxLDL) (Hoosdally *et al.*, 2009). AcLDL is known to be more stable than oxLDL and have a similar binding affinity as oxLDL for CD36 on the surface of cells. In this binding assay, increasing concentrations of alexa fluor 488-acLDL were added to purified CD36 ED-12His immobilised on a microtitre plate coated with Ni-NTA (see section 2.6.14). The data were analysed using GraphPad Prism software version 5.0 with a saturation binding curve which was best fitted by the Langmuir adsorption equation (Equation 3.1), that describes a single binding site being bound by a single ligand. When applied to alexa fluor 488-acLDL binding to immobilised CD36 ED-12His, **B** is bound alexa fluor 488-acLDL (relative fluorescence units), **[L]** is the concentration of alexa fluor 488-acLDL (µg/ml) and **K_D** is the concentration of alexa fluor 488-acLDL that gives half maximal binding and is used as a measure of the affinity of alexa fluor 488-acLDL for CD36 ED-12His

$$B = \frac{B_{max} \times [L]}{K_D + [L]} \longrightarrow K_D = \frac{[L](B_{max} - B)}{B}$$

Equation 3.1. The Langmuir Adsorption Equation.

The calculated mean K_D for the binding of alexa fluor 488-acLDL with immobilised CD36 ED-12His purified from Sf21 insect cells +/- standard error (SE) was 6.2µg/ml +/- 0.9µg/ml (n=3) (Figure 3.9). In 2009, it was shown that full-length CD36 purified from Sf21 insect cells bound acLDL with a K_D value +/- SE of 6.4µg/ml +/- 1.5µg/ml. It was also shown that the K_D value for the binding of acLDL to CD36 expressed transiently on the surface of mammalian HEK293T cells +/- SE was 8.3µg/ml +/- 1.4µg/ml (Hoosdally *et al*., 2009). Comparing the data obtained here with previously published data shows that the affinity of acLDL for CD36 ED-12His is similar to that of full-length CD36 suggesting that the ED is folded correctly and retains the ability to bind modified LDL independent of the rest of the protein.
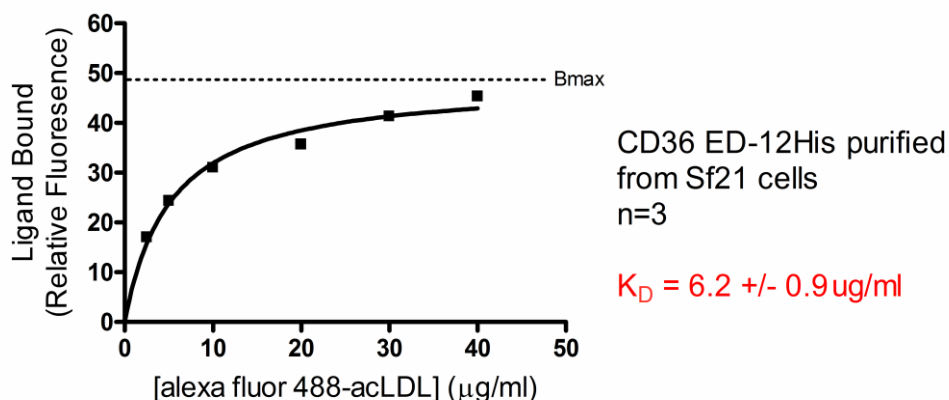
Figure 3.9. Interaction of CD36 ED-12His purified from Sf21 insect cells with alexa fluor 488-acLDL.

3.2.8. Deglycosylated CD36 ED retains affinity for acetylated low-density lipoprotein

It has been shown previously that N-linked glycosylation is necessary for efficient trafficking of CD36 to the plasma membrane, but the pattern of glycosylation sites occupied is not important and did not appear to have an impact on binding of acLDL (Hoosdally *et al*., 2009). This suggested but did not prove that the glycans were unimportant for acLDL binding. To investigate this further, purified CD36 ED-12His was deglycosylated under native conditions using PNGase F and immobilised on a microtitre plate coated with Ni-NTA. A ligand binding assay was performed as described previously and the K_D value for binding of alexa fluor 488-acLDL to deglycosylated CD36 ED-12His +/- SE was measured as 5.8μg/ml +/- 0.6μg/ml (Figure 3.10). This value is not significantly different to the K_D obtained for glycosylated CD36 ED-12His and demonstrates that N-linked glycosylation of CD36 ED is not required for binding of modified LDL. It also shows that the glycan structures can be removed from native CD36 with no loss in the ability of the CD36 ED to bind ligand and demonstrates the potential utility of this protein for biochemical and biophysical analyses.

The figure shows a binding curve with the y-axis labeled "Ligand Bound (Relative Fluorescence)" ranging from 0 to 60, and the x-axis labeled "[alexa fluor 488-acLDL] (μg/ml)" ranging from 0 to 50. A dashed line at 50 is labeled "Bmax". Text annotations read: "Deglycosylated CD36 ED-12His purified from Sf21 cells, n=3" and "K_D = 5.8 +/- 0.6ug/ml".
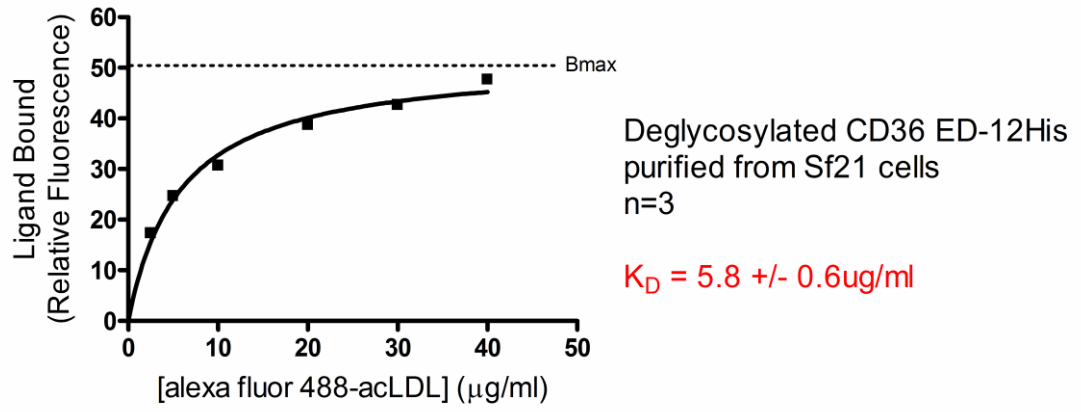
Figure 3.10. Interaction of deglycosylated CD36 ED-12His purified from Sf21 insect cells with alexa fluor 488-acLDL.

3.2.9. Large scale expression and purification of CD36 ED-12His from Sf21 insect cells

Scale-up of protein production is necessary for production of milligram quantities of CD36 ED-12His. I have shown already that Sf21 insect cells can produce maximum protein yields using a low MOI and that subsequent purification of CD36 ED-12His from a 100ml suspension culture could yield ~0.5mg of pure protein per litre of culture. To obtain milligram quantities of CD36 ED-12His, 5 litres of Sf21 insect cells were grown in suspension using a Wave Bioreactor (GE Healthcare) and infected with *flashBAC Gold*-CD36ED at an MOI of 0.05. Spent media was harvested 72 hours post-infection and centrifuged to remove cells and cell debris. Concentration and buffer exchange of spent media was achieved through use of a tangential cross-flow filtration hollow fibre cartridge. The spent media was concentrated to 500ml before buffer exchange using 5L of purification buffer.

An automated protein purifier (AKTA Prime Plus, GE Healthcare) was used to purify the CD36 ED-12His. The main advantage of this system is the ability to purify protein on a much larger scale while reducing the amount of contact time needed. In addition, protein binding and elution can be monitored in real-time with sensors recording numerous parameters including absorbance of the solution at 280nm (A280). The crude sample in binding buffer was passed through a 5ml a HisTrap HP binding column (GE Healthcare) at a low flow rate (0.3ml/min) to allow CD36 ED-12His to bind. To remove non-specific protein, the column was washed with purification buffer containing 100mM imidazole, passed continuously through the column for 20 column volumes at a flow rate of 0.5ml/min. The bound CD36

ED-12His was then eluted in purification buffer containing 500mM imidazole also at a flow rate of 0.5ml/min and collected in 2ml fractions. Fractions containing protein were identified based on the A280 reading (Figure 3.11 (a)). Samples from fractions 18-44 were separated by SDS-PAGE in the presence (Figure 3.11 (b)) and absence (Figure 3.11 (c)) of reducing agent and then stained with colloidal blue to identify fractions containing CD36 ED-12His.

Major contaminants that bound to the column in addition to CD36 ED-12His eluted early in the elution profile, causing a defined peak in the A280 trace (fractions 21-27). CD36 ED-12His eluted gradually (fractions 22-44) leading to the formation of a shoulder to the right of the initial A280 peak. This slow dissociation of His-tagged CD36 ED and subsequent A280 shoulder is characteristic of his-tagged proteins. Fractions separated by SDS-PAGE, prepared with reducing agents, showed that CD36 ED-12His eluted between fractions 22 to 44 (Figure 3.11 (b)). Compared to batch purification, performed previously (see section 3.2.4), purification of a large-scale suspension culture using this column format resulted in the elution of more non-specific proteins along with CD36 ED-12His. In the absence of reducing agent, clearly defined species were also evident migrating more slowly through the gel (Figure 3.11 (c)). These bands corresponded roughly to double, triple, and higher order molecular weights than would be expected for purified monomeric CD36 ED-12His, suggesting that these might represent higher order homo-multimers of CD36 ED-12His. Due to the complexity of the banding pattern generated following SDS-PAGE it was not possible to accurately calculate the yield from the large scale purification by the method used for the small scale purification (see section 3.2.4).

To understand the nature of the higher molecular weight species observed and to further purify CD36 ED-12His, size-exclusion chromatography (SEC) was performed under non-reducing conditions.

(a)

(b)

(c)
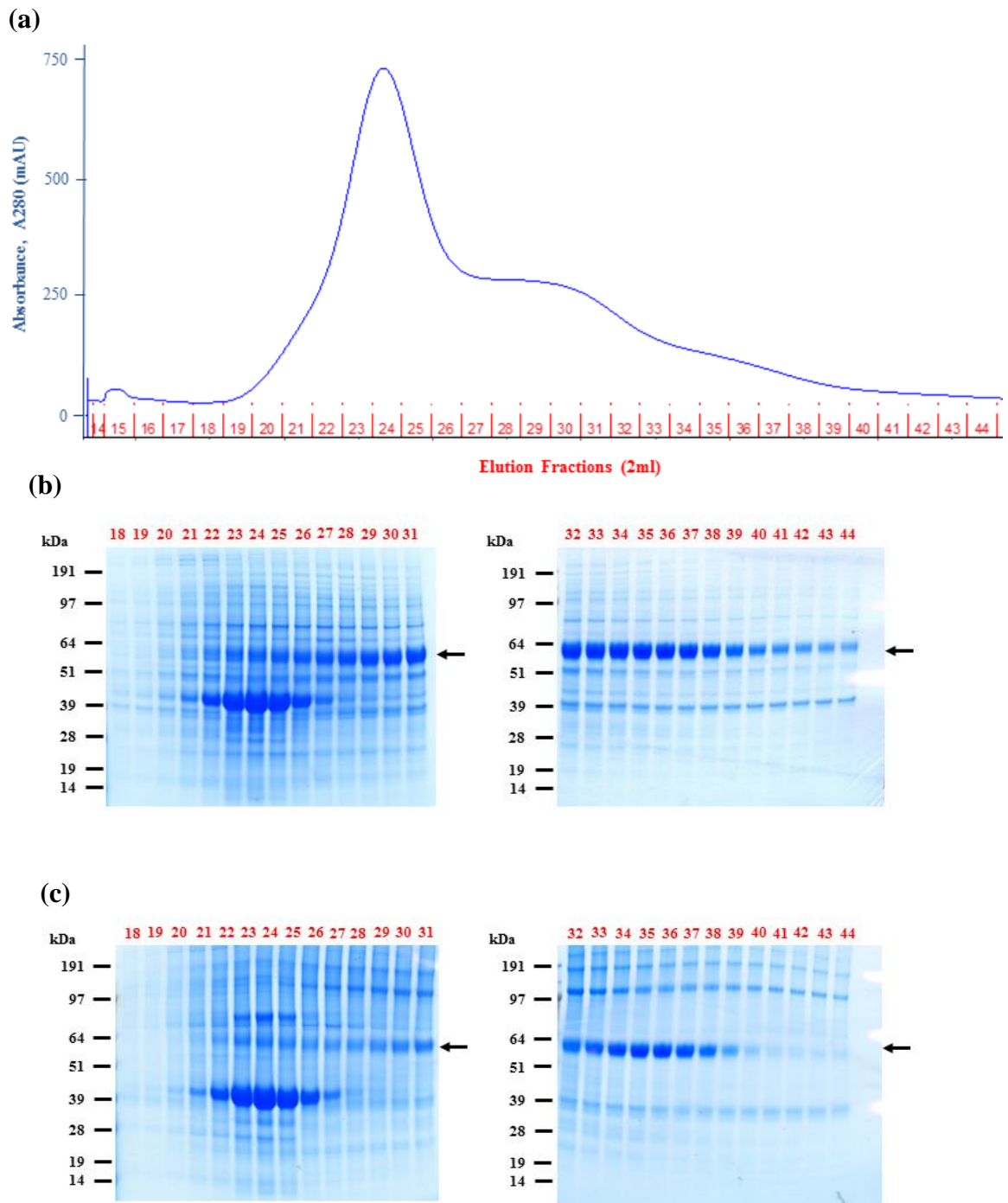
Figure 3.11. Large-scale nickel affinity purification of CD36 ED-12His secreted from a 5L culture of Sf21 insect cells.
CD36 ED-12His was eluted in 2ml fractions from a 5ml HisTrap HP column using 500mM Imidazole. **(a)** Eluted protein was observed as an increase in the A280 reading. Fractions (0.5% of the total volume) under the A280 peak and shoulder (18-44) were loaded onto a SDS polyacrylamide gel and the proteins separated by electrophoresis and stained with colloidal blue. Samples prior to loading were either heated at 75°C for 10mins in the presence **(b)** or the absence **(c)** of 5% β-mercaptoethanol. Arrows indicate predicted CD36 ED-12His.

3.2.10. Separation of purified proteins by size-exclusion chromatography

SEC is a chromatographic technique that allows the separation of proteins by size (Fekete *et al*., 2014). The basic principle is that as a protein mixture in solution is passed down a column packed with a porous matrix, the flow of smaller proteins is hampered as they pass through the pores in the matrix, whereas larger proteins cannot enter the pores as readily and so pass through the column with less hindrance. This results in large proteins eluting from the column first followed by the elution of progressively smaller proteins.

Previously, I showed that purification of CD36 ED-12His from a large-scale suspension culture resulted in the co-purification of proteins of sizes other than that the size expected of CD36 ED-12His. SEC was therefore employed to try to separate these proteins, further purifying CD36 ED-12His. Fractions (29-44) collected during nickel affinity purification (see 3.2.9) were pooled, dialysed against dialysis buffer (50mM HEPES, 300mM NaCl, pH7.4) and then concentrated to around 1ml. The sample was electrophoresed through an SDS-polyacrylamide gel in the presence and absence of reducing agent (Figure 3.12 (a)). When stained with colloidal blue, the complexity of the overloaded sample is apparent, but the highly enriched CD36 ED-12His migrating at around 63kDa remained evident. More monomeric CD36 ED-12His could still be observed in the reduced sample compared to the non-reduced sample. The sample was then passed through a Superdex 200 10/300 GL SEC column (GE Healthcare), with a separation range of 10-600kDa. Eluted protein was collected in 1ml fractions (Figure 3.12 (b)). The proteins in the fractions were then

separated by SDS-PAGE, prepared in the presence and absence of reducing agent (Figure 3.12 (c)). CD36 ED-12His eluted from the column in every fraction collected (Figure 3.12 (c)), suggesting that CD36 ED-12His existed at a range of molecular weights from 10kDa to 600kDa (the separation range of the column). More monomeric CD36 ED-12His could be seen at the expected molecular weight in the reduced samples. The lower amount of CD36 ED-12His detected in non-reduced samples corresponded with the appearance of clearly defined higher molecular weight proteins.

Taken together, these observations suggest that CD36 ED-12His may homo-associate in solution and that the higher molecular weight species detected represent oligomeric forms of the protein. To determine whether these higher molecular weight proteins were indeed CD36 ED-12His of origin, SEC elution fractions were analysed by western blotting using an antibody against CD36. SEC fractions (A7-A11) were separated by SDS-PAGE in the presence and absence of reducing agent prior to electroblotting onto a PVDF membrane and probing with the anti-CD36 antibody (Figure 3.13).

In addition to detecting CD36 ED-12His at the expected monomeric molecular weight of around 63kDa, higher molecular weight species were also detected. As shown previously with colloidal blue staining (Figure 3.12 (c)), more CD36 ED-12His was present at the monomeric molecular weight in reduced samples while the majority of the CD36-ED12His in the non-reduced samples migrated much more slowly through the gel. The presence of CD36 ED-12His at the monomeric molecular weight in early fractions, expected to elute proteins up to 600kDa (e.g. A6-A7) suggests the aggregation process may be dynamic and reversible. If this assumption is true then the detection of CD36 ED-12His predominantly at the

monomeric molecular weight in later fractions might suggest that homo-association

may be concentration dependent.
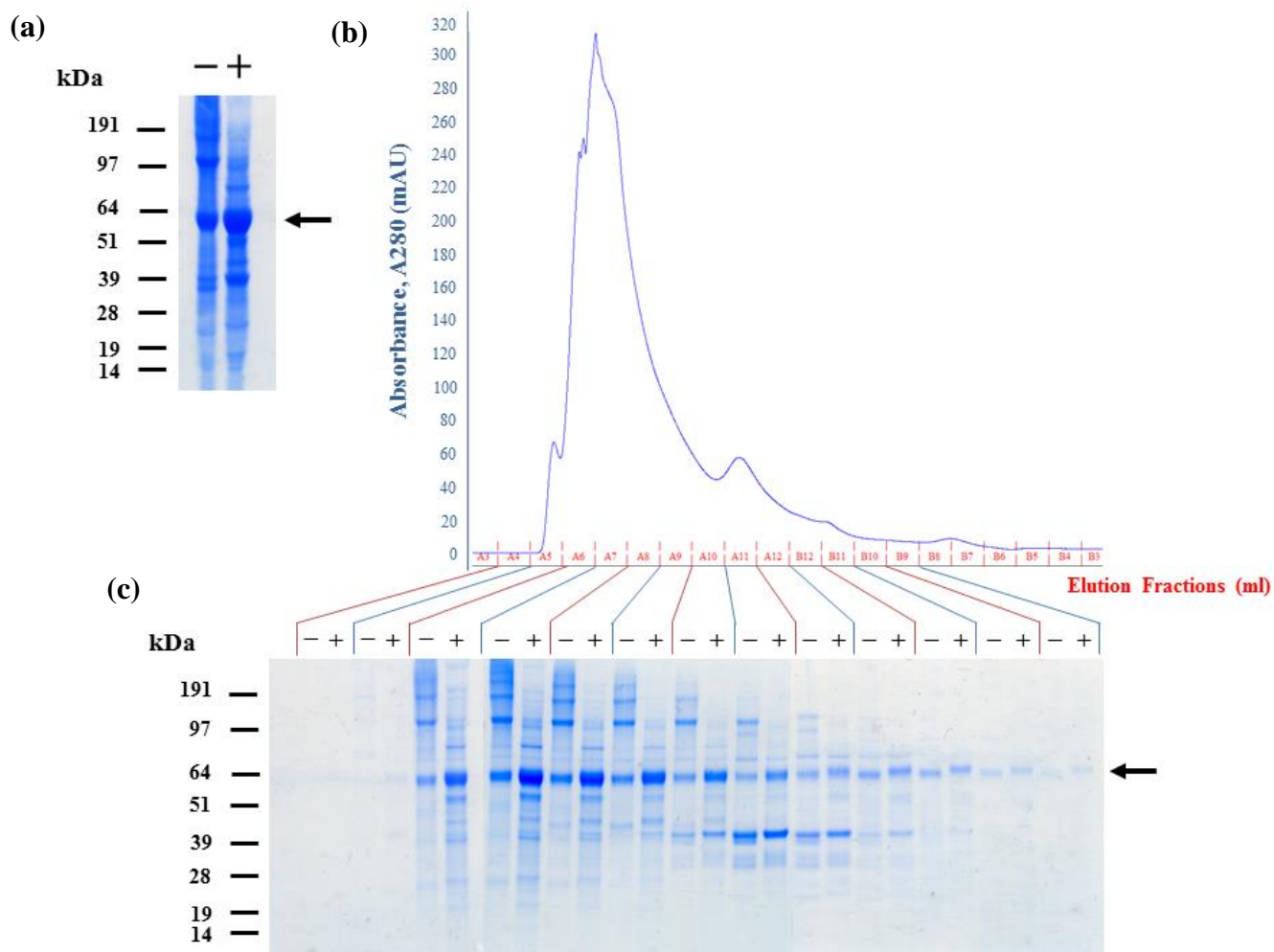
Figure 3.12. Separation of purified CD36 ED-12His and co-purifying proteins using size exclusion chromatography.
(a) Concentrated HisTrap-purified CD36 ED-12His (1%) was loaded onto a SDS polyacrylamide gel having in the absence (-) or presence (+) of 5% β-mercaptoethanol and then separated by electrophoresis and stained with colloidal blue. Arrow indicates the expected molecular weight of monomeric CD36 ED-12His **(b)** Separation of concentrated proteins was performed using a Superdex 200 10/300 GL size exclusion column (GE Healthcare). The separation range of the column was 10-600kDa. 1ml fractions were collected. **(c)** SEC fractions (1% of total volume) were loaded onto a SDS polyacrylamide gel in the absence (-) or presence (+) of 5% β-mercaptoethanol and then separated by electrophoresis and stained with colloidal blue.
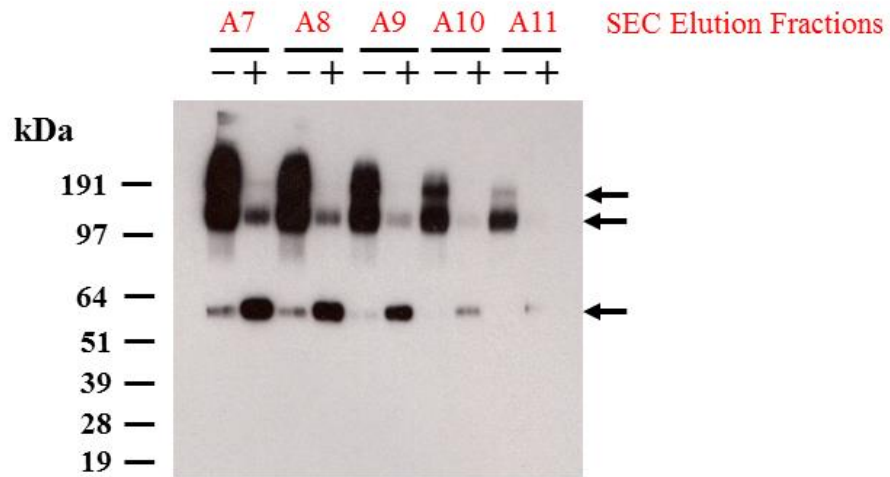
Figure 3.13. CD36 ED-12His exists as higher molecular weight species in solution.
SEC fractions (0.01%) were loaded onto a SDS polyacrylamide gel in the absence (-) or presence (+) of 5% β-mercaptoethanol. Proteins were separated by electrophoresis, blotted onto PVDF membrane and probed using anti-CD36 antibody, clone 1955 (R&D systems). Arrows indicate different molecular weight forms of CD36 ED-12His detected.

3.3. Discussion

The use of baculovirus expression systems to produce recombinant proteins is an attractive alternative to bacteria, yeast and mammalian expression systems. Although bacteria have now been discovered to be able to produce post-translational modifications such as N-linked glycosylation (Schwarz and Aebi, 2011), these biochemical pathways do not appear to be sufficient to mimic the type of glycans required for efficient trafficking of mammalian-like proteins such as CD36 to the plasma membrane. It is shown in this chapter that it is possible to express and secrete the ED of CD36 successfully from insect cells with protein yields comparable to the yield obtained from a mammalian cell line. Despite insect cells producing simpler N-linked glycosylation than mammalian cells, this simplicity may be an advantage for structural studies. During these studies the crystal structure of the soluble domain of another class B scavenger receptor, the lysosomal protein, LIMP-2, was solved (Neculai *et al*., 2013). Expressed and secreted from Sf9 insect cells this soluble domain was purified by nickel affinity chromatography and size-exclusion chromatography to produce milligram quantities of protein which subsequently led to the formation of crystals with the deduction of a 3Å resolution model. Furthermore, this domain was crystallised with glycans present on all 9 putative N-linked glycosylation sites. The LIMP-2 crystal structure has been used to model the structure of CD36, however the usefulness of such a model is debatable given the medium resolution of the LIMP-2 structure. The relevance of a homology model to CD36-ligand interaction would also be limited given that LIMP-2 is unlikely to share many ligands with CD36. A true structure of CD36, based on direct

biophysical analyses remains elusive, but would be needed to answer these questions.

The *flashBAC Gold* baculovirus expression system which lacks the non-essential *ChiA* and *v-cath* genes was found to produce more secreted CD36 ED-12His in both Hi5 and Sf21insect cell lines compared to both the *flashBAC* and the *Profold-ER1* expression systems. Despite the removal of the *v-cath* gene which encodes the protease v-cath endopeptidase, the increased yield of CD36 ED-12His generated using *flashBAC Gold* compared to the *flashBAC* system is unlikely to be caused by decreased proteolytic digestion of the newly translated protein. This is because v-cath endopeptidase is expressed as the inactive pro-v-cath form which is only activated to v-cath in the presence of chitinase, which is absent from both *flashBAC* expression systems. Increased CD36 ED-12His secretion using the *flashBAC Gold* system is therefore likely to be due to the absence of pro-v-cath accumulation within the ER, freeing up space within the secretory pathway, allowing the cellular mechanisms to fold and modify CD36 ED-12His more efficiently. The *profold-ER1* expression system produced the least amount of secreted CD36 ED-12His of all the baculovirus expression systems tested. It has been shown on numerous occasions, including during this study, that CD36 can be expressed, modified and trafficked to the plasma membrane without the aid of mammalian-like chaperones in insect cells (Hoosdally *et al*., 2009, Martin *et al*., 2007, Jimenez-Dalmaroni *et al*., 2009). A lower yield of CD36 ED-12His using the *Profold-ER1* system may be due to the insect cells having to produce two additional recombinant proteins (calreticulin and PDI) which may, effectively, compete with CD36 ED-12His for translation and translocation sites on the ER.

The ability to produce CD36 ED-12His using Sf21 insect cells infected with *flashBAC Gold* at a low MOI increases the appeal of using this baculovirus/insect cell system for large-scale protein production which would normally require large amounts of baculovirus to achieve optimal protein yields. Using a low MOI saves on cost and also saves on time by removing the need to amplify baculovirus as frequently to replenish working stocks. Other studies have shown that similar yields of protein can be obtained using a low MOI to produce recombinant within 72 hours and, by incubating the cells for longer, the overall yield of protein can be increased over infections using a high MOI over the same time period (Liebman *et al*., 1999). However, the production of heterologous proteins using baculoviruses is ultimately a cell-lytic expression system in insect cells and so therefore care should be taken to ensure longer infection times do not also increase the amount of cytosolic proteins, including proteases, released into the media which could have a negative impact on the yield.

Immobilised metal ion affinity chromatography (IMAC) is one of the most popular methods for purification of heterologous recombinant proteins (Cheung *et al*., 2012). Polyhistidine tags offer a simple purification process needing only the fusion of a few extra amino acids at either the N- or C-terminus of the protein (Paramban *et al*., 2004), which rarely have an impact on the protein fold or function (Terpe, 2003). The use of a double hexahistidine tag has been shown to improve the affinity of tagged protein for nickel (Khan *et al*., 2006) and has been shown previously to improve recombinant CD36 binding to a Ni-NTA matrix (Martin *et al*., 2007), allowing a higher degree of purification. Small-scale purification using nickel affinity chromatography exploiting the C-terminal double hexahistidine tag on CD36

ED was shown in these studies to be an effective method of purification, resulting in purified CD36 ED-12His of around 80-90% purity.

Deglycosylation experiments showed that Hi5 insect cells produced N-linked glycans on CD36 ED-12His which were insensitive to PNGase F. The inability to remove glycans from the Hi5 insect cell derived mouse Cd36 (mCd36) ED has been observed previously (Jimenez-Dalmaroni *et al*., 2009), and was attributed to the ability of Hi5 insect cells to produce core α(1-3)-linked fucose saccharides which would make N-linked glycans insensitive to cleavage by PNGase F (Tretter *et al*., 1991). The nature of N-linked glycosylation found on human CD36 ED-12His secreted from both Sf21 and Hi5 insect cells is explored in more detail in Chapter 4. The CD36 ED-12His derived from Sf21 insect cells was found to be sensitive to cleavage by PNGase F, and the resultant deglycosylated protein migrated with an observed molecular weight of ~50kDa. The subtle difference between this observed molecular weight and the predicted molecular weight based on the unmodified primary structure (~48kDa) is most likely attributed to anomalous migration through the gel. It is, however, possible that additional post-translational modifications such as O-linked glycosylation, (which has been identified previously on recombinant proteins expressed in insect cells (Klenk, 1996, Thomsen *et al*., 1990, Altmann *et al*., 1999) may be present that would slow migration. Thr92 of CD36 has also been shown previously to play an important regulatory role preventing the binding of TSP-1 to CD36 (Chu and Silverstein, 2012), however, mass spectrometry provided no evidence of phosphorylation of CD36 ED-12His secreted from either cell type.

CD36 ED-12His secreted from Sf21 insect cells retained affinity for modified LDL comparable with full-length CD36 purified from insect cells and CD36 on the surface of mammalian cells (Hoosdally *et al*., 2009). Furthermore, it was shown that

native CD36 ED-12His could be deglycosylated and still retain affinity for modified LDL, suggesting that N-linked glycosylation is irrelevant for the binding of this ligand. Previous studies suggested that N-linked glycosylation of CD36 is important for efficient trafficking of the protein to the plasma membrane (Hoosdally *et al.*, 2009). Lauzier *et al.*, have also shown that the glycosylation status of Cd36 in the Spontaneously Hypertensive Rat is altered (along with significant changes in primary amino acid sequence, and abundance in cardiac membranes) leading them to suggest that glycosylation affects the ability of Cd36 to utilise long chain fatty acids in cardiac tissue (Lauzier *et al.*, 2011).

Large-scale purification of CD36 ED-12His revealed the possible presence of higher molecular weight forms of CD36 ED-12His when fractions were analysed in the presence and absence of reducing agent. The inability to separate these different forms of CD36 ED-12His using SEC suggests that oligomer formation may be dynamic and reversible. During the purification of the soluble domain of LIMP-2, Neculai, *et al.*, reported similar higher molecular weight species. Despite this, they were able to isolate enough 'monomeric' protein following SEC to produce crystals (Neculai *et al.*, 2013). They suggested that the hydrophobic face of a helical-bundle located towards the apex of the protein may have been responsible for dimerization (a site also identified for ligand binding). The ability of CD36 to form oligomers has been documented previously. In 1997, it was shown that CD36 on the surface of platelets and transiently-transfected COS-7 cells formed multimers that could be disrupted by reducing agents (Thorne *et al.*, 1997). It was proposed that the association was mediated through intermolecular disulphide bridges. However, CD36 has no free cysteine residues within the ED, with all six involved in intramolecular disulphide bridging (Rasmussen *et al.*, 1998). A more likely

explanation is that the reducing agent disrupts the intramolecular disulphide bridging resulting in conformational change within the ED, to indirectly disrupt homo-dimeric interaction.

Further studies should be employed to assess the stability and possible disruption of these higher molecular weight species. The higher molecular weight species can be observed prior to buffer exchange or purification (Figure 3.5 (a)), suggesting that interaction occurs as soon as the protein is secreted from the insect cell with the rate of oligomer formation accelerated at higher concentrations. The use of additives, such as glycerol, to minimise aggregation (Vagenende *et al*., 2009, Hamada *et al*., 2009) was ineffective at reducing CD36 ED self-association (data not shown). However, imidazole has been reported to result in protein aggregation (Hefti *et al*., 2001). It was shown by Martin *et al*., that full-length rat Cd36 expressed in insect cells and purified using nickel affinity purification in the presence of the detergent octylglucoside could be isolated as a monomeric form. Interestingly, Cd36 was eluted from the nickel resin using only 250mM imidazole, compared to the 500mM imidazole that was used in the work presented here (Martin et al., 2007). Imidazole, like any other salt, at low concentration can help to stabilise a protein in solution. However, at high concentrations, imidazole may lead to a decrease in protein stability and encourage protein aggregation (Hamada et al., 2009). If this is the case, then it may be possible to avoid these effects by eluting CD36 ED-12His from the nickel surface by lowering of the pH instead of using imidazole, or by switching to a different affinity tag altogether.

The formation of higher molecular weight species of CD36 ED-12His may not ultimately be a problem for crystal formation and subsequent structural studies. Formation of crystals is based on the ability of the protein to form a regular lattice at high concentrations following dehydration (Smyth and Martin, 2000). The presence of CD36 ED-12His as homo-oligomers may therefore aid the formation of crystals. An empiric test of crystallisation conditions using the purified CD36 ED-12His should therefore be explored.

4. Analysis of CD36 Ectodomain N-linked Glycosylation in Insect Cells

4.1. Introduction

Protein post-translational modifications (PTMs) are enzyme-driven covalent chemical modifications of proteins following translation. These modifications can have a profound effect on both protein conformation and stability. Additionally, PTMs can influence cellular localisation as well as playing a role in the activity of those modified proteins. Currently there are over 400 known post-translational modifications, with phosphorylation, acetylation and glycosylation being among the most commonly encountered (Khoury *et al*., 2011, Creasy and Cottrell, 2004).

The ectodomain (ED) of CD36 is known to be heavily glycosylated, with 10 putative N-linked glycosylation sites. The glycosylation site occupancy has previously been characterised for full-length human CD36 heterologously expressed in both insect and mammalian cells (Hoosdally *et al*., 2009). Despite identifying nine of the ten glycan sites as being occupied, the nature of these glycans has never been characterised. In chapter 3 it was shown that CD36 ED could be secreted from Sf21 and Hi5 insect cells. It was subsequently shown that glycans present on CD36 ED secreted from Hi5 insect cells were insensitive to enzymatic cleavage using PNGase F. In contrast, the glycans present on purified CD36 ED from Sf21 insect cells were shown to be sensitive to PNGase F treatment. To better understand the nature of the

glycans added to the CD36 ED in insect cells, mass spectrometry was used to determine putative N-linked glycan site occupancy and the composition of the structures generated in each insect cell line.

4.1.1. N-linked Glycosylation

There are two main types of glycosylation; N-linked glycosylation and O-linked glycosylation (Moremen *et al*., 2012). These two modifications occur with attachment of a glycan to proteins either via an amide group (N-linked) or a hydroxyl group (O-linked). Another form of glycan attachment, termed C-linked glycosylation, involves the addition of a glycan via the indole C2 carbon atom on the side chain of tryptophan residues (Hofsteenge *et al*., 1994, Furmanek and Hofsteenge, 2000).

N-linked glycosylation is known to be important for a range of cellular functions including signal transduction, cell adhesion and cell migration (Isaji *et al*., 2004, Ono *et al*., 2000, Zhong *et al*., 2004). It has also been shown to confer protease resistance on proteins (Sareneva *et al*., 1995). Abnormal N-linked glycosylation has been implicated in a number of diseases including cancer (Leroy, 2006, Kobata and Amano, 2005).

4.1.1.1.   Biosynthesis of N-linked glycosylation

The synthesis of N-linked glycans on proteins in eukaryotes occurs in two separate compartments within the cell, the endoplasmic reticulum (ER) and the Golgi apparatus. The initial synthesis, addition and trimming of a core oligosaccharide to a growing nascent polypeptide chain occurs in the ER. At this stage all of the glycans are homogeneous. Correctly folded glycoproteins are then transported to the Golgi apparatus where the oligosaccharides are trimmed further before becoming elongated to form glycosylation which can be complex and heterogeneous.

4.1.1.2.   N-linked glycosylation in the ER

The N-glycosylation process begins with the formation of a 14 saccharide core unit attached to the amide nitrogen of asparagine residues within the N-linked glycosylation sequon, Asn-X-Ser/Thr, where X can be any amino acid except for a proline residue. This core glycan is shared by all eukaryotes, with a predefined structure of $Glc_3Man_9GlcNAc_2$ (Kornfeld and Kornfeld, 1985)(Figure 4.1).
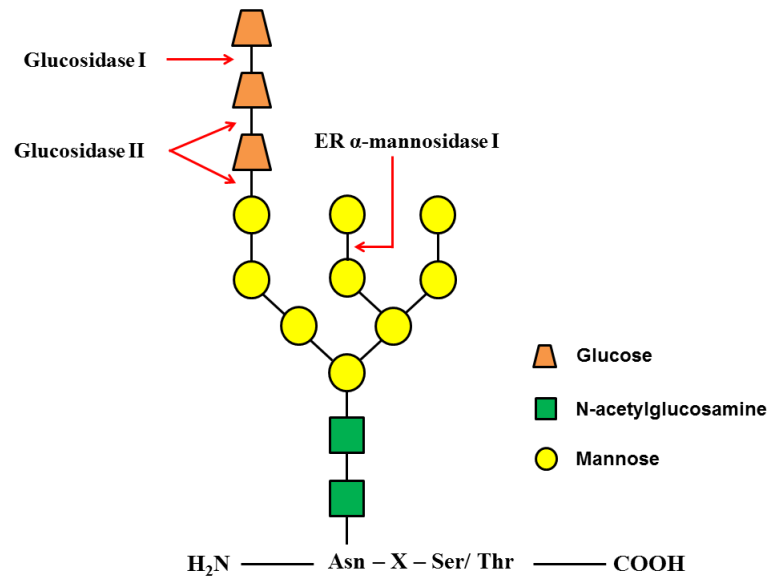
Figure 4.1. Common core N-linked glycan.
This predefined glycan is common to all eukaryotes. The core oligosaccharide which is initially synthesised on a lipid carrier molecule consists of two N-acetylglucosamines, nine mannoses and three glucoses. Arrows indicate sites of cleavage which occur as part of the quality control processes present within the ER. Modified from Helenius, A. & Aebi, M. 2001. Intracellular functions of N-linked glycans. *Science,* 291, 2364-9. Reprinted with permission from AAAS.

Presynthesis of the oligosaccharide occurs at the cytosolic face of the ER with the addition of saccharides to the lipid carrier molecule, dolichol-pyrophosphate (DPP), by monosaccharide transferases (Burda and Aebi, 1999) (Figure 4.2). Following the addition of the first seven saccharide units, an ATP-independent bi-directional floppase 'flops' the sugars to the luminal side of the ER membrane (Hirschberg and Snider, 1987, Helenius *et al*., 2002). Once the final terminal glucose unit has been added to form the core glycan, oligosaccharyltransferase (OST) recognises this structure and transfers it to the Asn on the nascent polypeptide (Burda and Aebi, 1998, Spiro, 2000, Zufferey *et al*., 1995). It is thought that the addition of glycans aids the folding of the protein either directly through stabilisation of the local protein structure (Petrescu *et al*., 2004) or indirectly through association with the molecular chaperones calnexin and calreticulin, which recognise and bind sugar groups

(Williams, 2006). It is in combination with calnexin and calreticulin that a quality control cycle is established to ensure proteins are processed correctly (Caramelo and Parodi, 2008). Immediately following transfer of the core glycan to the nascent polypeptide, the first and second glucose saccharides are cleaved by glucosidase I and then glucosidase II, respectively (Hammond *et al*., 1994). The resultant monoglucosylated glycan is then free to bind either calnexin (for a transmembrane ER proteins) or calreticulin (for soluble ER proteins), which facilitates the folding of the protein (Ou *et al*., 1993, Helenius *et al*., 1997). The remaining glucose saccharide is then cleaved by glucosidase II, releasing the protein from the chaperone. If the protein has folded incorrectly, it is recognised by UDP-Glc:glycoprotein glucosyltransferase (UGT), which re-glycosylates the glycan resulting in binding to the chaperone again to allow refolding (Sousa *et al*., 1992, Caramelo and Parodi, 2008). The process of binding to and release from the chaperone continues until the protein either folds correctly or alternatively is targeted to the proteasome in the cytosol for degradation (Caramelo and Parodi, 2008). Once the protein has been folded properly, ER α-mannosidase I cleaves one mannose saccharide from the glycan before export of the protein from the ER to the Golgi apparatus (Hammond *et al*., 1994).
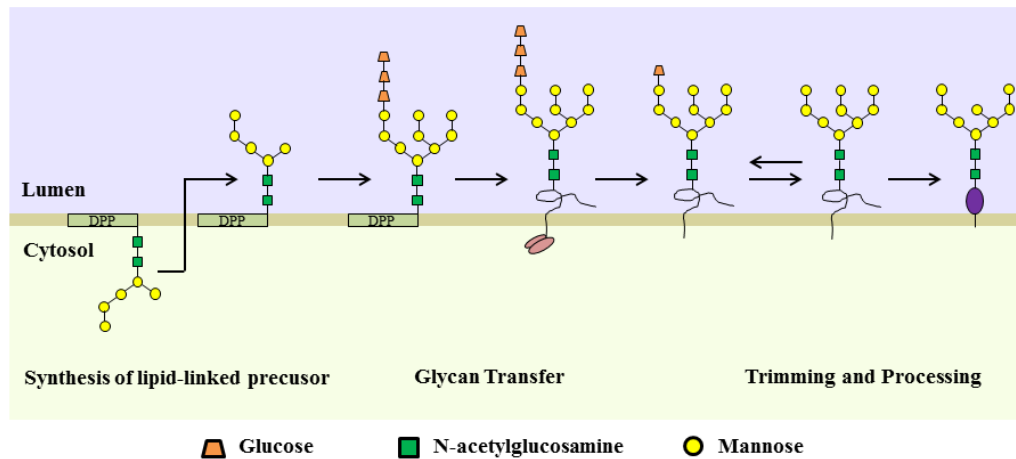
Figure 4.2. Processing of N-linked glycans in the ER.
N-linked glycans are synthesised initially as a precursor on the cytosolic side of the ER membrane before being flipped into the ER lumun. The core glycan is transferred onto the asparagine within the sequon of the growing polypeptide before being trimmed prior to entering a quality control cycle with calnexin/calreticulin. Following removal of one mannose saccharide, the correctly folded protein can be transported to the Golgi apparatus. Modified from Helenius, A. & Aebi, M. 2001. Intracellular functions of N-linked glycans. *Science,* 291, 2364-9. Reprinted with permission from AAAS.

4.1.1.3. N-linked glycosylation in the Golgi apparatus

As proteins pass through the Golgi apparatus, they are further modified before they are trafficked to their final destination. In the lumen of the cis-Golgi, core glycans are initially trimmed by a series of mannosidases to remove more mannose saccharides (Figure 4.3). As the protein passes from the cis- to the trans-Golgi, the glycans are elongated by a wide variety of glycosyltransferases with the use of soluble precursors such as nucleotide sugars (Hirschberg *et al*., 1998). The addition of saccharide units is dependent on both the presence of a particular glycosyltransferase and also the accessibility of the growing glycan (Hsieh *et al*., 1983, Elbein, 1991). Trafficking through the Golgi apparatus usually takes 5-15

minutes (Pelham and Rothman, 2000), allowing a high degree of glycosylation as well as diversity due to the lack of a quality control system. Once glycans have finished being added to the glycoprotein, it is trafficked to its final localisation. The Golgi apparatus lacks the quality control mechanisms of the ER resulting in glycoproteins with defective moieties still being readily exported (Elbein, 1991, Stanley, 1984).
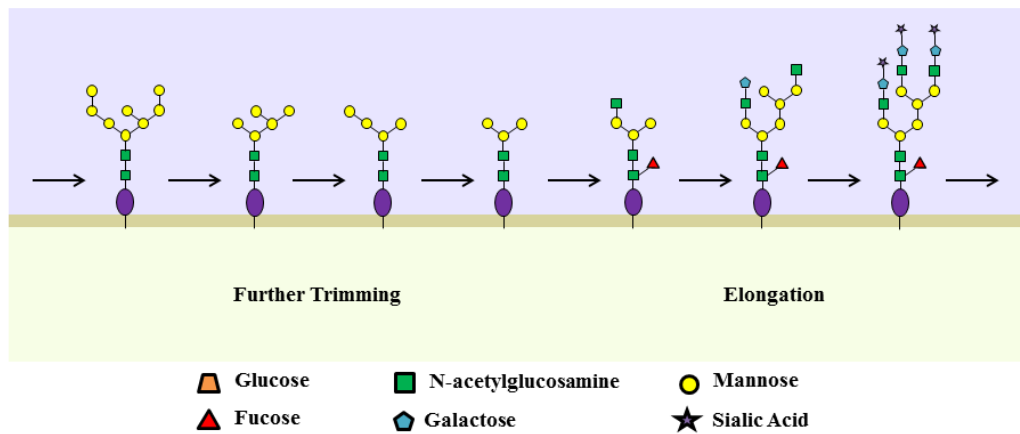
Figure 4.3. Processing of N-linked glycans in the Golgi apparatus.
N-linked glycans undergo further trimming, followed by elongation with the addition of different sugar units depending on the protein, or cell types in which the protein has been expressed. Modified from Helenius, A. & Aebi, M. 2001. Intracellular functions of N-linked glycans. *Science,* 291, 2364-9. Reprinted with permission from AAAS.

4.1.1.4. Insect and Mammalian N-linked Glycosylation

There are three main types of N-linked glycans produced as glycoproteins traffic through the Golgi apparatus: high mannose, hybrid and complex (Figure 4.4). High mannose glycans consist of two N-acetylglucosamines with multiple mannose units attached, resembling the core N-linked glycan structure initially created in the ER. Complex glycans consist of many different types of saccharide, including more than the two core N-acetylglucosamines. Hybrid glycans consist of both high mannose and complex glycans. As eukaryotes, both insect and mammalian cells recognise the same consensus sequon when it comes to addition of the core N-linked glycan in the ER. It is in the Golgi apparatus however that the glycosylation events in insect cells and mammalian cells differ. Whereas mammalian cells can produce glycans with diverse terminally sialylated complex glycan structures (Beyer *et al*., 1979, Aricescu and Owens, 2013), glycans from insect cells have traditionally been seen as high mannose, pauci-mannosidic in structure (Hsieh and Robbins, 1984). Despite this, there is increasing evidence that some insect cells lines may be capable of producing more complicated glycans, more closely resembling hybrid structures (Rendic *et al*., 2008). With the use of insect cells as a popular alternative host for the expression of recombinant proteins, it is therefore important to characterise the glycosylation status of these proteins to improve the understanding of the role that glycosylation may have on protein function, and also because the glycans may have an impact on downstream biophysical studies. This type of analysis is possible by mass spectrometry.
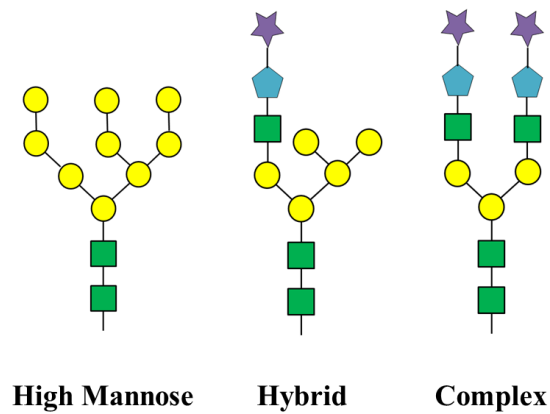
Figure 4.4. Three main types of N-linked glycans.
As glycoproteins move from the medial to trans- portion of the Golgi apparatus a variety of glycosyltransferases add sugar units to the core glycan forming three main types of glycans.

4.1.2. Mass Spectrometry

Mass spectrometry (MS) is an analytical chemistry technique that is used to determine the mass of a molecule by measuring the mass/charge (m/z) ratio of its ions. The use of MS has expanded greatly over the last few decades with MS playing an important role in the study of proteins, peptides and other biological molecules (Aebersold and Mann, 2003). Applications of MS include amino-acid sequencing to characterise peptides and identify interacting proteins, monitoring enzyme reactions, establishing purity of a sample and also the determination of post-translational modifications (Bantscheff *et al*., 2012).

Despite many different forms of mass analysers having been developed, the underlying principle remains the same (Figure 4.5). Following introduction into the instrument, the sample is converted into gaseous charged ions within an ionisation

146

chamber. These ions are then accelerated through a mass analyser consisting of an electric or magnetic field which deflects and separates ions according to the m/z ratio. Ions bombard a detector which amplifies the signal, displaying the relative abundance of each ion that is detected as a function of the m/z ratio. By correlating known masses or characteristic fragmentation patterns with those masses detected, sample identification is possible. To ensure that the sample is not hindered by air molecules when passing through the instrument, the ionisation chamber, mass analyser and detector are under a high vacuum.
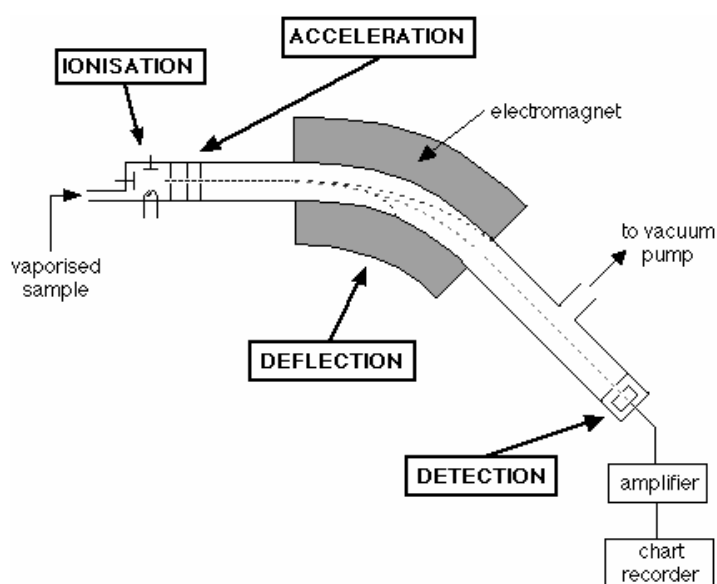
Figure 4.5. Basic components of a mass spectrometer.
A vaporised sample is ionised to form charged ions in the ionisation chamber. Ions are then accelerated through a mass analyser, deflected by a strong electromagnetic field onto a detector. Deflection of ions is based on the m/z ratio. The relative abundance for each ion as a function of the m/z ratio can be used in the identification of protein samples. (http://www.chemguide.co.uk/analysis/masspec/howitworks.html#top, website accessed: 31/08/14).

4.1.2.1. Liquid chromatography tandem mass spectroscopy (LC-MS/MS)

LC-MS/MS, using electrospray ionisation (ESI), combines the physical separation of a protein solution (using liquid chromatography, LC) with the mass analysis of a mass spectrometer (MS). The protein sample having been enzymatically digested is passed down a capillary liquid chromatography column to separate peptide fragments, reducing the complexity of the sample. As fragments are eluted from the column they pass through a needle in the presence of a strong electric field resulting in vaporisation of the sample forming a spray of multiply charged droplets, directed to the mass analyser.

Tandem mass spectrometry (MS/MS) consists of multiple mass spectrometric steps, usually involving further fragmentation of charged ions. Although multiple complex systems have been developed, they all follow the same basic principles. Ionised sample is introduced into the mass analyser (e.g. via ESI). These charged ions, termed precursor ions, are deflected and separated based on their m/z ratio. Isolated precursor ions are then further fragmented usually through high energy bombardment. The resulting charged product ions can provide more detailed information about the structure and composition of a protein compared to single step MS, a fact that has greatly enhanced the ability to study post-translational modifications such as glycosylation.

The successful fragmentation of precursor ions is critical for MS/MS. There are many different methods now available to further fragment precursor ions, each capable of producing different types of fragmentation. Collision-induced dissociation (CID) and other related fragmentation techniques have been used extensively of late to study the glycosylation status of many different proteins (Singh *et al*., 2012, Gonzalez *et al*., 1992).

4.1.2.2.   Collision-induced dissociation

During CID, one or more collisions occur between precursor ions and neutral gas molecules (such as helium, nitrogen or argon), producing a vibrational energy that redistributes over the precursor ion. This vibrational energy results in breakage of peptide bonds along the peptide backbone, generating b- and y-type fragments (Figure 4.6) (Paizs and Suhai, 2005) and/or leading to loss of small neutral molecules, such as water and/or ammonia or other fragments derived from side chains (Kertesz *et al*., 2009). By detecting progressively larger b-ions from the N- to C-termini and y-ions from the C- to N-termini it is possible to sequence the peptide fragment by correlating observed masses with the characteristic mass of each individual amino acid residue.
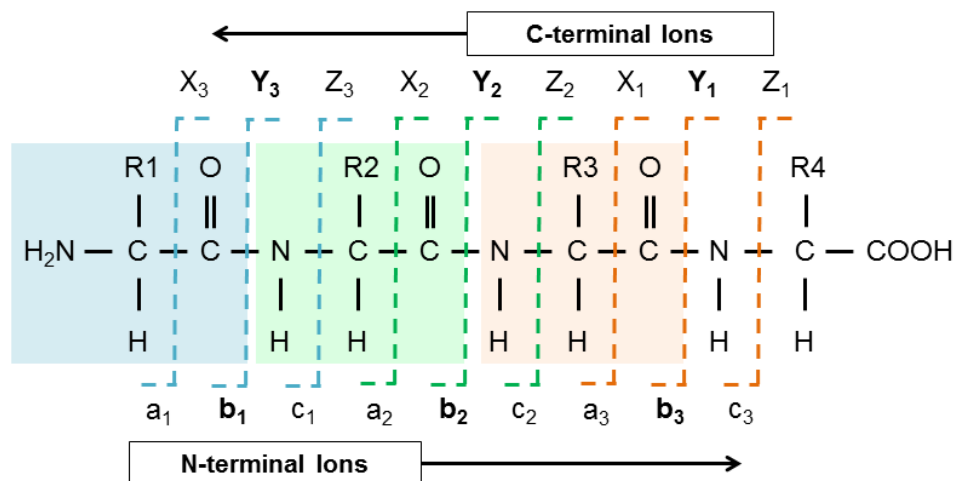
Figure 4.6. Fragmentation of charged precursor ions during LC-MS/MS.
Collision induced dissociation (CID) creates vibrational energy resulting in breakage of peptide bonds along the peptide backbone, generating b- and y-type ions. Other fragmentation methods can cause breakage of other bonds along the peptide backbone, such as electron transfer dissociation (ETD) which breaks N-Cα bonds, generating c- and z-type ions.

4.1.2.3. Higher Energy Collision Dissociation Product Ion-Triggered Electron Transfer Dissociation

Although CID is effective for analysis of small, low-charged peptide ions, CID is not suitable for detection of peptides with post-translational modifications. These modifications hinder the ability of CID to efficiently break peptide bonds and form b- and y-ions. Consequently it is possible to identify glycans present within a fragment population but not possible to localise the glycan to a particular amino acid residue. In contract to CID, which induces fragmentation of peptides at the site of peptide bonds, electron transfer dissociation (ETD) induces cleavage of N-Cα bonds generating c- and z-type ions (Figure 4.6) which can also be used for peptide

fragment sequencing. Another important feature of ETD-type dissociation is that it does not lead to the loss of post-translational modifications and so is therefore able to provide both sequence information and the localisation of modified sites. Another type of fragmentation method similar to CID is beam-type CID, as opposed to conventional ion-trap CID. Beam-type CID, also known as higher energy collision dissociation (HCD), uses higher activation energy over a shorter activation time, compared to traditional ion-trap CID. This results in not only producing b- and y-ions and glycan-peptide fragments, as with ion-trap CID, but also formation and detection of low-abundance oxonium product ions, such as N-acetylglucosamine (m/z 204) and mannose-N-acetylglucosamine (m/z 366), characteristic to all glycopeptides. One problem associated with studying N-linked glycosylation is the inherent heterogeneity in glycan structures found on a single protein as well as within a protein population. By coupling the glycan structures detected by CID and using the detection of oxonium ions by HCD as a trigger for subsequent ETD analysis of the same peptide precursor ion, it is possible to overcome the challenge of glycan heterogeneity, allowing targeted analysis of glycopeptides. This method of CID-HCD product-ion triggered ETD provides information on the site of glycosylation and peptide sequence (ETD spectrum) and through HCD (and CID) provides information on glycan structure (Singh *et al.*, 2012).

4.2. Results

4.2.1. Enzymatic deglycosylation of CD36 ED

To confirm the identity of the purified CD36 ED and to provide the first indication of glycosylation site occupancy approximately 2µg of purified CD36 ED-12His from both Sf21 and Hi5 insect cells was treated with endoglycosidase peptide-N-glycosidase F (PNGase F), which cleaves the innermost N-acetylglucosamine and asparagine (N) residue of high mannose, hybrid and complex N-linked oligosaccharides present on glycoproteins (Maley *et al*., 1989)(Figure 4.7 (a)). PNGase F cleaves N-linked glycans by hydrolysing the side chain of the asparagine residue, converting the asparagine residue into an asparartic acid. This process of deamidation is characterised by a mass increase of approximately +1Da. As PNGase F will only convert an asparagine residue into an aspartic acid when a cleavable glycan is present, protein sequencing by mass spectrometry can easily identify sites which have been occupied with a glycan.

One type of N-linked glycan is insensitive to PNGase F; where the innermost N-acetylglucosamine saccharide is attached to an α(1-3)-linked fucose sugar (Tretter *et al*., 1991). Fucose attached by this particular linkage is absent from mammalian glycoproteins but present on glycoproteins produced in plant cells, and some insect cells. The α(1-3)-linked fucose has been found to be immunogenic, acting as an epitope for antisera raised against plant glycoproteins (Kurosaka *et al*., 1991) as well as for IgE from individuals allergic to plant and insect material (Altmann, 2007).
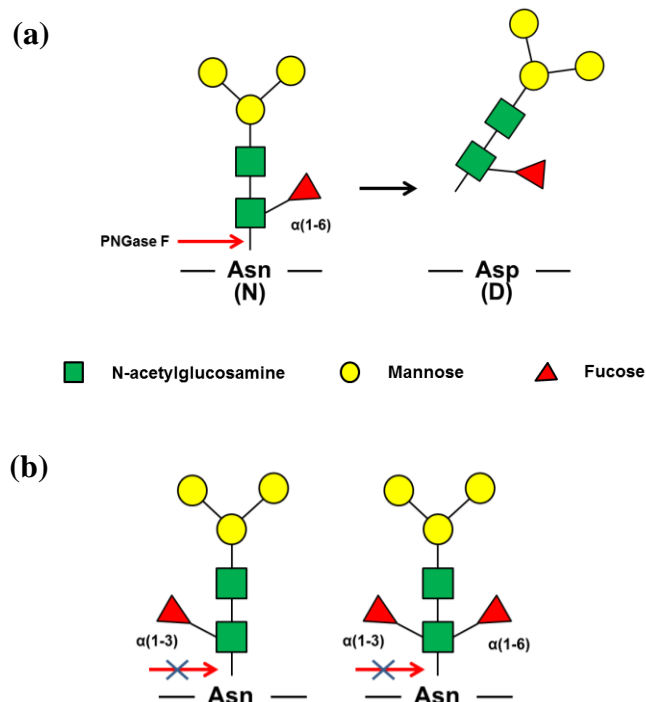
Figure 4.7. N-linked glycan cleavage using the enzyme PNGase F.
(a) PNGase F will cleave high mannose, hybrid and complex N-linked glycans between the innermost N-acetylglucosamine and asparagine residue. **(b)** An exception to this rule is found when a fucose residue is attached to the innermost N-acetylglucosamine residue via an core α(1-3) linked fucose.

4.2.2.   Preparation of protein for mass spectrometry

Purified CD36 ED-12His derived from both Sf21 and Hi5 insect cells was sent to the Advanced Mass Spectrometry Facility at Birmingham University for mass spectrometric analysis. Both glycosylated (25µg) and deglycosylated (2µg) purified CD36 ED-12His were excised from a SDS-PAGE gel and digested (in-gel) with trypsin to yield peptide fragments of known sizes, seven of which contain putative N-linked glycosylation sites (**Error! Reference source not found.**). Trypsin is a erine protease which preferentially cleaves at the carboxyl terminal of the amino

acids lysine and arginine, except if these residues are followed by a proline (Pan *et al*., 2014). Purified CD36 ED-12His derived from Hi5 cells was also digested with chymotrypsin in an attempt to improve coverage of CD36 ED-12His detected by mass spectrometric analysis. Chymotrypsin is another serine protease which preferentially cleaves at the carboxyl terminal of large hydrophobic amino acids (tyrosine, tryptophan and phenylalanine). Digestion of CD36 ED-12His with chymotrypsin was expected to yield 10 fragments, each containing one of the putative N-linked glycosylation sites (**Error! Reference source not found.**). igested protein was extracted from the gel using 0.1% formic acid and then analysed by LC-MS/MS.

Table 4.1. Complete tryptic digest of CD36 ED-12His.
Complete digestion of CD36-12His with typsin generates 42 fragments. Of these fragments, 7 contain putative N-linked glycosylation sites (N). There are 10 putative N-linked glycosylation sites in total. The putative glycosylated asparagines are numbered 1 to 10 with respect to their position within the primary sequence of the ED.

Mass	Amino Acid Number	Peptide Sequence
6953.72	70-133	EN(2)VTQDAEDNTVSFLQPNGAIFEPSLSVGTEADN(3)FTVLNLAVAAASHIYQNQFVQMILNSLIN(4)K
3535.87	307-337	PVYISLPHFLYASPDVSEPIDGLNPNEEEHR
3352.79	153-182	DPFLSLVPYPVTTTVGLFYPYN(5)NTADGVYK
2959.27	204-229	N(7)LSYWESHCDMIN(8)GTDAASFPPFVEK
2783.1	33-55	QFWIFDVQNPQEVMMN(1)SSNIQVK
2294.36	401-419	SQVTGHHHHHHHTGHHHHHH
2175.47	377-395	NYIVPILWLN(10)ETGTIGDEK
2035.24	268-285	AFASPVENPDNYCFCTEK
1957.26	338-354	TYLDIEPITGFTLQFAK
1529.74	230-242	SQVLQFFSSDICR
1484.67	243-255	SIYAVFESDVNLK
1367.65	356-367	LQVNLLVKPSEK

1333.55	10-21	QVVLEEGTIAFK
1299.47	290-301	N(9)CTSYGVLDISK
936.08	146-152	ELLWGYR
922.09	193-200	VAIIDTYK
854	136-142	SSMFQVR
824.89	26-32	TGTEVYR
755.83	58-63	GPYTYR
703.84	256-261	GIPVYR
689.85	262-267	FVLPSK
637.76	396-400	ANMFR
599.77	368-372	IQVLK
575.62	188-192	DN(6)ISK
563.65	183-187	VFNGK
545.64	22-25	NWVK
532.5	1-5	DPSSK
477.61	66-69	FLAK
459.59	286-289	IISK
388.47	143-145	TLR
373.45	373-375	NLK
360.45	6-8	TIK
360.37	304-306	EGR
302.33	56-57	QR
273.34	64-65	VR
249.33	302-303	CK
233.27	134-135	SK
203.24	201-202	GK
174.2	203	R
174.2	355	R
174.2	376	R
146.19	9	K

Table 4.2. Complete chymotrypsin digest of CD36 ED-12His.
Complete digestion of CD36-12His with chymotrypsin generates 47 fragments. Of these fragments, 10 contain putative N-linked glycosylation sites (N). There are 10 putative N-linked glycosylation sites in total. The putative glycosylated asparagines are numbered 1 to 10 with respect to their position within the primary sequence of the ED.

Mass	Amino Acid Number	Peptide Sequence
3093.76	352-378	AKRLQVNLLVKPSEKIQVLKNLKRNY
2662.99	38-60	DVQNPQEVMMN(1)SSNIQVKQRGPY
2469.56	318-339	ASPDVSEPIDGLNPNEEEHRTY
2450.55	400-419	RSQVTGHHHHHHTGHHHHHH
2190.52	1-20	DPSSKTIKKQVVLEEGTIAF
1940.36	123-139	VQMILNSLIN(4)KSKSSMF
1880.98	67-83	LAKEN(2)VTQDAEDNTVSF
1783.92	208-223	WESHCDMIN(8)GTDAASF
1663.96	295-309	GVLDISKCKEGRPVY
1650.85	185-199	NGKDN(6)ISKVAIIDTY
1639.81	385-399	LN(10)ETGTIGDEKANMF
1489.73	282-294	CTEKIISKN(9)CTSY
1442.68	105-118	TVLNLAVAAASHIY
1418.66	224-235	PPFVEKSQVLQF
1365.42	92-104	EPSLSVGTEADN(3)F
1333.51	249-260	ESDVNLKGIPVY
1313.57	140-149	QVRTLRELLW
1043.17	237-245	SSDICRSIY
1105.13	270-279	ASPVENPDNY
1004.15	340-348	LDIEPITGF
965.12	200-207	KGKRN(7)LSY
934.1	162-170	PVTTTVGLF
896.01	24-31	VKTGTEVY
858.99	84-91	LQPNGAIF
852.86	174-181	N(5)NTADGVY
760.93	263-269	VLPSKAF
739.96	379-384	IVPILW
712.85	310-315	ISLPHF

690.84	156-161	LSLVPY
576.7	63-66	RVRF
535.56	119-122	QNQF
533.59	152-155	RDPF
507.59	349-352	TLQF
449.51	32-34	RQF
446.51	21-23	KNW
392.5	182-184	KVF
335.4	246-248	AVF
321.38	260-261	RF
294.35	316-317	LY
282.3	61-62	TY
278.35	36-37	IF
278.31	172-173	PY
268.34	280-281	CF
238.24	150-152	GY
204.23	35	W
181.19	171	Y
165.19	236	F

4.2.3. Analysis of putative N-linked glycosylation sites on PNGase F-treated CD36 ED-12His secreted from insect cells

To determine whether putative N-linked glycan sites were occupied on CD36 ED-12His secreted from Hi5 and Sf21 insect cells, purified CD36 ED-12His was digested with PNGase F and analysed by LC-MS/MS using collision-induced

dissociation to allow sequencing of the protein. Peptides were first separated using a nano-reverse-phase liquid chromatography column before ionisation and direct loading into a LTQ Orbitrap Velos mass spectrometer using ESI. The resulting precursor ions were deflected and then subjected to ion-type CID to form b- and y-type fragments (Figure 4.8). Subsequent fragments were then analysed together to deduce the peptide sequence. Using this approach, PNGase F treated peptide fragments containing putative N-linked glycan sites were considered as occupied by a glycan when conversion of an asparagine residue (N) to an aspartic acid (D) was observed, i.e. had become deamidated (Figure 4.9).

b-ions (N-term) **y-ions (C-term)**

4 → 15
3 → 16
2 → 17
1 → 18

183 – VFNGKD**N(6)**ISKVAIIDTYK - 200
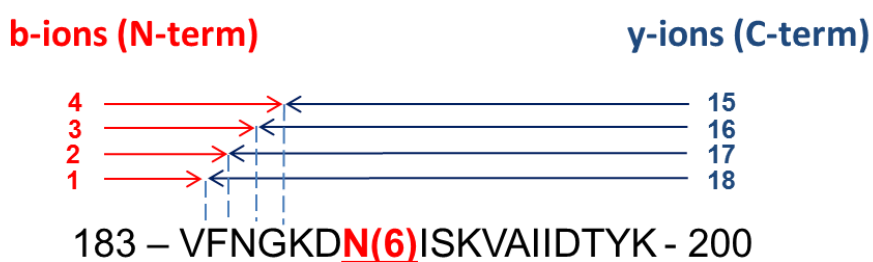
Figure 4.8. Fragmentation of charged precursor ions during LC-MS/MS.
Collision induced dissociation (CID) of precursor ions leads to breakage of peptide bonds along the peptide backbone generating b- and y-type ions. The fragment shown contains the sixth putative glycan site (N6) found within CD36 ED-12His.

(a)
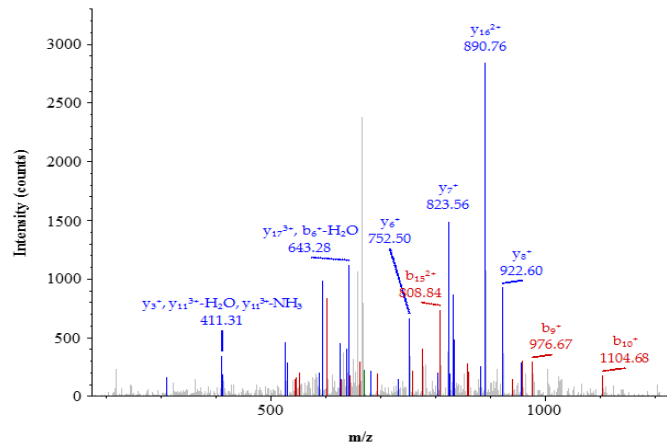
(b)

#1	b^+	b^{2+}	b^{3+}	Seq.	y^+	y^{2+}	y^{3+}	#2
1	100.07570	50.54149	34.03008	V				18
2	247.14412	124.07570	83.05289	F	1927.01720	964.01224	643.01058	17
3	361.18705	181.09716	121.06720	N	1779.94878	890.47803	593.98778	16
4	418.20852	209.60790	140.07436	G	1665.90585	833.45656	555.97347	15
5	546.30349	273.65538	182.77268	K	1608.88438	804.94583	536.96631	14
6	661.33044	331.16886	221.11500	D	1480.78941	740.89834	494.26799	13
7	776.35738	388.68233	259.45731	D (N6)	1365.76246	683.38487	455.92567	12
8	889.44145	445.22436	297.15200	I	1250.73551	625.87139	417.58335	11
9	976.47348	488.74038	326.16268	S	1137.65144	569.32936	379.88866	10
10	1104.56845	552.78786	368.86100	K	1050.61941	525.81334	350.87799	9
11	1203.63687	602.32207	401.88381	V	922.52444	461.76586	308.17966	8
12	1274.67399	637.84063	425.56285	A	823.45602	412.23165	275.15686	7
13	1387.75806	694.38267	463.25754	I	752.41890	376.71309	251.47782	6
14	1500.84213	750.92470	500.95223	I	639.33483	320.17105	213.78313	5
15	1615.86908	808.43818	539.29455	D	526.25076	263.62902	176.08844	4
16	1716.91676	858.96202	572.97711	T	411.22381	206.11554	137.74612	3
17	1879.98008	940.49368	627.33155	Y	310.17613	155.59170	104.06356	2
18				K	147.11281	74.06004	49.70912	1

(c)

#1	b^+	b^{2+}	b^{3+}	Seq.	y^+	y^{2+}	y^{3+}	#2
2	247.14412	124.07570	83.05289	F	1927.01720	964.01224	643.01058	17
3	361.18705	181.09716	121.06720	N	1779.94878	890.47803	593.98778	16
4	418.20852	209.60790	140.07436	G	1665.90585	833.45656	555.97347	15

$b3^+ - b2^+$
$= 114.04$

$b3^{2+} - b2^{2+}$
$= 57.02 \times 2$
$= 114.04$

$b3^{3+} - b2^{3+}$
$= 38.014 \times 3$
$= 114.04$

$y16^+ - y15^+$
$= 114.04$

$y16^{2+} - y15^{2+}$
$= 57.02 \times 2$
$= 114.04$

$y16^{3+} - y15^{3+}$
$= 38.014 \times 3$
$= 114.04$

#1	b^+	b^{2+}	b^{3+}	Seq.	y^+	y^{2+}	y^{3+}	#2
6	661.33044	331.16886	221.11500	D	1480.78941	740.89834	494.26799	13
7	776.35738	388.68233	259.45731	D (N6)	1365.76246	683.38487	455.92567	12
8	889.44145	445.22436	297.15200	I	1250.73551	625.87139	417.58335	11

$b7^+ - b6^+$
$= 115.03$

$b7^{2+} - b6^{2+}$
$= 57.51 \times 2$
$= 115.03$

$b7^{3+} - b6^{3+}$
$= 38.342 \times 3$
$= 115.03$

$y12^+ - y11^+$
$= 115.03$

$y12^{2+} - y11^{2+}$
$= 57.51 \times 2$
$= 115.03$

$b7^{3+} - b6^{3+}$
$= 38.342 \times 3$
$= 115.03$

Figure 4.9. LC-MS/MS analysis of CD36 ED-12His treated with PNGase F.
Collision-induced dissociation of charged precursor ions generated an array of b- and y-type ions as shown in the resulting (**a**) mass spectrum and corresponding (**b**) table of predicted m/z fragment values. Values in red correspond to observed b-type ions. Values in blue correspond to observed y-type ions. The fragment analysed here includes the sixth putative N-linked glycosylation site found in CD36 ED-12His (N6). Deamidated asparagine residues as a result of glycan cleavage by PNGase F are characterised by the conversion of asparagine (N) to an aspartic acid (D) and an apparent mass shift of approximately +1Da, as shown in (**c**).

Seven putative N-glycosylation sites on CD36 ED-12His (N1, N5-N10) purified from Sf21 insect cells were detected as being deamidated, suggesting glycan occupancy at these sites (Figure 4.10). Six putative N-glycosylation sites on CD36 ED-12His (N2-N3, N6 and N9 – N10) purified from Hi5 insect cells were detected as having been deamidated (Figure 4.10).

Putative N-linked Glycan Site	Sf21	Hi5
N1	Deamidated	Not found
N2	Not found	Deamidated
N3	Not found	Deamidated
N4	Not found	Not found
N5	Deamidated	Deamidated
N6	Deamidated	Deamidated
N7	Deamidated	Not found
N8	Deamidated	Not found
N9	Deamidated	Deamidated
N10	Deamidated	Deamidated

Figure 4.10. Summary of putative N-linked glycosylation sites on CD36 ED-12His secreted from insect cells found to be deamidated after digestion with PNGase F.
Purified CD36 ED-12His derived from Hi5 and Sf21 insect cells were treated with PNGase F and then analysed by LC-MS/MS using CID. Deamidated residues indicate putative N-linked glycosylation sites where glycans have been cleaved from asparagine residues, converting asparagine to an aspartic acid (becoming deamidated). Putative glycan sites on peptide fragments which were not detected by mass spectrometric analysis are labelled 'not found'.

4.2.4. Analysis of glycans present on CD36 ED-12His derived from Hi5 and Sf21 insect cells.

To support the mass spectrometry data obtained using CD36 ED-12His treated with PNGase F, a second approach was used to try to determine the exact glycan structures occupying N-linked glycan sites.

Initially LC-MS/MS using CID (ion-type) fragmentation was performed on glycosylated CD36 ED-12His. The CID spectrum (Figure 4.11 (a)) provided information about glycan occupancy on the peptide fragments. However, as the presence of N-linked glycans hindered the formation of b- and y-type ions from the associated peptides, a lack of peptide sequence information was observed. In separate LC-MS/MS experiments, HCD (beam-type CID) was used to produce b- and y-type ions as well as glycan-peptide fragments (Figure 4.11 (b)). HCD also resulted in the formation and subsequent detection of low-abundance oxonium product ions, such as N-acetylglucosamine (m/z 204) and mannose-N-acetylglucosamine (m/z 366), characteristic to all glycoproteins. On detecting these ions, ETD of the same precursor ions was triggered resulting in the formation of c- and z-type ions which enabled the localisation of the glycan to a particular site within the fragment (Figure 4.11 (c)). A list of the glycan structures identified on CD36 ED-12His secreted from Sf21 (Figure 4.12) and Hi5 (Figure 4.13) insect cells are shown.
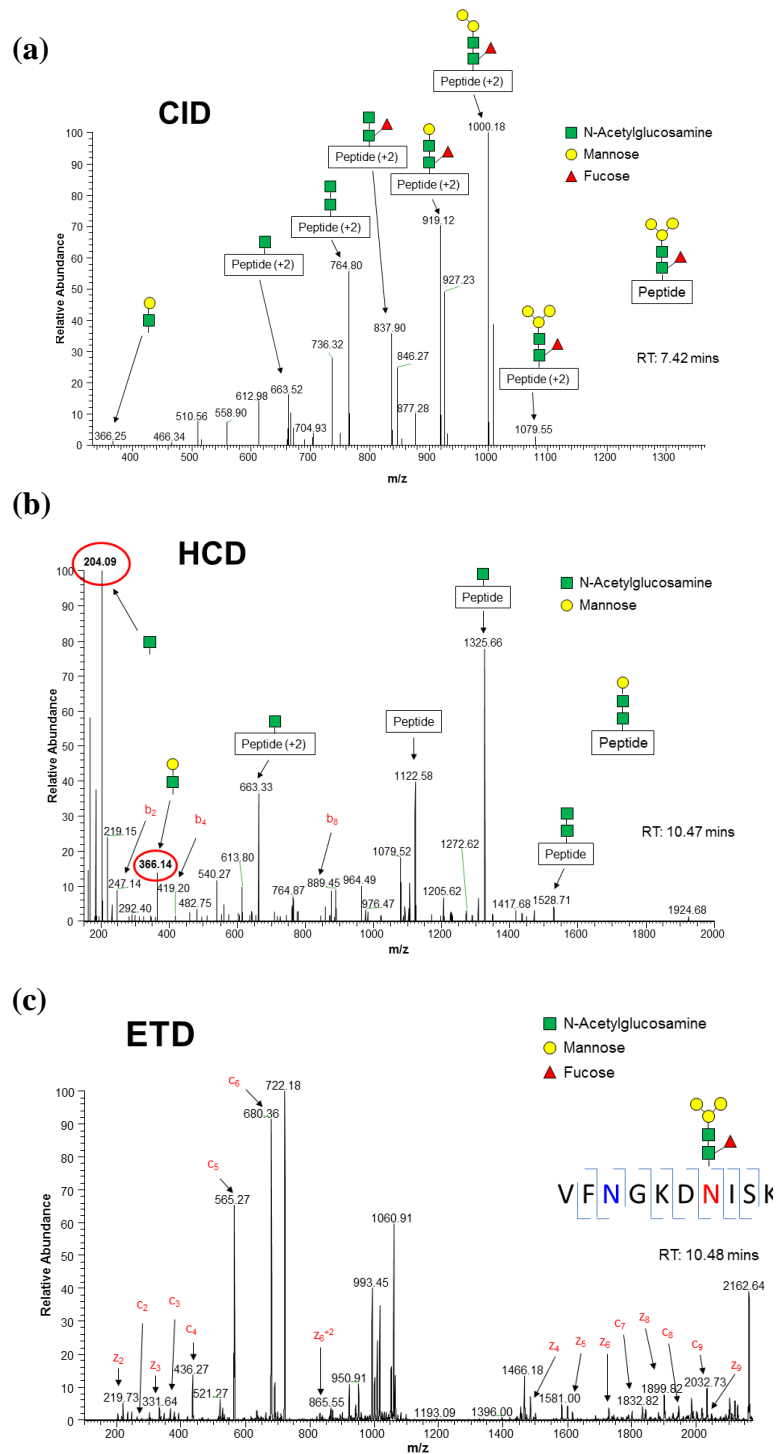
Figure 4.11. CID/HCD product-ion triggered ETD in determining glycan structures occupying specific N-linked glycosylation sites.
(a) Ion-trap collision induced dissociation (CID) fragmentation of precursor ions generated from glycosylated CD36 ED-12His was used to determine glycan structures present on a peptide fragment. The presence of N-linked glycans hindered formation of b- and y-type ions and prevented peptide sequencing and glycan localisation. (b) Higher energy collision dissociation (HCD) produced characteristic oxonium product ions (circled in red) which triggered (c) electron transfer dissociation (ETD) of the same charged precursor ion and subsequent generation of c- and z-type ions. Combination of glycan structures obtained from CID/HCD and peptide sequence information from ETD allowed identification of a glycan structure at a particular site. The fragment shown includes the sixth putative N-linked glycosylation site in CD36 ED derived from Sf21 insect cells.
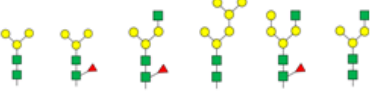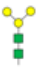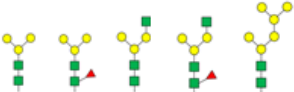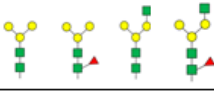
Figure 4.12. Summary of mass spectrometric analysis of glycosylation of CD36 ED-12His secreted from Sf21 insect cells.

Using CID/HCD product-ion triggered ETD, glycan structures were observed on six putative glycan sites on CD36 ED-12His secreted from Sf21 insect cells. CD36 Ed-12His was digested into fragments using trypsin prior to analysis. Glycan heterogeneity was observed between different sites as well as between glycans on the same site. Glycans were simple and core-like. ■- N-acetylglucosamine, ◯ - Mannose, ▲- Fucose. Glycan structures were deduced using the protein metric software, Byonic (Protein Metrics) against the human CD36 sequence. Precursor tolerance of 6ppm and fragmentation of 0.5Da. False discovery rate (FDR) was 1%.
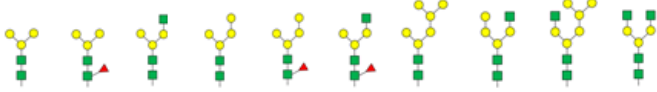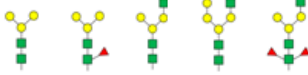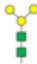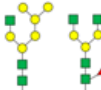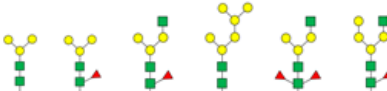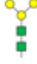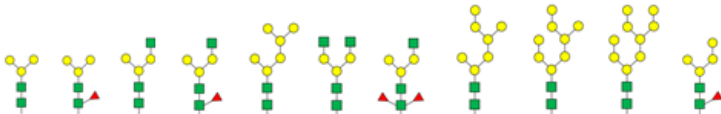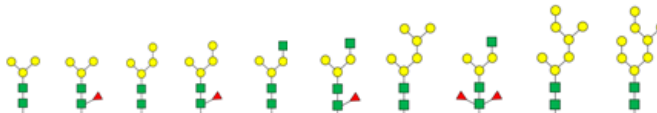
Figure 4.13. Summary of mass spectrometric analysis of glycosylation of CD36 ED-12His secreted from Hi5 insect cells.

Using CID/HCD product-ion triggered ETD, glycan structures were observed on eight putative glycan sites on CD36 ED-12His secreted from Hi5 insect cells. CD36 ED-12His was digested into fragments using either trypsin or chymotrypsin prior to analysis. Glycan heterogeneity was observed between different sites and also between glycans on the same site. Higher mannose-type sugars were observed in Hi5 derived CD36 ED-12His. Hi5 derived CD36 ED-12His was also found to contain difucosylated glycans increasing the likelihood of core α(1-3) linked fucose being present. ■ - N-acetylglucosamine, ○ - Mannose, ▲ - Fucose. Glycan structures were deduced using the protein metric software, Byonic (Protein Metrics) against the human CD36 sequence. Precursor tolerance of 6ppm and fragmentation of 0.5Da. False discovery rate (FDR) was 1%.

4.3. Discussion

N-linked glycosylation on proteins is known to play an important role in a range of cellular functions. It was previously shown that nine of the ten putative N-linked glycosylation sites on full-length CD36, heterologously expressed in Sf21 insect cells and mammalian cells, were occupied (Hoosdally *et al*., 2009). In this chapter mass spectrometry was used to determine the putative N-linked glycosylation site occupancy of purified CD36 ED expressed in two separate insect cells lines and identify the nature of this glycosylation.

Of the ten putative N-linked glycosylation sites found on CD36, glycan structures were identified on six sites from CD36 ED-12His secreted from Sf21 insect cells (Figure 4.12) and eight sites from CD36 ED-12His secreted from Hi5 insect cells (Figure 4.13). Both cell lines generated CD36 ED-12His with heterogeneous glycosylation. This heterogeneity was observed not only at different sites but also between glycans occupying the same site. Glycans found on CD36 ED-12His secreted from Hi5 insect cells showed greater heterogeneity. All glycans observed contained only N-acetylglucosamine, mannose and fucose. Although the same type of sugar groups were found on both CD36 ED-12His from both cells lines, Sf21 derived CD36 ED-12His glycosylation consisted of simple short glycans, whereas the glycans on Hi5 derived CD36 ED-12His glycosylation were elongated. The presence of difucosylated glycans on CD36 ED-12His derived from Hi5 suggests the presence of α(1-3)-linked fucose residues and provides an explanation for the inability to remove all glycans with PNGase F. This data is in line with other studies which have shown Hi5 insect cells to produce recombinant proteins with this

particular linkage as part of more complex and hybrid-like glycans (Hsu *et al*., 1997, Rudd *et al*., 2000, Ding *et al*., 2003). Although the presence of singly fucosylated glycans on Sf21 derived CD36 ED-12His does not rule out the presence of α(1-3)-linked fucose residues, the ability to deglycosylated the protein with PNGase F would suggest that these fucose residues are instead attached via α(1-6)-linkages. This is consistent with several studies which have failed to detect α(1-3)-linked fucose residues in Sf21 insect cells (Voss *et al*., 1993, Kuroda *et al*., 1990, Grabenhorst *et al*., 1993).

Despite being able to detect glycan structures on six of the putative N-linked glycosylation sites on CD36 ED-12His secreted from Sf21 insect cells, glycan structures on an additional two putative sites (N2 and N3) were detected on CD36 ED-12His secreted from Hi5 insect cells. This can be attributed to the chymotrypsin digestion of Hi5 derived CD36 ED-12His which resulted in shorter fragmentation with each product containing only one of the putative sites. In contrast, digestion of CD36 ED-12His with trypsin results in a large peptide fragment containing three putative N-linked glycosylation sites, which made glycan detection and assignment difficult (Baldwin, 2004).

Only one putative N-linked glycosylation site was shown to lack glycosylation in both insect cells lines (N4). This is in agreement with Hoosdally *et al*., who showed that the same site was not glycosylated on full-length CD36 from insect and mammalian cell lines (Hoosdally *et al*., 2009). This putative site is located within one of two alpha helices suggested to be involved in oxLDL binding and, possibly, in CD36 homo-oligomerisation based on the structural model of CD36, derived from the LIMP-2 crystal structure. An alignment of the primary sequences of CD36, LIMP-2 and SR-B1 is shown in (Figure 4.14). Several residues within and around

this predicted alpha helix in CD36 were suggested, by mutagenesis (L158E, L161E, double mutant K164/K166E), to be involved in the binding of DiI-oxLDL (Neculai *et al*., 2013). This finding however is based on very severe amino acid substitutions which may have had an indirect impact on binding of oxLDL, as opposed to these residues specifically being required for oxLDL binding.

Although the N-linked glycosylation sequon is thought to be recognised faithfully by oligosaccharyltransferase in the transfer of core glycan to asparagine residues (Schwarz and Aebi, 2011), the absence of a glycan within this proposed ligand binding region might suggest that there is a mechanism in place during trafficking through the ER to prevent glycosylation at this site. There are many examples reported where the presence of the sequon does not guarantee glycosylation (Gavel and von Heijne, 1990), and variability in site occupancy could be caused by different amino acids at positions +1 and +2 within the sequon (Shakin-Eshleman *et al*., 1996, Petrescu *et al*., 2004, Kasturi *et al*., 1997). Another mechanism to explain a non-glycosylated sequon is the possibility of neighbouring Ser/Thr becoming O-mannosylated, prior to core glycan transfer to the Asn, blocking N-linked glycosylation (Ecker *et al*., 2003).

```
hCD36    MGCDRNCGLIAGAV--IGAVLAVFGGILMPVGDLLIQKTIKKQVVLEEGTIAFKNWVKTG
hLIMP2   MG--RCCFYTAGTLSLLLLVTSV-TLLVARVFQKAVDQSIEKKIVLRNGTEAFDSWEKPP
hSR-B1   MGCSAKARWAAGALGVAGLLCAVLGAVMIVMVPSLIKQQVLKNVRIDPSSLSFNMWKEIP
         **     .   **::      : :*    ::  :    :.: : *:: :  .: :*. * :

                             N1                          N2
hCD36    TEVYRQFWIFDVQNPQEVMMNSSNIQVKQRGPYTYRVRFLAKENVTQDAEDNTVSFLQPN
hLIMP2   LPVYTQFYFFNVTNPEEILR-GETPRVEEVGPYTYRE-LRNKANIQFGDNGTTISAVSNK
hSR-B1   IPFYLSVYFFDVMNPSEILK-GEKPQVRERGPYVYRE-FRHKSNITFNNNDT-VSFLEYR
          .*  ..::*:* **.*::   ...  :*.: ***.** :  * *:     : . :* :. .

                           N3                              N4
hCD36    GAIFEPSLSVGTEA-DNFTVLNLAVAAASHIYQNQ--FVQMILNSLINKSKSSMFQVRTL
hLIMP2   AYVFERDQSVGDPKIDLIRTLNIPVLTV--IEWSQVHFLREIIEAMLKAYQQKLFVTHTV
hSR-B1   TFQFQPSKSHGSES-DYIVMPNILVLGAAVMMENKPMTLKLIMTLAFTTLGERAFMNRTV
          *:  . * *     * :    *: *   . :    :    :: *:   :.   .  *  :*:

                                      N5                  N6
hCD36    RELLWGYRDPFLSLVP------YPVTTTVGLFYPYNNTADGVYKVFNGKDNISKVAIIDT
hLIMP2   DELLWGYKDEILSLIHVFRPDISPY---FGLFYEKNGTNDGDYVFLTGEDSYLNFTKIVE
hSR-B1   GEIMWGYKDPLVNLINKYFPGMFPFKDKFGLFAELNNSDSGLFTVFTGVQNISRIHLVDK
          *::**:* ::.*:         *     .*** * :  .* .: ..* :.  ..  :

              N7          N8
hCD36    YKGKRNLSYWES-HCDMINGTDAASFPPFVEKSQVLQFFSSDICRSIYAVFESDVNLKGI
hLIMP2   WNGKTSLDWWITDKCNMINGTDGDSFHPLITKDEVLYVFPSDFCRSVYITFSDYESVQGL
hSR-B1   WNGLSKVDFWHSDQCNMINGTSGQMWPPFMTPESSLEFYSPEACRSMKLMYKESGVFEGI
          ::*  .:.:* : :*:*****..  : *::  ..  * .:  : ***:    :...   .:*:

                                          N9
hCD36    PVYRFVLPSKAFASPVENPDNYCFCTEKIISKNCTSYGVLDISKCKEGRPVYISLPHFLY
hLIMP2   PAFRYKVPAEILANTS---DNAGFCIP---EGNCLGSGVLNVSICKNGAPIIMSFPHFYQ
hSR-B1   PTYRFVAPKTLFANGSIYPPNEGFC-------PCLESGIQNVSTCRFSAPLFLSHPHFLN
          *.:*:  *   :*.      *  **        *   *: ::* *: . *: :* ***

hCD36    ASPDVSEPIDGLNPNEEEHRTYLDIEPITGFTLQFAKRLQVNLLVKPSEKIQVLKNLKRN
hLIMP2   ADERFVSAIEGMHPNQEDHETFVDINPLTGIIILKAAKRFQINIYVKKLDDFVETGD-IRT
hSR-B1   ADPVLAEAVTGLHPNQEAHSLFLDIHPVTGIPMNCSVKLQLSLYMKSVAGIGQTGK-IEP
          *.   . : *:..**:* *  :::**.*:** :: : ::*:.: :*     :    . .

            N10
hCD36    YIVPILWLNETGTIGDEKANMFRSQVTGKINLLGLIEMILLSVGVVMFVAFMISYCACRS
hLIMP2   MVFPVMYLNESVHIDKETASRLKSM-INTTLIITNIPYIIMALGVFFGLVFTWLACKGQG
hSR-B1   VVLPLLWFAESGAMEGETLHTFYTQLVLMPKVMHYAQYVLLALGCVLLLVP--VICQIRS
          :.*::::   *:  :   *.   : :           ::   :::::*  .: :.    *  :.

hCD36    KTIK--------------------------------------------------------
hLIMP2   SMDEGTADERAPLIRT--------------------------------------------
hSR-B1   QVGAGQRAARADSHSLACWGKGASDRTLWPTAAWSPPPAAVLRLCRSGSGHCWGLRSTLA
                                                                      .

hCD36    ------------------------
hLIMP2   ------------------------
hSR-B1   SFACRVATTLPVLEGLGPSLGGGTGS
```

Figure 4.14. Primary Sequence Alignment of Human CD36 Protein Family.
Clustal[15] sequence alignment of the human CD36 family of proteins with all 10 putative N-linked glycan sites underlined with corresponding asparagines highlighted in yellow. Sequences highlighted in green and blue indicate residues predicted to reside within the first (α5) and second (α7) alpha helices involved with ligand binding and homo-oligomerisation, based on the model generated by Neculai, *et al*,. LIMP-2 residues in red are those predicted to be important for homo-oligomerisation. Mutating CD36 residues in brown were shown to abrogate binding of DiI-oxLDL (Neculai *et al*., 2013). CD36 putative N-linked glycan sites are labelled N1-10. '*****': identical residues, '**:**' conserved residues, '**.**' Semi-conserved residues.

168

5. Analysis of Antibody Binding to the CD36 Ectodomain using Surface Plasmon Resonance

5.1.   Introduction

The ability to monitor binding interactions is of the upmost importance to the drug discovery and development process. It has been known since the beginning of the 20th century, when the receptor theory of drug action was first proposed, that for a drug to work it must bind to its target receptor (Langley, 1905). Much of the drug discovery process since then has focused on the direct measurement of the amount of drug bound to a receptor at equilibrium, i.e. the binding affinity or binding strength. This emphasis on binding affinity which is described in terms of an equilibrium dissociation constant - the drug concentration required to give half-maximum binding, is based on the assumption that affinity is an acceptable surrogate for determining *in vivo* efficacy (Pan *et al*., 2013). Although affinity determination has been behind the discovery of many highly efficacious drugs, it is becoming increasingly acknowledged that the rate of drug association and then the rate of drug dissociation from a receptor, i.e. the binding kinetics, has a direct effect drug efficacy as well as on drug safety (Swinney, 2009, Vauquelin *et al*., 2012, Chen *et al*., 1992, Pan *et al*., 2013). In an *in vivo* system, the concentration of drug at the target site will vary over time, on a timescale which may be faster than the binding

and unbinding to a receptor, such that a binding equilibrium may never be reached or maintained (Pan *et al*., 2013). For some drugs, reaching equilibrium may not even be desirable with possible toxic side effects being caused by the drug staying within the system too long and causing adverse effects to normal physiological processes (Chen *et al*., 1992).

The scavenger receptor CD36 is found on many different cell and tissue Types, including macrophages (Savill et al., 1991), endothelial cells (Swerlick *et al*., 1992) and smooth muscle (Harmon and Abumrad, 1993). It is this diverse expression pattern as well as the ability of the ectodomain (ED) of CD36 to bind a wide range of ligands that links this receptor to many different normal physiological processes as well as pathological states. With this in mind, the development of any therapeutic agents to target CD36, with the hope to relieve or cure a related pathosis, must take into account possible side-effects that may affect other essential physiological processes. Understanding the way in which a ligand or drug might bind to the ED of CD36, in particular the binding kinetics, is therefore vital for the development of effective therapeutic agents.

This chapter describes how Biacore™ (GE Healthcare), a technology which exploits the phenomena of surface plasmon resonance (SPR) spectroscopy, a label-free binding technique (Patching, 2014), was used to monitor the binding between unlabelled monoclonal antibodies and the purified ED of CD36 with the goal to determine binding affinities and the kinetics of these interactions. These initial experiments are the first steps in the development and optimisation of an approach which could then be used to analyse the binding affinity and binding kinetics of a range of CD36 ligands as well as for potential therapeutic agents designed to modulate or inhibit ligand binding to the ED of CD36.

5.1.1. Surface Plasmon Resonance

Although many different methods for monitoring ligand-receptor binding have been employed for decades in academia and the pharmaceutical industry (Swinney and Anthony, 2011), these assays have generally relied on the use of labels, such as radioactive tags, fluorescent tags or colorimetric reactions to report binding. These indirect detection methods not only make analysis more expensive but also introduces possible experimental uncertainty either through blocking of the active binding epitopes by the label or the label itself contributing to the overall binding event leading to a false-positive result (Beher *et al*., 2009, Hu *et al*., 2012). Although there is now a wide variety of labelled detection methods available, the use of label-free methods are becoming increasingly popular. Label-free methods greatly reduce the time and complexity required for binding analysis as well as removing the difficulties caused by steric hindrance or from false-positives produced by label participation (Fang, 2014).

Most label-free detection methods follow the same underlining principle involving a transducer that is capable of measuring a physical property of a substance, whether it is DNA, protein, lipid or even whole cells. All molecules and cells have finite properties such as mass, volume, and conductivity that can be exploited to indicate their presence or absence from a particular sensor surface (Cunningham *et al*., 2004). The sensor, acting as a transducer, converts one of these physical properties (such as the mass of a compound binding to the surface) into a quantifiable signal (e.g. current or voltage) which can then be gathered by an appropriate instrument (such as

voltage meter), providing a signal proportional to the amount of binding (Cunningham *et al*., 2004).

The phenomenon of surface plasmon resonance (SPR), which uses optical biosensors, has become one of the most popular label-free methods for measuring binding interactions in real-time (Karlsson, 2004). The use of optical biosensors in SPR systems is dominated by Biacore™ which in combination with their own microfluidic system for delivering sample to the biosensor surface, have become the main providers of this technology (Karlsson, 2004).

Through molecules binding to these optical biosensors it is possible to generate a response which is proportional to the mass of the molecule bound (Tanious *et al*., 2008). As the binding events are observed in real-time, it is possible to study a range of interaction characteristics which were previously unmeasurable using conventional equilibrium-based binding studies. By following the binding event in real-time, it is possible to monitor the binding kinetics of the interaction and in turn elucidate a clearer mechanism and understanding of the binding event (Tanious *et al*., 2008, Nordgren *et al*., 2001).

5.1.1.1. Biacore SPR Detection System

Biacore systems use the phenomenon of SPR to monitor the interaction between two molecules in real-time (Karlsson, 2004). The approach involves immobilising one interacting partner, termed the ligand (not to be confused with ligand-receptor terminology), to the surface of a sensor chip (Figure 5.1). The other interacting

partner, termed the analyte, is then passed over the sensor chip surface in solution where it is then able to interact with the immobilised ligand (Karlsson and Stahlberg, 1995).
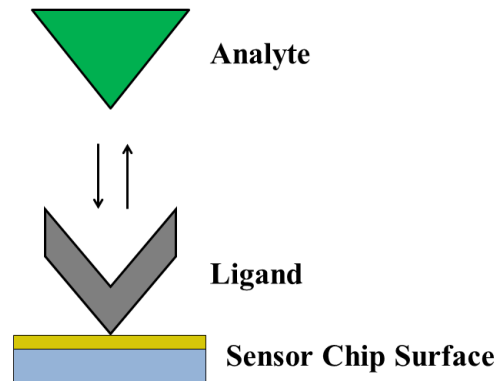
Figure 5.1. Surface plasmon resonance basic terminology.
The ligand is the interacting partner that is immobilised onto the surface of the sensor chip. The analyte is passed over the sensor chip surface in solution where it can then bind to the immobilised ligand.

SPR takes places within a thin conducting film at an interface between media of different refractive indices. The refractive index is a measure of how light, or any other form of radiation, passes through a medium (Cooper, 2003, Piliarik *et al*., 2009). In the SPR detection system the media are the glass of the sensor chip (high refractive index) and a buffer (low refractive index), the conducting film being a thin layer of gold at the surface of the sensor chip (Figure 5.2) (Hahnefeld *et al*., 2004). When polarized light, under conditions of total internal reflection, hits the electrically conducting gold layer interface between the two media, an electromagnetic field intensity, known as an evanescent wave, is generated (Cooper, 2003). The evanescent wave once generated leaks across the gold layer interface into the medium with lower refractive index (the buffer). The amplitude of the

evanescent wave decreases exponentially with distance from the sensor chip surface so that the effective penetrative depth in terms of sensitivity to refractive index is around 150nm (Cooper, 2003, Nunez *et al*., 2012). With a particular combination of angle of incidence and energy (wavelength), the polarized light excites plasmons (electron charge density waves) in the gold film. This results in a characteristic absorption of energy via the evanescent wave with the SPR being seen as a drop in intensity of the reflected light. SPR is very sensitive to the refractive index of the solution within the effective penetrative depth of the evanescent wave (within the buffer) (Cooper, 2003). A change in the solute concentration at the sensor chip surface causes a change in the refractive index of the solution within the evanescent wave. The resultant shift in light energy (wavelength), which is absorbed rather than reflected, can be measured as change in resonance angle or resonance wavelength (Nunez *et al*., 2012). Only refractive index changes within the effective penetrative depth (150nm away from the sensor chip surface) will affect the SPR signal. This means that only analyte binding to the sensor chip surface will generate a response change (Cooper, 2003, Nunez *et al*., 2012).
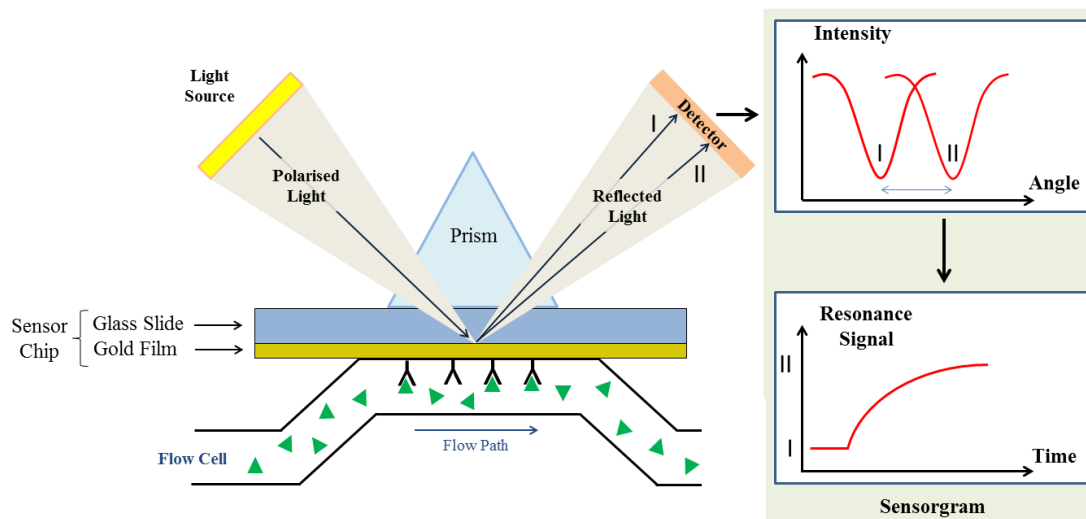
Figure 5.2. Basic configuration of a Surface Plasmon Resonance (SPR) sensor.
SPR is sensitive to refractive index changes that take place within close proximity to the sensor chip surface. As molecules bind the mass at the sensor surface increases, causing the SPR angle to shift (from I to II). The change in resonant angle can be monitored in real-time as a change in resonance signal over time. The degree of resonance increase is proportional to the mass change at the surface. Biacore is trademark of GE healthcare companies. © 2014 General Electric Company - Reproduced by permission of GE Healthcare.

5.1.1.2.   Sensor Chip Surface

The sensor chip, in particular, the sensor chip surface is fundamental to SPR in measuring molecular interactions (Cooper, 2003). The ability to monitor the binding between an analyte and a ligand is dependent on first being able to immobilise the ligand onto the chip surface and for it to retain its native active conformation. The ligand must then also remain bound throughout the course of the binding experiment. There are several ways with which ligands may be attached to the sensor chip surface. The first is through covalent immobilization where the ligand is attached to the surface through a covalent linkage. The second method of attachment is via

175

hydrophobic absorption which exploits hydrophobic effects to either attach a ligand of interest or a hydrophobic carrier such as a lipid-based monolayer or bilayer to the sensor chip surface. The final type of immobilisation is achieved through high affinity capture. In this method the ligand of interest is non-covalently attached to another molecule (which in turn is usually attached using covalent immobilisation) (Cooper, 2003, Hutsell *et al*., 2010, Piliarik *et al*., 2009). The type of sensor chip surface that is used is based on the nature of the ligand and the analyte-ligand interaction that is to be studied. There is now a wide range of sensor chips available which are capable of immobilising anything from small peptides to whole cells (Figure 5.3). Every sensor chip consists of the same glass surface coated with a thin layer of gold which forms the basic platform from which specialised surfaces have been designed to immobilise a variety of ligands with very different physical properties (Lofas and Johnsson, 1990, Karlsson and Lofas, 2002, Knecht *et al*., 2009, Hodnik and Anderluh, 2010).

The most widely used form of sensor chip consists of a gold layer which has been modified with a carboxymethylated dextran layer (Figure 5.3; CM5 Chip) (Lofas and Johnsson, 1990). This dextran layer creates a hydrophilic environment for the ligand attachment, maintaining the ligand in a native state. From this a range of modified surfaces have been designed which enables alternative immobilisation methods based on the nature of the ligand. All sensor chips (except CM1 and HPA sensor chips) are made up of a carboxymethylated dextran matrix covalently attached to the gold surface. Attachment of the ligand to this matrix is achieved through chemical reactions involving functional groups found on the ligand, such as aldehyde, thiol, and amino groups (Cooper, 2003). CM4 sensor chips have a lower degree of carboxymethylation than CM5 sensor chips and as such have a lower binding

176

capacity, thought to reduce non-specific binding (Lundquist et al., 2010, Hu et al., 2009, Hahnefeld et al., 2004). The CM3 sensor chip has the same amount of carboxymethylation as the CM5 sensor chip but instead consists of a matrix of shorter dextran chains which is designed to reduce possible steric hindrance when investigating larger molecules such as viruses or whole cells. An extreme variant of the CM5 sensor chip, the C1 sensor chip has a carboxymethylated surface without a dextran matrix (Zhao *et al*., 2013, Zhang and Oglesbee, 2003). C1 sensor chips also allow the immobilisation of large ligands but limit freedom of movement of the ligand on the dextran matrix of the CM3 sensor chip (Hahnefeld *et al*., 2004).

For hydrophobic ligands, HPA and L1 sensor chips are primarily used (Figure 5.3). The HPA sensor chip has alkanethiol molecules attached to the gold film creating a hydrophobic surface. This sensor chip is used for the immobilisation of lipids and membrane-associated molecules (Cooper *et al*., 1998, Hodnik and Anderluh, 2010). The L1 sensor chip has a carboxymethylated dextran matrix with covalently attached lipophilic residues allowing the capture of vesicles and liposomes directly (Besenicar *et al*., 2006, Hodnik and Anderluh, 2010, Hahnefeld *et al*., 2004).

The final types of sensor chip available are those allowing immobilisation of ligand through high affinity capture (Figure 5.3). The SA sensor chip has a dextran matrix with streptavidin covalently attached. Streptavidin is capable of binding biotinylated ligands tightly with an affinity similar to that of direct covalent immobilisation (Hodnik and Anderluh, 2010, Hutsell *et al*., 2010). Another type of high affinity capture sensor chip is the NTA sensor chip. The NTA sensor chip has nitrilotriacetic acid (NTA) covalently bound to a dextran matrix, allowing the capture of polyhistidine-tagged ligands (Hahnefeld *et al*., 2004). As with NTA-agarose (see 3.2.4), the immobilised NTA chelates metal ions, such as nickel (Ni^{2+}), leaving

coordination sites free which can bind to polyhisitine tagged proteins (Knecht *et al*., 2009).

The binding cycle of NTA sensor chips differs from that of other chips, which rely on the ligand remaining immobilised for the duration of the whole experiment (including the use of multiple concentrations of analyte). For NTA sensor chips each experiment consists of multiple binding cycles; each binding cycle involving one concentration of analyte binding to immobilised ligand. At the start of a binding cycle, the sensor chip surface is first 'activated' with nickel ions. Injection of nickel over the sensor chip surface results in the nickel coordinately binding to the immobilised NTA. With the nickel bound, the surface is then capable of binding polyhistidine tagged proteins. Injection of ligand over the activated surface results in the polyhistidine tag of the ligand binding to the sensor chip surface through the coordinately bound nickel. With the ligand immobilisaed, binding interactions between analyte and ligand can be observed when analyte is injected over the sensor chip surface. Following measurement of the association and dissociation of analyte to ligand, the surface is regenerated, to remove all bound analyte, ligand and nickel. This differs from conventional CM sensor chips which rely on only removing analyte during regeneration, leaving the ligand immobilised. To regenerate the NTA sensor chip, EDTA is injected over the surface. EDTA is a metal ion chelator which sequesters and strips the nickel from the immobolised NTA and in turn removes the ligand and analyte. The sensor chip is then ready for a new binding cycle with fresh reagents (Hahnefeld *et al*., 2004).

In the current study an NTA sensor chip was chosen for carrying out SPR analysis with the 12xhistidine tagged CD36 ED immobilised as a ligand. The NTA sensor chip surface chemistry exploits the same technology used previously in the metal-ion

affinity chromatography purification of the ED of CD36. The additional benefit of using this type of chip is that through immobilisation via the C-terminal 12-histidine tag, the ED is arrayed in a uniform orientation with the ED likely extending from the sensor chip surface and into the flow path of the analyte.
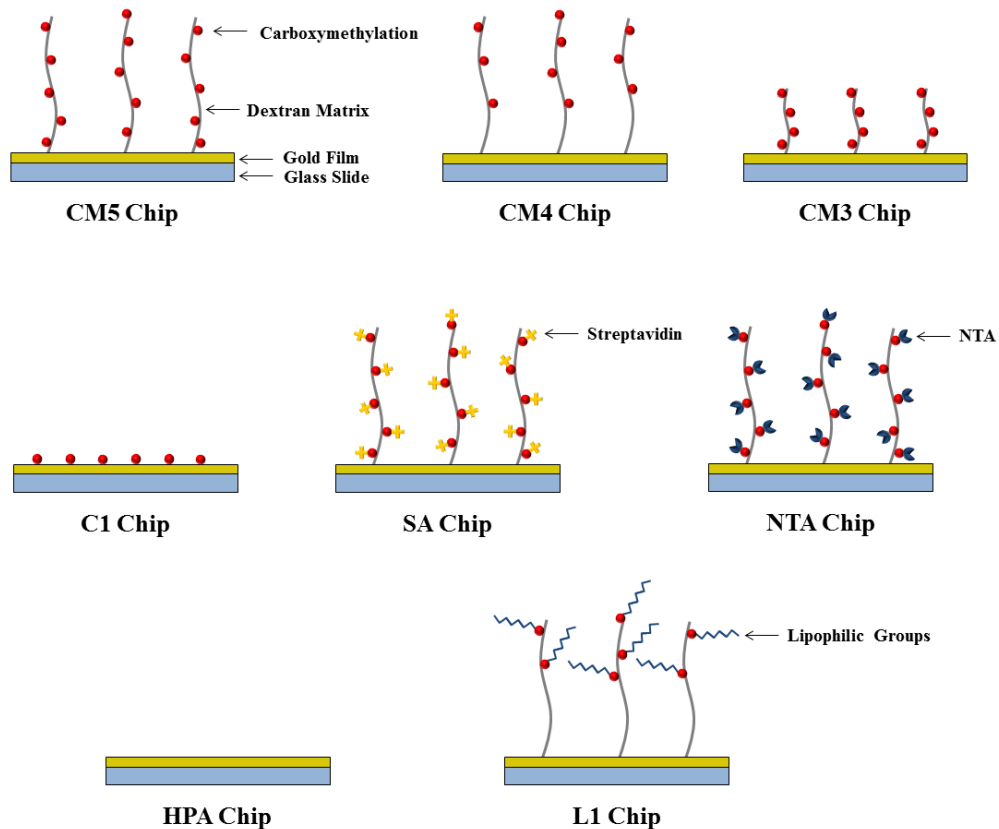
Figure 5.3. Biacore Sensor Chip Surface Chemistry.
There a number of optical biosensor chips available for the immobilisation of ligand during SPR analysis. The type of surface chemistry is dependent on the physical properties of the ligand that is to be immobilised. All sensor chips consist of the same glass surface coated with a thin layer of gold which forms the basic platform from which specialised surfaces have been designed. Biacore is trademark of GE healthcare companies. © 2014 General Electric Company - Reproduced by permission of GE Healthcare.

5.1.1.3. SPR Sensorgram

Throughout an SPR experiment, the resonance (also called response), measured in response units (RU), is continually measured with a continuous flow of running buffer (or sample) over the sensor chip surface at all times. RU is an arbitrary unit which describes the relative change in mass at the surface of the sensor chip as molecules associate and dissociate. The response is directly proportional to the concentration of the molecules at the surface of the sensor chip. The response is represented in real-time on an SPR sensorgram which is a plot showing response against time (Figure 5.4). As the analyte comes into close proximity to the sensor surface and binds ligand, a refractive index change within the effective penetrative depth occurs, represented by in an increase in response. As more analyte binds to ligand, a characteristic dose-dependent response curve is observed. Eventually all binding sites become occupied and the response level begins to plateau. Once injection of analyte over the sensor chip surface has stopped, dissociation of analyte is measured as running buffer is passed over the sensor chip surface. For the next binding cycle to begin, the sensor surface is regenerated to ensure any remaining analyte has been removed from the surface. The regeneration solution used will vary depending on the type of sensor chip used. Each sensor chip is made up of four flow cells, allowing the measurement of different analyte/ligand binding conditions in parallel. To control for non-specific binding, analyte is passed through one flow cell without immobilised ligand. The control flow cell binding response is then subtracted from ligand immobilised flow cell response. For NTA sensor chips, this control flow cell lacks both nickel activation and immobilised ligand.

The rate of binding and dissociation are represented by two different constants, together describing the kinetics of the interaction. During association, the rate of analyte binding, described by the association rate constant (K_a), is dependent on both concentration of analyte (M) and time (s). Therefore K_a values are given with the units $M^{-1}s^{-1}$. During dissociation, described by the dissociation rate constant (K_d), the analyte freely dissociates as running buffer passes over the sensor surface. As a result, dissociation of analyte is dependent only on time. K_d values are therefore given with the units s^{-1}.
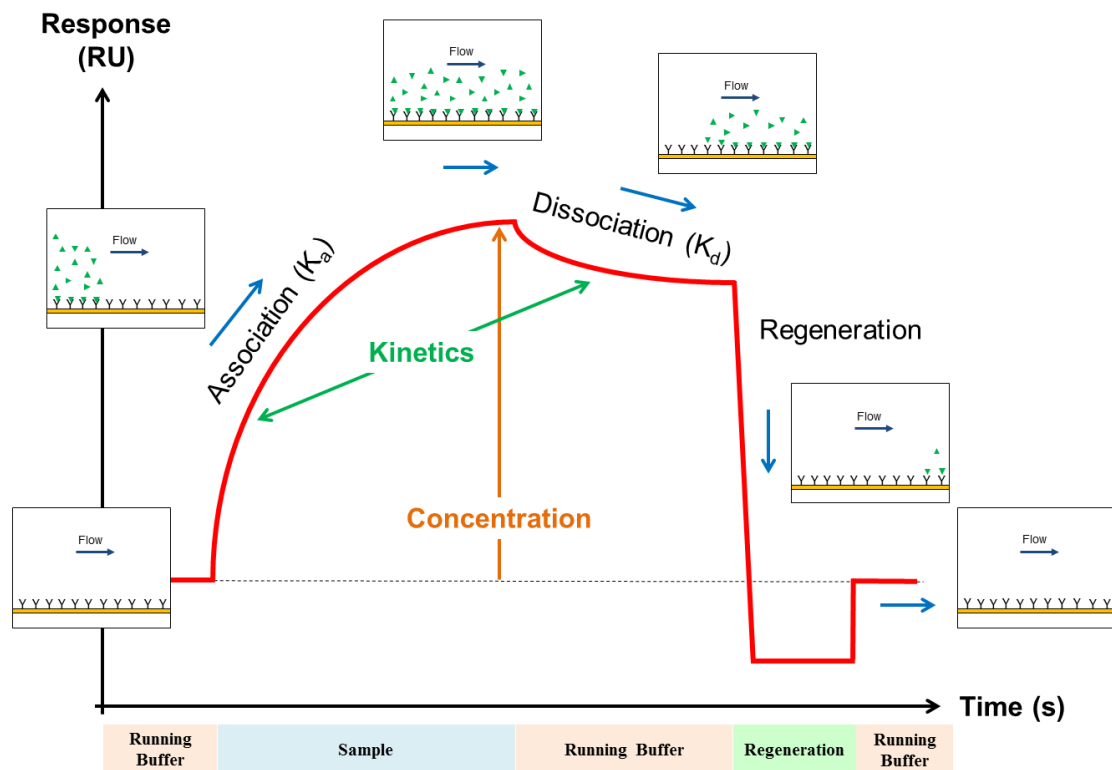
Figure 5.4. A typical SPR sensorgram showing analyte binding to immobilised ligand.
A typical sensorgram consists of three distinct phases: analyte association, analyte dissociation and surface regeneration. Biacore is trademark of GE healthcare companies. © 2014 General Electric Company - Reproduced by permission of GE Healthcare.

To predict the degree of response change brought about through analyte binding, it is important to know how much ligand is immobilised on the sensor chip surface. The amount of analyte binding is dependent on the amount of ligand present and therefore available binding sites. As all steps of the SPR experiment are monitored by the system, the amount of ligand immobilised is measured directly by the increase in response above the baseline. The analyte binding capacity, or Rmax (Equation 5.1) is calculated to give an indication of the expected maximum response in a binding cycle. The amount of ligand immobilised on the surface can be used to indicate the theoretical binding capacity of the surface with ligand immobilised. This is dependent on prior knowledge of the molecular weights of the analyte and ligand. For example: if the molecular weights of the analyte and ligand are 100kDa and 50kDa, respectively, and 50RU of ligand is immobilised, then a Rmax of 100RU would be expected.

$$\text{Analyte Binding Capacity (RU)} = \frac{\text{Analyte MW}}{\text{Ligand MW}} \ \text{X} \ \text{Immobilised Ligand Level (RU)}$$

Equation 5.1. Analyte Binding Capacity (Rmax) Equation.
The theoretical Rmax is calculated to determine the expected maximum response that would be observed for a given binding event. Comparison of theoretical and practical Rmax values give a measure of activity of the surface-bound ligand. A lower practical Rmax value obtained experimentally compared to the theoretical Rmax would suggest a lower activity of surface-bound ligand.

The practical analyte binding capacity can be obtained experimentally by injecting analyte at high concentration to saturate the sensor chip surface. Alternatively, the practical analyte binding capacity can be determined by extrapolating binding levels from measurements at a series of analyte concentrations.

5.2.   Results

5.2.1.   Immobilisation of CD36 ED-12His on a nickel-activated NTA sensor chip.

Prior to measuring analyte binding, SPR was used to determine whether purified CD36 ED could be immobilised onto an NTA sensor chip via the C-terminal 12xhistidine tag (-12His), and more importantly whether it would remain immobilised. The sensor chip was activated by passing a 0.5mM nickel solution over the sensor chip surface (Figure 5.5). A subsequent rise in baseline response following nickel addition corresponded with the immobilisation of nickel ions and the successful activation of the chip surface. Purified CD36 ED-12His, pre-dialysed into running buffer was diluted to ~5μg/ml and then injected over the activated sensor chip surface (Figure 5.5), resulting in a response increase of ~500RU. Following immobilisation of CD36 ED-12His, running buffer was passed over the sensor chip surface with no decrease in response level being observed, suggesting stable immobilisation of CD36 ED-12His on the nickel-activated NTA sensor chip surface.
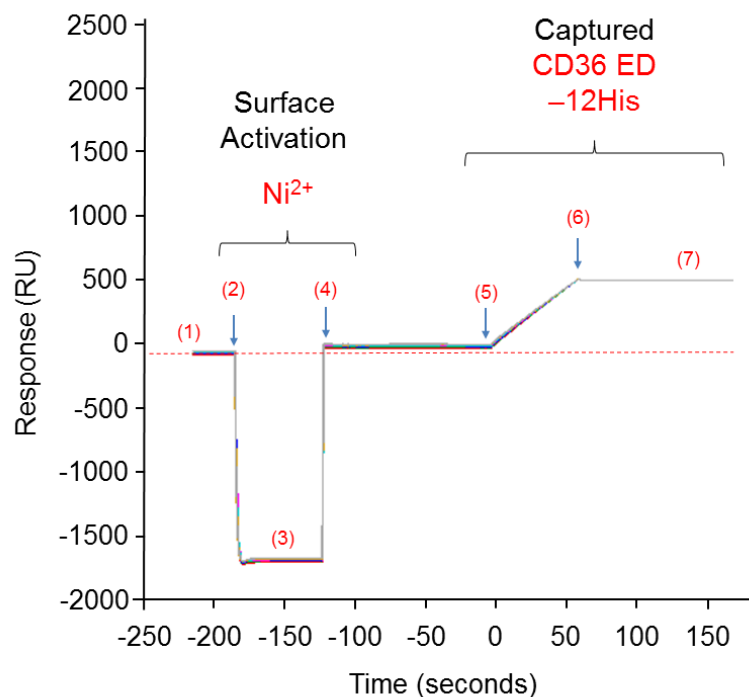
Figure 5.5. Overview of surface activation and immobilisation of CD36 ED-12His on an NTA sensor chip.

An NTA sensor chip was equilibrated using running buffer (1). On injection of a 0.5mM nickel solution (2) over the surface of the sensor chip for 1 minute (10µl/min), a drop in resonance (3) was observed due to the change in the refractive index of the solution flowed over the surface. Equilibration of the flow cell with running buffer following surface activation (4) shows a response ~40RU higher than the starting base-line response level, consistent with the immobilisation of nickel ions on the NTA coated surface. Injection of ~5µg/ml CD36 ED-12His over the activated surface (5) for 1 minute (10µl/min) resulted in a response increase of ~500RU (6). After CD36 ED-12His injection, running buffer was passed over the sensor surface to monitor dissociation of captured protein. CD36 ED-12His bound tightly to the nickel-activated surface of the NTA sensor chip with no decrease in response being observed (7). SPR was performed in a Biacore T200 (GE Healthcare) with all analysis undertaken at 25°C. The sensorgram was generated using BIA evaluation software version 2 (GE Healthcare). Experiments were performed in triplicate (triplicate traces are superimposed).

5.2.2. Analyte binding to immobilised CD36 ED-12His on an NTA sensor chip

Having shown that purified CD36 ED-12His could be immobilised on a nickel-activated NTA sensor chip surface without subsequent loss of attachment, SPR was performed to see whether analyte binding to CD36 ED-12His could be measured. The monoclonal antibody mAb1955 (Rat IgG2B, ~150kDa, R&D Systems, clone 255619) is known to recognise CD36 ED-12His, having been shown previously to bind to CD36 ED-12His in western blotting experiments (see 3.2.1). MAb1955 has also been shown to bind native human CD36 expressed on the surface of transiently transfected mammalian cells (Linton, K; personal communication). MAb1955 was therefore used as analyte in initial binding experiments as proof of principle to test analyte binding to immobilised CD36 ED-12His.

The NTA sensor chip was activated with a 0.5mM nickel solution followed by immobilisation of CD36 ED-12His (~500RU) as shown previously (see 5.2.1). Each binding cycle (Figure 5.6) consisted of surface activation of the NTA sensor chip surface with nickel, immobilisation of CD36 ED-12His, followed by injection of mAb1955 at set concentrations (ranging from 0nM up to 20nM) over the chip surface. During mAb1955 injection, association of antibody was observed as a response increase. After injection, running buffer alone was passed over the sensor chip surface to monitor mAb1955 dissociation, represented by a decrease in response. Following the dissociation phase, the sensor chip surface was regenerated using 350mM EDTA to sequester and strip nickel ions from the sensor chip surface and in turn remove immobilised CD36 ED-12His and mAb1955.

With increasing concentration of mAb1955, a greater response increase was observed corresponding to increased mAb1955 binding (Figure 5.7). Despite a concentration dependent increase in binding response, mAb1955 binding did not produce sensorgrams with the expected curvature. All concentrations of mAb1955 produced a near linear response during association, as opposed to the characteristic curved response expected with conventional analyte/ligand interactions (Figure 5.4). This was especially true for higher concentrations of antibody. With the molecular weights of CD36 ED-12His and mAb1955 as ~63kDa and ~150kDa, respectively, and ~500RU of CD36 ED-12His having been immobilised, an Rmax value of ~1190RU was expected (Equation 5.1). The Rmax is the point at which all available binding sites are occupied and so no further response increase should be observed beyond ~1190RU. Biacore evaluation software (BIA evaluation) predicted, based on the binding curves generated, an Rmax value of around 7000RU. An additional point worth noting is that the binding curves appear similiar in their linearity to that of CD36 ED-12His immobilisation to the nickel-acitvated sensor chip surface. Together, the data suggested a non-specific interaction of mAb1955 with the nickel-activated NTA sensor chip surface that is independent of CD36 ED-12His. mAb1955 concentrations up to 2.5nM produced stable binding profiles with no loss of binding during the dissociation phase. However, increasing the concentration of mAb1955 (from 5nM to 20nM) led to unstable binding, represented by a greater decrease in reponse during the disocciation phase with higher concentrations of mAb1955.
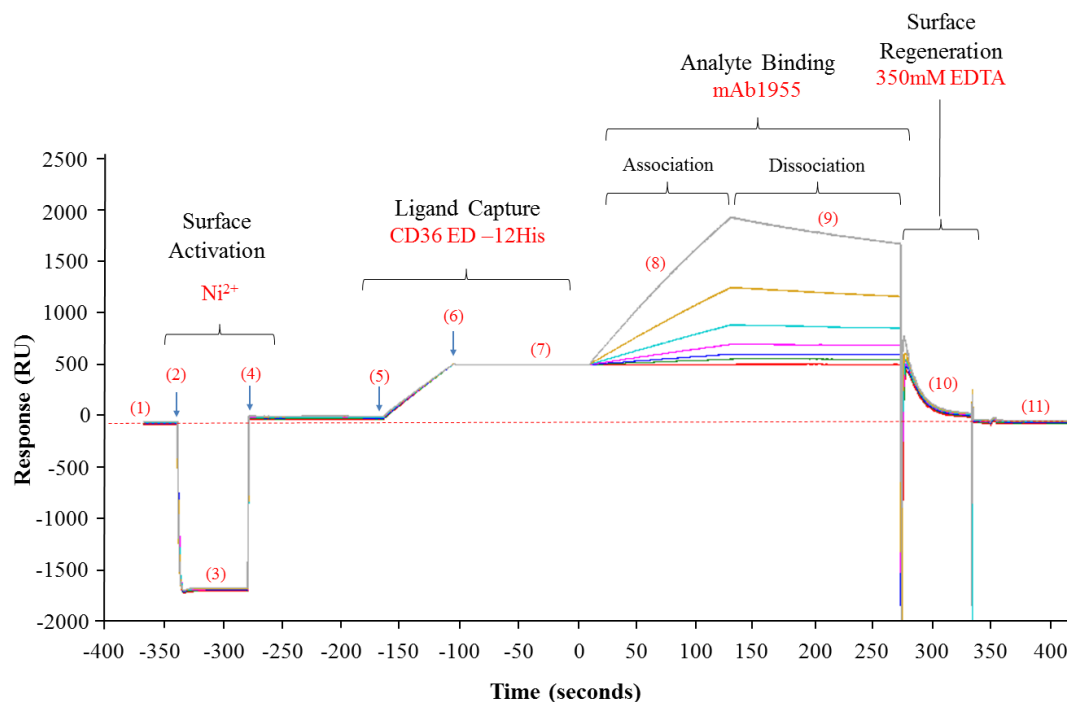
Figure 5.6. Overview of SPR analysis of the interaction of mAb1955 with CD36 ED-12His immobilised on an NTA Sensor Chip.

Overview of nickel activation, immobilisation of CD36 ED-12His and binding of mAb1955. An NTA sensor chip was equilibrated using running buffer (1). On injection of a 0.5mM nickel solution (10µl/min) (2), a drop in resonance (3) was observed due to the change in refractive index of the solution being flowed over the surface. Equilibration of flow cell with running buffer following surface activation (4) revealed a response ~40RU higher than the starting base-line level, corresponding to nickel ions co-ordinately bound to the NTA coated surface. Injection of ~5µg/ml CD36 ED-12His (5) over the activated surface for 60 seconds (10µl/min) resulted in a response increase of ~500RU. After CD36 ED-12His injection (6), running buffer was passed over the sensor surface to monitor dissociation of captured protein. CD36 ED-12His bound tightly to the nickel activated surface of the NTA sensor chip with no decrease in response observed (7). MAb1955 was diluted in running buffer to concentrations from 0nM up to 20nM. One concentration of mAb1955 was injected (30µl/ml for two minutes) over the chip surface per binding cycle (8). Association of mAb1955 was measured by an increase in response level (9). Following the association phase, running buffer alone was passed over the sensor chip surface (10) (30µl/min for 2.5 minutes) with dissociation of mAb1955 measured by a drop in response level (11). The sensor chip surface was regenerated by passing 350mM EDTA over the surface (12), resulting in a decrease in response level (13). Following re-equilibration with running buffer (14), starting base-line response level was restored (15), with the sensor chip surface ready for the next binding cycle. SPR was performed in a Biacore T200 (GE Healthcare) with all analysis undertaken at 25°C. Sensorgrams were generated using BIAevaluation software version 2 (GE Healthcare). Experiments were performed in triplicate (triplicate traces are superimposed).
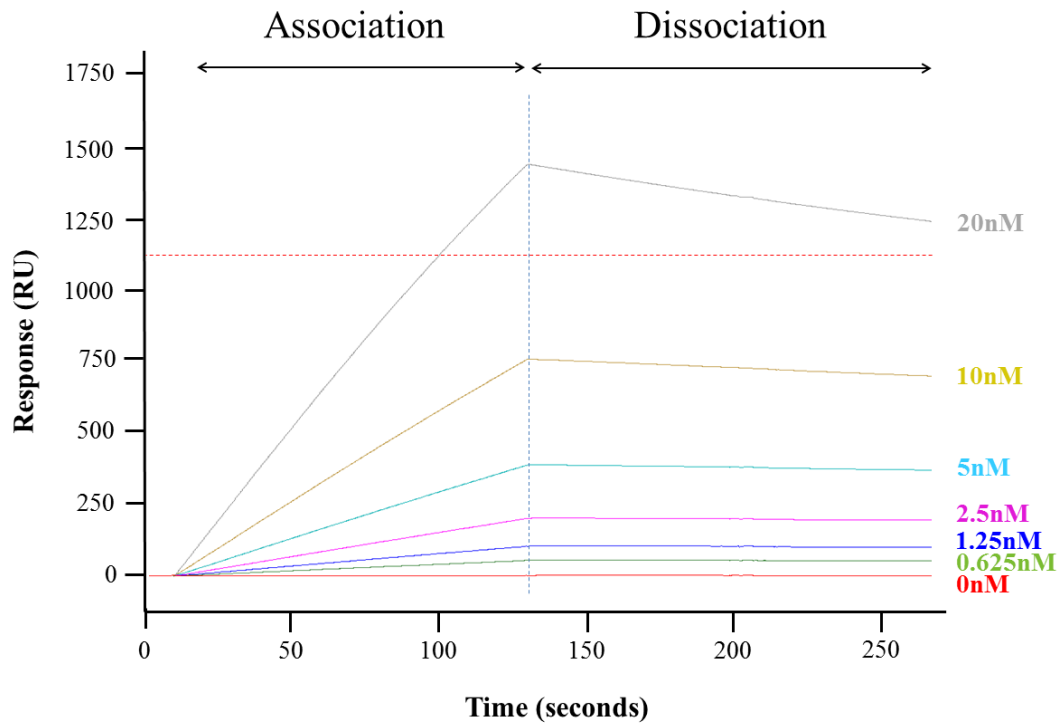
Figure 5.7. SPR analysis of the interaction of mAb1955 with CD36 ED-12His immobilised on an NTA Sensor Chip.
SPR sensorgram for the interaction of mAb1955 to CD36 ED-12His immobilised on an NTA sensor chip. mAb1955 diluted in running buffer to 0nM (blank reference), 0.625nM, 1.25nM, 2.5nM, 5nM, 10nM and 20nM was injected over the sensor chip with immobilised CD36 ED-12His (30µl/min for 2 minutes) in separate binding cycles. Dissociation of mAb1955 was measured by passing running buffer alone over the sensor chip surface. - - - represents the expected Rmax level based on immobilisation of ~500RU CD36 ED-12His with the molecular weights of CD36 ED-12His and mAb1955 being ~63kDa and ~150kDa, respectively. SPR was performed in a Biacore T200 (GE Healthcare) with all analysis undertaken at 25°C. Sensorgrams were generated using BIAevaluation software version 2 (GE Healthcare). Experiments were performed in triplicate (triplicate traces are superimposed).

5.2.3. Specificity of monoclonal antibodies for CD36 ED-12His immobilised on an NTA sensor chip

The shape of the sensorgram curves (the linearity of mAb1955 association and dissociation with the chip) and the unexpectedly high response level, prompted a more rigorous examination of the specificity of mAb1955 binding. In parallel, the binding specificity of two other monoclonal anti-CD36 antibodies for immobilised CD36 ED-12His was performed. In these experiments, one flow cell of a NTA sensor chip was activated with nickel, followed by immobilisation of CD36 ED-12His (~50RU). A second flow cell was only activated with nickel without subsequent CD36 ED-12His immobilisation. Three anti-CD36 monoclonal antibodies; mAb1955, mAb1258 and mAbFA6-152 were flowed over the surface of the two flow cells in different binding cycles to determine antibody specificity for CD36 ED-12His.

5.2.3.1. mAb1955

During injection of 5nM mAb1955 over the NTA sensor chip with CD36-ED-12His immobilised on the surface (Figure 5.8 (a)), a near linear increase in response was observed with the same characteristics as shown previously (Figure 5.7). When 5nM mAb1955 was injected over the nickel-activated surface lacking immobilised CD36 ED-12His (Figure 5.8 (b)), a similar response curve was generated. This result suggests that mAb1955 binding is non-specific and that the antibody has an affinity

for the nickel-activated NTA sensor surface. This similarity is made more apparent when the two traces are merged (Figure 5.8 (c)).
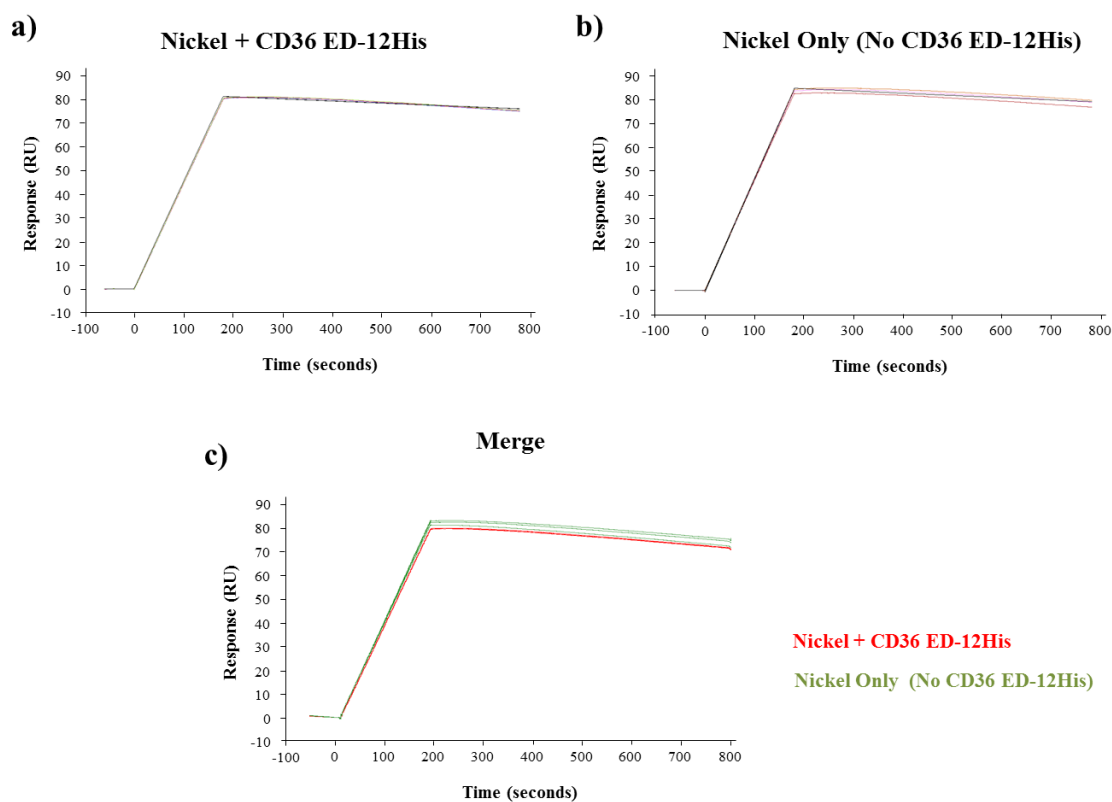
Figure 5.8. Specificity of mAb1955 for CD36 ED-12His immobilised on a nickel-activated NTA Sensor Chip.
Curves show response generated when analyte was flown over sensor chip surface. mAb1955 (5nM) was injected (30µl/min for 3 minutes) over two flow cells of an NTA sensor chip. A flow cell was either **(a)** nickel-activated with CD36 ED-12His (~50RU) immobilised on the surface, or **(b)** activated with nickel alone. Dissociation was measured for 10 minutes (~30µl/min). Sensorgrams from both experiments were merged for comparison **(c)**. SPR was performed in a Biacore T200 (GE Healthcare) with all analysis undertaken at 25°C. Sensorgrams were generated using BIA evaluation software version 2 (GE Healthcare). Experiments were performed in triplicate (triplicate traces are superimposed).

5.2.3.2.   mAb1258

The anti-CD36 antibody mAb1258 (Merck Millipore, Clone 63) is a monoclonal antibody (Mouse IgAκ, ~320kDa) sold primarily for use in detecting CD36 by flow cytometry, immunofluorescence and immunoprecipitation (Hoosdally *et al*., 2009, Keizer *et al*., 2004). In addition, mAb1258 has been shown to be effective at inhibiting the uptake of oxLDL by murine macrophages and adipocytes *in vitro* (Masella *et al*., 2006). However, mAb1258 has been found to be ineffective at detecting CD36 during western blotting analysis, suggesting that epitope recognition is dependent on the tertiary fold.

During injection of 5nM mAb1258 over the NTA sensor chip with CD36 ED-12His immobilised on the surface (Figure 5.9 (a)), an increase in response was observed with similar characteristics to that of mAb1955 binding to the nickel-activated NTA sensor chip surface (Figure 5.9 (b)). When 5nM mAb1258 was injected over the nickel-activated sensor chip surface lacking immobilised CD36 ED-12His (Figure 5.9 (b)), an almost identical response curve, as with mAb1955, was generated. Merged binding traces for mAb1258 are shown (Figure 5.9 (c)) to highlight this similarity. Like mAb1955, mAb1258 appeared to associate with the nickel activated NTA sensor chip surface to the same extent in the presence or absence of immobilised CD36 ED-12His, again suggesting a non-specific interaction independent of CD36 ED-12His.

a) Nickel + CD36 ED-12His

b) Nickel Only (No CD36 ED-12His)

c) Merge

Nickel + CD36 ED-12His

Nickel Only (No CD36 ED-12His)
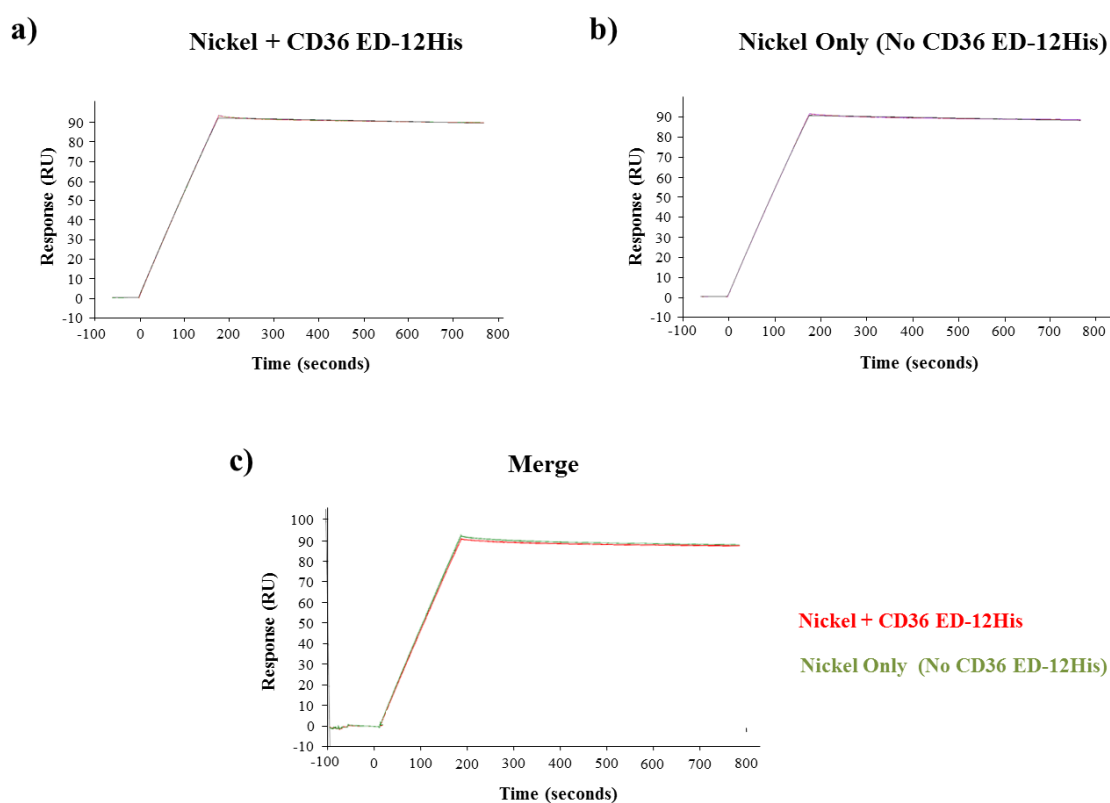
Figure 5.9. Specificity of mAb1258 for CD36 ED-12His immobilised on a nickel activated NTA Sensor Chip.
Curves show response generated when analyte was flown over sensor chip surface. MAb1258 (5nM) was injected (30µl/min for 3 minutes) over two flow cells of an NTA sensor chip. A flow cell was either **(a)** nickel-activated with CD36 ED-12His (~50RU) immobilised on the surface, or **(b)** activated with nickel alone. Dissociation was measured for 10 minutes (~30µl/min). Sensorgrams from both experiments were merged for comparison **(c)**. SPR was performed in a Biacore T200 (GE Healthcare) with all analysis undertaken at 25°C. Sensorgrams were generated using BIA evaluation software version 2 (GE Healthcare). Experiments were performed in triplicate (triplicate traces are superimposed).

5.2.4. mAbFA6-152

The anti-CD36 antibody mAbFA6-152 (Abcam) is a monoclonal antibody (mouse IgG1, ~150kDa) sold for use in a wide range of applications including blocking and functional studies, flow cytometry, immunofluorescence, immunohistochemistry and

193

western blotting analysis (Chu and Silverstein, 2012, Olivetta *et al*., 2014, Maleszewski *et al*., 2007, Thelen *et al*., 2010).

On injection of 5nM mAbFA6-152 over the NTA sensor chip with CD36 ED-12His immobilised on the surface (Figure 5.10 (a)), a response increase is generated as the antibody binds to the sensor chip surface. Unlike, mAb1955 and mAb1258, the response generated when mAbFA6-152 associates with the sensor chip surface has curvature and is more characteristic of an analyte/ligand interaction (Figure 5.4). After injection over the surface, no dissociation of mAbFA6-152 was detected with the response level remaining constant, suggesting a strong stable interaction. When mAbFA6-152 was injected over the nickel activated surface lacking immobilised CD36 ED-12His (Figure 5.10 (b)), a completely different response profile was generated. The maximum response achieved on the nickel-activated only surface was ~6.5RU, whereas ~46RU were achieved when mAbFA6-152 was passed over the surface with immobilised CD36 ED-12His (Figure 5.10 (c)). Additionally, once the flow mAbFA6-152 over the nickel-activated surface (in the absence of CD36 ED-12His) was discontinued and replaced by buffer only, the sensorgram trace returned to baseline, suggesting that the antibody does not stably associate with the nickel-activated surface.

a) Nickel + CD36 ED-12His

b) Nickel Only (No CD36 ED-12His)

c) Merge

Nickel + CD36 ED-12His

Nickel Only (No CD36 ED-12His)
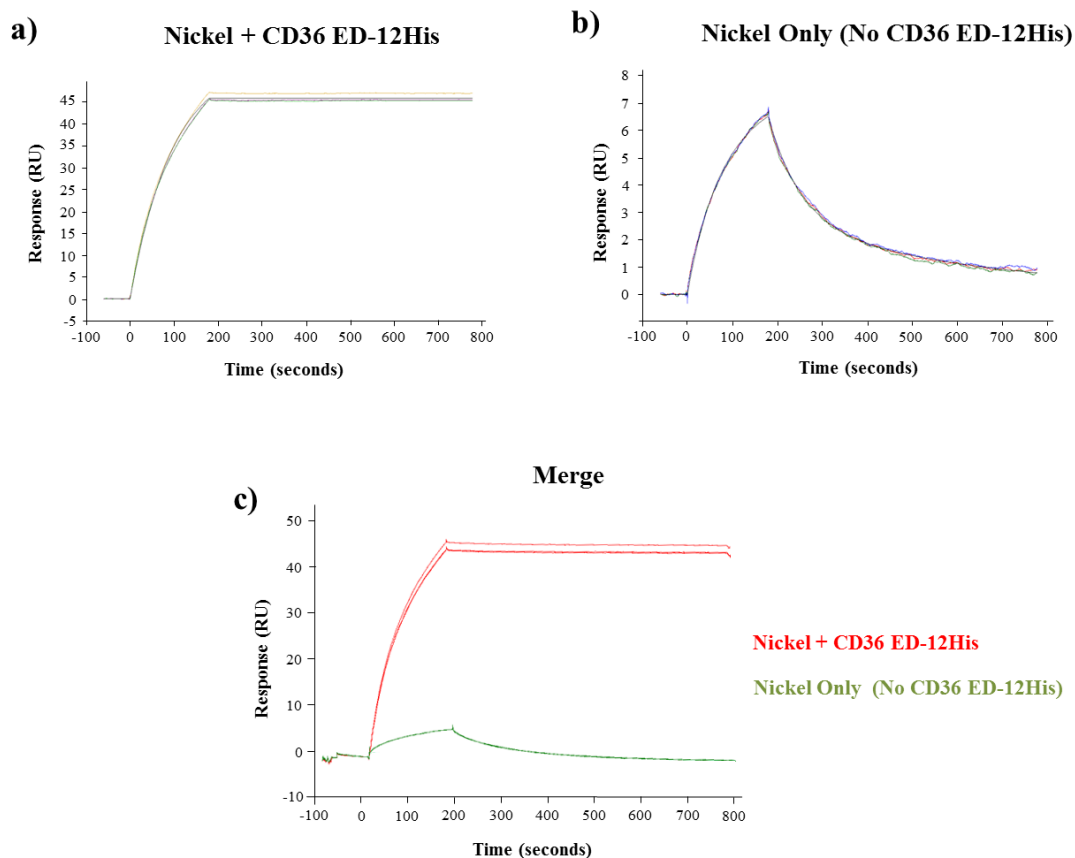
Figure 5.10. Specificity of mAbFA6-152 for CD36 ED-12His immobilised on a nickel activated NTA Sensor Chip.
Curves show response generated when analyte was flown over sensor chip surface. MAbFA6-152 (5nM) was injected (30μl/min for 3 minutes) over two flow cells of an NTA sensor chip. A flow cell either had **(a)** CD36 ED-12His immobilised (~50RU) on a nickel-activated surface, **(b)** activated with nickel alone. Dissociation was measured for 10 minutes (~30μ/min). Sensorgrams from both experiments were merged for comparison and shown in **(c)**. SPR was performed in a Biacore T200 (GE Healthcare) with all analysis undertaken at 25°C. Sensorgrams were generated using BIA evaluation software version 2 (GE Healthcare). Experiments were performed in triplicate (triplicate traces are superimposed).

5.2.5. Determination of an equilibrium dissociation constant for mAbFA6-152 binding to CD36 ED-12His

Of the three antibodies tested, only mAbFA6-152 failed to react with the Ni-charged NTA chip, but specifically recognised CD36 ED-12His. The microkinetics of mAbFA6-152 binding could therefore be analysed further. First, the apparent equilibrium binding affinity of mAbFA6-152 for CD36 ED was measured by SPR. As previously described, affinity is the strength of binding of one molecule to another and is typically measured and reported by a K_D value at equilibrium, (i.e. the concentration of analyte at equilibrium that binds 50% of all ligand binding sites). At equilibrium, the rate of analyte binding is equal to the rate of analyte dissociation (the lower the K_D, the greater the affinity).

The affinity of a binding interaction (expressed as the K_D value) can be determined using two independent approaches. The first is by measuring the dependence of steady-state binding levels on analyte concentrations and then extrapolating a K_D value from a binding curve. The second is by calculating the K_D value as the ratio between kinetic rate constants. Of the two methods, the simplest is by measurement of steady-state binding levels and involves analysing the level of binding at equilibrium for a range of analyte concentrations. Analysis of steady-state binding is achieved through plotting the amount of analyte bound against the concentration of analyte used. From the curve generated it is then possible to calculate the Rmax value and therefore the K_D value.

MAbFA6-152 was diluted in running buffer to a range of concentrations from 0.15625nM to 20nM (including 0nM as a blank reference). Each sample was injected over the nickel-activated NTA sensor chip surface with immobilised CD36 ED-12His (Figure 5.11 (a)). Binding sensorgrams generated showed a concentration-dependent increase in response during mAbFA6-152 injection (association) exhibiting the expected curvature characteristic of analyte/ligand interactions (Figure 5.4).

A steady-state binding curve was then plotted from the maximum response levels generated for each concentration of mAbFA6-162 used, having first subtracted the 0nM blank reference (Figure 5.11(b)). The Rmax value, based on the curve plotted, was found to be 100.5RU $\pm$ 2.3RU (Figure 5.11 (c)). With the molecular weights of CD36 ED-12His and mAbFA6-152 as ~63kDa and ~150kDa, respectively, and ~50RU of CD36 ED-12His having been immobilised, an Rmax value of ~119RU was expected (Equation 5.1). The K_D value for the interaction between mAbFA6-152 and CD36 ED-12His was found to be 5.06nM $\pm$ 0.4nM. The offset value (Figure 5.11 (c)) (a constant that indicates where the curve intercepts the y-axis) is measured at 4.08RU $\pm$ 0.94RU and the Chi^2 value (the total average deviation between the experimental data and the fitted curve) for the binding curve was found to be 4.39RU^2 indicative of the reliability of the data.

(a)

(b)

(c)
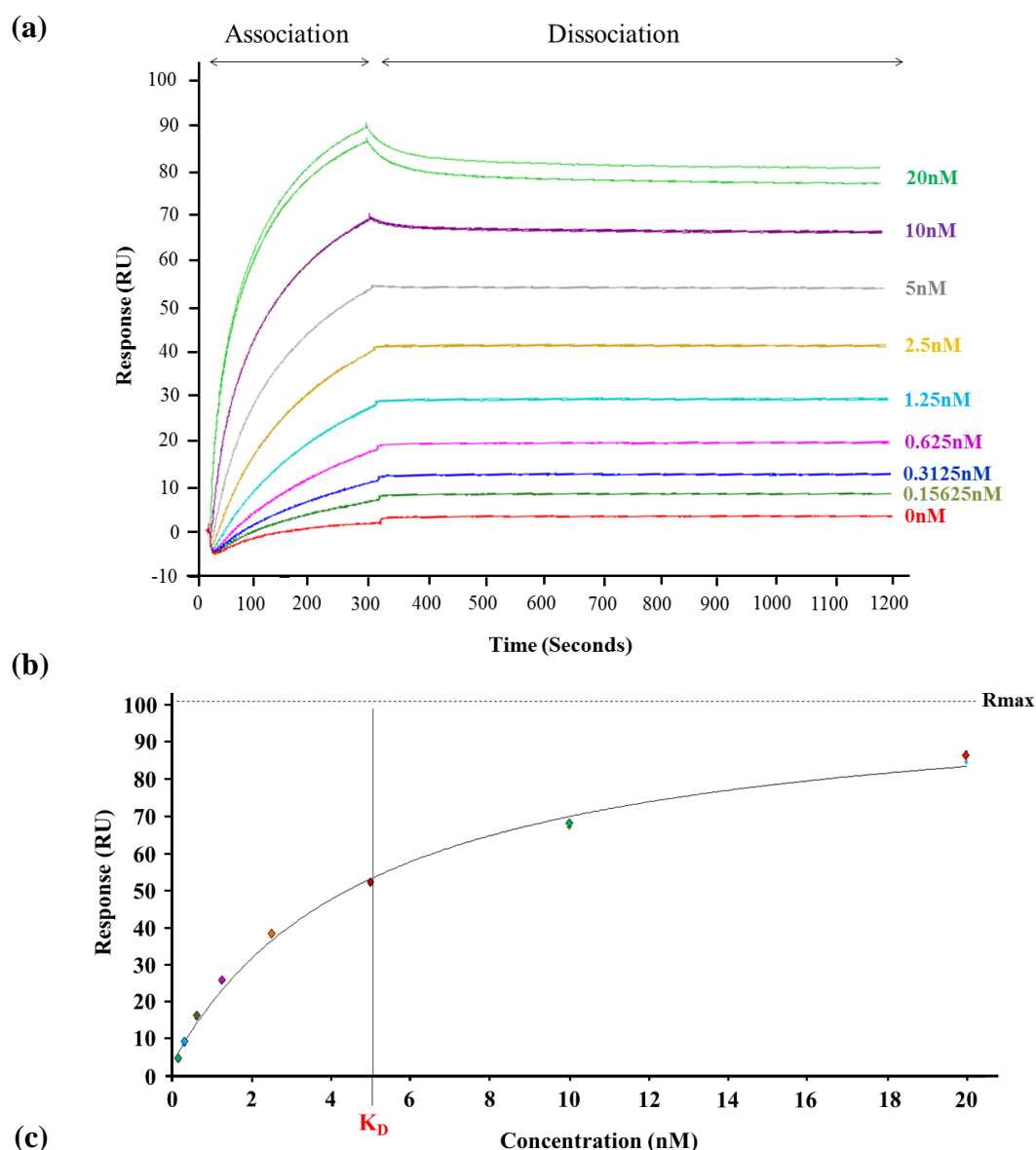
mAbFA6-152 binding to CD36 ED-12His, n=3						
K_D (nM)	S.E. (nM)	Rmax (RU)	S.E. (RU)	Offset (RU)	S.E. (RU)	Chi^2 (RU^2)
5.06	0.40	100.50	2.30	4.08	0.94	4.39

Figure 5.11. SPR analysis of the interaction of mAbFA6-152 with CD36 ED-12His immobilised on an NTA Sensor Chip.
(a) Overlay of sensorgrams for the interaction of mAbFA6-152 to CD36 ED-12His immobilised on an NTA sensor chip. MAbFA6-152 diluted in running buffer to 0nM (blank), 0.625nM, 1.25nM, 2.5nM, 5nM, 10nM and 20nM was injected over the sensor chip surface (30μl/min for 2 minutes) in separate binding cycles. Dissociation of mAbFA6-152 was then measured by passing running buffer over the sensor chip surface (30μl/min for 15 minutes. **(b)** A Steady-state binding model using the blank-subtracted sensorgrams with maximum responses plotted against mAbFA6-152 concentration. From the generated binding curve, Rmax (100.5 ± 2.3RU) and K_D (5.06 ± 0.4nM) values were determined **(c)**, as well as an offset constant (4.08 ± 0.94RU) and a Chi^2 value (4.39RU^2) describing the closeness of experimental data to the fitted steady-state model. SPR was performed in a Biacore T200 (GE Healthcare) with all analysis undertaken at 25°C. Sensorgrams and steady-state curve were generated using BIA evaluation software version 2 (GE Healthcare). Experiments were performed in triplicate (triplicate traces are superimposed).

198

5.2.6. Determination of binding microkinetics of the interaction between mAbFA6-152 and CD36 ED-12His

Having determined the equilibrium binding affinity of mAbFA6-152 for CD36 ED-12His (K_D = 5.06 ± 0.4nM), interaction models were applied to the SPR data to try and ascertain the microkinetics of the interaction, i.e. the on (K_a) and off (K_d) rates of binding and dissociation.

Kinetic data are typically interpreted in terms of a model which best describes the interaction process. The binding constants obtained are apparent constants and are only valid within the context of the model used. As a rule of thumb, the simplest model is usually adequate for generating interpretable data. The simplest model that could potentially apply is the 1:1 binding model (O'Shannessy *et al*., 1993). In this model, the system assumes that the interaction involves one analyte binding to one immobilised ligand. From this it is possible to deduce a single association (K_a) and dissociation (K_d) rate constant for the interaction (Equation 5.2). Another model that may be used to describe binding data is the bivalent analyte binding model (Muller *et al*., 1998). This model is traditionally used when the analyte has two separate binding sites, as is the case with antibodies, such as IgG immunoglobulins, which have two antigen binding sites (Cuesta *et al*., 2010). In this model two separate binding events occur (Equation 5.3). The association and dissociation of the first binding event is described using K_{a1} and K_{d1}, respectively, whereas the association and dissociation of the second interaction is described by K_{a2} and K_{d2}, respectively. The first binding event yields a conventional 1:1 binding fit whereas the second

binding event stabilises the analyte-ligand complex and thus changes the kinetics of

the overall reaction. The sensorgram produced from a bivalent analyte binding to a

ligand would therefore be the result of two different kinetic processes occurring in

tandem.

$$A + B \underset{K_d}{\overset{K_a}{\rightleftharpoons}} AB$$
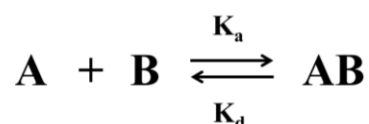
Equation 5.2. 1:1 Binding Model Rate Equation.
One analyte is capable of binding one ligand, described by a single association and dissociation rate
constant. A – Analyte, B – Ligand, AB – Analyte/Ligand Complex, K_a – Association rate constant, K_d
– Dissociation rate constant.

$$A + B1 \underset{K_{d1}}{\overset{K_{a1}}{\rightleftharpoons}} AB1 + B2 \underset{K_{d2}}{\overset{K_{a2}}{\rightleftharpoons}} AB1\text{-}AB2$$
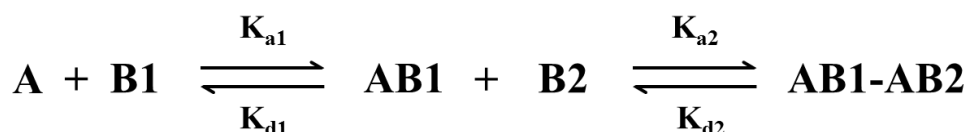
Equation 5.3. Bivalent Analyte Binding Model Rate Equation.
In a bivalent analyte model an analyte is capable of binding two separate ligands. A – Analyte, B –
Ligand, AB – Analyte/Ligand Complex, K_a – Association rate constant, K_d – Dissociation rate
constant.

To determine the binding kinetics for the interaction of mAbFA6-152 to CD36 ED-

12His, a 1:1 binding fit model was first applied (Figure 5.12 (a)). The poor fit during

association and dissociation phases suggested that the 1:1 binding model is not

applicable for the interaction between mAbFA6-152 and CD36 ED-12His. When the

bivalent analyte model was applied to the experimental data (Figure 5.12 (b)), a

much better fit was observed. The closeness of the fit during both association and

dissociation of mAbFA6-152 to CD36 ED-12His suggests that the antibody is binding to either two sites on the same molecule of CD36 ED-12His or that the antibody is binding to one CD36 ED-12His and then binding to another in close proximity to the first. By fitting the bivalent analyte model to the data, two sets of association and dissociation constants were calculated (Figure 5.12 (c)). The first binding event was described by an association rate constant (K_{a1}) of $1.46 \times 10^6 \pm 3.8 \times 10^3 M^{-1} s^{-1}$ with a dissociation rate constant (K_{d1}) of $8.92 \times 10^{-5} \pm 2.5 \times 10^{-7} s^{-1}$. As the second binding event takes place in tandem with the first binding event, the second association rate constant (K_{a2}) was measured in $RU^{-1} s^{-1}$ with a value of $183.5 \pm 19 RU^{-1} s^{-1}$ being calculated. The second dissociation rate constant value was determined to be $1658 \pm 1.7 \times 10^2 s^{-1}$. The closeness of the bivalent analyte binding model to the experimental data was supported by a low Chi^2 value of $0.201 RU^2$.

Although it was possible to generate association and dissociation rate constants for the interaction between mAbFA6-152 and CD36 ED-12His, it was not possible to then deduce an equilibrium dissociation constant (K_D) as a ratio of kinetic rate constants from this data. The ability to determine K_D values based on the kinetic rate constants is dependent on their being a 1:1 binding event, with one analyte binding to one ligand. As mAbFA6-152 binding to CD36 ED-12His proceeds in two-step binding process, where the two binding events are linked, it is not possible to ascertain a single K_D value. Therefore the K_D value obtained previously (see 5.2.5) of 5.06nM is not a description of affinity, but instead avidity, which can be defined as the combined binding strength of multiple interactions.

(a)

← 10nM
← 5nM
← 2.5nM
← 1.25nM
← 0.625nM
← 0.3125nM
← 0.15625nM

(b)

← 10nM
← 5nM
← 2.5nM
← 1.25nM
← 0.625nM
← 0.3125nM
← 0.15625nM

(c)

Bivalent Analyte Model Fit for mAbFA6-152 binding to CD36 ED-12His, n=3								
K_a1 $(M^{-1}s^{-1})$	SE (K_a1)	K_d1 (s^{-1})	SE (K_d1)	K_a2 $(RU^{-1}s^{-1})$	SE $(RU^{-1}s^{-1})$	K_d2 (s^{-1})	SE (s^{-1})	Chi^2 (RU^2)
1.46×10^6	3.8×10^3	8.92×10^{-5}	2.5×10^{-7}	183.5	19	1658	1.7×10^2	0.201
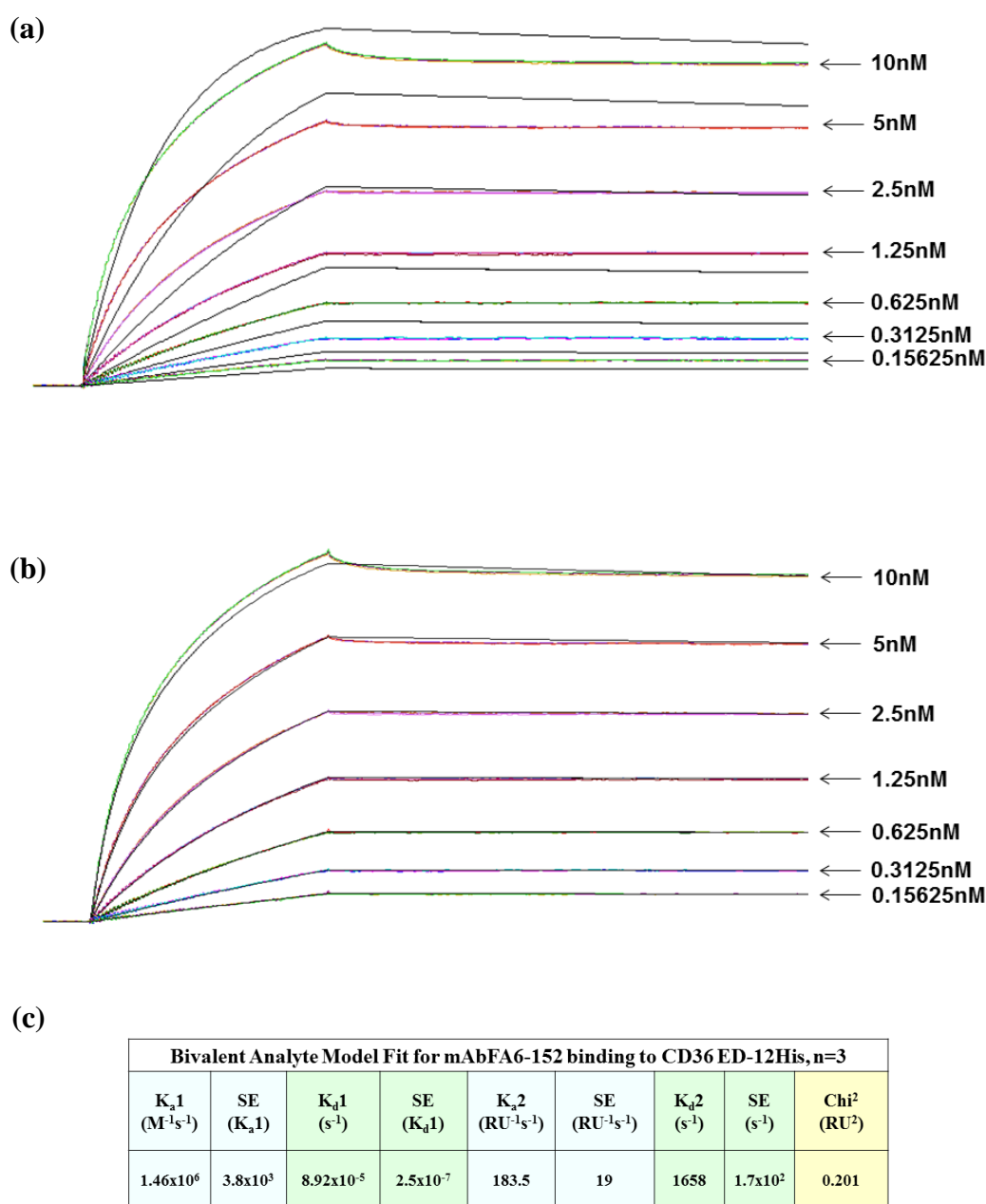
Figure 5.12. Kinetic Analysis of mAbFA6-152 binding to CD36 ED-12His.
Sensorgrams generated from seven concentrations of mAbFA6-152 (coloured lines) binding to immobilised CD36 ED-12His (blank subtracted) were globally fit (black lines) to **(a)** a 1:1 binding model or **(b)** a bivalent analyte binding model. A bivalent analyte model was found to fit experimental data better than a 1:1 binding model. Instead of a single set of Ka and Kd values (1:1 binding kinetics), bivalent analyte binding is dependent on two separate binding events, and so two separate sets of rate constants are measured **(c)**. The second binding event rate constants are dependent on the first and so second K_a values are measured relatively in response units (RU). SPR was performed in a Biacore T200 (GE Healthcare) with all analysis undertaken at 25°C. Kinetic binding models were fit to experimental data using BIA evaluation software version 2 (GE Healthcare). Experiments were performed in triplicate (triplicate traces are superimposed).

5.3. Discussion

The ability to monitor the rate at which a molecule binds and then dissociates from a target receptor is just as important as the affinity with which it binds. To begin to understand the way in which molecules bind the ED of CD36, SPR was used to monitor binding between CD36 ED and monoclonal antibodies. Purified CD36 ED was immobilised onto a nickel-activated NTA sensor chip and exposed to each antibody in the analyte flow to monitor binding events. Of the three antibodies tested, two showed non-specific binding to the nickel-activated sensor chip surface (but not in the absence of nickel). The remaining antibody was found to bind to immobilised CD36 ED specifically.

The ability of both mAb1955 and mAb1258 to associate with the nickel-activated NTA sensor chip surface suggests that these two antibodies interact with the nickel ions independent of immobilised CD36 ED-12His. Based on these findings, it could be speculated that these antibodies may contain a polyhistidine sequence, a possible consequence of the purification processes used during production. However, according to R&D systems, the immunogen used in the production of mAb1955 is a recombinant protein spanning Gly30-Asn439 (covering the ED) of human CD36, expressed and secreted from Sf21 insect cells. Using the hybridoma technique (Kennett, 1981, Tomita and Tsumoto, 2011), this recombinant protein was used to generate a single monoclonal anti-CD36 antibody which was then purified from a hybridoma cell culture supernatant using either protein A or G. The hybridoma technique involves the fusion of a specific antibody-producing B cell, isolated from the spleen of an immunised mammal (for mAb1955, a rat), with a myeloma cell to

form an immortalised hybridoma (Kohler and Milstein, 1975, Kohler and Milstein, 1976). The resultant hybridoma will produce a monoclonal antibody with a single specificity. Based on this procedure it is highly unlikely that the antibody produced would contain a polyhistidine tag. MAb1258 was also produced using the hybridoma technique where the immunogen was a recombinant adenovirus vector encoding murine CD36. Both antibodies are provided in simple buffers, lacking additives (mAb1955, PBS; mAb1258, TBS). This affinity of mAb1955 and mAb1258 for nickel therefore remains unexplained. It may be possible to experimentally verify the presence or absence of a histidine tag on these antibodies by SPR by immobilising an anti-histidine antibody onto a CM5 sensor chip and then injecting either of the two antibodies over the surface. As both antibodies have been shown to bind the ED of CD36 expressed on the surface of cells previously, it was surprising not to have observed a greater (and biphasic) response when these antibodies were injected over the immobilised CD36 ED. This may be explained by the small amount of CD36 ED immobilised on the surface of the NTA chip, which could result in the antibody coming into contact with the nickel-activated surface first and binding with high affinity, thereby blocking subsequent binding to immobilised CD36 ED through a steric hindrance effect. The microkinetics of mAb1955 and mAb1258 binding to CD36 ED could yet be measured by immobilising ED to different chip surface that does not chelate divalent cations, such as a CM5 chip or, following biotinylation of the ED, a SA chip.

In contrast, mAbFA6-152 was found to bind specifically to CD36 ED-12His with high avidity (5.06nM). The small response increase observed when the antibody was injected over the surface lacking CD36 ED-12His could be attributed to a number of factors. Firstly, mAbFA6-152 is provided in PBS buffer containing 0.1% BSA. The

BSA which is likely to be present as a stabilising agent may have a weak affinity for the nickel-activated surface. Secondly, the non-specific binding may be due to a mass transport effect, a diffusion-dependent supply of analyte to the sensor chip surface. Mass transport is a problem commonly encountered at high analyte concentrations or when the analyte flow rate is too low. At very high analyte concentrations or at very low flow rates, where the flow rate is slower than the association rate, the observed response increase is a measure of the diffusion rate rather than the interaction of analyte and ligand. In the current study the analyte flow over the surface was at 30µl/min, the recommended flow rate to minimise mass transport effects. Although increasing the flow rate further may have reduced possible mass transport effects, the shape of the response curve generated during analyte injection on the nickel-activated surface suggests a dose-dependent interaction with the surface. However, the non-specific interaction between mAbFA6-152 (and/or BSA) and the nickel-activated surface is subtle in comparison to the response generated when mAbFA6-152 interacts with CD36 ED and would only have a minimal effect on the calculated K_D and microkinetic rate constants. Previous work by Pambakian and Poston showed that the Fc fragment of IgG antibodies can bind non-specifically to solid phase cationic sites in the absence of competing proteins (Pambakian and Poston, 1987). When the nickel coordinates with the NTA sensor chip, it forms a cationic surface. This therefore might be responsible for the observed binding of mAb1955 and mAb1258 to the activated sensor chip surface. Furthermore, the presence of BSA, which is a common blocking reagent used in antibody based assays, in the mAbFA6-152 solution might act to block non-specific binding allowing specific binding to take place.

MAbFA6-152 was found to interact with CD36 ED-12His via a 2-step binding process. The bivalent analyte binding model describes an analyte which has two identical binding sites, a property that is true of all IgG immunoglobulins (such as mAbFA6-152) (Cuesta *et al*., 2010). This bivalent binding property allows cross-linking of two identical antigenic sites, increasing affinity and therefore improving retention time, maximising an immune response (Cuesta *et al*., 2010). The result of this model is the measurement of two separate sets of binding rate constant which together describe the avidity rather than the affinity of antibody to ED. As very little CD36 ED was immobilised onto the sensor chip surface, far from saturating levels (CD36 ED binding response does not plateau during ligand capture, Figure 5.5), it is unlikely based on this that mAbFA6-152 was cross-linking different CD36 ED molecules. This however is based on the assumption that the purified CD36 ED was immobilised in a monomeric, dispersed, non-aggregated-like fashion. It was shown previously (see 3.2.10) that at high concentrations purified CD36 ED was more likely to be found as higher molecular weight species with molecular weights equating to possible a dimer, trimer, tetramer, etc, formation. Although the concentration of CD36 ED in SPR experimentation was low enough to observe the protein in a predominantly monomeric state by SDS-PAGE, by passing the ED through the microfluidics of the Biacore system, the protein may have become close enough in proximity to self-associate either prior to or during immobilisation.

This initial study, along with other recent publications, shows the potential of using SPR to study the interactions between CD36 and its associated ligands. In 2012, Bao *et al.,* demonstrated a binding affinity (in the micro-molar range) for SAB and hexarelin for CD36 ED immobilised on the surface of a CM5 sensor chip. Interestingly, the binding of these molecules to the commercially bought insect cell-

derived CD36 ED (R&D Systems, Minneapolis, MN) was fitted with a 1:1 binding model (Bao *et al*., 2012). Although it was not shown whether the CD36 ED was forming homo-oligomers, it is unlikely that these small ligands are bivalent and therefore capable of binding more than one CD36 ED at a time. In contrast to mAbFA6-152 which is a large bivalent IgG molecule, hexarelin is a six-amino acid peptide (Massoud *et al*., 1996) and SAB is a water-soluble 718.6Da phenolic acid derived from plants (Ho and Hong, 2011).

With further optimisation it may be possible to measure the binding affinity, and more importantly the binding kinetics, of more physiologically relevant ligands such as oxLDL or TSP-1. In 2011, Ohki *et al*. demonstrated how the binding affinity of modified LDL binding to the LOX-1 receptor could be achieved with LOX-1 immobilised on the surface of a SA sensor chip. From this they managed to observe differing binding affinities based on whether LOX-1 was immobilised as a monomer, dimer or as a cluster (Ohki et al., 2011). Although successful binding information was generated from mAbFA6-152 binding to CD36 ED immobilised to the surface of a nickel-activated NTA sensor chip, caution should be taken to detect and limit non-specific binding events which may interfere with reliable data acquisition. Thrombospondin-1 has been shown to associate with polyhistidine sequences with high affinity (Vanguri *et al*., 2000). This therefore most likely rules out being able to study thromobospondin-1 interacting with CD36 ED immobilised to the NTA surface via the 12His tag. Further optimisation may be required to measure oxLDL binding to the ED of CD36. To formulate oxLDL, LDL is typically incubated with the salt of a transition element, such as copper sulphate, to oxidise lipid and protein moieties (Heinecke *et al*., 1984). The NTA sensor chip is nickel-activated and, as a transition element, nickel could potentially increase the oxidation

level of the analyte during the experiment leading to erroneous binding data. Preliminary results (not shown) suggest that native unmodified LDL binds and possibly undergoes modification as it is passed over a nickel-activated NTA sensor chip. Taken together these possible complications suggest careful consideration is required to identify the appropriate surface chemistry for immobilising CD36 ED and that this is likely to be dependent on the ligand tag used. By testing interactions with CD36 ED on a variety of different sensor surfaces, such as with SA and CM5 chips, methods could be optimised to enhance the quality of the data obtained while reducing non-specific, erroneous binding events.

6. General Discussion

The aim of this study was to establish a method to express and purify milligram quantities of CD36 to allow the initiation of crystallisation trials and to perform SPR to measure the microkinetics of ligand binding. In chapter 3, a mammalian expression system and three baculovirus expression systems in two different insect cell lines were compared to provide the highest yield of CD36 ED. CD36 ED expressed from *FlashBAC Gold* from Sf21 and Hi5 insect cells was purified using nickel affinity chromatography. The Sf21-derived material could be deglycosylated with PNGase F without denaturation and was shown to retain affinity for modified LDL irrespective of its glycosylation status. Expression and purification on a large-scale format showed that recombinant CD36 ED forms homo-oligomers, especially at higher concentrations. In chapter 4, the glycosylation status and glycan composition of CD36 ED expressed and purified from insect cells was assessed using mass spectrometry. The glycans present on CD36 derived from both Sf21 and Hi5 insect cells lines were simple (high mannose) but heterogeneous. Hi5 insect cells were capable of producing glycans with a di-fucosylated core N-acetylglucosamine offering an explanation for the incomplete deglycosylation by PNGase F for CD36 ED purified from these cells. No evidence was found for glycosylation at one (N4) of the ten putative glycan sites, as described for full length CD36 expressed in mammalian or insect cells (Hoosdally *et al*., 2009). When mapped to the structure of the homologous LIMP-2, N4 was localised to a helix suggested to be involved in ligand binding and homo-oligomerisation. Finally in chapter 5, purified CD36 ED was immobilised on a sensor chip and SPR was used to investigate the binding

affinity and microkinetic interaction of three monoclonal anti-CD36 antibodies. Although two antibodies, mAb1955 and mAb1258, were found to bind non-specifically to the nickel-activated sensor chip surface, an equilibrium binding constant was obtained for mAbFA6-152. Microkinetic analysis was consistent with a two-step process with the bivalent antibody binding to two separate sites. As a result, the binding data was expressed as a measure of avidity, the strength of multiple binding events rather than affinity which is the strength of a single binding event.

In the following sections, the findings of this study are summarized and discussed in relation to the data in the literature, and possible further work is considered that may lead to a fuller understanding of the structure as well as the ligand binding dynamics of human CD36.

6.1.   Expression and purification of CD36 ED

Endogenous CD36 has previously been purified from human platelets (Tandon et al., 1989b), human and bovine mammary epithelial cells (Greenwalt *et al*., 1990), rat adipocytes (Jochen and Hays, 1993) and rat cardiomyocytes (Brinkmann *et al*., 2006) using the detergent (Triton X-100/114) to solubilize the protein from the membrane with a combination of different purification techniques including ion exchange, lectin-affinity and size-exclusion chromatography (SEC). Despite it being possible to isolate endogenous CD36 with high purity, for example >95% (0.2mg Cd36/250mg total heart protein) from rat cardiomyocytes, it required initial solubilisation of membrane proteins with detergent and then the continual presence of detergent during purification to prevent protein aggregation (Brinkmann et al.,

2006). In addition to this, the existence of detergent might have hindered downstream applications such as crystallography and surface plasmon resonance (Tan and Ting, 2000, Garavito et al., 1996). It is therefore advantageous to express the ED of CD36 alone as it removes the need to solubilise the membrane and to maintain the protein in detergent throughout purification and downstream applications.

The need for structural and ligand binding studies means that it is important to maximise the expression of the protein to obtain a suitable yield, preferably milligram quantities. In this project, CD36 ED was expressed in insect cells using a baculovirus expression vector. The protein was fused, in frame, to an amino-terminal cleavable secretory signal and a carboxy-terminal 12 histidine tag, which allowed the protein to be secreted into the surrounding culture media and subsequently purified using nickel affinity chromatography; all in the absence of detergent. This approach allowed 55-115µg of CD36 ED to be purified from small-scale (100ml) insect cell cultures. The process was scalable to 5 litre Sf21 insect cell culture despite the apparent formation of homo-oligomers. Similar approaches have been used in the past to obtain high yields of scavenger receptor protein. For example, Neculai *et al*., demonstrated that it was possible to express and secrete the ectodomain of LIMP-2 (amino acids 35-430; LIMP-2 ED) from Sf9 insect cells and subsequently use nickel affinity chromatography and SEC to isolate a sufficient yield of pure protein to allow successful protein crystallisation. Despite the yield not being quoted, it was reported that the protein, following SEC, was concentrated to 15mg/ml for subsequent crystallisation (Neculai *et al*., 2013). This reinforced the idea that the baculovirus/insect cell expression system was indeed a good system to use for producing a high yield of protein which could then be used for structural studies.

Interestingly, the same study showed that LIMP-2 ED was also prone to forming homo-oligomers. However, a predominantly monomeric form could be isolated following SEC. The unit cell of the crystal consisted of six molecules, four of which formed head-to-head dimers with extensive crystal contacts between the alpha-helical bundles including α5 and α7 (Neculai *et al*., 2013). It is possible that this reflects the homo-dimeric interaction that the purified LIMP-2 ED is prone to, but equally this packing arrangement could just as likely represent crystal contacts that have no physiological relevance.

In 2009, Jimenez-Dalmaroni *et al*., also showed that it was possible to express and secrete the ectodomain of mCd36 using a baculovirus expression vector, this time from Hi5 insect cells (Jimenez-Dalmaroni *et al*., 2009). The protocol used nickel affinity, cationic exchange and SEC, to achieve 'highly purified' mCd36 ED, however, no yield or purity values were quoted. mCd36 ED did however appear to be monomeric in solution, eluting as a single defined peak from a SEC column. SEC was also used to provide evidence of mCd36 ED binding to diacylglycerides by observing changes in the relative protein elution times following incubation of mCd36 ED with the ligand (Jimenez-Dalmaroni *et al*., 2009). Ligand binding to mCd36 ED was associated with earlier elution during SEC, represented on the chromatogram by a defined peak shift to the left, suggesting an overall increase in size due to the interaction. This would be difficult with a protein that homo-oligomerises. The primary sequences of human CD36 and mouse Cd36 within the regions proposed to be involved with homo-oligomerisation are almost identical (Figure 6.1). The primary difference is the presence of a putative N-linked glycosylation site within the human sequence, which is absent from the mouse sequence. However, as shown in chapter 4, and consistent with the data reported for

full length human CD36 by Hoosdally *et al*., this site is not occupied by a glycan and therefore the apparent difference in behaviour of the two proteins is not likely to be due to differences in glycosylation at this locus (Hoosdally *et al*., 2009). Overall, it seems unlikely that these apical helices are responsible for the homo-oligomerisation of CD36 ED observed in the present study.

Another curiosity that is worth noting is that primary sequence alignment of LIMP-2 with CD36 is far from perfect over the helical bundle. In particular, the presence of multiple proline residues within the primary sequence of mouse and human CD36, proposed to form the α7 helix makes it less likely that this region is even helical in CD36. It is well known that proline residues have a poor helix propensity, producing either kinks or breaks within helices due to sterically rigid side-chains (Pace and Scholtz, 1998). In addition, α5 in LIMP-2 is an amphipathic α helix with charged residues at three to four periodicity separated by neutral or hydrophobic amino acids. This is not apparent in the primary sequence proposed to form α5 from CD36. The meaning of this is not yet clear; it is possible that the alpha-helical bundle is important for ligand interaction and simply reflects that the ligands of LIMP-2 and CD36 are different. However, it is also possible that the fold of CD36 differs from LIMP-2 in these apparently important regions of the protein and should caution against using a low resolution LIMP-2 crystal structure to infer the structure of CD36.

```
                                               α5 helix
                                       ┌─────────────────────────┐
                                                        N4
CD36     GAIFEPSLSVG-TEADNFTVLNLAVAAASHIYQNQ--FVQMILNSLINKSKSSMFQVRTL 175
mCd36    GAIFEPSLSVG-TEDDNFTVLNLAVAAAPHIYQNS--FVQVVLNSLIKKSKSSMFQTRSL 175
hLIMP-2  AYVFERDQSVGDPKIDLIRTLNIPVL--TVIEWSQVHFLREIIEAMLKAYQQKLFVTHTV 173
hSR-BI   TFQFQPSKSHG-SESDYIVMPNILVLGAAVMMENKPMTLKLIMTLAFTTLGERAFMNRTV 176
                *:  .  *  *  .:  *  :    *:  *         ::  ::    :.    .   *   :::

            α7 helix
         ┌────────────────┐
CD36     RELLWGYRDPFLSLVP------YPVTTTVGLFYPYNNTADGVYKVFNGKDNISKVAIIDT 229
mCd36    KELLWGYKDPFLSLVP------YPISTTVGVFYPYNDTVDGVYKVFNGKDNISKVAIIES 229
hLIMP-2  DELLWGYKDEILSLIHVFRPDISPY---FGLFYEKNGTNDGDYVFLTGEDSYLNFTKIVE 230
hSR-BI   GEIMWGYKDPLVNLINKYFPGMFPFKDKFGLFAELNNSDSGLFTVFTGVQNISRIHLVDK 236
              *::***:*  ::.*:          *     .*:*    *.:  .*  :  .:.*  :.  ..   :
```

Figure 6.1. Primary Sequence Alignment of Human CD36 Protein Family with the mouse CD36 Protein.
Clustal[15] sequence alignment of the human CD36 family of proteins and mouse CD36. The fourth putative N-linked glycosylation site (N4) in CD36 is underlined with corresponding asparagine highlighted in yellow. Sequences highlighted in green and blue indicate residues predicted to reside within the first (α5) and second (α7) alpha helices involved with ligand binding and homo-oligomerisation, based on the model generated by Neculai, *et al*,. LIMP-2 residues in red are those predicted to be important for homo-oligomerisation. Mutating CD36 residues in brown were shown to abrogate binding of DiI-oxLDL (Neculai *et al*., 2013). '*****': identical residues, '**:**' conserved residues, '**.**' Semi-conserved residues.

6.2.   Glycosylation of CD36 ED expressed in insect cells

There is increasing evidence that insect cells are capable of producing more elaborate forms of glycosylation than the paucimannosidic glycans previously described (Rendic *et al*., 2008). In chapter 3, it was shown that N-linked glycans on CD36 ED derived from Hi5 insect cells could not be cleaved using PNGase F, whereas those from CD36 ED derived from Sf21 insect cells could be cleaved. Insensitivity to PNGase F is attributed to the presence of α(1-3) core-linked fucose residues (Tretter *et al*., 1991). In chapter 4, mass spectrometric analysis of purified CD36 ED showed the presence of di-fucosylated glycan structures on CD36 ED

prepared from Hi5 cells. Sf21 cells were found to produce only singly fucosylated glycans. This suggests that CD36 ED purified from Sf21 cells contains PNGase F-sensitive α(1-6) core-linked glycans whereas Hi5 cells produces CD36 ED with glycans containing both α(1-6) and PNGase F-resistant α(1-3) core-linked glycans. This conclusion is supported by other studies which have also looked at the expression of CD36 from insect cells. In 2009, when mCd36 ED was purified from Hi5 insect cells, it was reported that PNGase F was not able to release all N-linked glycans. The theoretical molecular weight of unmodified mCd36 ED was predicted to be ~47.4kDa, however after digestion the electrophoretic mobility suggested a molecular weight above 50kDa. This inability to remove all glycans was also attributed to the presence of α(1-3) core-linked fucose residues (Jimenez-Dalmaroni *et al*., 2009). In contrast, Hoosdally *et al*., showed N-linked glycans on full-length CD36 purified from Sf21 cells could be removed when digested with PNGase F. Digested CD36 had an electrophoretic mobility corresponding to a molecular weight of around 50kDa (the predicted unmodified molecular weight being ~53kDa) (Hoosdally *et al*., 2009). The difference in glycosylation found in both insect cell lines could have a significant impact on the crystallisation of CD36. The inability to remove heterogeneous glycans, as was found with Hi5 derived CD36 ED, could hinder efficient crystal formation. On the other hand, the ED of LIMP-2, purified from Sf9 insect cells, was crystallised with N-linked glycans consisting of between 1-5 mannose units still present (similar to those detected on CD36 ED (chapter 4)). However, the resultant crystals diffracted poorly, and the eventual resolution obtained was only to 3Å (Neculai *et al*., 2013). By removing the glycans it may be possible to obtain crystals that diffract to a higher resolution, and obtain a more accurate structural model of CD36.

This study is unique in that it is the first example describing the removal of N-linked glycans from CD36 without prior denaturation. Deglycosylated, native, CD36 ED (purified from Sf21 insect cells), binds modified LDL with the same affinity as the glycosylated native protein. It was concluded therefore that N-linked glycosylation does not play a role in binding of modified LDL to CD36. As discussed in chapter 4, there is only one sequon within CD36 that was not occupied by a glycan. This sequon (N4) is located within the region of CD36 suggested to be important for modified LDL binding. The asparagine is not buried in secondary structure (based on the LIMP-2 crystal structure) and none of the other sequons are located near this region. It is unclear why this site is not recognised by the glycosyltransferases that catalyse glycosylation events in the ER. There may be a mechanism which prevents glycosylation at this site, perhaps because it is critical for ligand binding and the inclusion of a glycan would inhibit ligand binding due to steric hindrance. To date, a precise role for N-linked glycosylation of CD36 function has not been defined. Hoosdally *et al*., demonstrated the need for a minimal level of N-glycosylation to ensure trafficking of CD36 to the plasma membrane in transiently-transfected HEK293T mammalian cells, but no individual glycosylation site or event was found to be critical (Hoosdally *et al*., 2009). This was interpreted as a requirement to engage lectin-like chaperones in the folding pathway, however a role in protein stability remains a possibility, particularly for an ectodomain exposed to proteases in the circulation. This remains to be tested. It was reported by Lauzier *et al*., that Cd36 N-linked glycosylation, in particular on Asn102, is important for uptake of LCFA. This was proposed following the observation that SHR, which express Cd36 lacking the putative N-linked glycosylation site at Asn102 (N2), were less able to utilise exogenous LCFA (Lauzier et al., 2011). In SHR this residue is a serine instead of an

asparagine. This data is however debatable as Cd36 from SHR is known to have multiple alterations in its primary amino acid sequence not just at amino acid position 102 (Aitman et al., 1999). These variations in primary amino acid sequence could have a significant impact of the overall fold of the protein and potentially alter ligand binding sites. Additionally, Asn102 is located away from the proposed LCFA binding site on CD36 which includes Lys164 and Lys166 (Kuda et al., 2013b), further questioning whether N-linked glycosylation has a role in LCFA utilisation by CD36.

6.3. Modified low density lipoprotein binding to CD36 ED purified from insect cells

The presence of correctly folded CD36 ED purified from Sf21 insect cells was demonstrated by the ability to bind acLDL. Modified LDL bound to the purified CD36 ED with the same affinity as full-length CD36 purified from Sf21 insect cells and more importantly, with the same affinity as full length CD36 expressed on the surface of mammalian cells (Hoosdally *et al*., 2009). It was suggested by Kar *et al*., that the region of CD36 between amino acids 160-168 (α5) contains the binding site for oxLDL and furthermore that Lys164 and Lys166 are crucial for this interaction (Kar *et al*., 2008). More recently the apparent importance of these two residues in modified LDL binding was shown by mutating both Lys164 and Lys166 to glutamates (K164E/K166E), in addition to mutating Leu158 and Leu161 to glutamates (L158E, L161E) independently. Introduction of these mutations was reported to abolish the ability of CD36 (tagged with an enhanced green fluorescent

protein, EGFP) expressed on the surface of CHO cells to bind modified LDL (Neculai *et al*., 2013). Confocal images, however, provided little evidence based on EGFP signal to suggest plasma membrane localisation. This is especially true for the lysine double mutant (K164E/K166E) and L158E mutant which appear to be retained intracellularly. It should be noted that these mutations significantly change the character of the side chain, changing positively charged (Lysine) or hydrophobic (Leucine) residues to negatively charged (Glutamic acid) residues. This could potentially have a significant effect on the protein fold. For example, the introduction of a negatively charged side chain close to another negatively charged side chain (which would be the case if one or more of the lysines in the native protein is involved in a salt bridge) could result in repulsion thus distorting the native fold. The chosen mutations may therefore affect ligand binding allosterically, bringing into question their direct involvement in binding modified LDL. The localisation of these mutants would suggest a folding defect which is either causing the protein to be retained within the secretory pathway or it being trafficked for degradation. Nevertheless, if it is presumed that amino acids 158-168 are involved directly in oxLDL binding then this would implicate α5, the same helix proposed to be responsible for homo-oligomerisation, as discussed above. If the modified LDL binding site on CD36 is indeed the same site as that involved in homo-oligomerisation then it would be expected that homo-oligomerisation of purified CD36 might prevent modified LDL binding, and this may have consequences for ligand binding studies. For example, if oligomeric CD36 ED cannot bind modified LDL this would likely reduce the binding maxima, but the affinity and microkinetics of binding to the monomeric domain would be unaffected.

6.4. Using SPR to measure the microkinetics of ligand binding to CD36

As discussed in chapter 5, the rate of association and dissociation of a one molecule to another is arguably more relevant than the overall binding affinity at equilibrium, especially when considering these binding events within the dynamic environment found within the human body. SPR is a powerful label-free tool for measuring these binding events in real time (Karlsson, 2004). MAbFA6-152 was shown to bind to immobilised purified CD36 ED with an equilibrium binding constant, K_D = 5.06nM, however analysis of the microkinetics of binding, showed that this antibody bound to the immobilised CD36 ED via a two-step process meaning that the binding constant is more accurately referred to as a measure of avidity, the strength of multiple binding events, rather than affinity. MAbFA6-152 has been used in a number of studies to block TSP-1, oxLDL and *P. falciparum* infected erythrocytes from binding to CD36 (Nergiz-Unal *et al*., 2011, Volf *et al*., 1999, Baruch *et al*., 1999). The assumption that this antibody can therefore recognise the binding site of all these ligands is questionable as these ligands have been reported to have completely separate binding sites. Daviet *et al*., proposed having used homologue-replacement mutagenesis, that the likely binding site for mAbFA6-152 was within the region containing amino acids 155-183, with Asn162 being a key residue for binding (Daviet *et al*., 1995). This would suggest that mAbFA6-152 recognises the region on CD36 proposed as the binding site for modified LDL and *P. falciparum* infected erythrocytes (Neculai et al., 2013, Kar et al., 2008, Baruch et al., 1999). The ability of this antibody to block binding of TSP-1 may therefore be due to steric hindrance

or allostery by inducing a conformational change in CD36 that masks the relevant binding sites.

The SPR analysis of mAbFA6-152 binding to immobilised CD36 ED was best fitted by a two-step binding model to generate two sets of rate constants. MAbFA6-152 is an IgG molecule (~150kDa) and, as with all IgG antibodies, it is bivalent with two identical antigen binding sites. At the end of chapter 5 it was proposed that mAbFA6-152 bound to two separate sites from two different CD36 molecules. Furthermore, combined with the observation in chapter 3 that CD36 ED can form homo-oligomers, it is possible that mAbFA6-152 binds to two CD36 ED molecules that were in association. If this theory is correct then it once again brings into question whether the proposed homo-oligomerisation site on LIMP-2 is the same for CD36. If mAbFA6-152 binds to the region containing amino acids 155-183 with Asn162 being critical (Daviet *et al*., 1995), and if homo-oligomerisation occurred via the same region, then mAbFA6-152 would be unable to bind to oligomeric CD36 ED. It seems likely therefore that homo-oligomerisation of CD36 ED is not mediated by the alpha-helical bundle identified in the LIMP-2 crystal structure as a putative homo-dimerisation interface. To further explore whether mAbFA6-152 is indeed binding through a two-step process to CD36, a monovalent antigen-binding fragment (fab) of this IgG antibody could be generated which should give a 1:1 binding kinetics profile.

The data presented in chapter 5 and other studies indicates the potential of SPR to measure the affinity and microkinetics of physiological ligand binding to CD36. It is also a useful technique to screen pharmacological agents which might be used against CD36 in the treatment of a range of disease states. Bao *et al*., showed by SPR that equilibrium binding affinities could be measured for SAB and hexarelin binding

to immobilised CD36 ED (Bao *et al*., 2012). Both have been shown to have an anti-atherosclerotic effect in mice by blocking binding of oxLDL to Cd36 (Bao *et al*., 2012, Demers *et al*., 2004). Both hexarelin and SAB are likely to be good candidates for further SPR analysis to determine the microkinetics of binding, i.e. the rate of association and dissociation to CD36. In contrast to mAbFA6-152 which is a large bivalent IgG molecule, hexarelin is a six-amino acid peptide (Massoud *et al*., 1996) and SAB is a water-soluble 718.6Da phenolic acid derived from plants (Ho and Hong, 2011). Other examples of molecules that could be studied by SPR include the CD36 inhibitors AP5055, AP5258 and ursolic acid which, like SAB, are also small and unlikely to be bivalent (Geloen et al., 2012, Wilkinson et al., 2011). To predict how these compounds may actually perform in the context of a living organism such as a rodent or humans, the ability to determine the microkinetics of binding is crucial. It is clear that CD36 is important for normal physiology as well as pathological conditions. By understanding the rate at which a potential therapeutic agent associates and then dissociates from CD36 is fundamental to improving efficacy and also for reducing the risk of possible toxic side-effects.

6.5.   Summary and Future Perspectives

CD36 is a scavenger receptor present on the surface of a variety of cell and tissue types implicated in normal physiological processes as well as a number of pathological states. This can be attributed to the poly-specific nature of the receptor being able to bind a wide range of ligands. One of the most studied diseases associated with CD36 is atherosclerosis which is characterised by the thickening and

hardening of the arterial wall in the form of a plaque. The development and progression of plaque formation is closely related to the uptake of oxLDL via CD36 into white blood cells ultimately leading to the formation fat-laden foam cells (a key component of the fatty plaque). Irrespective of studies predicting the sites of ligand binding such as oxLDL on CD36, proposed binding sites are questionable as the precise structure of CD36 remains unknown. In order to aid the development of effective therapeutics for conditions such as atherosclerosis that can specifically inhibit ligand binding to CD36, it is imperative to improve the current knowledge of multi-ligand binding to CD36 with the use of a structure of CD36 to which binding sites can be mapped.

This study describes a method of expressing and purifying sufficient quantities of pure CD36 ED in its native fold that can be used for two important future directions. The first involves using purified CD36 ED in crystallisation trials with the aim of generating protein crystals. Using pure uniform CD36 ED crystals X-ray crystallography would describe the three-dimensional shape of the receptor and allow modelling of ligand binding sites. The recently solved crystal structure of LIMP-2 ED using similar expression and purification processes suggests that it is highly likely that purified CD36 ED can also be crystallised. Furthermore, the crystallisation process may be improved by reducing the complexity and asymmetry of purified CD36 ED (e.g. removal of sugar groups) without losing overall protein shape and without reducing the ability to bind ligand (e.g. acLDL in this study). This might serve to increase the resolution of the calculated structure and provide a more accurate scaffold to map ligand binding sites. Ideally, to clearly define CD36 ligand binding sites, purified CD36 ED would be co-crystallised with ligand bound,

however further optimisation of crystallisation conditions would need to be determined empirically.

The second avenue of investigation involves measuring the microkinetics of ligand and putative inhibitor interactions with purified CD36 ED. Although CD36 is not an essential protein (with natural deficiencies occurring in healthy human populations) it is critical to the pathophysiology of diseases such as atherosclerosis. Subsequently, this makes it a good target for therapeutic intervention as inhibiting CD36 activity is less likely to be detrimental providing that the inhibitor is specific and potent (i.e. producing only the desired biological response). The microkinetics of binding are a set of parameters which are more physiologically-relevant than the overall strength of interaction, describing the rates at which an inhibitor binds (on-rate) and dissociates (off-rate) from a receptor. These rate constants report physiological binding events in more detail and produce a more accurate predictor of the potency of putative inhibitors, i.e. the amount of inhibitor required to block ligand binding. To be specific and potent, inhibitors would need to display fast on-rates and slow off-rates, binding to the specific target receptor readily and remaining bound, blocking ligand binding. In drug discovery and development it is thus critical to measure the microkinetics of inhibitor interactions to aid the therapeutic selection process, meaning that only the inhibitors with the best characteristics are tested in animal models, resulting in a reduced demand for animal testing prior to human studies.

A method for measuring the microkinetics of an antibody binding to purified CD36 ED using SPR was described in this study. Using SPR it was possible to observe the interaction between antibody and purified CD36 ED in real-time. In addition to measuring the strength of antibody binding to purified CD36 ED, SPR also revealed

that this antibody bound to CD36 ED with a fast on-rate and slow-off rate, making it an ideal candidate for further testing as an inhibitor of ligand binding to CD36. Using similar methods to the one described in this study it would be possible to not only measure the microkinetics of physiologically-relevant ligands such as oxLDL binding to CD36, but also to assess the ability of candidate therapeutics to inhibit ligand binding. A number of compounds such as SAB from the red sage *Salvia miltiorrhzia* have been identified which were previously reported to have cardioprotective properties. Furthermore, recent studies have demonstrated the ability of SAB to bind CD36 and block uptake of oxLDL into white blood cells. This study highlights the potential of SPR to be able to rapidly screen such putative therapeutics for the treatment of diseases such as atherosclerosis. By understanding the microkinetics of the interaction between SAB and CD36, a more informed decision can be made about how to administer SAB as well as aiding in the design and development of new drugs with similar properties. To complement microkinetic data generated for inhibitors shown to block oxLDL binding to CD36, cell-based studies would need to be undertaken prior to testing in animals to ensure that an inhibitor would bind specifically to CD36 and also that the inhibitor itself would not cause progression and development of plaque formation or any other unwanted side-effects.

The data presented and methods described in this study pave the way to generating a greater understanding of the polyspecificity of CD36 as well as aiding the design and development of therapeutics to block ligand binding. Together this will provide a greater insight into the involvement of CD36 in a range of pathological states including atherosclerosis, type 2 diabetes and Alzheimer's disease.

Bibliography

ABUMRAD, N. A., EL-MAGHRABI, M. R., AMRI, E. Z., LOPEZ, E. & GRIMALDI, P. A. 1993. Cloning of a rat adipocyte membrane protein implicated in binding or transport of long-chain fatty acids that is induced during preadipocyte differentiation. Homology with human CD36. *J Biol Chem,* 268**,** 17665-8.

ACTON, S., RESNICK, D., FREEMAN, M., EKKEL, Y., ASHKENAS, J. & KRIEGER, M. 1993. The collagenous domains of macrophage scavenger receptors and complement component C1q mediate their similar, but not identical, binding specificities for polyanionic ligands. *J Biol Chem,* 268**,** 3530-7.

ACTON, S. L., SCHERER, P. E., LODISH, H. F. & KRIEGER, M. 1994. Expression cloning of SR-BI, a CD36-related class B scavenger receptor. *J Biol Chem,* 269**,** 21003-9.

AEBERSOLD, R. & MANN, M. 2003. Mass spectrometry-based proteomics. *Nature,* 422**,** 198-207.

AICART-RAMOS, C., VALERO, R. A. & RODRIGUEZ-CRESPO, I. 2011. Protein palmitoylation and subcellular trafficking. *Biochim Biophys Acta,* 1808**,** 2981-94.

AITMAN, T. J., COOPER, L. D., NORSWORTHY, P. J., WAHID, F. N., GRAY, J. K., CURTIS, B. R., MCKEIGUE, P. M., KWIATKOWSKI, D., GREENWOOD, B. M., SNOW, R. W., HILL, A. V. & SCOTT, J. 2000. Malaria susceptibility and CD36 mutation. *Nature,* 405**,** 1015-6.

AITMAN, T. J., GLAZIER, A. M., WALLACE, C. A., COOPER, L. D., NORSWORTHY, P. J., WAHID, F. N., AL-MAJALI, K. M., TREMBLING, P. M., MANN, C. J., SHOULDERS, C. C., GRAF, D., ST LEZIN, E., KURTZ, T. W., KREN, V., PRAVENEC, M., IBRAHIMI, A., ABUMRAD, N. A., STANTON, L. W. & SCOTT, J. 1999. Identification of Cd36 (Fat) as an insulin-resistance gene causing defective fatty acid and glucose metabolism in hypertensive rats. *Nature genetics,* 21**,** 76-83.

AITMAN, T. J., GODSLAND, I. F., FARREN, B., CROOK, D., WONG, H. J. & SCOTT, J. 1997a. Defects of insulin action on fatty acid and carbohydrate metabolism in familial combined hyperlipidemia. *Arterioscler Thromb Vasc Biol,* 17**,** 748-54.

AITMAN, T. J., GOTODA, T., EVANS, A. L., IMRIE, H., HEATH, K. E., TREMBLING, P. M., TRUMAN, H., WALLACE, C. A., RAHMAN, A., DORE, C., FLINT, J., KREN, V., ZIDEK, V., KURTZ, T. W., PRAVENEC, M. & SCOTT, J. 1997b. Quantitative trait loci for cellular defects in glucose and fatty acid metabolism in hypertensive rats. *Nat Genet,* 16**,** 197-201.

AKIYAMA, H. 1994. Inflammatory response in Alzheimer's disease. *Tohoku J Exp Med,* 174**,** 295-303.

ALTMANN, F. 2007. The role of protein glycosylation in allergy. *Int Arch Allergy Immunol,* 142**,** 99-115.

ALTMANN, F., STAUDACHER, E., WILSON, I. B. & MARZ, L. 1999. Insect cells as hosts for the expression of recombinant glycoproteins. *Glycoconj J,* 16**,** 109-23.

AMEZAGA, N., SANJURJO, L., JULVE, J., ARAN, G., PEREZ-CABEZAS, B., BASTOS-AMADOR, P., ARMENGOL, C., VILELLA, R., ESCOLA-GIL, J. C., BLANCO-VACA, F., BORRAS, F. E., VALLEDOR, A. F. & SARRIAS, M. R. 2014. Human scavenger protein AIM increases foam cell formation and CD36-mediated oxLDL uptake. *J Leukoc Biol,* 95**,** 509-20.

ANDERSEN, M., LENHARD, B., WHATLING, C., ERIKSSON, P. & ODEBERG, J. 2006. Alternative promoter usage of the membrane glycoprotein CD36. *BMC Mol Biol,* 7**,** 8.

ANGIN, Y., STEINBUSCH, L. K., SIMONS, P. J., GREULICH, S., HOEBERS, N. T., DOUMA, K., VAN ZANDVOORT, M. A., COUMANS, W. A., WIJNEN, W., DIAMANT, M., OUWENS, D. M., GLATZ, J. F. & LUIKEN, J. J. 2012. CD36 inhibition prevents lipid accumulation and contractile dysfunction in rat cardiomyocytes. *Biochem J,* 448**,** 43-53.

APPENZELLER-HERZOG, C. & ELLGAARD, L. 2008. The human PDI family: versatility packed into a single fold. *Biochim Biophys Acta,* 1783**,** 535-48.

ARAI, S., SHELTON, J. M., CHEN, M., BRADLEY, M. N., CASTRILLO, A., BOOKOUT, A. L., MAK, P. A., EDWARDS, P. A., MANGELSDORF, D. J., TONTONOZ, P. & MIYAZAKI, T. 2005. A role for the apoptosis inhibitory factor AIM/Spalpha/Api6 in atherosclerosis development. *Cell Metab,* 1**,** 201-13.

ARESCHOUG, T. & GORDON, S. 2009. Scavenger receptors: role in innate immunity and microbial pathogenesis. *Cell Microbiol,* 11**,** 1160-9.

ARICESCU, A. R. & OWENS, R. J. 2013. Expression of recombinant glycoproteins in mammalian cells: towards an integrative approach to structural biology. *Curr Opin Struct Biol,* 23**,** 345-56.

ARMESILLA, A. L. & VEGA, M. A. 1994. Structural organization of the gene for human CD36 glycoprotein. *J Biol Chem,* 269**,** 18985-91.

ASCH, A. S., BARNWELL, J., SILVERSTEIN, R. L. & NACHMAN, R. L. 1987. Isolation of the thrombospondin membrane receptor. *J Clin Invest,* 79**,** 1054-61.

ASCH, A. S., LIU, I., BRICCETTI, F. M., BARNWELL, J. W., KWAKYE-BERKO, F., DOKUN, A., GOLDBERGER, J. & PERNAMBUCO, M. 1993. Analysis of CD36 binding domains: ligand specificity controlled by dephosphorylation of an ectodomain. *Science (New York, N Y),* 262**,** 1436-40.

AYODO, G., PRICE, A. L., KEINAN, A., AJWANG, A., OTIENO, M. F., ORAGO, A. S., PATTERSON, N. & REICH, D. 2007. Combining evidence of natural selection with association analysis increases power to detect malaria-resistance variants. *Am J Hum Genet,* 81**,** 234-42.

AYRES, M. D., HOWARD, S. C., KUZIO, J., LOPEZ-FERBER, M. & POSSEE, R. D. 1994. The complete DNA sequence of Autographa californica nuclear polyhedrosis virus. *Virology,* 202**,** 586-605.

BALDWIN, M. A. 2004. Protein identification by mass spectrometry: issues to be considered. *Mol Cell Proteomics,* 3**,** 1-9.

BAMBERGER, M. E., HARRIS, M. E., MCDONALD, D. R., HUSEMANN, J. & LANDRETH, G. E. 2003. A cell surface receptor complex for fibrillar beta-amyloid mediates microglial activation. *J Neurosci,* 23**,** 2665-74.

BANTSCHEFF, M., LEMEER, S., SAVITSKI, M. M. & KUSTER, B. 2012. Quantitative mass spectrometry in proteomics: critical review update from 2007 to the present. *Anal Bioanal Chem,* 404**,** 939-65.

BAO, Y., WANG, L., XU, Y., YANG, Y., WANG, L., SI, S., CHO, S. & HONG, B. 2012. Salvianolic acid B inhibits macrophage uptake of modified low density lipoprotein (mLDL) in a scavenger receptor CD36-dependent manner. *Atherosclerosis,* 223**,** 152-9.

BARUCH, D. I., MA, X. C., PASLOSKE, B., HOWARD, R. J. & MILLER, L. H. 1999. CD36 peptides that block cytoadherence define the CD36 binding region for Plasmodium falciparum-infected erythrocytes. *Blood,* 94**,** 2121-7.

BASTA, G., SCHMIDT, A. M. & DE CATERINA, R. 2004. Advanced glycation end products and vascular inflammation: implications for accelerated atherosclerosis in diabetes. *Cardiovasc Res,* 63**,** 582-92.

BEHER, D., WU, J., CUMINE, S., KIM, K. W., LU, S. C., ATANGAN, L. & WANG, M. 2009. Resveratrol is not a direct activator of SIRT1 enzyme activity. *Chem Biol Drug Des,* 74**,** 619-24.

BENTON, R., VANNICE, K. S. & VOSSHALL, L. B. 2007. An essential role for a CD36-related receptor in pheromone detection in Drosophila. *Nature,* 450**,** 289-93.

BESENICAR, M., MACEK, P., LAKEY, J. H. & ANDERLUH, G. 2006. Surface plasmon resonance in protein-membrane interactions. *Chem Phys Lipids,* 141**,** 169-78.

BESSI, V. L., LABBE, S. M., HUYNH, D. N., MENARD, L., JOSSART, C., FEBBRAIO, M., GUERIN, B., BENTOURKIA, M., LECOMTE, R., CARPENTIER, A. C., ONG, H. & MARLEAU, S. 2012. EP 80317, a selective CD36 ligand, shows cardioprotective effects against post-ischaemic myocardial damage in mice. *Cardiovasc Res,* 96**,** 99-108.

BEYER, T. A., REARICK, J. I., PAULSON, J. C., PRIEELS, J. P., SADLER, J. E. & HILL, R. L. 1979. Biosynthesis of mammalian glycoproteins. Glycosylation pathways in the synthesis of the nonreducing terminal sequences. *J Biol Chem,* 254**,** 12531-4.

BIRNBOIM, H. C. & DOLY, J. 1979. A rapid alkaline extraction procedure for screening recombinant plasmid DNA. *Nucleic Acids Res,* 7**,** 1513-23.

BLISSARD, G. W. & WENZ, J. R. 1992. Baculovirus gp64 envelope glycoprotein is sufficient to mediate pH-dependent membrane fusion. *J Virol,* 66**,** 6829-35.

BODART, V., FEBBRAIO, M., DEMERS, A., MCNICOLL, N., POHANKOVA, P., PERREAULT, A., SEJLITZ, T., ESCHER, E., SILVERSTEIN, R. L., LAMONTAGNE, D. & ONG, H. 2002. CD36 mediates the cardiovascular action of growth hormone-releasing peptides in the heart. *Circ Res,* 90**,** 844-9.

BONEN, A., DYCK, D. J., IBRAHIMI, A. & ABUMRAD, N. A. 1999. Muscle contractile activity increases fatty acid metabolism and transport and FAT/CD36. *Am J Physiol,* 276**,** E642-9.

BONEN, A., LUIKEN, J. J., ARUMUGAM, Y., GLATZ, J. F. & TANDON, N. N. 2000. Acute regulation of fatty acid uptake involves the cellular redistribution of fatty acid translocase. *J Biol Chem,* 275**,** 14501-8.

BRAAKMAN, I. & BULLEID, N. J. 2011. Protein folding and modification in the mammalian endoplasmic reticulum. *Annu Rev Biochem,* 80**,** 71-99.

BRINKMANN, J. F., PELSERS, M. M., VAN NIEUWENHOVEN, F. A., TANDON, N. N., VAN DER VUSSE, G. J. & GLATZ, J. F. 2006. Purification, immunochemical quantification and localization in rat heart of putative fatty acid translocase (FAT/CD36). *Mol Cell Biochem,* 284**,** 127-34.

BROWN, M. S. & GOLDSTEIN, J. L. 1979. Receptor-mediated endocytosis: insights from the lipoprotein receptor system. *Proc Natl Acad Sci U S A,* 76**,** 3330-7.

BROWN, M. S., GOLDSTEIN, J. L., KRIEGER, M., HO, Y. K. & ANDERSON, R. G. 1979. Reversible accumulation of cholesteryl esters in macrophages incubated with acetylated lipoproteins. *J Cell Biol,* 82**,** 597-613.

BROWNLEE, M., VLASSARA, H. & CERAMI, A. 1985. Nonenzymatic glycosylation products on collagen covalently trap low-density lipoprotein. *Diabetes,* 34**,** 938-41.

BURDA, P. & AEBI, M. 1998. The ALG10 locus of Saccharomyces cerevisiae encodes the alpha-1,2 glucosyltransferase of the endoplasmic reticulum: the terminal glucose of the lipid-linked oligosaccharide is required for efficient N-linked glycosylation. *Glycobiology,* 8**,** 455-62.

BURDA, P. & AEBI, M. 1999. The dolichol pathway of N-linked glycosylation. *Biochim Biophys Acta,* 1426**,** 239-57.

BURNETT, M. S., GAYDOS, C. A., MADICO, G. E., GLAD, S. M., PAIGEN, B., QUINN, T. C. & EPSTEIN, S. E. 2001. Atherosclerosis in apoE knockout mice infected with multiple pathogens. *J Infect Dis,* 183**,** 226-231.

CALVO, D., GOMEZ-CORONADO, D., LASUNCION, M. A. & VEGA, M. A. 1997. CLA-1 is an 85-kD plasma membrane glycoprotein that acts as a high-affinity receptor for both native (HDL, LDL, and VLDL) and modified (OxLDL and AcLDL) lipoproteins. *Arterioscler Thromb Vasc Biol,* 17**,** 2341-9.

CALVO, D., GOMEZ-CORONADO, D., SUAREZ, Y., LASUNCION, M. A. & VEGA, M. A. 1998. Human CD36 is a high affinity receptor for the native lipoproteins HDL, LDL, and VLDL. *J Lipid Res,* 39**,** 777-88.

CANTON, J., NECULAI, D. & GRINSTEIN, S. 2013. Scavenger receptors in homeostasis and immunity. *Nat Rev Immunol,* 13**,** 621-34.

CAO, G., GARCIA, C. K., WYNE, K. L., SCHULTZ, R. A., PARKER, K. L. & HOBBS, H. H. 1997. Structure and localization of the human gene encoding SR-BI/CLA-1. Evidence for transcriptional control by steroidogenic factor 1. *J Biol Chem,* 272**,** 33068-76.

CARAMELO, J. J. & PARODI, A. J. 2008. Getting in and out from calnexin/calreticulin cycles. *J Biol Chem,* 283**,** 10221-5.

CARLSON, S. E. 1985. N-acetylneuraminic acid concentrations in human milk oligosaccharides and glycoproteins during lactation. *Am J Clin Nutr,* 41**,** 720-6.

CARLSON, S. E. & HOUSE, S. G. 1986. Oral and intraperitoneal administration of N-acetylneuraminic acid: effect on rat cerebral and cerebellar N-acetylneuraminic acid. *J Nutr,* 116**,** 881-6.

CARPENTIER, D. C., GRIFFITHS, C. M. & KING, L. A. 2008. The baculovirus P10 protein of Autographa californica nucleopolyhedrovirus forms two distinct cytoskeletal-like structures and associates with polyhedral occlusion bodies during infection. *Virology,* 371**,** 278-91.

CHABOWSKI, A., GORSKI, J., CALLES-ESCANDON, J., TANDON, N. N. & BONEN, A. 2006. Hypoxia-induced fatty acid transporter translocation increases fatty acid transport and contributes to lipid accumulation in the heart. *FEBS Lett,* 580**,** 3617-23.

CHEN, H. S., PELLEGRINI, J. W., AGGARWAL, S. K., LEI, S. Z., WARACH, S., JENSEN, F. E. & LIPTON, S. A. 1992. Open-channel block of N-methyl-D-

aspartate (NMDA) responses by memantine: therapeutic advantage against NMDA receptor-mediated neurotoxicity. *J Neurosci,* 12**,** 4427-36.

CHEN, Y. R., ZHONG, S., FEI, Z., HASHIMOTO, Y., XIANG, J. Z., ZHANG, S. & BLISSARD, G. W. 2013. The transcriptome of the baculovirus Autographa californica multiple nucleopolyhedrovirus in Trichoplusia ni cells. *J Virol,* 87**,** 6391-405.

CHEUNG, R. C., WONG, J. H. & NG, T. B. 2012. Immobilized metal ion affinity chromatography: a review on its applications. *Appl Microbiol Biotechnol,* 96**,** 1411-20.

CHU, L. Y. & SILVERSTEIN, R. L. 2012. CD36 ectodomain phosphorylation blocks thrombospondin-1 binding: structure-function relationships and regulation by protein kinase C. *Arterioscler Thromb Vasc Biol,* 32**,** 760-7.

COBURN, C. T., KNAPP, F. F., JR., FEBBRAIO, M., BEETS, A. L., SILVERSTEIN, R. L. & ABUMRAD, N. A. 2000. Defective uptake and utilization of long chain fatty acids in muscle and adipose tissues of CD36 knockout mice. *J Biol Chem,* 275**,** 32523-9.

COLLOT-TEIXEIRA, S., MARTIN, J., MCDERMOTT-ROE, C., POSTON, R. & MCGREGOR, J. L. 2007. CD36 and macrophages in atherosclerosis. *Cardiovasc Res,* 75**,** 468-77.

CONIBEAR, E. & DAVIS, N. G. 2010. Palmitoylation and depalmitoylation dynamics at a glance. *J Cell Sci,* 123**,** 4007-10.

COOPER, M. A. 2003. Label-free screening of bio-molecular interactions. *Analytical and bioanalytical chemistry,* 377**,** 834-42.

COOPER, M. A., TRY, A. C., CARROLL, J., ELLAR, D. J. & WILLIAMS, D. H. 1998. Surface plasmon resonance analysis at a supported lipid monolayer. *Biochim Biophys Acta,* 1373**,** 101-11.

CORACI, I. S., HUSEMANN, J., BERMAN, J. W., HULETTE, C., DUFOUR, J. H., CAMPANELLA, G. K., LUSTER, A. D., SILVERSTEIN, S. C. & EL-KHOURY, J. B. 2002. CD36, a class B scavenger receptor, is expressed on microglia in Alzheimer's disease brains and can mediate production of reactive oxygen species in response to beta-amyloid fibrils. *Am J Pathol,* 160**,** 101-12.

CORPELEIJN, E., VAN DER KALLEN, C. J., KRUIJSHOOP, M., MAGAGNIN, M. G., DE BRUIN, T. W., FESKENS, E. J., SARIS, W. H. & BLAAK, E. E. 2006. Direct association of a promoter polymorphism in the CD36/FAT fatty acid transporter gene with Type 2 diabetes mellitus and insulin resistance. *Diabet Med,* 23**,** 907-11.

CORY, J. S. & BISHOP, D. H. 1997. Use of baculoviruses as biological insecticides. *Mol Biotechnol,* 7**,** 303-13.

CREASY, D. M. & COTTRELL, J. S. 2004. Unimod: Protein modifications for mass spectrometry. *Proteomics,* 4**,** 1534-6.

CREIGHTON, T. E. 1988. Disulphide bonds and protein stability. *Bioessays,* 8**,** 57-63.

CROMBIE, R. & SILVERSTEIN, R. 1998. Lysosomal integral membrane protein II binds thrombospondin-1. Structure-function homology with the cell adhesion molecule CD36 defines a conserved recognition motif. *The Journal of biological chemistry,* 273**,** 4855-63.

CROMBIE, R., SILVERSTEIN, R. L., MACLOW, C., PEARCE, S. F., NACHMAN, R. L. & LAURENCE, J. 1998. Identification of a CD36-related thrombospondin 1-binding domain in HIV-1 envelope glycoprotein gp120:

relationship to HIV-1-specific inhibitory factors in human saliva. *J Exp Med,* 187**,** 25-35.

CUESTA, A. M., SAINZ-PASTOR, N., BONET, J., OLIVA, B. & ALVAREZ-VALLINA, L. 2010. Multivalent antibodies: when design surpasses evolution. *Trends Biotechnol,* 28**,** 355-62.

CUNNINGHAM, B. T., LI, P., SCHULZ, S., LIN, B., BAIRD, C., GERSTENMAIER, J., GENICK, C., WANG, F., FINE, E. & LAING, L. 2004. Label-free assays on the BIND system. *J Biomol Screen,* 9**,** 481-90.

CURTISS, L. K. 2006. Is two out of three enough for ABCG1? *Arterioscler Thromb Vasc Biol,* 26**,** 2175-7.

DAVIET, L., BUCKLAND, R., PUENTE NAVAZO, M. D. & MCGREGOR, J. L. 1995. Identification of an immunodominant functional domain on human CD36 antigen using human-mouse chimaeric proteins and homologue-replacement mutagenesis. *Biochem J,* 305 (Pt 1)**,** 221-4.

DAVIET, L., CRAIG, A. G., MCGREGOR, L., PINCHES, R., WILD, T. F., BERENDT, A. R., NEWBOLD, C. I. & MCGREGOR, J. L. 1997. Characterization of two vaccinia CD36 recombinant-virus-generated monoclonal antibodies (10/5, 13/10): effects on malarial cytoadherence and platelet functions. *Eur J Biochem,* 243**,** 344-9.

DAVIS, T. R., TROTTER, K. M., GRANADOS, R. R. & WOOD, H. A. 1992. Baculovirus expression of alkaline phosphatase as a reporter gene for evaluation of production, glycosylation and secretion. *Biotechnology (N Y),* 10**,** 1148-50.

DAWSON, D. W., PEARCE, S. F., ZHONG, R., SILVERSTEIN, R. L., FRAZIER, W. A. & BOUCK, N. P. 1997. CD36 mediates the In vitro inhibitory effects of thrombospondin-1 on endothelial cells. *J Cell Biol,* 138**,** 707-17.

DE VRIES, R. P., DE VRIES, E., BOSCH, B. J., DE GROOT, R. J., ROTTIER, P. J. & DE HAAN, C. A. 2010. The influenza A virus hemagglutinin glycosylation state affects receptor-binding specificity. *Virology,* 403**,** 17-25.

DEMERS, A., MCNICOLL, N., FEBBRAIO, M., SERVANT, M., MARLEAU, S., SILVERSTEIN, R. & ONG, H. 2004. Identification of the growth hormone-releasing peptide binding site in CD36: a photoaffinity cross-linking study. *Biochem J,* 382**,** 417-24.

DING, H., GRIESEL, C., NIMTZ, M., CONRADT, H. S., WEICH, H. A. & JAGER, V. 2003. Molecular cloning, expression, purification, and characterization of soluble full-length, human interleukin-3 with a baculovirus-insect cell expression system. *Protein Expr Purif,* 31**,** 34-41.

DOI, T., HIGASHINO, K., KURIHARA, Y., WADA, Y., MIYAZAKI, T., NAKAMURA, H., UESUGI, S., IMANISHI, T., KAWABE, Y., ITAKURA, H. & ET AL. 1993. Charged collagen structure mediates the recognition of negatively charged macromolecules by macrophage scavenger receptors. *J Biol Chem,* 268**,** 2126-33.

ECKER, M., MRSA, V., HAGEN, I., DEUTZMANN, R., STRAHL, S. & TANNER, W. 2003. O-mannosylation precedes and potentially controls the N-glycosylation of a yeast cell wall glycoprotein. *EMBO Rep,* 4**,** 628-32.

EHRLICH, Y. H., HOGAN, M. V., PAWLOWSKA, Z., NAIK, U. & KORNECKI, E. 1990. Ectoprotein kinase in the regulation of cellular responsiveness to extracellular ATP. *Ann N Y Acad Sci,* 603**,** 401-16.

EL KHOURY, J., HICKMAN, S. E., THOMAS, C. A., CAO, L., SILVERSTEIN, S. C. & LOIKE, J. D. 1996. Scavenger receptor-mediated adhesion of microglia to beta-amyloid fibrils. *Nature,* 382**,** 716-9.

EL KHOURY, J. B., MOORE, K. J., MEANS, T. K., LEUNG, J., TERADA, K., TOFT, M., FREEMAN, M. W. & LUSTER, A. D. 2003. CD36 mediates the innate host response to beta-amyloid. *J Exp Med,* 197**,** 1657-66.

ELBEIN, A. D. 1991. Glycosidase inhibitors: inhibitors of N-linked oligosaccharide processing. *FASEB J,* 5**,** 3055-63.

EMI, M., ASAOKA, H., MATSUMOTO, A., ITAKURA, H., KURIHARA, Y., WADA, Y., KANAMORI, H., YAZAKI, Y., TAKAHASHI, E., LEPERT, M. & ET AL. 1993. Structure, organization, and chromosomal mapping of the human macrophage scavenger receptor gene. *J Biol Chem,* 268**,** 2120-5.

ENDEMANN, G., STANTON, L. W., MADDEN, K. S., BRYANT, C. M., WHITE, R. T. & PROTTER, A. A. 1993. CD36 is a receptor for oxidized low density lipoprotein. *The Journal of biological chemistry,* 268**,** 11811-6.

FANG, Y. 2014. Label-free drug discovery. *Front Pharmacol,* 5**,** 52.

FEBBRAIO, M., ABUMRAD, N. A., HAJJAR, D. P., SHARMA, K., CHENG, W., PEARCE, S. F. & SILVERSTEIN, R. L. 1999. A null mutation in murine CD36 reveals an important role in fatty acid and lipoprotein metabolism. *J Biol Chem,* 274**,** 19055-62.

FEBBRAIO, M., GUY, E. & SILVERSTEIN, R. L. 2004. Stem cell transplantation reveals that absence of macrophage CD36 is protective against atherosclerosis. *Arterioscler Thromb Vasc Biol,* 24**,** 2333-8.

FEBBRAIO, M., PODREZ, E. A., SMITH, J. D., HAJJAR, D. P., HAZEN, S. L., HOFF, H. F., SHARMA, K. & SILVERSTEIN, R. L. 2000. Targeted disruption of the class B scavenger receptor CD36 protects against atherosclerotic lesion development in mice. *The Journal of clinical investigation,* 105**,** 1049-56.

FEBBRAIO, M. & SILVERSTEIN, R. L. 2007. CD36: implications in cardiovascular disease. *Int J Biochem Cell Biol,* 39**,** 2012-30.

FEKETE, S., BECK, A., VEUTHEY, J. L. & GUILLARME, D. 2014. Theory and practice of size exclusion chromatography for the analysis of protein aggregates. *J Pharm Biomed Anal*.

FENG, J., HAN, J., PEARCE, S. F., SILVERSTEIN, R. L., GOTTO, A. M., JR., HAJJAR, D. P. & NICHOLSON, A. C. 2000. Induction of CD36 expression by oxidized LDL and IL-4 by a common signaling pathway dependent on protein kinase C and PPAR-gamma. *J Lipid Res,* 41**,** 688-96.

FERNANDEZ-RUIZ, E., ARMESILLA, A. L., SANCHEZ-MADRID, F. & VEGA, M. A. 1993. Gene encoding the collagen type I and thrombospondin receptor CD36 is located on chromosome 7q11.2. *Genomics,* 17**,** 759-61.

FINNEMANN, S. C. & SILVERSTEIN, R. L. 2001. Differential roles of CD36 and alphavbeta5 integrin in photoreceptor phagocytosis by the retinal pigment epithelium. *J Exp Med,* 194**,** 1289-98.

FRANC, N. C., DIMARCQ, J. L., LAGUEUX, M., HOFFMANN, J. & EZEKOWITZ, R. A. 1996. Croquemort, a novel Drosophila hemocyte/macrophage receptor that recognizes apoptotic cells. *Immunity,* 4**,** 431-43.

FRASER, M. J. 1989. Expression of eukaryotic genes in insect cultures. *In Vitro Cell Dev Biol,* 25**,** 225-35.

FREEMAN, M., ASHKENAS, J., REES, D. J., KINGSLEY, D. M., COPELAND, N. G., JENKINS, N. A. & KRIEGER, M. 1990. An ancient, highly conserved family of cysteine-rich protein domains revealed by cloning type I and type II murine macrophage scavenger receptors. *Proc Natl Acad Sci U S A,* 87**,** 8810-4.

FRIEDA, S., PEARCE, A., WU, J. & SILVERSTEIN, R. L. 1995. Recombinant GST/CD36 fusion proteins define a thrombospondin binding domain. Evidence for a single calcium-dependent binding site on CD36. *The Journal of biological chemistry,* 270**,** 2981-6.

FRY, A. E., GHANSA, A., SMALL, K. S., PALMA, A., AUBURN, S., DIAKITE, M., GREEN, A., CAMPINO, S., TEO, Y. Y., CLARK, T. G., JEFFREYS, A. E., WILSON, J., JALLOW, M., SISAY-JOOF, F., PINDER, M., GRIFFITHS, M. J., PESHU, N., WILLIAMS, T. N., NEWTON, C. R., MARSH, K., MOLYNEUX, M. E., TAYLOR, T. E., KORAM, K. A., ODURO, A. R., ROGERS, W. O., ROCKETT, K. A., SABETI, P. C. & KWIATKOWSKI, D. P. 2009. Positive selection of a CD36 nonsense variant in sub-Saharan Africa, but no association with severe malaria phenotypes. *Hum Mol Genet,* 18**,** 2683-92.

FURMANEK, A. & HOFSTEENGE, J. 2000. Protein C-mannosylation: facts and questions. *Acta Biochim Pol,* 47**,** 781-9.

FURUHASHI, M., URA, N., NAKATA, T. & SHIMAMOTO, K. 2003. Insulin sensitivity and lipid metabolism in human CD36 deficiency. *Diabetes Care,* 26**,** 471-4.

FURUHASHI, M., URA, N., NAKATA, T., TANAKA, T. & SHIMAMOTO, K. 2004. Genotype in human CD36 deficiency and diabetes mellitus. *Diabet Med,* 21**,** 952-3.

GARAVITO, R. M., PICOT, D. & LOLL, P. J. 1996. Strategies for crystallizing membrane proteins. *J Bioenerg Biomembr,* 28**,** 13-27.

GARDNER, M. J., HALL, N., FUNG, E., WHITE, O., BERRIMAN, M., HYMAN, R. W., CARLTON, J. M., PAIN, A., NELSON, K. E., BOWMAN, S., PAULSEN, I. T., JAMES, K., EISEN, J. A., RUTHERFORD, K., SALZBERG, S. L., CRAIG, A., KYES, S., CHAN, M. S., NENE, V., SHALLOM, S. J., SUH, B., PETERSON, J., ANGIUOLI, S., PERTEA, M., ALLEN, J., SELENGUT, J., HAFT, D., MATHER, M. W., VAIDYA, A. B., MARTIN, D. M., FAIRLAMB, A. H., FRAUNHOLZ, M. J., ROOS, D. S., RALPH, S. A., MCFADDEN, G. I., CUMMINGS, L. M., SUBRAMANIAN, G. M., MUNGALL, C., VENTER, J. C., CARUCCI, D. J., HOFFMAN, S. L., NEWBOLD, C., DAVIS, R. W., FRASER, C. M. & BARRELL, B. 2002. Genome sequence of the human malaria parasite Plasmodium falciparum. *Nature,* 419**,** 498-511.

GAVEL, Y. & VON HEIJNE, G. 1990. Sequence differences between glycosylated and non-glycosylated Asn-X-Thr/Ser acceptor sites: implications for protein engineering. *Protein Eng,* 3**,** 433-42.

GELOEN, A., HELIN, L., GEERAERT, B., MALAUD, E., HOLVOET, P. & MARGUERIE, G. 2012. CD36 inhibitors reduce postprandial hypertriglyceridemia and protect against diabetic dyslipidemia and atherosclerosis. *PLoS One,* 7**,** e37633.

GLATZ, J. F., BONEN, A., OUWENS, D. M. & LUIKEN, J. J. 2006. Regulation of sarcolemmal transport of substrates in the healthy and diseased heart. *Cardiovasc Drugs Ther,* 20**,** 471-6.

GLATZ, J. F. & LUIKEN, J. J. 2014. Fatty acids in cell signaling: Historical perspective and future outlook. *Prostaglandins Leukot Essent Fatty Acids*.

GLATZ, J. F., LUIKEN, J. J. & BONEN, A. 2010. Membrane fatty acid transporters as regulators of lipid metabolism: implications for metabolic disease. *Physiol Rev,* 90**,** 367-417.

GLATZ, J. F., SCHAAP, F. G., BINAS, B., BONEN, A., VAN DER VUSSE, G. J. & LUIKEN, J. J. 2003. Cytoplasmic fatty acid-binding protein facilitates fatty acid utilization by skeletal muscle. *Acta Physiol Scand,* 178**,** 367-71.

GONZALEZ, J., TAKAO, T., HORI, H., BESADA, V., RODRIGUEZ, R., PADRON, G. & SHIMONISHI, Y. 1992. A method for determination of N-glycosylation sites in glycoproteins by collision-induced dissociation analysis in fast atom bombardment mass spectrometry: identification of the positions of carbohydrate-linked asparagine in recombinant alpha-amylase by treatment with peptide-N-glycosidase F in 18O-labeled water. *Anal Biochem,* 205**,** 151-8.

GOOD, D. J., POLVERINI, P. J., RASTINEJAD, F., LE BEAU, M. M., LEMONS, R. S., FRAZIER, W. A. & BOUCK, N. P. 1990. A tumor suppressor-dependent inhibitor of angiogenesis is immunologically and functionally indistinguishable from a fragment of thrombospondin. *Proc Natl Acad Sci U S A,* 87**,** 6624-8.

GOTODA, T., IIZUKA, Y., KATO, N., OSUGA, J., BIHOREAU, M. T., MURAKAMI, T., YAMORI, Y., SHIMANO, H., ISHIBASHI, S. & YAMADA, N. 1999. Absence of Cd36 mutation in the original spontaneously hypertensive rats with insulin resistance. *Nat Genet,* 22**,** 226-8.

GOUDRIAAN, J. R., DAHLMANS, V. E., TEUSINK, B., OUWENS, D. M., FEBBRAIO, M., MAASSEN, J. A., ROMIJN, J. A., HAVEKES, L. M. & VOSHOL, P. J. 2003. CD36 deficiency increases insulin sensitivity in muscle, but induces insulin resistance in the liver in mice. *J Lipid Res,* 44**,** 2270-7.

GRABENHORST, E., HOFER, B., NIMTZ, M., JAGER, V. & CONRADT, H. S. 1993. Biosynthesis and secretion of human interleukin 2 glycoprotein variants from baculovirus-infected Sf21 cells. Characterization of polypeptides and posttranslational modifications. *Eur J Biochem,* 215**,** 189-97.

GREAVES, D. R. & GORDON, S. 2009. The macrophage scavenger receptor at 30 years of age: current knowledge and future challenges. *J Lipid Res,* 50 Suppl**,** S282-6.

GREENBERG, M. E., LI, X. M., GUGIU, B. G., GU, X., QIN, J., SALOMON, R. G. & HAZEN, S. L. 2008. The lipid whisker model of the structure of oxidized cell membranes. *J Biol Chem,* 283**,** 2385-96.

GREENBERG, M. E., SUN, M., ZHANG, R., FEBBRAIO, M., SILVERSTEIN, R. & HAZEN, S. L. 2006. Oxidized phosphatidylserine-CD36 interactions play an essential role in macrophage-dependent phagocytosis of apoptotic cells. *J Exp Med,* 203**,** 2613-25.

GREENWALT, D. E., WATT, K. W., SO, O. Y. & JIWANI, N. 1990. PAS IV, an integral membrane protein of mammary epithelial cells, is related to platelet and endothelial cell CD36 (GP IV). *Biochemistry,* 29**,** 7054-9.

GROOP, L. C., BONADONNA, R. C., DELPRATO, S., RATHEISER, K., ZYCK, K., FERRANNINI, E. & DEFRONZO, R. A. 1989. Glucose and free fatty

acid metabolism in non-insulin-dependent diabetes mellitus. Evidence for multiple sites of insulin resistance. *J Clin Invest,* 84**,** 205-13.

GROSSE, S. D., ODAME, I., ATRASH, H. K., AMENDAH, D. D., PIEL, F. B. & WILLIAMS, T. N. 2011. Sickle cell disease in Africa: a neglected cause of early childhood mortality. *Am J Prev Med,* 41**,** S398-405.

GRUARIN, P., SITIA, R. & ALESSIO, M. 1997. Formation of one or more intrachain disulphide bonds is required for the intracellular processing and transport of CD36. *Biochem J,* 328 (Pt 2)**,** 635-42.

GUY, E., KUCHIBHOTLA, S., SILVERSTEIN, R. & FEBBRAIO, M. 2007. Continued inhibition of atherosclerotic lesion development in long term Western diet fed CD36o /apoEo mice. *Atherosclerosis,* 192**,** 123-30.

HAHNEFELD, C., DREWIANKA, S. & HERBERG, F. W. 2004. Determination of kinetic data using surface plasmon resonance biosensors. *Methods Mol Med,* 94**,** 299-320.

HAMADA, H., ARAKAWA, T. & SHIRAKI, K. 2009. Effect of additives on protein aggregation. *Curr Pharm Biotechnol,* 10**,** 400-7.

HAMMOND, C., BRAAKMAN, I. & HELENIUS, A. 1994. Role of N-linked oligosaccharide recognition, glucose trimming, and calnexin in glycoprotein folding and quality control. *Proc Natl Acad Sci U S A,* 91**,** 913-7.

HAMMOND, J. R. & ZARENDA, M. 1996. Effect of detergents on ligand binding and translocation activities of solubilized/reconstituted nucleoside transporters. *Arch Biochem Biophys,* 332**,** 313-22.

HARMON, C. M. & ABUMRAD, N. A. 1993. Binding of sulfosuccinimidyl fatty acids to adipocyte membrane proteins: isolation and amino-terminal sequence of an 88-kD protein implicated in transport of long-chain fatty acids. *J Membr Biol,* 133**,** 43-9.

HART, K. & WILCOX, M. 1993. A Drosophila gene encoding an epithelial membrane protein with homology to CD36/LIMP II. *J Mol Biol,* 234**,** 249-53.

HARTVIGSEN, K., CHOU, M. Y., HANSEN, L. F., SHAW, P. X., TSIMIKAS, S., BINDER, C. J. & WITZTUM, J. L. 2009. The role of innate immunity in atherogenesis. *J Lipid Res,* 50 Suppl**,** S388-93.

HARUTA, I., KATO, Y., HASHIMOTO, E., MINJARES, C., KENNEDY, S., UTO, H., YAMAUCHI, K., KOBAYASHI, M., YUSA, S., MULLER, U., HAYASHI, N. & MIYAZAKI, T. 2001. Association of AIM, a novel apoptosis inhibitory factor, with hepatitis via supporting macrophage survival and enhancing phagocytotic function of macrophages. *J Biol Chem,* 276**,** 22910-4.

HASEGAWA, Y., SUEHIRO, A., HIGASA, S., NAMBA, M. & KAKISHITA, E. 2002. Enhancing effect of advanced glycation end products on serotonin-induced platelet aggregation in patients with diabetes mellitus. *Thromb Res,* 107**,** 319-23.

HAWKES, M., LI, X., CROCKETT, M., DIASSITI, A., FINNEY, C., MIN-OO, G., LILES, W. C., LIU, J. & KAIN, K. C. 2010a. CD36 deficiency attenuates experimental mycobacterial infection. *BMC Infect Dis,* 10**,** 299.

HAWKES, M., LI, X., CROCKETT, M., DIASSITI, A., LILES, W. C., LIU, J. & KAIN, K. C. 2010b. Malaria exacerbates experimental mycobacterial infection in vitro and in vivo. *Microbes Infect,* 12**,** 864-74.

HAWTIN, R. E., ARNOLD, K., AYRES, M. D., ZANOTTO, P. M., HOWARD, S. C., GOODAY, G. W., CHAPPELL, L. H., KITTS, P. A., KING, L. A. &

POSSEE, R. D. 1995. Identification and preliminary characterization of a chitinase gene in the Autographa californica nuclear polyhedrosis virus genome. *Virology,* 212**,** 673-85.

HAWTIN, R. E., ZARKOWSKA, T., ARNOLD, K., THOMAS, C. J., GOODAY, G. W., KING, L. A., KUZIO, J. A. & POSSEE, R. D. 1997. Liquefaction of Autographa californica nucleopolyhedrovirus-infected insects is dependent on the integrity of virus-encoded chitinase and cathepsin genes. *Virology,* 238**,** 243-53.

HEBBEL, R. P., BOOGAERTS, M. A., EATON, J. W. & STEINBERG, M. H. 1980. Erythrocyte adherence to endothelium in sickle-cell anemia. A possible determinant of disease severity. *N Engl J Med,* 302**,** 992-5.

HEFTI, M. H., VAN VUGT-VAN DER TOORN, C. J., DIXON, R. & VERVOORT, J. 2001. A novel purification method for histidine-tagged proteins containing a thrombin cleavage site. *Anal Biochem,* 295**,** 180-5.

HEINECKE, J. W., ROSEN, H. & CHAIT, A. 1984. Iron and copper promote modification of low density lipoprotein by human arterial smooth muscle cells in culture. *J Clin Invest,* 74**,** 1890-4.

HELENIUS, A., TROMBETTA, E. S., HEBERT, D. N. & SIMONS, J. F. 1997. Calnexin, calreticulin and the folding of glycoproteins. *Trends Cell Biol,* 7**,** 193-200.

HELENIUS, J., NG, D. T., MAROLDA, C. L., WALTER, P., VALVANO, M. A. & AEBI, M. 2002. Translocation of lipid-linked oligosaccharides across the ER membrane requires Rft1 protein. *Nature,* 415**,** 447-50.

HENRIKSEN, T., MAHONEY, E. M. & STEINBERG, D. 1981. Enhanced macrophage degradation of low density lipoprotein previously incubated with cultured endothelial cells: recognition by receptors for acetylated low density lipoproteins. *Proc Natl Acad Sci U S A,* 78**,** 6499-503.

HERRMANN, J., LERMAN, L. O. & LERMAN, A. 2007. Ubiquitin and ubiquitin-like proteins in protein regulation. *Circ Res,* 100**,** 1276-91.

HINK, W. F., THOMSEN, D. R., DAVIDSON, D. J., MEYER, A. L. & CASTELLINO, F. J. 1991. Expression of three recombinant proteins using baculovirus vectors in 23 insect cell lines. *Biotechnol Prog,* 7**,** 9-14.

HIRANO, K., KUWASAKO, T., NAKAGAWA-TOYAMA, Y., JANABI, M., YAMASHITA, S. & MATSUZAWA, Y. 2003. Pathophysiology of human genetic CD36 deficiency. *Trends Cardiovasc Med,* 13**,** 136-41.

HIRSCHBERG, C. B., ROBBINS, P. W. & ABEIJON, C. 1998. Transporters of nucleotide sugars, ATP, and nucleotide sulfate in the endoplasmic reticulum and Golgi apparatus. *Annu Rev Biochem,* 67**,** 49-69.

HIRSCHBERG, C. B. & SNIDER, M. D. 1987. Topography of glycosylation in the rough endoplasmic reticulum and Golgi apparatus. *Annu Rev Biochem,* 56**,** 63-87.

HITCHMAN, R. B., POSSEE, R. D., SIATERLI, E., RICHARDS, K. S., CLAYTON, A. J., BIRD, L. E., OWENS, R. J., CARPENTIER, D. C., KING, F. L., DANQUAH, J. O., SPINK, K. G. & KING, L. A. 2010. Improved expression of secreted and membrane-targeted proteins in insect cells. *Biotechnol Appl Biochem,* 56**,** 85-93.

HO, J. H. & HONG, C. Y. 2011. Salvianolic acids: small compounds with multiple mechanisms for cardiovascular protection. *J Biomed Sci,* 18**,** 30.

HO, M., HOANG, H. L., LEE, K. M., LIU, N., MACRAE, T., MONTES, L., FLATT, C. L., YIPP, B. G., BERGER, B. J., LOOAREESUWAN, S. &

ROBBINS, S. M. 2005. Ectophosphorylation of CD36 regulates cytoadherence of Plasmodium falciparum to microvascular endothelium under flow conditions. *Infect Immun,* 73**,** 8179-87.

HOCHULI, E., DOBELI, H. & SCHACHER, A. 1987. New metal chelate adsorbent selective for proteins and peptides containing neighbouring histidine residues. *J Chromatogr,* 411**,** 177-84.

HODNIK, V. & ANDERLUH, G. 2010. Capture of intact liposomes on biacore sensor chips for protein-membrane interaction studies. *Methods Mol Biol,* 627**,** 201-11.

HOEBE, K., GEORGEL, P., RUTSCHMANN, S., DU, X., MUDD, S., CROZAT, K., SOVATH, S., SHAMEL, L., HARTUNG, T., ZAHRINGER, U. & BEUTLER, B. 2005. CD36 is a sensor of diacylglycerides. *Nature,* 433**,** 523-7.

HOFSTEENGE, J., MULLER, D. R., DE BEER, T., LOFFLER, A., RICHTER, W. J. & VLIEGENTHART, J. F. 1994. New type of linkage between a carbohydrate and a protein: C-glycosylation of a specific tryptophan residue in human RNase Us. *Biochemistry,* 33**,** 13524-30.

HOM, L. G., OHKAWA, T., TRUDEAU, D. & VOLKMAN, L. E. 2002. Autographa californica M nucleopolyhedrovirus ProV-CATH is activated during infected cell death. *Virology,* 296**,** 212-8.

HOM, L. G. & VOLKMAN, L. E. 2000. Autographa californica M nucleopolyhedrovirus chiA is required for processing of V-CATH. *Virology,* 277**,** 178-83.

HOOSDALLY, S. J., ANDRESS, E. J., WOODING, C., MARTIN, C. A. & LINTON, K. J. 2009. The Human Scavenger Receptor CD36: glycosylation status and its role in trafficking and function. *The Journal of biological chemistry,* 284**,** 16277-88.

HORIUCHI, S., UNNO, Y., USUI, H., SHIKATA, K., TAKAKI, K., KOITO, W., SAKAMOTO, Y., NAGAI, R., MAKINO, K., SASAO, A., WADA, J. & MAKINO, H. 2005. Pathological roles of advanced glycation end product receptors SR-A and CD36. *Ann N Y Acad Sci,* 1043**,** 671-5.

HSIEH, P. & ROBBINS, P. W. 1984. Regulation of asparagine-linked oligosaccharide processing. Oligosaccharide processing in Aedes albopictus mosquito cells. *J Biol Chem,* 259**,** 2375-82.

HSIEH, P., ROSNER, M. R. & ROBBINS, P. W. 1983. Selective cleavage by endo-beta-N-acetylglucosaminidase H at individual glycosylation sites of Sindbis virion envelope glycoproteins. *J Biol Chem,* 258**,** 2555-61.

HSU, T. A. & BETENBAUGH, M. J. 1997. Coexpression of molecular chaperone BiP improves immunoglobulin solubility and IgG secretion from Trichoplusia ni insect cells. *Biotechnol Prog,* 13**,** 96-104.

HSU, T. A., TAKAHASHI, N., TSUKAMOTO, Y., KATO, K., SHIMADA, I., MASUDA, K., WHITELEY, E. M., FAN, J. Q., LEE, Y. C. & BETENBAUGH, M. J. 1997. Differential N-glycan patterns of secreted and intracellular IgG produced in Trichoplusia ni cells. *J Biol Chem,* 272**,** 9062-70.

HSU, T. A., WATSON, S., EIDEN, J. J. & BETENBAUGH, M. J. 1996. Rescue of immunoglobulins from insolubility is facilitated by PDI in the baculovirus expression system. *Protein Expr Purif,* 7**,** 281-8.

HU, H., DENG, H. & FANG, Y. 2012. Label-free phenotypic profiling identified D-luciferin as a GPR35 agonist. *PLoS One,* 7**,** e34934.

HU, Y., GUIMOND, S. E., TRAVERS, P., CADMAN, S., HOHENESTER, E., TURNBULL, J. E., KIM, S. H. & BOULOUX, P. M. 2009. Novel mechanisms of fibroblast growth factor receptor 1 regulation by extracellular matrix protein anosmin-1. *J Biol Chem,* 284**,** 29905-20.

HULST, M. M., WESTRA, D. F., WENSVOORT, G. & MOORMANN, R. J. 1993. Glycoprotein E1 of hog cholera virus expressed in insect cells protects swine from hog cholera. *J Virol,* 67**,** 5435-42.

HUNTER, T. 1995. Protein kinases and phosphatases: the yin and yang of protein phosphorylation and signaling. *Cell,* 80**,** 225-36.

HUSEMANN, J., LOIKE, J. D., KODAMA, T. & SILVERSTEIN, S. C. 2001. Scavenger receptor class B type I (SR-BI) mediates adhesion of neonatal murine microglia to fibrillar beta-amyloid. *J Neuroimmunol,* 114**,** 142-50.

HUTSELL, S. Q., KIMPLE, R. J., SIDEROVSKI, D. P., WILLARD, F. S. & KIMPLE, A. J. 2010. High-affinity immobilization of proteins using biotin- and GST-based coupling strategies. *Methods Mol Biol,* 627**,** 75-90.

IBRAHIMI, A., BONEN, A., BLINN, W. D., HAJRI, T., LI, X., ZHONG, K., CAMERON, R. & ABUMRAD, N. A. 1999. Muscle-specific overexpression of FAT/CD36 enhances fatty acid oxidation by contracting muscle, reduces plasma triglycerides and fatty acids, and increases plasma glucose and insulin. *J Biol Chem,* 274**,** 26761-6.

IRITANI, N., FUKUDA, E., NARA, Y. & YAMORI, Y. 1977. Lipid metabolism in spontaneously hypertensive rats (SHR). *Atherosclerosis,* 28**,** 217-22.

ISAJI, T., GU, J., NISHIUCHI, R., ZHAO, Y., TAKAHASHI, M., MIYOSHI, E., HONKE, K., SEKIGUCHI, K. & TANIGUCHI, N. 2004. Introduction of bisecting GlcNAc into integrin alpha5beta1 reduces ligand binding and down-regulates cell adhesion and cell migration. *J Biol Chem,* 279**,** 19747-54.

ITABE, H., OBAMA, T. & KATO, R. 2011. The Dynamics of Oxidized LDL during Atherogenesis. *J Lipids,* 2011**,** 418313.

JARVIS, D. L. 2003. Developing baculovirus-insect cell expression systems for humanized recombinant glycoprotein production. *Virology,* 310**,** 1-7.

JIMENEZ-DALMARONI, M. J., XIAO, N., CORPER, A. L., VERDINO, P., AINGE, G. D., LARSEN, D. S., PAINTER, G. F., RUDD, P. M., DWEK, R. A., HOEBE, K., BEUTLER, B. & WILSON, I. A. 2009. Soluble CD36 ectodomain binds negatively charged diacylglycerol ligands and acts as a co-receptor for TLR2. *PLoS One,* 4**,** e7411.

JIMENEZ, B., VOLPERT, O. V., CRAWFORD, S. E., FEBBRAIO, M., SILVERSTEIN, R. L. & BOUCK, N. 2000. Signals leading to apoptosis-dependent inhibition of neovascularization by thrombospondin-1. *Nat Med,* 6**,** 41-8.

JOCHEN, A. & HAYS, J. 1993. Purification of the major substrate for palmitoylation in rat adipocytes: N-terminal homology with CD36 and evidence for cell surface acylation. *J Lipid Res,* 34**,** 1783-92.

JOCHEN, A. L., HAYS, J. & MICK, G. 1995. Inhibitory effects of cerulenin on protein palmitoylation and insulin internalization in rat adipocytes. *Biochim Biophys Acta,* 1259**,** 65-72.

JOHNSON, I. S. 1983. Human insulin from recombinant DNA technology. *Science,* 219**,** 632-7.

KAJIHARA, S., HISATOMI, A., OGAWA, Y., YASUTAKE, T., YOSHIMURA, T., HARA, T., MIZUTA, T., OZAKI, I., IWAMOTO, N. & YAMAMOTO,

K. 2001. Association of the Pro90Ser CD36 mutation with elevated free fatty acid concentrations but not with insulin resistance syndrome in Japanese. *Clin Chim Acta,* 314**,** 125-30.

KAR, N. S., ASHRAF, M. Z., VALIYAVEETTIL, M. & PODREZ, E. A. 2008. Mapping and characterization of the binding site for specific oxidized phospholipids and oxidized low density lipoprotein of scavenger receptor CD36. *J Biol Chem,* 283**,** 8765-71.

KARLSSON, K. A. 1998. Meaning and therapeutic potential of microbial recognition of host glycoconjugates. *Mol Microbiol,* 29**,** 1-11.

KARLSSON, O. P. & LOFAS, S. 2002. Flow-mediated on-surface reconstitution of G-protein coupled receptors for applications in surface plasmon resonance biosensors. *Anal Biochem,* 300**,** 132-8.

KARLSSON, R. 2004. SPR for molecular interaction analysis: a review of emerging application areas. *J Mol Recognit,* 17**,** 151-61.

KARLSSON, R. & STAHLBERG, R. 1995. Surface plasmon resonance detection and multispot sensing for direct monitoring of interactions involving low-molecular-weight analytes and for determination of low affinities. *Anal Biochem,* 228**,** 274-80.

KASHIWAGI, H., HONDA, S., TOMIYAMA, Y., MIZUTANI, H., TAKE, H., HONDA, Y., KOSUGI, S., KANAYAMA, Y., KURATA, Y. & MATSUZAWA, Y. 1993. A novel polymorphism in glycoprotein IV (replacement of proline-90 by serine) predominates in subjects with platelet GPIV deficiency. *Thromb Haemost,* 69**,** 481-4.

KASHIWAGI, H., TOMIYAMA, Y., HONDA, S., KOSUGI, S., SHIRAGA, M., NAGAO, N., SEKIGUCHI, S., KANAYAMA, Y., KURATA, Y. & MATSUZAWA, Y. 1995. Molecular basis of CD36 deficiency. Evidence that a 478C-->T substitution (proline90-->serine) in CD36 cDNA accounts for CD36 deficiency. *J Clin Invest,* 95**,** 1040-6.

KASHIWAGI, H., TOMIYAMA, Y., NOZAKI, S., KIYOI, T., TADOKORO, S., MATSUMOTO, K., HONDA, S., KOSUGI, S., KURATA, Y. & MATSUZAWA, Y. 2001. Analyses of genetic abnormalities in type I CD36 deficiency in Japan: identification and cell biological characterization of two novel mutations that cause CD36 deficiency in man. *Hum Genet,* 108**,** 459-66.

KASTURI, L., CHEN, H. & SHAKIN-ESHLEMAN, S. H. 1997. Regulation of N-linked core glycosylation: use of a site-directed mutagenesis approach to identify Asn-Xaa-Ser/Thr sequons that are poor oligosaccharide acceptors. *Biochem J,* 323 (Pt 2)**,** 415-9.

KAUR, B., CORK, S. M., SANDBERG, E. M., DEVI, N. S., ZHANG, Z., KLENOTIC, P. A., FEBBRAIO, M., SHIM, H., MAO, H., TUCKER-BURDEN, C., SILVERSTEIN, R. L., BRAT, D. J., OLSON, J. J. & VAN MEIR, E. G. 2009. Vasculostatin inhibits intracranial glioma growth and negatively regulates in vivo angiogenesis through a CD36-dependent mechanism. *Cancer Res,* 69**,** 1212-20.

KEIZER, H. A., SCHAART, G., TANDON, N. N., GLATZ, J. F. & LUIKEN, J. J. 2004. Subcellular immunolocalisation of fatty acid translocase (FAT)/CD36 in human type-1 and type-2 skeletal muscle fibres. *Histochem Cell Biol,* 121**,** 101-7.

KENNEDY, D. J., KUCHIBHOTLA, S., WESTFALL, K. M., SILVERSTEIN, R. L., MORTON, R. E. & FEBBRAIO, M. 2011. A CD36-dependent pathway

enhances macrophage and adipose tissue inflammation and impairs insulin signalling. *Cardiovasc Res,* 89**,** 604-13.

KENNETT, R. H. 1981. Hybridomas: a new dimension in biological analyses. *In Vitro,* 17**,** 1036-50.

KERTESZ, T. M., HALL, L. H., HILL, D. W. & GRANT, D. F. 2009. CE50: quantifying collision induced dissociation energy for small molecule characterization and identification. *Journal of the American Society for Mass Spectrometry,* 20**,** 1759-67.

KHAN, F., HE, M. & TAUSSIG, M. J. 2006. Double-hexahistidine tag with high-affinity binding for protein immobilization, purification, and detection on ni-nitrilotriacetic acid surfaces. *Anal Chem,* 78**,** 3072-9.

KHOURY, G. A., BALIBAN, R. C. & FLOUDAS, C. A. 2011. Proteome-wide post-translational modification statistics: frequency analysis and curation of the swiss-prot database. *Sci Rep,* 1.

KIEFFER, N., BETTAIEB, A., LEGRAND, C., COULOMBEL, L., VAINCHENKER, W., EDELMAN, L. & BRETON-GORIUS, J. 1989. Developmentally regulated expression of a 78 kDa erythroblast membrane glycoprotein immunologically related to the platelet thrombospondin receptor. *Biochem J,* 262**,** 835-42.

KIM, K. Y., STEVENS, M. V., AKTER, M. H., RUSK, S. E., HUANG, R. J., COHEN, A., NOGUCHI, A., SPRINGER, D., BOCHAROV, A. V., EGGERMAN, T. L., SUEN, D. F., YOULE, R. J., AMAR, M., REMALEY, A. T. & SACK, M. N. 2011. Parkin is a lipid-responsive regulator of fat uptake in mice and mutant human cells. *J Clin Invest,* 121**,** 3701-12.

KITTS, P. A., AYRES, M. D. & POSSEE, R. D. 1990. Linearization of baculovirus DNA enhances the recovery of recombinant virus expression vectors. *Nucleic Acids Res,* 18**,** 5667-72.

KITTS, P. A. & POSSEE, R. D. 1993. A method for producing recombinant baculovirus expression vectors at high frequency. *Biotechniques,* 14**,** 810-7.

KLENK, H. D. 1996. Post-translational modifications in insect cells. *Cytotechnology,* 20**,** 139-44.

KNECHT, S., RICKLIN, D., EBERLE, A. N. & ERNST, B. 2009. Oligohis-tags: mechanisms of binding to Ni2+-NTA surfaces. *J Mol Recognit,* 22**,** 270-9.

KOBATA, A. & AMANO, J. 2005. Altered glycosylation of proteins produced by malignant cells, and application for the diagnosis and immunotherapy of tumours. *Immunol Cell Biol,* 83**,** 429-39.

KODAMA, T., FREEMAN, M., ROHRER, L., ZABRECKY, J., MATSUDAIRA, P. & KRIEGER, M. 1990. Type I macrophage scavenger receptor contains alpha-helical and collagen-like coiled coils. *Nature,* 343**,** 531-5.

KOHLER, G. & MILSTEIN, C. 1975. Continuous cultures of fused cells secreting antibody of predefined specificity. *Nature,* 256**,** 495-7.

KOHLER, G. & MILSTEIN, C. 1976. Derivation of specific antibody-producing tissue culture and tumor lines by cell fusion. *Eur J Immunol,* 6**,** 511-9.

KOMANDER, D. 2009. The emerging complexity of protein ubiquitination. *Biochem Soc Trans,* 37**,** 937-53.

KORNFELD, R. & KORNFELD, S. 1985. Assembly of asparagine-linked oligosaccharides. *Annu Rev Biochem,* 54**,** 631-64.

KRABBE, G., HALLE, A., MATYASH, V., RINNENTHAL, J. L., EOM, G. D., BERNHARDT, U., MILLER, K. R., PROKOP, S., KETTENMANN, H. & HEPPNER, F. L. 2013. Functional impairment of microglia coincides with

Beta-amyloid deposition in mice with Alzheimer-like pathology. *PLoS One,* 8**,** e60921.

KROGH, A., LARSSON, B., VON HEIJNE, G. & SONNHAMMER, E. L. 2001. Predicting transmembrane protein topology with a hidden Markov model: application to complete genomes. *J Mol Biol,* 305**,** 567-80.

KUANG, M., FEBBRAIO, M., WAGG, C., LOPASCHUK, G. D. & DYCK, J. R. 2004. Fatty acid translocase/CD36 deficiency does not energetically or functionally compromise hearts before or after ischemia. *Circulation,* 109**,** 1550-7.

KUDA, O., PIETKA, T. A., DEMIANOVA, Z., KUDOVA, E., CVACKA, J., KOPECKY, J. & ABUMRAD, N. A. 2013a. Sulfo-N-succinimidyl Oleate (SSO) inhibits fatty acid uptake and signaling for intracellular calcium via binding CD36 lysine 164. SSO also Inhibits oxLDL uptake by macrophages. *J Biol Chem.*

KUDA, O., PIETKA, T. A., DEMIANOVA, Z., KUDOVA, E., CVACKA, J., KOPECKY, J. & ABUMRAD, N. A. 2013b. Sulfo-N-succinimidyl Oleate (SSO) Inhibits Fatty Acid Uptake and Signaling for Intracellular Calcium via Binding CD36 Lysine 164: SSO ALSO INHIBITS OXIDIZED LOW DENSITY LIPOPROTEIN UPTAKE BY MACROPHAGES. *The Journal of biological chemistry,* 288**,** 15547-55.

KURODA, K., GEYER, H., GEYER, R., DOERFLER, W. & KLENK, H. D. 1990. The oligosaccharides of influenza virus hemagglutinin expressed in insect cells by a baculovirus vector. *Virology,* 174**,** 418-29.

KUROSAKA, A., YANO, A., ITOH, N., KURODA, Y., NAKAGAWA, T. & KAWASAKI, T. 1991. The structure of a neural specific carbohydrate epitope of horseradish peroxidase recognized by anti-horseradish peroxidase antiserum. *J Biol Chem,* 266**,** 4168-72.

KUWASAKO, T., HIRANO, K., SAKAI, N., ISHIGAMI, M., HIRAOKA, H., YAKUB, M. J., YAMAUCHI-TAKIHARA, K., YAMASHITA, S. & MATSUZAWA, Y. 2003. Lipoprotein abnormalities in human genetic CD36 deficiency associated with insulin resistance and abnormal fatty acid metabolism. *Diabetes Care,* 26**,** 1647-8.

LACZY, B., FULOP, N., ONAY-BESIKCI, A., DES ROSIERS, C. & CHATHAM, J. C. 2011. Acute regulation of cardiac metabolism by the hexosamine biosynthesis pathway and protein O-GlcNAcylation. *PLoS One,* 6**,** e18417.

LAEMMLI, U. K. 1970. Cleavage of structural proteins during the assembly of the head of bacteriophage T4. *Nature,* 227**,** 680-5.

LANGLEY, J. N. 1905. On the reaction of cells and of nerve-endings to certain poisons, chiefly as regards the reaction of striated muscle to nicotine and to curari. *J Physiol,* 33**,** 374-413.

LAUZIER, B., MERLEN, C., VAILLANT, F., MCDUFF, J., BOUCHARD, B., BEGUIN, P. C., DOLINSKY, V. W., FOISY, S., VILLENEUVE, L. R., LABARTHE, F., DYCK, J. R., ALLEN, B. G., CHARRON, G. & DES ROSIERS, C. 2011. Post-translational modifications, a key process in CD36 function: lessons from the spontaneously hypertensive rat heart. *J Mol Cell Cardiol,* 51**,** 99-108.

LAZARTE, J. E., TOSI, P. F. & NICOLAU, C. 1992. Optimization of the production of full-length rCD4 in baculovirus-infected Sf9 cells. *Biotechnol Bioeng,* 40**,** 214-7.

LEPRETRE, F., LINTON, K. J., LACQUEMANT, C., VATIN, V., SAMSON, C., DINA, C., CHIKRI, M., ALI, S., SCHERER, P., SERON, K., VASSEUR, F., AITMAN, T. & FROGUEL, P. 2004. Genetic study of the CD36 gene in a French diabetic population. *Diabetes Metab,* 30**,** 459-63.

LEROY, J. G. 2006. Congenital disorders of N-glycosylation including diseases associated with O- as well as N-glycosylation defects. *Pediatr Res,* 60**,** 643-56.

LEUNG, L. L., LI, W. X., MCGREGOR, J. L., ALBRECHT, G. & HOWARD, R. J. 1992. CD36 peptides enhance or inhibit CD36-thrombospondin binding. A two-step process of ligand-receptor interaction. *The Journal of biological chemistry,* 267**,** 18244-50.

LI, G., WANG, J., DENG, R. & WANG, X. 2008. Characterization of AcMNPV with a deletion of ac68 gene. *Virus Genes,* 37**,** 119-27.

LICARI, P. & BAILEY, J. E. 1992. Modeling the population dynamics of baculovirus-infected insect cells: Optimizing infection strategies for enhanced recombinant protein yields. *Biotechnol Bioeng,* 39**,** 432-41.

LIEBMAN, J. M., LASALA, D., WANG, W. & STEED, P. M. 1999. When less is more: enhanced baculovirus production of recombinant proteins at very low multiplicities of infection. *Biotechniques,* 26**,** 36-8, 40, 42.

LINDER, M. E. & DESCHENES, R. J. 2007. Palmitoylation: policing protein stability and traffic. *Nat Rev Mol Cell Biol,* 8**,** 74-84.

LOFAS, S. & JOHNSSON, B. 1990. A novel hydrogel matrix on gold surfaces in surface plasmon resonance sensors for fast and efficient covalent immobilization of ligands. *Journal of the Chemical Society, Chemical Communications***,** 1526-1528.

LOVE-GREGORY, L., SHERVA, R., SUN, L., WASSON, J., SCHAPPE, T., DORIA, A., RAO, D. C., HUNT, S. C., KLEIN, S., NEUMAN, R. J., PERMUTT, M. A. & ABUMRAD, N. A. 2008. Variants in the CD36 gene associate with the metabolic syndrome and high-density lipoprotein cholesterol. *Hum Mol Genet,* 17**,** 1695-704.

LU, C., QIU, F., ZHOU, H., PENG, Y., HAO, W., XU, J., YUAN, J., WANG, S., QIANG, B., XU, C. & PENG, X. 2006. Identification and characterization of selenoprotein K: an antioxidant in cardiomyocytes. *FEBS Lett,* 580**,** 5189-97.

LUIKEN, J. J., SCHAAP, F. G., VAN NIEUWENHOVEN, F. A., VAN DER VUSSE, G. J., BONEN, A. & GLATZ, J. F. 1999. Cellular fatty acid transport in heart and skeletal muscle as facilitated by proteins. *Lipids,* 34 Suppl**,** S169-75.

LUNDQUIST, A., HANSEN, S. B., NORDSTROM, H., DANIELSON, U. H. & EDWARDS, K. 2010. Biotinylated lipid bilayer disks as model membranes for biosensor analyses. *Anal Biochem,* 405**,** 153-9.

LYNN, D. E. 1996. Development and characterization of insect cell lines. *Cytotechnology,* 20**,** 3-11.

MA, X., BACCI, S., MLYNARSKI, W., GOTTARDO, L., SOCCIO, T., MENZAGHI, C., IORI, E., LAGER, R. A., SHROFF, A. R., GERVINO, E. V., NESTO, R. W., JOHNSTONE, M. T., ABUMRAD, N. A., AVOGARO, A., TRISCHITTA, V. & DORIA, A. 2004. A common haplotype at the CD36 locus is associated with high free fatty acid levels and increased cardiovascular risk in Caucasians. *Hum Mol Genet,* 13**,** 2197-205.

MALAUD, E., HOURTON, D., GIROUX, L. M., NINIO, E., BUCKLAND, R. & MCGREGOR, J. L. 2002. The terminal six amino-acids of the carboxy

cytoplasmic tail of CD36 contain a functional domain implicated in the binding and capture of oxidized low-density lipoprotein. *Biochem J,* 364**,** 507-15.

MALESZEWSKI, J., LU, J., FOX-TALBOT, K. & HALUSHKA, M. K. 2007. Robust immunohistochemical staining of several classes of proteins in tissues subjected to autolysis. *J Histochem Cytochem,* 55**,** 597-606.

MALEY, F., TRIMBLE, R. B., TARENTINO, A. L. & PLUMMER, T. H., JR. 1989. Characterization of glycoproteins and their associated oligosaccharides through the use of endoglycosidases. *Anal Biochem,* 180**,** 195-204.

MARLEAU, S., HARB, D., BUJOLD, K., AVALLONE, R., IKEN, K., WANG, Y., DEMERS, A., SIROIS, M. G., FEBBRAIO, M., SILVERSTEIN, R. L., TREMBLAY, A. & ONG, H. 2005. EP 80317, a ligand of the CD36 scavenger receptor, protects apolipoprotein E-deficient mice from developing atherosclerotic lesions. *FASEB J,* 19**,** 1869-71.

MARTIN, C. A., LONGMAN, E., WOODING, C., HOOSDALLY, S. J., ALI, S., AITMAN, T. J., GUTMANN, D. A. P., FREEMONT, P. S., BYRNE, B. & LINTON, K. J. 2007. Cd36, a class B scavenger receptor, functions as a monomer to bind acetylated and oxidized low-density lipoproteins. *Protein science : a publication of the Protein Society,* 16**,** 2531-41.

MASELLA, R., VARI, R., D'ARCHIVIO, M., SANTANGELO, C., SCAZZOCCHIO, B., MAGGIORELLA, M. T., SERNICOLA, L., TITTI, F., SANCHEZ, M., DI MARIO, U., LETO, G. & GIOVANNINI, C. 2006. Oxidised LDL modulate adipogenesis in 3T3-L1 preadipocytes by affecting the balance between cell proliferation and differentiation. *FEBS Lett,* 580**,** 2421-9.

MASSOUD, A. F., HINDMARSH, P. C., MATTHEWS, D. R. & BROOK, C. G. 1996. The effect of repeated administration of hexarelin, a growth hormone releasing peptide, and growth hormone releasing hormone on growth hormone responsivity. *Clin Endocrinol (Oxf),* 44**,** 555-62.

MEANS, T. K. 2010. Fungal pathogen recognition by scavenger receptors in nematodes and mammals. *Virulence,* 1**,** 37-41.

MEANS, T. K., MYLONAKIS, E., TAMPAKAKIS, E., COLVIN, R. A., SEUNG, E., PUCKETT, L., TAI, M. F., STEWART, C. R., PUKKILA-WORLEY, R., HICKMAN, S. E., MOORE, K. J., CALDERWOOD, S. B., HACOHEN, N., LUSTER, A. D. & EL KHOURY, J. 2009. Evolutionarily conserved recognition and innate immunity to fungal pathogens by the scavenger receptors SCARF1 and CD36. *J Exp Med,* 206**,** 637-53.

MEILER, S., BAUMER, Y., HUANG, Z., HOFFMANN, F. W., FREDERICKS, G. J., ROSE, A. H., NORTON, R. L., HOFFMANN, P. R. & BOISVERT, W. A. 2013. Selenoprotein K is required for palmitoylation of CD36 in macrophages: implications in foam cell formation and atherogenesis. *J Leukoc Biol,* 93**,** 771-80.

MILLER, L. H., ACKERMAN, H. C., SU, X. Z. & WELLEMS, T. E. 2013. Malaria biology and disease pathogenesis: insights for new treatments. *Nat Med,* 19**,** 156-67.

MILLER, L. K. 1989. Insect baculoviruses: powerful gene expression vectors. *Bioessays,* 11**,** 91-5.

MIYAOKA, K., KUWASAKO, T., HIRANO, K., NOZAKI, S., YAMASHITA, S. & MATSUZAWA, Y. 2001. CD36 deficiency associated with insulin resistance. *Lancet,* 357**,** 686-7.

MOORE, K. J., KUNJATHOOR, V. V., KOEHN, S. L., MANNING, J. J., TSENG, A. A., SILVER, J. M., MCKEE, M. & FREEMAN, M. W. 2005. Loss of receptor-mediated lipid uptake via scavenger receptor A or CD36 pathways does not ameliorate atherosclerosis in hyperlipidemic mice. *J Clin Invest,* 115**,** 2192-201.

MOREMEN, K. W., TIEMEYER, M. & NAIRN, A. V. 2012. Vertebrate protein glycosylation: diversity, synthesis and function. *Nat Rev Mol Cell Biol,* 13**,** 448-62.

MORGAN, B. L. & WINICK, M. 1980. Effects of environmental stimulation on brain N-acetylneuraminic acid content and behavior. *J Nutr,* 110**,** 425-32.

MULLER, K. M., ARNDT, K. M. & PLUCKTHUN, A. 1998. Model and simulation of multivalent binding to fixed ligands. *Anal Biochem,* 261**,** 149-58.

MUNGER, J. S., HUANG, X., KAWAKATSU, H., GRIFFITHS, M. J., DALTON, S. L., WU, J., PITTET, J. F., KAMINSKI, N., GARAT, C., MATTHAY, M. A., RIFKIN, D. B. & SHEPPARD, D. 1999. The integrin alpha v beta 6 binds and activates latent TGF beta 1: a mechanism for regulating pulmonary inflammation and fibrosis. *Cell,* 96**,** 319-28.

MURAO, K., TERPSTRA, V., GREEN, S. R., KONDRATENKO, N., STEINBERG, D. & QUEHENBERGER, O. 1997. Characterization of CLA-1, a human homologue of rodent scavenger receptor BI, as a receptor for high density lipoprotein and apoptotic thymocytes. *J Biol Chem,* 272**,** 17551-7.

NAGY, L., TONTONOZ, P., ALVAREZ, J. G., CHEN, H. & EVANS, R. M. 1998. Oxidized LDL regulates macrophage gene expression through ligand activation of PPARgamma. *Cell,* 93**,** 229-40.

NAKAJOU, K., HORIUCHI, S., SAKAI, M., HIRATA, K., TANAKA, M., TAKEYA, M., KAI, T. & OTAGIRI, M. 2005. CD36 is not involved in scavenger receptor-mediated endocytic uptake of glycolaldehyde- and methylglyoxal-modified proteins by liver endothelial cells. *J Biochem,* 137**,** 607-16.

NAKATA, N., FURUKAWA, K., GREENWALT, D. E., SATO, T. & KOBATA, A. 1993. Structural study of the sugar chains of CD36 purified from bovine mammary epithelial cells: occurrence of novel hybrid-type sugar chains containing the Neu5Ac alpha 2-->6GalNAc beta 1-->4GlcNAc and the Man alpha 1-->2Man alpha 1-->3Man alpha 1-->6Man groups. *Biochemistry,* 32**,** 4369-83.

NECULAI, D., SCHWAKE, M., RAVICHANDRAN, M., ZUNKE, F., COLLINS, R. F., PETERS, J., NECULAI, M., PLUMB, J., LOPPNAU, P., PIZARRO, J. C., SEITOVA, A., TRIMBLE, W. S., SAFTIG, P., GRINSTEIN, S. & DHE-PAGANON, S. 2013. Structure of LIMP-2 provides functional insights with implications for SR-BI and CD36. *Nature*.

NERGIZ-UNAL, R., LAMERS, M. M., VAN KRUCHTEN, R., LUIKEN, J. J., COSEMANS, J. M., GLATZ, J. F., KUIJPERS, M. J. & HEEMSKERK, J. W. 2011. Signaling role of CD36 in platelet activation and thrombus formation on immobilized thrombospondin or oxidized low-density lipoprotein. *J Thromb Haemost,* 9**,** 1835-46.

NGUYEN, B., JARNAGIN, K., WILLIAMS, S., CHAN, H. & BARNETT, J. 1993. Fed-batch culture of insect cells: a method to increase the yield of recombinant human nerve growth factor (rhNGF) in the baculovirus expression system. *J Biotechnol,* 31**,** 205-17.

NICHOLS, Z. & VOGT, R. G. 2008. The SNMP/CD36 gene family in Diptera, Hymenoptera and Coleoptera: Drosophila melanogaster, D. pseudoobscura, Anopheles gambiae, Aedes aegypti, Apis mellifera, and Tribolium castaneum. *Insect Biochem Mol Biol,* 38**,** 398-415.

NISHIMURA, S. L. 2009. Integrin-mediated transforming growth factor-beta activation, a potential therapeutic target in fibrogenic disorders. *Am J Pathol,* 175**,** 1362-70.

NORDGREN, S., SLAGTER-JAGER, J. G. & WAGNER, G. H. 2001. Real time kinetic studies of the interaction between folded antisense and target RNAs using surface plasmon resonance. *J Mol Biol,* 310**,** 1125-34.

NOZAKI, S., KASHIWAGI, H., YAMASHITA, S., NAKAGAWA, T., KOSTNER, B., TOMIYAMA, Y., NAKATA, A., ISHIGAMI, M., MIYAGAWA, J., KAMEDA-TAKEMURA, K. & ET AL. 1995. Reduced uptake of oxidized low density lipoproteins in monocyte-derived macrophages from CD36-deficient subjects. *J Clin Invest,* 96**,** 1859-65.

NUNEZ, S., VENHORST, J. & KRUSE, C. G. 2012. Target-drug interactions: first principles and their application to drug discovery. *Drug Discov Today,* 17**,** 10-22.

O'SHANNESSY, D. J., BRIGHAM-BURKE, M., SONESON, K. K., HENSLEY, P. & BROOKS, I. 1993. Determination of rate and equilibrium binding constants for macromolecular interactions using surface plasmon resonance: use of nonlinear least squares analysis methods. *Anal Biochem,* 212**,** 457-68.

OCKENHOUSE, C. F., HO, M., TANDON, N. N., VAN SEVENTER, G. A., SHAW, S., WHITE, N. J., JAMIESON, G. A., CHULAY, J. D. & WEBSTER, H. K. 1991. Molecular basis of sequestration in severe and uncomplicated Plasmodium falciparum malaria: differential adhesion of infected erythrocytes to CD36 and ICAM-1. *J Infect Dis,* 164**,** 163-9.

OHGAMI, N., NAGAI, R., IKEMOTO, M., ARAI, H., MIYAZAKI, A., HAKAMATA, H., HORIUCHI, S. & NAKAYAMA, H. 2002. CD36, serves as a receptor for advanced glycation endproducts (AGE). *J Diabetes Complications,* 16**,** 56-9.

OHKAWA, T., VOLKMAN, L. E. & WELCH, M. D. 2010. Actin-based motility drives baculovirus transit to the nucleus and cell surface. *J Cell Biol,* 190**,** 187-95.

OHKI, I., AMIDA, H., YAMADA, R., SUGIHARA, M., ISHIGAKI, T. & TATE, S. 2011. Surface plasmon resonance study on functional significance of clustered organization of lectin-like oxidized LDL receptor (LOX-1). *Biochim Biophys Acta,* 1814**,** 345-54.

OLIVETTA, E., TIRELLI, V., CHIOZZINI, C., SCAZZOCCHIO, B., ROMANO, I., ARENACCIO, C. & SANCHEZ, M. 2014. HIV-1 Nef impairs key functional activities in human macrophages through CD36 downregulation. *PLoS One,* 9**,** e93699.

OMI, K., OHASHI, J., PATARAPOTIKUL, J., HANANANTACHAI, H., NAKA, I., LOOAREESUWAN, S. & TOKUNAGA, K. 2003. CD36 polymorphism is associated with protection from cerebral malaria. *Am J Hum Genet,* 72**,** 364-74.

ONO, M., HANDA, K., WITHERS, D. A. & HAKOMORI, S. 2000. Glycosylation effect on membrane domain (GEM) involved in cell adhesion and motility: a preliminary note on functional alpha3, alpha5-CD82 glycosylation complex in ldlD 14 cells. *Biochem Biophys Res Commun,* 279**,** 744-50.

OQUENDO, P., HUNDT, E., LAWLER, J. & SEED, B. 1989. CD36 directly mediates cytoadherence of Plasmodium falciparum parasitized erythrocytes. *Cell,* 58**,** 95-101.

OU, W. J., CAMERON, P. H., THOMAS, D. Y. & BERGERON, J. J. 1993. Association of folding intermediates of glycoproteins with calnexin during protein maturation. *Nature,* 364**,** 771-6.

OUWENS, D. M., DIAMANT, M., FODOR, M., HABETS, D. D., PELSERS, M. M., EL HASNAOUI, M., DANG, Z. C., VAN DEN BROM, C. E., VLASBLOM, R., RIETDIJK, A., BOER, C., COORT, S. L., GLATZ, J. F. & LUIKEN, J. J. 2007. Cardiac contractile dysfunction in insulin-resistant rats fed a high-fat diet is associated with elevated CD36-mediated fatty acid uptake and esterification. *Diabetologia,* 50**,** 1938-48.

PACE, C. N. & SCHOLTZ, J. M. 1998. A helix propensity scale based on experimental studies of peptides and proteins. *Biophys J,* 75**,** 422-7.

PAIN, A., URBAN, B. C., KAI, O., CASALS-PASCUAL, C., SHAFI, J., MARSH, K. & ROBERTS, D. J. 2001. A non-sense mutation in Cd36 gene is associated with protection from severe malaria. *Lancet,* 357**,** 1502-3.

PAIZS, B. & SUHAI, S. 2005. Fragmentation pathways of protonated peptides. *Mass spectrometry reviews,* 24**,** 508-48.

PAMBAKIAN, S. & POSTON, R. N. 1987. The binding of immunoglobulin Fc to cationic proteins. *Clin Exp Immunol,* 68**,** 402-8.

PAN, A. C., BORHANI, D. W., DROR, R. O. & SHAW, D. E. 2013. Molecular determinants of drug-receptor binding kinetics. *Drug Discov Today,* 18**,** 667-73.

PAN, X. D., ZHU, Y. G., LIN, N., ZHANG, J., YE, Q. Y., HUANG, H. P. & CHEN, X. C. 2011. Microglial phagocytosis induced by fibrillar beta-amyloid is attenuated by oligomeric beta-amyloid: implications for Alzheimer's disease. *Mol Neurodegener,* 6**,** 45.

PAN, Y., CHENG, K., MAO, J., LIU, F., LIU, J., YE, M. & ZOU, H. 2014. Quantitative proteomics reveals the kinetics of trypsin-catalyzed protein digestion. *Anal Bioanal Chem.*

PARAMBAN, R. I., BUGOS, R. C. & SU, W. W. 2004. Engineering green fluorescent protein as a dual functional tag. *Biotechnol Bioeng,* 86**,** 687-97.

PATCHING, S. G. 2014. Surface plasmon resonance spectroscopy for characterisation of membrane protein-ligand interactions and its potential for drug discovery. *Biochim Biophys Acta,* 1838**,** 43-55.

PEARCE, S. F., ROY, P., NICHOLSON, A. C., HAJJAR, D. P., FEBBRAIO, M. & SILVERSTEIN, R. L. 1998. Recombinant glutathione S-transferase/CD36 fusion proteins define an oxidized low density lipoprotein-binding domain. *J Biol Chem,* 273**,** 34875-81.

PELHAM, H. R. & ROTHMAN, J. E. 2000. The debate about transport in the Golgi--two sides of the same coin? *Cell,* 102**,** 713-9.

PETRESCU, A. J., MILAC, A. L., PETRESCU, S. M., DWEK, R. A. & WORMALD, M. R. 2004. Statistical analysis of the protein environment of N-glycosylation sites: implications for occupancy, structure, and folding. *Glycobiology,* 14**,** 103-14.

PILIARIK, M., VAISOCHEROVA, H. & HOMOLA, J. 2009. Surface plasmon resonance biosensing. *Methods Mol Biol,* 503**,** 65-88.

PITTONI, V. & VALESINI, G. 2002. The clearance of apoptotic cells: implications for autoimmunity. *Autoimmun Rev,* 1**,** 154-61.

PLUDDEMANN, A., MUKHOPADHYAY, S. & GORDON, S. 2006. The interaction of macrophage receptors with bacterial ligands. *Expert Rev Mol Med,* 8**,** 1-25.

POSSEE, R. D. & HOWARD, S. C. 1987. Analysis of the polyhedrin gene promoter of the Autographa californica nuclear polyhedrosis virus. *Nucleic Acids Res,* 15**,** 10233-48.

POSSEE, R. D., SUN, T. P., HOWARD, S. C., AYRES, M. D., HILL-PERKINS, M. & GEARING, K. L. 1991. Nucleotide sequence of the Autographa californica nuclear polyhedrosis 9.4 kbp EcoRI-I and -R (polyhedrin gene) region. *Virology,* 185**,** 229-41.

PRAVENEC, M., LANDA, V., ZIDEK, V., MUSILOVA, A., KREN, V., KAZDOVA, L., AITMAN, T. J., GLAZIER, A. M., IBRAHIMI, A., ABUMRAD, N. A., QI, N., WANG, J. M., ST LEZIN, E. M. & KURTZ, T. W. 2001. Transgenic rescue of defective Cd36 ameliorates insulin resistance in spontaneously hypertensive rats. *Nat Genet,* 27**,** 156-8.

PRIVE, G. G. 2007. Detergents for the stabilization and crystallization of membrane proteins. *Methods,* 41**,** 388-97.

PUENTE NAVAZO, M. D., DAVIET, L., NINIO, E. & MCGREGOR, J. L. 1996. Identification on human CD36 of a domain (155-183) implicated in binding oxidized low-density lipoproteins (Ox-LDL). *Arterioscler Thromb Vasc Biol,* 16**,** 1033-9.

QIAO, L., MACDOUGALD, O. A. & SHAO, J. 2006. CCAAT/enhancer-binding protein alpha mediates induction of hepatic phosphoenolpyruvate carboxykinase by p38 mitogen-activated protein kinase. *J Biol Chem,* 281**,** 24390-7.

QIAO, L., ZOU, C., SHAO, P., SCHAACK, J., JOHNSON, P. F. & SHAO, J. 2008. Transcriptional regulation of fatty acid translocase/CD36 expression by CCAAT/enhancer-binding protein alpha. *J Biol Chem,* 283**,** 8788-95.

RAC, M. E., SAFRANOW, K. & PONCYLJUSZ, W. 2007. Molecular basis of human CD36 gene mutations. *Mol Med,* 13**,** 288-96.

RASMUSSEN, J. T., BERGLUND, L., RASMUSSEN, M. S. & PETERSEN, T. E. 1998. Assignment of disulfide bridges in bovine CD36. *Eur J Biochem,* 257**,** 488-94.

REAVEN, G. M. 1988. Banting lecture 1988. Role of insulin resistance in human disease. *Diabetes,* 37**,** 1595-607.

REAVEN, G. M., CHANG, H., HOFFMAN, B. B. & AZHAR, S. 1989. Resistance to insulin-stimulated glucose uptake in adipocytes isolated from spontaneously hypertensive rats. *Diabetes,* 38**,** 1155-60.

REAVEN, G. M., LITHELL, H. & LANDSBERG, L. 1996. Hypertension and associated metabolic abnormalities--the role of insulin resistance and the sympathoadrenal system. *N Engl J Med,* 334**,** 374-81.

RECZEK, D., SCHWAKE, M., SCHRODER, J., HUGHES, H., BLANZ, J., JIN, X., BRONDYK, W., VAN PATTEN, S., EDMUNDS, T. & SAFTIG, P. 2007. LIMP-2 is a receptor for lysosomal mannose-6-phosphate-independent targeting of beta-glucocerebrosidase. *Cell,* 131**,** 770-83.

REGE, T. A., STEWART, J., JR., DRANKA, B., BENVENISTE, E. N., SILVERSTEIN, R. L. & GLADSON, C. L. 2009. Thrombospondin-1-induced apoptosis of brain microvascular endothelial cells can be mediated by TNF-R1. *J Cell Physiol,* 218**,** 94-103.

RENDIC, D., WILSON, I. B. H. & PASCHINGER, K. 2008. The glycosylation capacity of insect cells. *Croatica Chemica Acta,* 81**,** 7-21.

RIGOTTI, A., ACTON, S. L. & KRIEGER, M. 1995. The class B scavenger receptors SR-BI and CD36 are receptors for anionic phospholipids. *J Biol Chem,* 270**,** 16221-4.

RIOS, F. J., FERRACINI, M., PECENIN, M., KOGA, M. M., WANG, Y., KETELHUTH, D. F. & JANCAR, S. 2013. Uptake of oxLDL and IL-10 production by macrophages requires PAFR and CD36 recruitment into the same lipid rafts. *PLoS One,* 8**,** e76893.

ROCKS, O., PEYKER, A., KAHMS, M., VERVEER, P. J., KOERNER, C., LUMBIERRES, M., KUHLMANN, J., WALDMANN, H., WITTINGHOFER, A. & BASTIAENS, P. I. 2005. An acylation cycle regulates localization and activity of palmitoylated Ras isoforms. *Science,* 307**,** 1746-52.

ROHRER, L., FREEMAN, M., KODAMA, T., PENMAN, M. & KRIEGER, M. 1990. Coiled-coil fibrous domains mediate ligand binding by macrophage scavenger receptor type II. *Nature,* 343**,** 570-2.

ROHRMANN, G. F. 1986. Polyhedrin structure. *J Gen Virol,* 67 (Pt 8)**,** 1499-513.

RUDD, P. M., DOWNING, A. K., CADENE, M., HARVEY, D. J., WORMALD, M. R., WEIR, I., DWEK, R. A., RIFKIN, D. B. & GLEIZES, P. E. 2000. Hybrid and complex glycans are linked to the conserved N-glycosylation site of the third eight-cysteine domain of LTBP-1 in insect cells. *Biochemistry,* 39**,** 1596-603.

RYEOM, S. W., SILVERSTEIN, R. L., SCOTTO, A. & SPARROW, J. R. 1996. Binding of anionic phospholipids to retinal pigment epithelium may be mediated by the scavenger receptor CD36. *J Biol Chem,* 271**,** 20536-9.

SALAWU, F. K., UMAR, J. T. & OLOKOBA, A. B. 2011. Alzheimer's disease: a review of recent developments. *Ann Afr Med,* 10**,** 73-9.

SALMON, V., LEGRAND, D., GEORGES, B., SLOMIANNY, M. C., CODDEVILLE, B. & SPIK, G. 1997. Characterization of human lactoferrin produced in the baculovirus expression system. *Protein Expr Purif,* 9**,** 203-10.

SARENEVA, T., PIRHONEN, J., CANTELL, K. & JULKUNEN, I. 1995. N-glycosylation of human interferon-gamma: glycans at Asn-25 are critical for protease resistance. *Biochem J,* 308 (Pt 1)**,** 9-14.

SARRIAS, M. R., GRONLUND, J., PADILLA, O., MADSEN, J., HOLMSKOV, U. & LOZANO, F. 2004. The Scavenger Receptor Cysteine-Rich (SRCR) domain: an ancient and highly conserved protein module of the innate immune system. *Crit Rev Immunol,* 24**,** 1-37.

SATO, O., KURIKI, C., FUKUI, Y. & MOTOJIMA, K. 2002. Dual promoter structure of mouse and human fatty acid translocase/CD36 genes and unique transcriptional activation by peroxisome proliferator-activated receptor alpha and gamma ligands. *J Biol Chem,* 277**,** 15703-11.

SAVILL, J., HOGG, N. & HASLETT, C. 1991. Macrophage Vitronectin Receptor, Cd36, and Thrombospondin Cooperate in Recognition of Neutrophils Undergoing Programmed Cell-Death. *Chest,* 99**,** S6-S7.

SAVILLE, G. P., PATMANIDI, A. L., POSSEE, R. D. & KING, L. A. 2004. Deletion of the Autographa californica nucleopolyhedrovirus chitinase KDEL motif and in vitro and in vivo analysis of the modified virus. *J Gen Virol,* 85**,** 821-31.

SCHMIDT, A. M., HORI, O., BRETT, J., YAN, S. D., WAUTIER, J. L. & STERN, D. 1994. Cellular receptors for advanced glycation end products. Implications for induction of oxidant stress and cellular dysfunction in the pathogenesis of vascular lesions. *Arterioscler Thromb,* 14**,** 1521-8.

SCHWARZ, F. & AEBI, M. 2011. Mechanisms and principles of N-linked protein glycosylation. *Curr Opin Struct Biol,* 21**,** 576-82.

SEDDON, A. M., CURNOW, P. & BOOTH, P. J. 2004. Membrane proteins, lipids and detergents: not just a soap opera. *Biochim Biophys Acta,* 1666**,** 105-17.

SELKOE, D. J. 2000. The origins of Alzheimer disease: a is for amyloid. *JAMA,* 283**,** 1615-7.

SERJEANT, G. R. 2013. The natural history of sickle cell disease. *Cold Spring Harb Perspect Med,* 3**,** a011783.

SETTY, B. N., KULKARNI, S. & STUART, M. J. 2002. Role of erythrocyte phosphatidylserine in sickle red cell-endothelial adhesion. *Blood,* 99**,** 1564-71.

SEVIER, C. S. & KAISER, C. A. 2002. Formation and transfer of disulphide bonds in living cells. *Nat Rev Mol Cell Biol,* 3**,** 836-47.

SHAKIN-ESHLEMAN, S. H., SPITALNIK, S. L. & KASTURI, L. 1996. The amino acid at the X position of an Asn-X-Ser sequon is an important determinant of N-linked core-glycosylation efficiency. *J Biol Chem,* 271**,** 6363-6.

SHAMSUL, H. M., HASEBE, A., IYORI, M., OHTANI, M., KIURA, K., ZHANG, D., TOTSUKA, Y. & SHIBATA, K. 2010. The Toll-like receptor 2 (TLR2) ligand FSL-1 is internalized via the clathrin-dependent endocytic pathway triggered by CD14 and CD36 but not by TLR2. *Immunology,* 130**,** 262-72.

SHARMA, S., ADROGUE, J. V., GOLFMAN, L., URAY, I., LEMM, J., YOUKER, K., NOON, G. P., FRAZIER, O. H. & TAEGTMEYER, H. 2004. Intramyocardial lipid accumulation in the failing human heart resembles the lipotoxic rat heart. *FASEB J,* 18**,** 1692-700.

SHEPPARD, D. 2005. Integrin-mediated activation of latent transforming growth factor beta. *Cancer Metastasis Rev,* 24**,** 395-402.

SIMANTOV, R., FEBBRAIO, M., CROMBIE, R., ASCH, A. S., NACHMAN, R. L. & SILVERSTEIN, R. L. 2001. Histidine-rich glycoprotein inhibits the antiangiogenic effect of thrombospondin-1. *J Clin Invest,* 107**,** 45-52.

SINGH, C., ZAMPRONIO, C. G., CREESE, A. J. & COOPER, H. J. 2012. Higher energy collision dissociation (HCD) product ion-triggered electron transfer dissociation (ETD) mass spectrometry for the analysis of N-linked glycoproteins. *J Proteome Res,* 11**,** 4517-25.

SINGH, R. B., MENGI, S. A., XU, Y. J., ARNEJA, A. S. & DHALLA, N. S. 2002. Pathogenesis of atherosclerosis: A multifactorial process. *Exp Clin Cardiol,* 7**,** 40-53.

SINHA, S., QIDWAI, T., KANCHAN, K., ANAND, P., JHA, G. N., PATI, S. S., MOHANTY, S., MISHRA, S. K., TYAGI, P. K., SHARMA, S. K., INDIAN GENOME VARIATION, C., VENKATESH, V. & HABIB, S. 2008. Variations in host genes encoding adhesion molecules and susceptibility to falciparum malaria in India. *Malar J,* 7**,** 250.

SLACK, J. M., KUZIO, J. & FAULKNER, P. 1995. Characterization of v-cath, a cathepsin L-like proteinase expressed by the baculovirus Autographa californica multiple nuclear polyhedrosis virus. *J Gen Virol,* 76 (Pt 5)**,** 1091-8.

SMATHERS, R. L. & PETERSEN, D. R. 2011. The human fatty acid-binding protein family: evolutionary divergences and functions. *Hum Genomics,* 5**,** 170-91.

SMITH, G. E., SUMMERS, M. D. & FRASER, M. J. 1983. Production of human beta interferon in insect cells infected with a baculovirus expression vector. *Mol Cell Biol,* 3**,** 2156-65.

SMITH, J., SU, X., EL-MAGHRABI, R., STAHL, P. D. & ABUMRAD, N. A. 2008. Opposite regulation of CD36 ubiquitination by fatty acids and insulin: effects on fatty acid uptake. *J Biol Chem,* 283**,** 13578-85.

SMOTRYS, J. E. & LINDER, M. E. 2004. Palmitoylation of intracellular signaling proteins: regulation and function. *Annu Rev Biochem,* 73**,** 559-87.

SMYTH, M. S. & MARTIN, J. H. 2000. x ray crystallography. *Mol Pathol,* 53**,** 8-14.

SOUSA, M. C., FERRERO-GARCIA, M. A. & PARODI, A. J. 1992. Recognition of the oligosaccharide and protein moieties of glycoproteins by the UDP-Glc:glycoprotein glucosyltransferase. *Biochemistry,* 31**,** 97-105.

SPIRO, R. G. 2000. Glucose residues as key determinants in the biosynthesis and quality control of glycoproteins with N-linked oligosaccharides. *J Biol Chem,* 275**,** 35657-60.

STANLEY, P. 1984. Glycosylation mutants of animal cells. *Annu Rev Genet,* 18**,** 525-52.

STEINBUSCH, L. K., SCHWENK, R. W., OUWENS, D. M., DIAMANT, M., GLATZ, J. F. & LUIKEN, J. J. 2011. Subcellular trafficking of the substrate transporters GLUT4 and CD36 in cardiomyocytes. *Cell Mol Life Sci,* 68**,** 2525-38.

STEWART, C. R., STUART, L. M., WILKINSON, K., VAN GILS, J. M., DENG, J., HALLE, A., RAYNER, K. J., BOYER, L., ZHONG, R., FRAZIER, W. A., LACY-HULBERT, A., EL KHOURY, J., GOLENBOCK, D. T. & MOORE, K. J. 2010. CD36 ligands promote sterile inflammation through assembly of a Toll-like receptor 4 and 6 heterodimer. *Nature immunology,* 11**,** 155-61.

STREMMEL, W., POHL, L., RING, A. & HERRMANN, T. 2001. A new concept of cellular uptake and intracellular trafficking of long-chain fatty acids. *Lipids,* 36**,** 981-9.

SUGIHARA, K., SUGIHARA, T., MOHANDAS, N. & HEBBEL, R. P. 1992. Thrombospondin mediates adherence of CD36+ sickle reticulocytes to endothelial cells. *Blood,* 80**,** 2634-42.

SUMMERS, M. D. & SMITH, G. E. 1978. Baculovirus structural polypeptides. *Virology,* 84**,** 390-402.

SWERLICK, R. A., LEE, K. H., WICK, T. M. & LAWLEY, T. J. 1992. Human dermal microvascular endothelial but not human umbilical vein endothelial cells express CD36 in vivo and in vitro. *J Immunol,* 148**,** 78-83.

SWINNEY, D. C. 2009. The role of binding kinetics in therapeutically useful drug action. *Curr Opin Drug Discov Devel,* 12**,** 31-9.

SWINNEY, D. C. & ANTHONY, J. 2011. How were new medicines discovered? *Nat Rev Drug Discov,* 10**,** 507-19.

TALLE, M. A., RAO, P. E., WESTBERG, E., ALLEGAR, N., MAKOWSKI, M., MITTLER, R. S. & GOLDSTEIN, G. 1983. Patterns of antigenic expression on human monocytes as defined by monoclonal antibodies. *Cellular immunology,* 78**,** 83-99.

TAN, Y.-J. & TING, A. E. 2000. Non-ionic detergent affects the conformation of a functionally active mutant of Bcl-XL. *Protein Engineering,* 13**,** 887-892.

TANDON, N. N., KRALISZ, U. & JAMIESON, G. A. 1989a. Identification of glycoprotein IV (CD36) as a primary receptor for platelet-collagen adhesion. *The Journal of biological chemistry,* 264**,** 7576-83.

TANDON, N. N., LIPSKY, R. H., BURGESS, W. H. & JAMIESON, G. A. 1989b. Isolation and characterization of platelet glycoprotein IV (CD36). *J Biol Chem,* 264**,** 7570-5.

TANG, Y., TAYLOR, K. T., SOBIESKI, D. A., MEDVED, E. S. & LIPSKY, R. H. 1994. Identification of a human CD36 isoform produced by exon skipping. Conservation of exon organization and pre-mRNA splicing patterns with a CD36 gene family member, CLA-1. *J Biol Chem,* 269**,** 6011-5.

TANIOUS, F. A., NGUYEN, B. & WILSON, W. D. 2008. Biosensor-surface plasmon resonance methods for quantitative analysis of biomolecular interactions. *Methods Cell Biol,* 84**,** 53-77.

TAO, N., WAGNER, S. J. & LUBLIN, D. M. 1996. CD36 is palmitoylated on both N- and C-terminal cytoplasmic tails. *The Journal of biological chemistry,* 271**,** 22315-20.

TERPE, K. 2003. Overview of tag protein fusions: from molecular and biochemical fundamentals to commercial systems. *Appl Microbiol Biotechnol,* 60**,** 523-33.

THELEN, T., HAO, Y., MEDEIROS, A. I., CURTIS, J. L., SEREZANI, C. H., KOBZIK, L., HARRIS, L. H. & ARONOFF, D. M. 2010. The class A scavenger receptor, macrophage receptor with collagenous structure, is the major phagocytic receptor for Clostridium sordellii expressed by human decidual macrophages. *J Immunol,* 185**,** 4328-35.

THOMAS, C. J., BROWN, H. L., HAWES, C. R., LEE, B. Y., MIN, M. K., KING, L. A. & POSSEE, R. D. 1998. Localization of a baculovirus-induced chitinase in the insect cell endoplasmic reticulum. *J Virol,* 72**,** 10207-12.

THOMSEN, D. R., POST, L. E. & ELHAMMER, A. P. 1990. Structure of O-glycosidically linked oligosaccharides synthesized by the insect cell line Sf9. *J Cell Biochem,* 43**,** 67-79.

THORNE, R. F., MELDRUM, C. J., HARRIS, S. J., DORAHY, D. J., SHAFREN, D. R., BERNDT, M. C., BURNS, G. F. & GIBSON, P. G. 1997. CD36 forms covalently associated dimers and multimers in platelets and transfected COS-7 cells. *Biochem Biophys Res Commun,* 240**,** 812-8.

THORNE, R. F., RALSTON, K. J., DE BOCK, C. E., MHAIDAT, N. M., ZHANG, X. D., BOYD, A. W. & BURNS, G. F. 2010. Palmitoylation of CD36/FAT regulates the rate of its post-transcriptional processing in the endoplasmic reticulum. *Biochim Biophys Acta,* 1803**,** 1298-307.

THORNTON, J. M. 1981. Disulphide bridges in globular proteins. *J Mol Biol,* 151**,** 261-87.

TOMITA, M. & TSUMOTO, K. 2011. Hybridoma technologies for antibody production. *Immunotherapy,* 3**,** 371-80.

TOWBIN, H., STAEHELIN, T. & GORDON, J. 1979. Electrophoretic transfer of proteins from polyacrylamide gels to nitrocellulose sheets: procedure and some applications. *Proceedings of the National Academy of Sciences of the United States of America,* 76**,** 4350-4.

TRETTER, V., ALTMANN, F. & MARZ, L. 1991. Peptide-N4-(N-acetyl-beta-glucosaminyl)asparagine amidase F cannot release glycans with fucose

attached alpha 1----3 to the asparagine-linked N-acetylglucosamine residue. *Eur J Biochem,* 199**,** 647-52.

TRINH-TRANG-TAN, M. M., VILELA-LAMEGO, C., PICOT, J., WAUTIER, M. P. & CARTRON, J. P. 2010. Intercellular adhesion molecule-4 and CD36 are implicated in the abnormal adhesiveness of sickle cell SAD mouse erythrocytes to endothelium. *Haematologica,* 95**,** 730-7.

UBERSAX, J. A. & FERRELL, J. E., JR. 2007. Mechanisms of specificity in protein phosphorylation. *Nat Rev Mol Cell Biol,* 8**,** 530-41.

VAGENENDE, V., YAP, M. G. & TROUT, B. L. 2009. Mechanisms of protein stabilization and prevention of protein aggregation by glycerol. *Biochemistry,* 48**,** 11084-96.

VAN ANKEN, E. & BRAAKMAN, I. 2005. Versatility of the endoplasmic reticulum protein folding factory. *Crit Rev Biochem Mol Biol,* 40**,** 191-228.

VAN REE, J. H., VAN DEN BROEK, W. J., DAHLMANS, V. E., GROOT, P. H., VIDGEON-HART, M., FRANTS, R. R., WIERINGA, B., HAVEKES, L. M. & HOFKER, M. H. 1994. Diet-induced hypercholesterolemia and atherosclerosis in heterozygous apolipoprotein E-deficient mice. *Atherosclerosis,* 111**,** 25-37.

VANGURI, V. K., WANG, S., GODYNA, S., RANGANATHAN, S. & LIAU, G. 2000. Thrombospondin-1 binds to polyhistidine with high affinity and specificity. *Biochem J,* 347**,** 469-73.

VAUGHN, J. L., GOODWIN, R. H., TOMPKINS, G. J. & MCCAWLEY, P. 1977. The establishment of two cell lines from the insect Spodoptera frugiperda (Lepidoptera; Noctuidae). *In Vitro,* 13**,** 213-7.

VAUQUELIN, G., BOSTOEN, S., VANDERHEYDEN, P. & SEEMAN, P. 2012. Clozapine, atypical antipsychotics, and the benefits of fast-off D2 dopamine receptor antagonism. *Naunyn Schmiedebergs Arch Pharmacol,* 385**,** 337-72.

VEGA, M. A., SEGUI-REAL, B., GARCIA, J. A., CALES, C., RODRIGUEZ, F., VANDERKERCKHOVE, J. & SANDOVAL, I. V. 1991. Cloning, sequencing, and expression of a cDNA encoding rat LIMP II, a novel 74-kDa lysosomal membrane protein related to the surface adhesion protein CD36. *J Biol Chem,* 266**,** 16818-24.

VOLF, I., MOESLINGER, T., COOPER, J., SCHMID, W. & KOLLER, E. 1999. Human platelets exclusively bind oxidized low density lipoprotein showing no specificity for acetylated low density lipoprotein. *FEBS Lett,* 449, 141-5.

VOLPERT, O. V., ZAICHUK, T., ZHOU, W., REIHER, F., FERGUSON, T. A., STUART, P. M., AMIN, M. & BOUCK, N. P. 2002. Inducer-stimulated Fas targets activated endothelium for destruction by anti-angiogenic thrombospondin-1 and pigment epithelium-derived factor. *Nat Med,* 8**,** 349-57.

VOSS, T., ERGULEN, E., AHORN, H., KUBELKA, V., SUGIYAMA, K., MAURER-FOGY, I. & GLOSSL, J. 1993. Expression of human interferon omega 1 in Sf9 cells. No evidence for complex-type N-linked glycosylation or sialylation. *Eur J Biochem,* 217**,** 913-9.

WANG, X., CHEN, Y., LV, L. & CHEN, J. 2009. Silencing CD36 gene expression results in the inhibition of latent-TGF-beta1 activation and suppression of silica-induced lung fibrosis in the rat. *Respir Res,* 10**,** 36.

WANG, X., WANG, Y. R., YANG, D. Y. & ZHANG, M. 2013. [The inhibitory effect of latent transforming growth factor beta1 activation and silicosis by

CD36 targeted RNA interference in silicosis model of rat]. *Zhonghua Lao Dong Wei Sheng Zhi Ye Bing Za Zhi,* 31**,** 518-21.

WANG, Y., WU, W., LI, Z., YUAN, M., FENG, G., YU, Q., YANG, K. & PANG, Y. 2007. ac18 is not essential for the propagation of Autographa californica multiple nucleopolyhedrovirus. *Virology,* 367**,** 71-81.

WICKHAM, T. J., DAVIS, T., GRANADOS, R. R., SHULER, M. L. & WOOD, H. A. 1992. Screening of insect cell lines for the production of recombinant proteins and infectious virus in the baculovirus expression system. *Biotechnol Prog,* 8**,** 391-6.

WICKHAM, T. J. & NEMEROW, G. R. 1993. Optimization of growth methods and recombinant protein production in BTI-Tn-5B1-4 insect cells using the baculovirus expression system. *Biotechnol Prog,* 9**,** 25-30.

WILKINSON, K., BOYD, J. D., GLICKSMAN, M., MOORE, K. J. & EL KHOURY, J. 2011. A high content drug screen identifies ursolic acid as an inhibitor of amyloid beta protein interactions with its receptor CD36. *The Journal of biological chemistry,* 286**,** 34914-22.

WILLIAMS, D. B. 2006. Beyond lectins: the calnexin/calreticulin chaperone system of the endoplasmic reticulum. *J Cell Sci,* 119**,** 615-23.

WITZTUM, J. L. 2005. You are right too! *J Clin Invest,* 115**,** 2072-5.

WONG, K. T., PETER, C. H., GREENFIELD, P. F., REID, S. & NIELSEN, L. K. 1996. Low multiplicity infection of insect cells with a recombinant baculovirus: The cell yield concept. *Biotechnol Bioeng,* 49**,** 659-66.

WYNN, T. A. 2008. Cellular and molecular mechanisms of fibrosis. *The Journal of pathology,* 214**,** 199-210.

YABE, U., SATO, C., MATSUDA, T. & KITAJIMA, K. 2003. Polysialic acid in human milk. CD36 is a new member of mammalian polysialic acid-containing glycoprotein. *J Biol Chem,* 278**,** 13875-80.

YAMAJI, H., TAGAI, S. & FUKUDA, H. 1999. Optimal production of recombinant protein by the baculovirus-insect cell system in shake-flask culture with medium replacement. *J Biosci Bioeng,* 87**,** 636-41.

YAMASHITA, S., HIRANO, K., KUWASAKO, T., JANABI, M., TOYAMA, Y., ISHIGAMI, M. & SAKAI, N. 2007. Physiological and pathological roles of a multi-ligand receptor CD36 in atherogenesis; insights from CD36-deficient patients. *Mol Cell Biochem,* 299**,** 19-22.

YANAI, H., CHIBA, H., MORIMOTO, M., JAMIESON, G. A. & MATSUNO, K. 2000. Type I CD36 deficiency in humans is not associated with insulin resistance syndrome. *Thromb Haemost,* 83**,** 786.

YANG, Y.-L., LIN, S.-H., CHUANG, L.-Y., GUH, J.-Y., LIAO, T.-N., LEE, T.-C., CHANG, W.-T., CHANG, F.-R., HUNG, M.-Y., CHIANG, T.-A. & HUNG, C.-Y. 2007. CD36 is a novel and potential anti-fibrogenic target in albumin-induced renal proximal tubule fibrosis. *Journal of cellular biochemistry,* 101**,** 735-44.

YEHUALAESHET, T., O'CONNOR, R., BEGLEITER, A., MURPHY-ULLRICH, J. E., SILVERSTEIN, R. & KHALIL, N. 2000. A CD36 synthetic peptide inhibits bleomycin-induced pulmonary inflammation and connective tissue synthesis in the rat. *Am J Respir Cell Mol Biol,* 23**,** 204-12.

YEHUALAESHET, T., O'CONNOR, R., GREEN-JOHNSON, J., MAI, S., SILVERSTEIN, R., MURPHY-ULLRICH, J. E. & KHALIL, N. 1999. Activation of rat alveolar macrophage-derived latent transforming growth factor beta-1 by plasmin requires interaction with thrombospondin-1 and its

cell surface receptor, CD36. *The American journal of pathology,* 155**,** 841-51.

YIPP, B. G., BARUCH, D. I., BRADY, C., MURRAY, A. G., LOOAREESUWAN, S., KUBES, P. & HO, M. 2003. Recombinant PfEMP1 peptide inhibits and reverses cytoadherence of clinical Plasmodium falciparum isolates in vivo. *Blood,* 101**,** 331-7.

ZENG, Y., TAO, N., CHUNG, K. N., HEUSER, J. E. & LUBLIN, D. M. 2003. Endocytosis of oxidized low density lipoprotein through scavenger receptor CD36 utilizes a lipid raft pathway that does not require caveolin-1. *J Biol Chem,* 278**,** 45931-6.

ZHANG, L., WU, G., TATE, C. G., LOOKENE, A. & OLIVECRONA, G. 2003. Calreticulin promotes folding/dimerization of human lipoprotein lipase expressed in insect cells (sf21). *J Biol Chem,* 278**,** 29344-51.

ZHANG, X. & OGLESBEE, M. 2003. Use of surface plasmon resonance for the measurement of low affinity binding interactions between HSP72 and measles virus nucleocapsid protein. *Biol Proced Online,* 5**,** 170-181.

ZHAO, H., GORSHKOVA, II, FU, G. L. & SCHUCK, P. 2013. A comparison of binding surfaces for SPR biosensing using an antibody-antigen system and affinity distribution analysis. *Methods,* 59**,** 328-35.

ZHONG, X., KRIZ, R., SEEHRA, J. & KUMAR, R. 2004. N-linked glycosylation of platelet P2Y12 ADP receptor is essential for signal transduction but not for ligand binding or cell surface expression. *FEBS Lett,* 562**,** 111-7.

ZHU, W., LI, W. & SILVERSTEIN, R. L. 2012. Advanced glycation end products induce a prothrombotic phenotype in mice via interaction with platelet CD36. *Blood,* 119**,** 6136-44.

ZINGG, J. M., RICCIARELLI, R., ANDORNO, E. & AZZI, A. 2002. Novel 5' exon of scavenger receptor CD36 is expressed in cultured human vascular smooth muscle cells and atherosclerotic plaques. *Arterioscler Thromb Vasc Biol,* 22**,** 412-7.

ZUFFEREY, R., KNAUER, R., BURDA, P., STAGLJAR, I., TE HEESEN, S., LEHLE, L. & AEBI, M. 1995. STT3, a highly conserved protein required for yeast oligosaccharyl transferase activity in vivo. *EMBO J,* 14**,** 4949-60.

Appendices

Appendix 1

pBacPAK9-HMSS-CD36ED-12His

```
                                    >EcoRV
                                      |
          1130      1140      1150      1160      1170      1180      1190      1200
ACAAACTGGAAATGTCTATCAATATATAGTTGCTGATATCATGGAGATAATTAAAATGATAACCATCTCGCAAATAAATA


          1210      1220      1230      1240      1250      1260      1270      1280
AGTATTTTACTGTTTTCGTAACAGTTTTGTAATAAAAAAACCTATAAATATGAAATTCTTAGTCAACGTTGCCCTTGTTT
                                                      M  K  F  L  V  N  V  A  L  V>
                                                      _____>


                                    >SacI
                                      |
          1290      1300      1310      1320 |    1330      1340      1350      1360
TTATGGTCGTATACATTTCTTACATCTATGCGGATCCGAGCTCGAAGACAATTAAAAAGCAAGTTGTCCTCGAAGAAGGT
 F  M  V  V  Y  I  S  Y  I  Y  A  D  P  S  S  K  T  I  K  K  Q  V  V  L  E  E  G>
_____      >


          1370      1380      1390      1400      1410      1420      1430      1440
ACAATTGCTTTTAAAAATTGGGTTAAAACAGGCACAGAAGTTTACAGACAGTTTTGGATCTTTGATGTGCAAAATCCACA
  T  I  A  F  K  N  W  V  K  T  G  T  E  V  Y  R  Q  F  W  I  F  D  V  Q  N  P  Q>
                                                                               >


          1450      1460      1470      1480      1490      1500      1510      1520
GGAAGTGATGATGAACAGCAGCAACATTCAAGTTAAGCAAAGAGGTCCTTATACGTACAGAGTTCGTTTTCTAGCCAAGG
  E  V  M  M  N  S  S  N  I  Q  V  K  Q  R  G  P  Y  T  Y  R  V  R  F  L  A  K>
                                                                            >


          1530      1540      1550      1560      1570      1580      1590      1600
AAAATGTAACCCAGGACGCTGAGGACAACACAGTCTCTTTCCTGCAGCCCAATGGTGCCATCTTCGAACCTTCACTATCA
 E  N  V  T  Q  D  A  E  D  N  T  V  S  F  L  Q  P  N  G  A  I  F  E  P  S  L  S>
                                                                             >


          1610      1620      1630      1640      1650      1660      1670      1680
GTTGGAACAGAGGCTGACAACTTCACAGTTCTCAATCTGGCTGTGGCAGCTGCATCCCATATCTATCAAAATCAATTTGT
  V  G  T  E  A  D  N  F  T  V  L  N  L  A  V  A  A  A  S  H  I  Y  Q  N  Q  F  V>
                                                                               >


          1690      1700      1710      1720      1730      1740      1750      1760
TCAAATGATCCTCAATTCACTTATTAACAAGTCAAAATCTTCTATGTTCCAAGTCAGAACTTTGAGAGAACTGTTATGGG
  Q  M  I  L  N  S  L  I  N  K  S  K  S  S  M  F  Q  V  R  T  L  R  E  L  L  W>
                                                                            >


          1770      1780      1790      1800      1810      1820      1830      1840
GCTATAGGGATCCATTTTTGAGTTTGGTTCCATACCCTGTTACTACCACAGTTGGTCTGTTTTATCCTTACAACAATACT
 G  Y  R  D  P  F  L  S  L  V  P  Y  P  V  T  T  T  V  G  L  F  Y  P  Y  N  N  T>
                                                                             >


          1850      1860      1870      1880      1890      1900      1910      1920
GCAGATGGAGTTTATAAAGTTTTCAATGGAAAAGATAACATAAGTAAAGTTGCCATAATCGACACATATAAAGGTAAAAG
```

```
            A  D  G  V  Y  K  V  F  N  G  K  D  N  I  S  K  V  A  I  I  D  T  Y  K  G  K  R>
    _____>


         1930      1940      1950      1960      1970      1980      1990      2000
GAATCTGTCCTATTGGGAAAGTCACTGCGACATGATTAATGGTACAGATGCAGCCTCATTTCCACCTTTTGTTGAGAAAA
     N  L  S  Y  W  E  S  H  C  D  M  I  N  G  T  D  A  A  S  F  P  P  F  V  E  K>
    _____>


         2010      2020      2030      2040      2050      2060      2070      2080
GCCAGGTATTGCAGTTCTTTTCTTCTGATATTTGCAGGTCAATCTATGCTGTATTTGAATCCGACGTTAATCTGAAAGGA
  S  Q  V  L  Q  F  F  S  S  D  I  C  R  S  I  Y  A  V  F  E  S  D  V  N  L  K  G>
    _____>


         2090      2100      2110      2120      2130      2140      2150      2160
ATCCCTGTGTATAGATTTGTTCTTCCATCCAAGGCCTTTGCCTCTCCAGTTGAAAACCCAGACAACTATTGTTTCTGCAC
  I  P  V  Y  R  F  V  L  P  S  K  A  F  A  S  P  V  E  N  P  D  N  Y  C  F  C  T>
    _____>


         2170      2180      2190      2200      2210      2220      2230      2240
AGAAAAAATTATCTCAAAAAATTGTACATCATATGGTGTGCTAGACATCAGCAAATGCAAAGAAGGGAGACCTGTGTACA
  E  K  I  I  S  K  N  C  T  S  Y  G  V  L  D  I  S  K  C  K  E  G  R  P  V  Y>
    _____>


         2250      2260      2270      2280      2290      2300      2310      2320
TTTCACTTCCTCATTTTCTGTATGCAAGTCCTGATGTTTCAGAACCTATTGATGGATTAAACCCAAATGAAGAAGAACAT
  I  S  L  P  H  F  L  Y  A  S  P  D  V  S  E  P  I  D  G  L  N  P  N  E  E  H>
    _____>


         2330      2340      2350      2360      2370      2380      2390      2400
AGGACATACTTGGATATTGAACCTATAACTGGATTCACTTTACAATTTGCAAAACGGCTGCAGGTCAACCTATTGGTCAA
  R  T  Y  L  D  I  E  P  I  T  G  F  T  L  Q  F  A  K  R  L  Q  V  N  L  L  V  K>
    _____>


         2410      2420      2430      2440      2450      2460      2470      2480
GCCATCAGAAAAAATTCAAGTATTAAAGAATCTGAAGAGGAACTATATTGTGCCTATTCTTTGGCTTAATGAGACTGGGA
  P  S  E  K  I  Q  V  L  K  N  L  K  R  N  Y  I  V  P  I  L  W  L  N  E  T  G>
    _____>


                                              >BstEII
                                               |
         2490      2500      2510      2520     | 2530      2540      2550      2560
CCATTGGTGATGAGAAGGCAAACATGTTCAGAAGTCAAGTAACTGGTCACCATCACCATCACCACACCGGTCATCATCAC
  T  I  G  D  E  K  A  N  M  F  R  S  Q  V  T  G  H  H  H  H  H  H  T  G  H  H  H>
    _____>


                                                                     >XbaI
                                                                      |
         2570      2580      2590      2600      2610      2620      2630    | 2640
CATCACCATTGAGTTTATCTGACTAAATCTTAGTTTGTATTGTCATGTTTTAATACAATATGTTATGTTTGGGTCTAGAT
  H  H  H  *>
    _____>
```